STUDIES ON DIRECT AND INDIRECT ELECTROCHEMICAL IMMUNOASSAYS

by

Eileen Buckley B.Sc.

A thesis submitted for the Degree of

Doctor of Philosophy

Dublin City University

September 1989

DECLARATION

I hereby declare that the contents of this thesis, except where otherwise stated, are based entirely on my own work, which was carried out in the School of Chemical Sciences, Dublin City University, Dublin and in the University of Cincinnati, Cincinnati, Ohio, U.S.A.

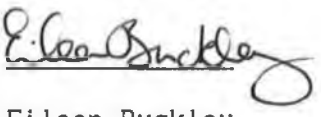

Eileen Buckley

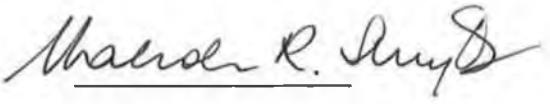

Malcolm R. Smyth

(Supervisor)

For my mother, Maura Taylor-Buckley and

in memory of my father Patrick Denis Buckley

Acknowledgements

I would like to acknowledge my supervisor Dr. Malcolm R. Smyth for giving me the opportunity to do this research and his continued help and guidance throughout the course of the work. Also to Professor A. Pratt and the School of Chemical Sciences, Dublin City University, for the use of facilities.

I wish to thank the technicians for all of their help, advice and patience, Teresa McDonald, Ita Kinehan, Mick Burke, Peig Ward and also Veronica, Fintan and Maurice.

Many thanks to the School of Biological Science, in particular Dr. Richard O'Kennedy for a lot of helpful advice and ideas also Patricia Carty and Patricia O'Reilly.

My thanks to my fellow postgrad's for their freindship and diversion, in particular "AS7" Bernie, Mary, Paula and Andrew. I would like to thank Dr. Juana Rodriquez-Flores and Dr. Jose-Maria Fernandez for their help and useful discussion.

I wish to thank, Dr. William R. Heineman for giving me the opportunity to work in his lab in the University of Cincinnati and for his hospitality throughout my stay. Also my thanks to Dr. Brian Halsall, George, Peter, Yan, John, Sam and Kiam. In particular Dr. Sarah H. Jenkins and Carlos Nazario for their kindness, hospitality and helpful discussions during my stay in Cincinnati.

I would like to acknowledge the staff of the library at D.C.U. especially Helen and Ann, and thanks to Gillian and Mick for their help in the preparation of this manuscript.

Finally my gratitude to my family for their endless support from the very beginning.

Contents page

"The case has, in some respects, been not entirely devoid of interest."

"A case of Identity"
Sir Arthur Conan Doyle.

ABSTRACT

STUDIES ON DIRECT AND INDIRECT ELECTROCHEMICAL IMMUNOASSAYS

Eileen Buckley

Two approaches to electrochemical immunoassay are reported. The first approach was an indirect method, involving an electroactive, enzyme-catalysed, substrate to product reaction. Conditions were optimised for the amperometric detection of para-aminophenol, the electroactive product of the alkaline phosphatase catalysed hydrolysis of a new substrate, p-aminophenylphosphate, after separation by HPLC.

The second approach involved the direct electrochemical detection of an immunoglobulin species, IgG, and the electrochemical monitoring of the immunological interaction. In an attempt to characterise the electrochemical response of such proteins, studies were carried out on the adsorptive stripping voltammetry of the immunoglobulin fragments, $F(ab')_2$ and Fab.

The globular proteins avidin and streptavidin, were then studied as these were similarly constructed proteins, except avidin had a disulphide bond, and streptavidin has not. The interaction of avidin and streptavidin with biotinylated IgG was also reported as this is an important labelling procedure in immunoassay.

CHAPTER 1

INTRODUCTION

1.1. Introduction

Electrochemistry is the oldest defined branch of physical science. Electricity itself was first reported by Thales (600 BC) who noticed that upon rubbing amber it attracted light substances[1].

> "Bright amber shines on his electric throne
> and adds etheral lustres to his own."

The initial studies of the effect of electricity on biological materials goes back to the first experiments of Luigi Galvani between 1786 and 1791, but it was with the development of polarography that bioelectrochemistry as a discipline began in earnest. Heyrovsky and Babicka[2] studied albumins by polarography and cited the work of Herles and Vancura[3] who applied polarographic methods to investigations of solutions containing blood and serum. At the same time, Brdicka was investigating the polarography of blood serum[4], and the electroreduction of proteins containing cystine[5]. Today, bioelectrochemistry is being applied to a wide variety of biological, medical and clinical problems. Areas of study such as electrochemical immunoassay (EIA) and biosensors combine the selectivity of biological recognition systems with the sensitivity of modern electroanalytical techniques. To get full value from these techniques, a fundamental understanding of protein electrochemistry is required and research is currently on-going in this area.

1.2. ELECTROCHEMICAL IMMUNOASSAY

Immunoassays exploit the molecular recognition properties of biological molecules such as immunoglobulins. The method exploits the very high specificity of an antibody for a given antigen. It was with the introduction of competitive radioimmunoassay (RIA) by Yalow and Berson[6] that the detection of very low concentrations of antigens (Ag) and antibodies (Ab) became practical. RIA has had a tremendous impact in the clinical and research laboratory which was reflected in the award of the Nobel prize to Yalow for the "development of radioimmunoassays of peptide hormones" in 1977. The theory of immunoassay has been outlined in section 2.4.1. RIA offers high sensitivity and specificity and has been the most popular immunoassay procedure to date. There are, however, disadvantages associated with the technique such as health hazards, disposal difficulties and short shelf life of the isotopic labels used e.g. I^{125}, I^{131} or H^3, that have prompted the search for alternative non-isotopic approaches.

Of the alternative labels explored, enzymes have become the most popular. These biological catalysts offer an amplification effect (as outlined in section 2.4.1.3.), and may be combined with a variety of detection systems depending on the substrate used. Most of the electrochemical immunoassay systems discussed below, both amperometric and potentiometric, exploit the enzyme both as an amplification mechanism and to generate an electroactive product. This product may be detected amperometrically at a glassy carbon electrode, such as

the product of the alkaline phosphatase catalysed reaction, i.e. para-aminophenyl phosphate (discussed in chapter 3). Alternatively a change in ion concentration can be detected using an ion selective electrode (ISE), such as the change in iodide ion concentration following the reaction of hydrogen peroxide with iodide as catalysed by horseradish peroxidase[7].

In the following section, electrochemical immunoassay (not to be confused with electroimmunoassay, a technique based on immunoprecipitation and electrophoresis described by Laurall[8]) will be classified under the means of detection employed. This will be divided first into amperometric or potentiometric based methods, and further subdivided by the type of electrode or technique used. It is inevitable that some overlap may occur, particularly in the area of biosensors. Whether an immunoelectrode should be discussed under the heading "electrochemical immunoassay" was decided on the basis of the direct use of an electrode in an immunoassay procedure. Otherwise it was classified as a "biosensor", and discussed in section 1.3.

1.2.1. Amperometric Detection in Electrochemical Immunoassay

1.2.1.1. Differential Pulse Methods

Differential pulse techniques were among the first reported voltammetric techniques applied to immunoassay with electrochemical detection. In the beginning, the approaches reported involved either modifying the analyte so that it

became electroactive, or 'tagging' it with an electroactive label. Strategies employed involved both homogeneous and heterogeneous immunoassays. In a heterogeneous immunoassay, after incubation of the antibody and antigen, the resulting complex is separated from the free antibody and antigen. In a homogeneous assay, no separation is necessary. This is discussed further in section 2.4. Homogeneous voltammetric assays function at least in part due to the difference in diffusion coefficients between the "free" labelled antigen and the labelled antigen "bound" to a much larger antibody molecule.

Heineman and co-workers used two different approaches to label the hormone, estriol, for use in a competitive homogeneous immunoassay. In the first approach,[9] differential pulse polarography (DPP) was used to detect estriol labelled with 4-mercuric acetate. The assay depended on the competition of labelled and unlabelled estriol for a specific estriol antibody. As the unlabelled estriol was electroinactive in the region -0.20 to -0.90 V (vs saturated calomel electrode (SCE)), it did not interfere with the signal from the labelled estriol which gave a distinct reduction peak at -0.30 V (vs SCE). The reduction wave for the labelled estriol occurred at a more negative potential than that for free labelled estriol, hence no separation step was necessary. In the second approach, estriol was labelled with nitro groups in the 2- and 4-positions, giving 2,4-dinitroestriol (DNE) which is electroactive and gives rise to two reduction waves at -0.422 V and at -0.481 mV (vs Ag/AgCl) respectively[10]. The peak current was found to be linear relative to concentration over

the range 60 ng/ml to 3.7 μg/ml. The antibody, the unlabelled estriol and the supporting buffer were all electroinactive in the region -0.20 to -1.00 V (vs Ag/AgCl). The assay was again based on competition of the labelled and unlabelled estriol for Ab binding sites. In this case the binding of the DNE and Ab could be monitored by a decrease in the reduction waves of DNE. It was suggested that this was due to a sequestering of the electroactive nitro-groups at the electrode surface by the antibody, or a decrease in the diffusion coefficient of DNE when bound to the larger antibody molecule. Hence the Ab-bound labelled analyte and free labelled analyte could be detected without interference from each other and no separation step was needed.

Lead was used as an electroactive label by Alam and Christian[11]. The analyte human serum albumin (HSA) was bound non-specifically to the ion:

$$HSA + Pb^{2+} \rightleftharpoons [HSA.Pb]^{2+}$$

and gave rise to a reduction peak at -0.68 V (vs SCE), whereas Pb(II) gives rise to a reduction peak at -0.58 V (vs SCE). After the immunochemical reaction of the labelled Ag with its Ab, raised in a goat (G-Ab):

$$G\text{-}Ab + [HSA.Pb]^{2+} \rightleftharpoons [G\text{-}Ab.HSA.Pb]^{2+}$$

the reduction peak at -0.68 V decreased in size, and the binding of the Ab and Ag could be detected by DPP without the need for a separation step.

This tagging approach was also used by Doyle et al. for HSA, where a heterogeneous assay was based on the determination of a releasable metal ion[12]. The analyte HSA was labelled with In(III) via the bifunctional chelating agent, diethylenetriamine pentaacetic acid (DTPA). The ion and the protein are very tightly bound by DTPA making a stable complex until the label is released through acidification. In(III) is not normally found in biological tissues and fluids, and exhibits a characteristic reversible electrochemical reduction peak at -0.59 V (vs Ag/AgCl) in complexing media, which makes it a suitable label for such an assay. Following a competitive heterogeneous equilibration, the In(III) label was released by acidification, separated from the assay mixture and detected by differential pulse anodic stripping voltammetry (DPASV) at the hanging mercury electrode without interference from the biological matrix.

1.2.1.2. Detection of an Electroactive Enzyme Product at the Carbon Electrode

Carbon electrodes, either in the form of carbon paste or glassy carbon, have been the most widely used detection systems in electrochemical immunoassay. In the literature, such detection systems have been used for those immunoassays that combine the amplification effect of an enzyme label with the low detection capabilities of an amperometric measurement, and have been applied to both competitive heterogenous immunoassays and homogeneous immunoassays. An enzyme label that generates an electroactive product which may be detected electrochemically

without interference from the substrate or other constituents of the assay matrix is chosen, and the immunoassay is performed as outlined in section 2.4.1. In many methods, a flow analysis procedure is used (involving either high performance liquid chromatography (HPLC) or flow injection analysis (FIA)) so that the site of the immunoreaction is spatially separated from the site of electrochemical detection.

The enzyme alkaline phosphatase is a well documented enzyme label system for immunoassay, and its substrate to product reaction may be monitored both by spectrophotometric or electrochemical techniques. Doyle et al.[13] labelled the analyte α_1-acid glycoprotein with this enzyme to catalyse the conversion of phenylphosphate to phenol by hydrolysis of the ester linkage. Phenol can be oxidised at +0.75 V (vs Ag/AgCl) and was detected (after separation from the assay mixture by HPLC) with a carbon paste electrode without interference from the substrate phenylphosphate which is electroinactive at these potentials.

The conversion of phenylphosphate to phenol by alkaline phosphatase was also used in an immunoassy procedure by Wehmeyer et al[14]. The analyte rabbit immunoglobulin G (IgG) was used as a model compound, and after the competitive "sandwich"-type immunoassay was carried out, the generated phenol was quantified at a carbon paste electode at +0.87 V (vs Ag/AgCl) after separation on a C_{18}-column, to remove the assay buffer and possible interferents. A detection limit of 10 ng/L was reported for this assay. In a subsequent paper[15] the group of Heineman applied such a detection system for the heart drug digoxin. Digoxin is a cardioactive drug used to

treat chronic heart disease, and has been used as a model analyte in the optimisation of a number of immunoassays, because of its clinical importance due to its widespread usage, low therapeutic levels and narrow therapeutic range. Two methods involving electrochemical detection, following HPLC and FIA procedures, i.e. LCEC and FIAEC were described, and the methods were compared to an established RIA method for analysis of the drug. The heterogeneous immunoassay protocol is illustrated in Figure 1.1. The detection limit for LCEC was reported to be $5x10^{-9}$ M and the linear range was over three orders of magnitude; the detection limit for FIAEC was $1.5x10^{-7}$ M. In FIAEC the faradaic current is superimposed on the capacitative current blank signal, as this procedure involves no separation of the phenol from the assay buffer. To minimise this capacitive current, the mobile phase used in FIAEC should be carefully matched with the sample matrix. The major advantage of FIAEC over LCEC was its relatively short analysis time; 25 seconds as opposed to 2.5 min with LCEC. The LCEC method was compared to RIA and a good correlation (correlation coefficient = 0.93) obtained.

Jenkins et al.[16] lowered the detection limits of a sandwich immunoassay for mouse IgG with detection of enzyme-generated phenol by FIAEC with a carbon paste electrode (at a fixed potential of +0.895 V (vs Ag/AgCl) by limiting non-specific adsorption of the enzyme conjugate. This was acheived by blocking possible sites for such adsorption with a combination of Tween 20 (a non-ionic detergent) and bovine serum albumin (BSA) as an additional blocker. In addition, the carbonate buffer system used previously[14,15] was replaced by a

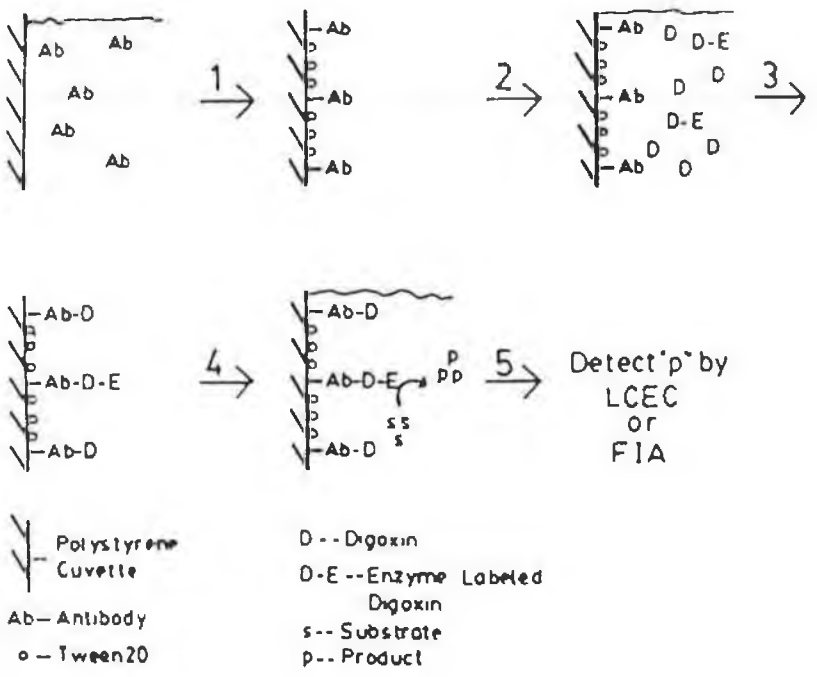

Figure 1.1 A heterogeneous enzyme immunoassay for the heart drug digoxin. (1) The walls of the polystyrene cuvette are coated with antibody (Ab) and tween, to block any non-specific adsorption, (2) the analyte (D) and enzyme-labelled analyte (D-E) are added, (3) the solution is aspirated from the cuvette and the cuvette is rinced, (4) the substrate is added, and (5) the electroactive producted is detected.

tris-based buffer, which was reported to permit a higher enzyme activity (i.e. substrate to product turnover). This method was tested on real samples using human serum controls, and despite this complex protein matrix, no increase in background current was observed. The detection limit of the assay was reduced from 100 to 7.5 pg (50 attomol).

Para-aminophenyl phosphate was then reported to be an improved substrate for electrochemical immunoassay by Tang et al[17]. This substrate is converted by alkaline phosphatase to para-aminophenol which may be detected by LCEC with a glassy carbon electrode. The product p-aminophenol exhibits electrochemically reversible behaviour at +0.10 V (vs Ag/AgCl), and is also easier to oxidise than phenol. Hence the interference from compounds such as ascorbic acid or other electroactive matrix constituents may be eliminated. Phenol has been reported to foul the electrode at high concentrations[17,18], whereas p-aminophenyl phosphate does not. The limit of detection for a heterogeneous immunoassay for digoxin using this new substrate was reported to be 30 pg/ml compared to 50 pg/ml with the substrate phenylphosphate. One major disadvantage of this substrate is that it is not available commercially.

A different approach, using a ferrocene-linked substrate for alkaline phosphatase, was developed by McNeil et al[18]. The substrate [N-ferrocenoyl]-4-aminophenyl phosphate was prepared by a modification of previously reported methods[19,20]. The immunoassay procedure was based on a commercial "ENDAB" immunoassay kit (CMD (UK) Ltd.) for the determination of unconjugated oestriol in serum, and modified so that the enzyme

product could be quantified by direct current cyclic voltammetry at a glassy carbon electrode. The oxidation of the ferrocene-based substrate to the ferricinium ion was monitored at +0.18 V (vs SCE). The substrate could also be monitored spectrophotometrically at 306 nm, and it was suggested that similar ferrocene-linked substrates could be developed for the enzyme β-galactosidase and peroxidase.

Rosen and Rishpon[21] developed an assay where the electrode itself was used as the solid phase. The antibody was immobilised onto the working electrode (glassy carbon or gold) based on the method of Laval and Bourdillon[22]. The glassy carbon electrode was activated electrochemically to form carboxylic groups on the surface, and the Ab was immobilised onto the gold electrode using an insoluble polymer. An assay was developed for the detection of dog IgG. Serum was immobilised on the surface of the gold electrode and the electrode was then incubated in a solution containing anti-dog IgG labelled with alkaline phosphatase. A bare electrode was used as a control to ensure the signal was not as a result of non-specific adsorption. Detection of phenol as the electroactive product of the enzymatic reaction was unfavourable because of electrode fouling, which was experienced by both the glassy carbon and gold electrodes. To solve the fouling problem, the electrode was held at a negative potential (-1.40 V vs SCE) to desorb the electrooxidation products. Application of these very negative potentials, however, was found to degrade the antibodies. The substrate used was p-aminophenyl phosphate,and the product p-aminophenol was detected by cyclic voltammety in tris buffer, pH 8.0.

Para-aminophenol gave rise to a peak at +0.05 V (vs SCE), whereas the substrate p-aminophenyl phosphate gave rise to a peak at +0.45 V (vs SCE). A dynamic electrochemical system of measurement was chosen as it was found to be more sensitive. The electrode was connected and disconnected repeatedly and the current was integrated 20 ms after the potential application, to minimise the contribution from the capacative current. The optimised immunosensor was then used in both a sandwich and a double sandwich method to detect human chorionic gonadotropin (hCG) in urine. The double sandwich method with p-aminophenyl phosphate as a substrate for alkaline phosphatase was reported to be the more sensitive of the two immunoassay procedures, but a limit of detection was not reported.

Preliminary studies of a novel carbon electrode, prepared by silk screening graphite paint onto cardboard was reported by Weetall and Hotaling[23]. The planar three electrode configuration, coated to prevent poisoning by protein adsorption, was tested for the detection and quantitation of H_2O_2 and NADH for use in a glucose oxidase enzyme immunoassay. This assay was combined with the method of Robinson et al.[24] which involved coupling the antibodies via magnetic particles to the solid phase to facilitate rapid, simple regeneration of the solid phase.

A homogeneous assay in a flowing system was devised by Weber and Purdy[25], to differentiate between the bound and unbound electroactive antigen, morphine. Advantage was taken of the slow dissociation rate of an Ab-Ag complex with a large equilibrium constant for binding. A fast electrochemical measurement (relative to the slow dissociation) would thus only

measure the free unbound antigen. To achieve this Weber, and Purdy used a flowing system so that the mean residence time for the Ab-Ag complex in the flow cell was short relative to the dissociation time. Morphine was chosen as a test analyte because it is electroactive and therefore no tagging of the analyte was necessary. In addition, morphine is a small molecule and represents a "worst case" situation, as the binding constant is decreased for smaller antigens. The assay solutions were pumped through an injector loop and then through the electrochemical cell which consisted of a laminar-flow cell with a glassy carbon working electrode, held at +0.50 V (vs SCE). The samples were introduced to the flow through the injector. The system could be used to detect the binding of the analyte to its Ab. Morphine was then labelled with ferrocene to yield ferrocenyl morphine (FCM) to demonstrate whether the Ab would have the same affinity for an electrochemically-labelled antigen. The second method was less sensitive, as the labelled molecule was found to be light sensitive. Codeine also binds to the morphine Ab, and addition of this second (though electroinactive) antigen increased the electrochemical signal, as it displaced morphine from the antibody. The technique described was found to be useful for monitoring the interaction of an electroactive Ag with its Ab, whereas for other non-electroactive antigens some sample pretreatment would be necessary to label the molecule. These workers also suggested the use of a dual electrode detection system to eliminate background noise.

1.2.1.3. Determination of Enzymatically Produced NADH

The enzyme, glucose-6-phosphate dehydrogenase (G6PD), converts the substrate glucose-6-phosphate (G6P) to glucono-γ-lactone 6-phosphate, and converts NAD^+ (nicotinamide adenine dinucleotide) to dihydronicotinamide adenine dinucleotide (NADH). This reaction (illustrated in Figure 1.2.), is well documented for use in enzyme labelled immunoassays, and the conversion of NAD^+ to NADH can be monitored spectrophotometrically at 340 nm. However, NADH can be electrochemically oxidised in the nicotinamide portion of the molecule according to:

$$NADH \longrightarrow NAD^+ + 2e^- + H^+$$

and may be monitored using amperometric detection at a solid electrode such as glassy carbon or platinum. The electrochemistry of the oxidation of NADH at the carbon electrode is well documented[26].

Eggers et al.[27] have developed an enzyme immunoassay for phenytoin using LCEC with detection at a glassy carbon electrode at +0.75 V (vs Ag/AgCl). The electrode was electrochemically pretreated prior to the detection of NADH by cycling between +1.5 and -1.50 V at a scan rate of 100 mV/s for 20 min, then applying a constant potential of +1.5 V for a further 2 min (repeated twice). The immunoassy procedure was based on a commercial "EMIT"[28] kit (Syva Co.). A standard curve for NADH exhibited a linear response (for peak current vs concentration) over the range 0.87 to 17.5 μmol/L.

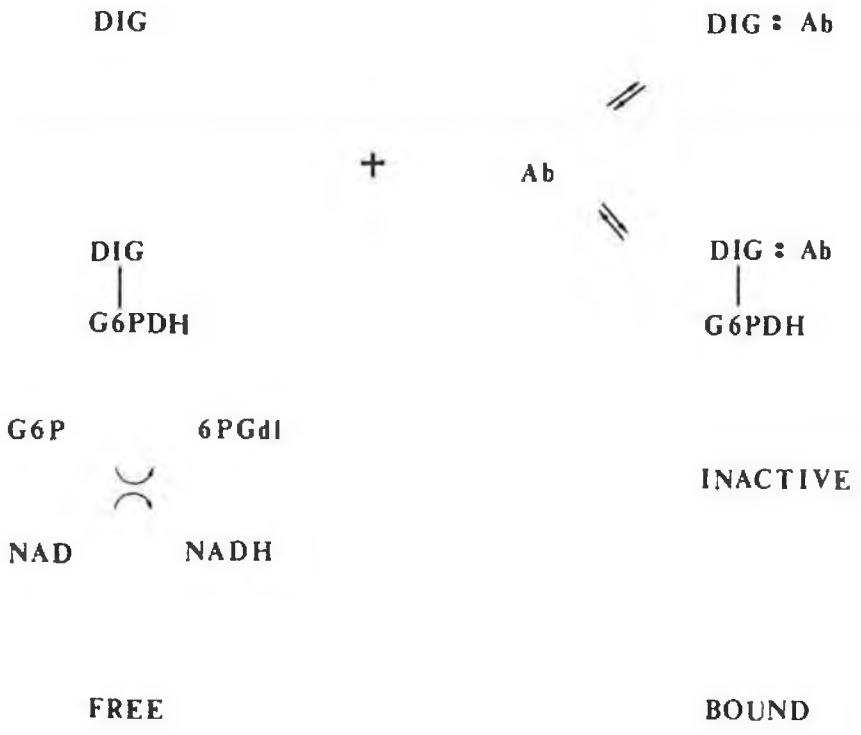

Figure 1.2. A competitive homogeneous immunoassay for the antigen, Digoxin (DIG), labelled with the enzyme glucose-6-phosphatase dehydrogenase, which catalyses the conversion of NAD^+ to NADH, which is detected amperometrically.

Concentrations above 10 μmol/L caused electrode fouling due to the adsorption of NAD^+ on the electrode surface[26]. HPLC was used to separate the proteins in the assay solution as the NADH current response decreased in the presence of protein due to its adsorption on the electrode surface. This amperometric immunoassay technique was compared with the standard "EMIT" spectrophotometric procedure. The correlation between the two methods was good (correlation coefficient = 0.99) and the electrochemical procedure compared favourably for the analysis of phenytoin in serum over a concentration range exceeding the therapeutic range of 10-20 mg/l.

Wright et al.[29] have applied a similar homogeneous immunoassay with amperometric detection of NADH to the analysis of digoxin. The immunoassay was based on an EMIT digoxin kit (Syva Co.). After the immunoassay procedure, the NADH was separated from the serum-based assay mixture using HPLC. A column switching technique[30] was used to separate the NADH chromatographic zone from both early and late eluting zones which contained electrochemical interferences. A precolumn was used to separate high molecular weight components (on the basis of size exclusion) and direct them to waste. The zone containing the NADH fraction was switched onto the analytical column and then the system switched back to route late eluting interferences such as uric acid to waste. This technique provided a convenient on-line sample clean-up which excluded any serum constituents, (which may have fouled the electrode) from the electrochemical cell. It also excluded other electroactive constituents such as uric acid, which gave an anodic peak at +0.43 V (vs Ag/AgCl) and could not be

discriminated against by means of the selected working potential. The NADH was detected with a carbon paste electrode at +0.75 V (vs Ag/AgCl). Using this assay regime, NADH could be detected in the range 6.2×10^{-8} M to 2.95×10^{-9} M. The technique was compared with a commercially available digoxin radioimmunoassay ("ARIA HT" digoxin system). There was good correlation between the methods (correlation coefficient = 0.942). The amperometric method had a major advantage over the spectrophotometric method, requiring an enzyme incubation time of 5 min (compared to 30 min with the spectrophotometric method), as the more sensitive electrochemical technique required less product. NADH has also been detected at the platinum electrode for use in immunoassay. Broyles and Rechnitz have described a homogeneous enzyme immunoassay, using the drug lidocaine as a model compound, based on the inhibition of the enzyme activity of the enzyme-antigen-conjugate by the lidocaine-specific antibody that was to be detected[31]. The activity of the enzyme (G6PD) was monitored through amperometric detection of NADH at the platinum electrode. The overall reaction for this assay is given below;

$$G6P + NAD^+ + Ab \xrightarrow{G6PD\text{-}Ag} 6\text{-phosphoglucono-}\delta\text{-lactone} + NADH + H^+ + Ab + G6PD\text{-}Ag{:}Ab \text{ (inactive)} + G6Pd\text{-}Ag \text{ (active)}.$$

The platinum electrode had previously been designed for the amperometric detection of H_2O_2, and consisted of a platinum anode, surrounded by a silver cathode (held at +0.70 V). A collagen membrane protected the electrode tip and also served to define the diffusion path to the tip. The enzyme-labelled

Ab-Ag complex gave rise to no signal at the electrode, nor did any of the reactants in the assay solution, ensuring a steady baseline. The electrode gave rise to a linear response to NADPH at millimolar concentrations. The assay was carried out in the presence of BSA to approximate the high protein content of serum samples, although the addition of BSA did not adversely affect the assay. Exposure of the electrode to high concentrations of the protein resulted in some adsorption of protein to the collagen membrane. The adsorbed protein could be removed by washing in tris buffer for 5 to 10 minutes. The total assay time (10 min) was not long enough for protein adsorption to restrict the diffusion of NADH through the membrane.

Electrochemical immunoassay has also been applied to the detection of creatine kinase isoenzyme MB (CK-MB), which if present in serum is a very important indication of acute myocardial infarction. A commercial test for the isoenzyme has been developed by Roche Diagnostics which combines an immunoinhibition test, in which the activity of the isoenzyme is monitored, and an immunoprecipitation test which subtracts out interfering activities. Normally, the assay is carried out spectrophotometrically through the determination of NADPH, the reduced form of nicotinamide adenine dincleotide phosphate, ($NADP^+$), in a coupled reaction. Kuan and Guilbault[32] and Yuan et al.[33] monitored this reaction amperometrically by coupling the ferricyanide-diaphorase reaction to monitor the NADPH produced.

The electron transfer reactions:

$$Fe(CN)_6^{3-} + NADPH \overset{diaphorase}{\rightleftharpoons} Fe(CN)_6^{4-} + NADP^+$$

and:

$$Fe(CN)_6^{4-} \rightleftharpoons Fe(CN)_6^{3-} + e^-$$

were studied at a platinum working electrode at a fixed potential of +0.36 V, and the solution was stirred at 800 rpm to increase sensitivity. Although the activator of creatine kinase, i.e. reduced glutathione, reacts with the electron acceptor ferricyanide, this interference was overcome by reducing the concentration of activator and preincubating the enzyme for about 2 min. This electrochemical method was compared with a standard clinical assay (involving electrophoresis) and the correlation using real serum samples was found to be excellent (correlation coefficient = 0.999).

The detection of H_2O_2 at the platinum electrode has been exploited for a number of other immunochemical methods. A platinum electrode protected with a cellulose acetate (CA) film has been designed for LCEC[34]. This inert film prevents the adsorption of protein, while at the same time facilitates selective transport of the electroactive species of interest to the electrode surface. The film is also reported to selectively eliminate some electroactive interferents, such as ascorbate, from the electrode surface making it a very attractive electrode for clinical analysis.

De Alwis and Wilson used such an electrode to monitor hydrogen

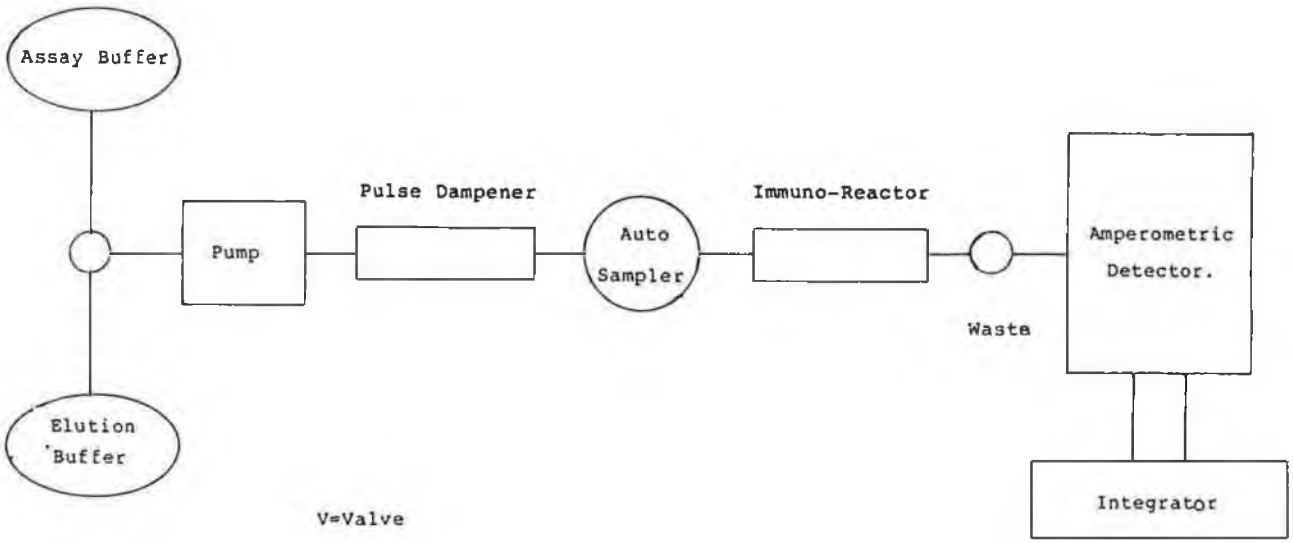

Figure 1.3. Schematic diagram of a FIA immunoassay apparatus[35].

peroxide, the electroactive product of a sandwich enzyme linked immunosorbent assay (ELISA) method[35]. Mouse anti-bovine IgG was used as a model analyte and the immunoassay system was coupled to an FIA system, as outlined in Figure 1.3. The assay reagents and samples were introduced via an automatic sampling valve and flowed through the immunoreactor at approximately 0.5 ml/min. Under these conditions the Ab-Ag reaction in the immunoreactor is extremely fast and long incubation times are not required. The final measurement step involved the determination of the activity of the enzyme label immobilised in the immunoreactor as a consequence of the assay sequence. The mobile phase containing the assay solution was diverted to waste until the solution containing the analyte was ready to enter the electrochemical detector. This method of protecting the electrochemical cell from possible damage by serum constituents was analagous to the column switching technique described above[29]. The enzyme label used was glucose oxidase, and the product, hydrogen peroxide, was detected amperometrically. The limit of detection for this assay was reported to be as low as 1 pmol in the presence of control serum and the assay time was 12 min. Suggested improvements for the system included pulse dampening of the HPLC pump to improve the limit of detection and the use of parellel immunoreactor columns combined with a column switching technique to increase sample throughput.

N-2,4-dinitrophenyl-6-aminocaproic acid (DNP-ACA) was used as a model analyte for a homogeneous amperometric immunoassay by Ngo et al.[36,37] An apoenzyme, apoglucose oxidase, was used as the enzyme label, and the product of the enzyme catalysed

reaction, i.e. H_2O_2, was monitored using a YSI-Clark type oxygen electrode in conjunction with an oxidase meter.

1.2.1.4. Determination of Enzymatically Produced Oxygen

Amperometric detection of oxygen, either generated[38] or consumed[39] during an enzyme-catalysed reaction has been applied to electrochemical immunoassay. The oxygen probe is often combined a membrane which may be used to bind antibodies, and thus the Ab-Ag interaction may be studied in close proximity to the electrode surface (Figure 1.4.). A technique has been developed by Boitieux et al.[38] for the analyte goat IgG. A sensor consisting of a protein-based membrane (pig skin gelatin) activated with thiol groups was fixed over an oxygen electrode. The goat IgG specific antibody was linked to this membrane with ribonuclease (RNase) and the assay solution was introduced to a continuous flow cell. The antigen was labelled with glucose oxidase and its activity in the presence of the substrate glucose was monitored through the measurement of oxygen consumed during the reaction. This sensor could be re-used over many months with no apparant loss in response. The disulphide bridges formed between the thiol groups of the membrane and the RNase labelled antigen were broken by incubation with 25 mM dithiothreitol for 15 min. A limit of detection was not reported for this preliminary study. Aizawa et al.[39] have described a similar strategy. In this case the antigen hCG was labelled with the enzyme catalase which

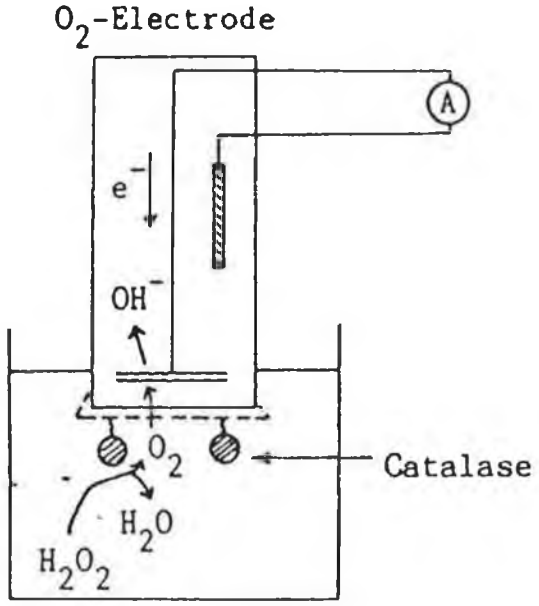

Figure 1.4. An enzyme immunosensor prepared by attaching an antibody bound membrane to a Clark type oxygen electrode.

catalyses the reaction:

$$H_2O_2 \longrightarrow H_2O + 1/2\ O_2$$

An antibody bound membrane specific for hCG was attached to the electrode surface and a competitive enzyme immunoassay was carried out between the hCG and the enzyme-labelled hCG. After the immunoassay procedure, the substrate H_2O_2 was added and the amount of immobilised enzyme (proportional to the amount of labelled Ag) was determined by determining the oxygen evolved, which was monitored through its reduction at the cathode:

$$O_2 + 2H_2O + 4e^- \longrightarrow 4OH^-$$

The response for this assay was linear in the range 2.8×10^{-7} g/ml to 1.4×10^{-5} g/ml. Aizawa et al. also developed a similar sensor for the analysis of both α-fetoprotein (AFP)[40], which had a linear dynamic range between 5×10^{-11} and 10^{-8} g/ml, and for ochratoxin A (OTA)[41], the assay for which was linear between 10^{-6} and 10^{-8} g/ml, with a minimum detection limit of the order of 10^{-10} g/ml.

1.2.2. Potentiometric Detection in Electrochemical Immunoassay

Potentiometric measurements, especially using ion-selective electrodes (ISE's) are of vital importance in the clinical laboratory[42]. The most widely used ISE is the pH electrode. The common laboratory pH electrode is usually made of glass, but pH measurements may also be made with other types of potentiometric probes, such as the quinhydrone electrode (based on a proton transfer redox reaction of the quinone/hydroquinone couple) or metal-metal oxide couples (e.g. palladium-palladium oxide). ISE's are included in most commercial clinical analyzers, such as the Technicon SMAC analyser, used for routine analysis in hospitals, and are rapidly replacing techniques like flame photometry for the analysis of such clinically important analytes as sodium, potassium, calcium and carbon dioxide etc. in biological samples. Their use has increased enormously with the rapid development in sensor technologies in the last 20 years[43,44].

ISE's have been used as the basis of many biosensors and lately have been applied to electrochemical immunoassay[45]. The strategies for potentiometric measurements in electrochemical immunoassay include the development of potentiometric immunosensors (or affinity probes) or coupling potentiometry with enzyme immunoassay resulting in a potentiometric enzyme immunoassay.

1.2.2.1. Potentiometric Antibody Electrodes in Immunoassay

An affinity probe is usually constructed with an ISE as the basic internal component, and either covalently linking the Ab or Ag directly onto the ISE surface, or binding it to a membrane or nitrocellulose chip. The immunochemical reaction that occurs at the probe's tip is converted to an electrical impulse. This type of probe may be used to selectively determine an analyte in a complex matrix or can be applied directly to an immunoassay.

A potentiometric ionophore modulation immunoassay (PIMIA) for the measurement of digoxin antibodies has been described by Keating and Rechnitz[46]. The probe was constructed by chemically coupling the antigen or hapten, corresponding to the Ab that was to be measured, to an ionophore, resulting in an antigen-carrier conjugate. This digoxin-carrier conjugate was immobilised in a poly(vinyl chloride) (PVC) membrane and placed on the potassium ion selective electrode tip (Figure 1.5.). The resulting probe was then exposed to a constant activity of the marker ion (K^+). The antibody to be measured was then added to the electrolyte. This, antibody then became bound to the antigen portion of the conjugate, and the resulting potential change was found to be proportional to the Ab concentration.

The probe was found to have excellent specificity in the presence of other non-specific Ab's and proteins, and could be used for 1 to 2 weeks before membrane replacement. This PIMIA technique was also successfully applied to a competitive immunoassay of the drug digoxin itself.

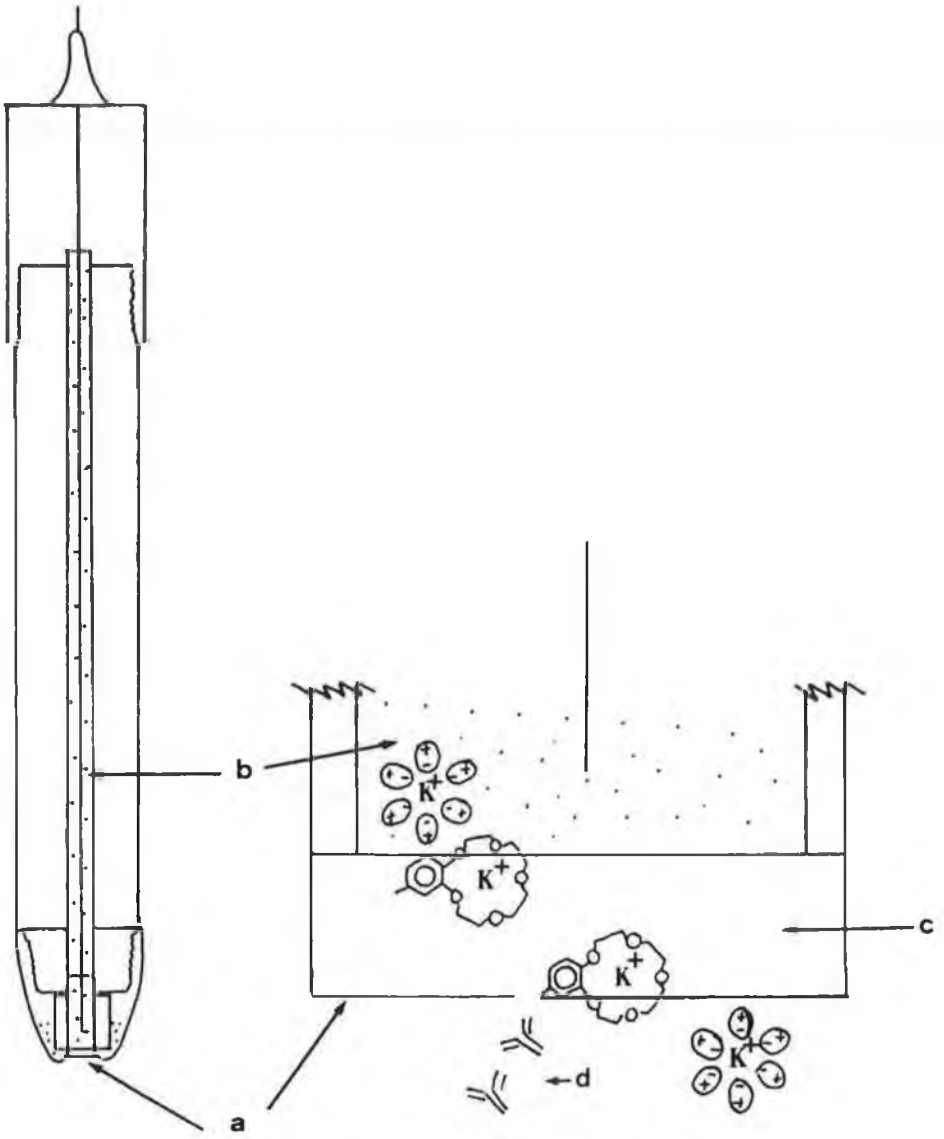

Figure 1.5. A digoxin antibody-sensing electrode: (a) PVC membrane containing digoxin carrier conjugate, (b) inner filling solution, (c) plasticizer, (d) digoxin antibodies.

1.2.2.2. Potentiometric Enzyme Immunoassay

One of the first potentiometric enzyme immunoassays was described by Boitieux et al.[47,48] It involved combining an enzyme-linked immunoassay sandwich technique for the determination of hepatitis B surface Ag with an iodide selective electrode. The specific antibodies were immobilised in a gelatine membrane which covered the tip of the ISE. The probe was then immersed in a stirred, dilute solution of the antigen in the presence of substrate (H_2O_2) and potassium iodide (I^-), and the enzyme activity (proportional to enzyme labelled Ag) measured. The enzyme, horseradish peroxidase (HRP), catalyses the reaction:

$$H_2O_2 + 2I^- + 2H^+ \xrightarrow{HRP} I_2 + 2H_2O$$

and the production of I_2 was monitored by the ISE. This reaction was first proposed by Nagy et al.[49] for the estimation of glucose in blood.

The limit of detection for this method was 6.5 mg/l and the linear range was been 0.5 and 50 mg/l. The assay compared well with a RIA technique. The technique was also applied to a low molecular weight molecule[50], 17 β-oestradiol , and the assay gave satisfactory results for the determination of the molecule in biological fluids at levels ranging from 57 pmol/l to 9.2 nmol/l.

Gas sensing probes, such as those used for the determination of carbon dioxide and ammonia, have been in use for almost thirty years. These potentiometric probes incorporate the

conventional ISE surrounded by an electrolyte solution and enclosed by a gas permeable membrane. The analyte gas diffuses through this membrane and comes to equilibrium with the internal electrolyte solution. The gas then undergoes a chemical reaction resulting in the consumption or formation of an ion which is detected by the ISE. The selectivity of such a sensor is dictated by type of the membrane used.

Broyles and Rechnitz[51] reviewed the use of carbon dioxide electrodes in potentiometric immunoassay (PIA). The CO_2 electrode has been applied to a typical competitive heterogeneous immunoassay for digoxin by Keating and Rechnitz[52]. Free digoxin and digoxin-BSA (bovine serum albumin) coated onto polystyrene beads compete for enzyme-labelled anti-digoxin antibodies in solution. The concentration of digoxin is inversely proportional to the amount of enzyme-labelled anti-digoxin bound to the beads. The beads are separated from the assay mixture by centrifugation and the carbon dioxide produced by the enzyme (HRP)/pyrogallol system is measured. The technique was reported to be sensitive in the ng range. A second assay, described by Fonong and Rechnitz[53], was a homogeneous immunoassay for the determination of human IgG. The enzyme used (chloroperoxidase) was conjugated to anti-human IgG, and the enzyme activity was subsequently inhibited by the binding of the Ag (human IgG). The enzymatic reaction in the assay solution containing β-ketoadipic acid, bromide and peroxide, produced CO_2 which was monitored by the electrode as an indicator of the decreased enzyme activity, and thus the Ab-Ag interaction.

Broyles and Rechnitz[51] have discussed the advantages and restrictions of CO_2 electrodes in PIA. The electrode functions best in acidic conditions, which restricts its use in immunoassay procedures, since the optimum pH for most immunochemical reactions for optimum enzyme activity normally lies close to the physiological pH, i.e. 7.4. Other disadvantages of such probes lie in their long recovery times and bulky size, prohibiting their use in assays requiring a small sample size or "in vivo" measurements. Before the CO_2 electrode is commonly used in immunoassay techniques, the basic design of the electrode needs to be adapted. Its redeeming features with regard to clinical samples are its selectivity, stability, and decreased contamination by proteins and serum constituents compared to the electrodes commonly used in voltammetry i.e. platinum or carbon.

The ammonia gas sensing electrode was first applied to EIA measurements by Meyerhoff and Rechnitz[54], using a urease enzyme label for the determination of BSA. Gebauer and Rechnitz [55] evaluated three deaminating enzyme labels for EIA, and the most promising, asparaginase, was used in an assay for dinitrophenol (DNP) (a model hapten) and for the clinically important steroid hormone, cortisol. As with the CO_2 electrode, the pH dependency of the NH_3 electrode was a limiting factor. The assay pH was a compromise between the optimum sensor pH and the optimum enzyme activity pH. This was determined by the construction of enzyme/sensor pH profiles. The measurement of the enzyme activity was evaluated to find the most suitable enzyme for potentiometric immunoassay. The limits of detection that were reported for the three enzymes,

asparaginase, urease and adenosine deaminase were 30, 35 and 160 fmol respectively (defined as the concentration of enzyme required to give a rate of 1 mV/min). The enzymes were also optimised with respect to the immunoassay procedure, and asparaginase was reported to be the most suitable for PIA.

Potentiometric immunoassays offer many advantages to the clinical chemist, in terms of selectivity and sensitivity combined with low cost, simplicity, ease of measurement and their suitability to automation.

1.2.3. Liposome-Mediated Immunoassay

Liposome-mediated immunoassay (LIA) is a relatively recently developed technique[56]. A liposome is a tiny artificial spherical assembly of concentric phospholipid bilayers. It may be filled (or loaded) with up to 10^4 marker molecules (i.e. an ion that can be detected potentiometrically, or an enzyme) and may be lysed using a complement. The classical complement pathway is an antigen-antibody specific reaction that occurs when an antigen-sensitised liposome immunospecifically binds with a corresponding antibody. In the presence of the complement, usually a serum protein, the marker is released and detected, and is an indication that the immunoreaction has taken place. LIA is simple to operate in practice and consists of three basic steps: the immunological reaction, the lysis, and the potentiometric detection of the released marker. A known amount of antibody specific for the sample antigen is mixed with that antigen, the liposome (which is sensitised on the outer surface with the same antigen) is then added, and the

free and liposome-labelled Ag's then compete for Ab binding sites. When the Ab-Ag reaction occurs at the surface of the liposome, the added complement is activated and liposome lysis occurs releasing the marker molecule, the concentration of which is proportional to the immune lysis response. This procedure has been further simplified by the use of cytolysin conjugates[57]. Cytolysins (e.g. bee venom melittin) are compounds that immediately lyse unsensitised liposomes and enable direct homogeneous non-competitive assays to be performed. Such a strategy would involve the conjugation of cytolysin to the Ag (to be measured). Then, on addition of the test sample, the antigen-cytolysin conjugate binds to the specific antibodies. Any unbound cytolysin conjugates remain free to immediately lyse the liposomes subsequently added. The immune reaction, however, quenches the cytotoxic effects of the conjugate and lysis does not take place. LIA combines a successful amplification technique with an instantaneous assay. One disadvantage, however, is the uncertainty of producing uniform batches of liposomes that do not leak, and hence give rise to background interference.

One of the earliest uses of liposome technologies for the monitoring of immunological reactions was the development of a immunoelectrode, where Ab levels in microliter amounts of serum were quantified using a thin-layer potentiometric measurement of the liposome marker, tetrapentylammonium ions (TPA^+), by Shiba et al.[58] LIA is not confined, however, to a potentiometric finish. Kannuck et al.[59] for instance, described a system of measuring liposome-released ferrocyanide with a dual function polymer modified electrode, and discussed

its potential use in homogeneous immunoassays. Amperometric oxygen sensing electrodes have been used to detect released liposome encapsulated glucose molecules in the presence of glucose oxidase[60]. Haga[61] has described a technique involving the entrapment of the enzyme HRP and monitoring the enzyme activity (which is directly proportional to the immune lysis and inversly proportional to the concentration of free Ag) by measuring oxygen consumption during the enzyme-catalysed oxidation of NADH. The liposome technique described was then applied to an assay for theophylline. This assay compared well with RIA with a sensitivity range of about 4×10^{-9} M for the liposome sensor and about 10^{-4} M for RIA. This, combined with other advantages such as fast measurment times and capabilities of measuring small samples, promise LIA a bright future.

1.3. Biosensors

1.3.1. Introduction

Biosensor technology is another area where rapid developments are currently taking place. This is a multi-disciplinarian field of activity with contributions from researchers in biochemistry, microelectronics, optics, electrochemistry etc. On reviewing the extensive literature, it may be seen that as yet, biosensors have many problems in their application. It is a science in its infancy and it has been suggested "that there tends to be too much hype at too early a stage"[62]. What is even more confusing is the wide variety of names for these sensors. Nagy and Pungor[63] in a review on bioelectroanalytical sensors, divide the field into two basic categories. Group 1 sensors are called "Biomatrix Chemical Sensors", which they define as "sensors specifically well capable of giving quantitative analytical information on biological matrices". Group 2 sensors are called "Biomimetric Sensors" which "exploit biological or biochemical phenomena for their selective operation."

In this work, a biosensor is considered as an analytical probe made up of a biochemical recognition phase and a sensor phase. The major processes involved are analyte recognition, signal transduction and readout of results. Sensors used for these purposes to date have included[64]: (i) electrochemical devices, both amperometric and potentiometric; (ii) optical sensors, based on fluorescence or fibre optics etc; (iii) semiconductor devices, such as the field effect transistor

(FET); and (iv) piezoelectric devices, such as surface acoustic wave (SAW) devices.

The molecular recognition phase can involve any selective biological reaction. The earliest electrode based biosensor was the enzyme electrode. Today, the recognition site could be based on anything from intact microrganisms to magnolia petals[65]. The biosensors of interest to this work are: enzyme electrodes, immunological electrodes and bio-affinity probes.

1.3.2. Enzyme Electrodes

Enzyme electrodes may be divided into two categories, amperometric or potentiometric. The enzyme is immobilised in some way onto the tip of the electrode which monitors changes occurring as a result of the enzymatic reaction. The immobilisation of the enzyme onto the electrode is a research area its own right[66] since the enzyme must not lose its catalytic activity if it is to be of use as a biosensor. Most enzyme electrodes make use of an ISE as the sensor, an important example being the penicillin electrode[67] which has been used to monitor the level of penicillin in fermentation broths. The enzyme, penicillinase, was immobilised onto a pH probe and the changes in concentration of hydrogen ion from the dissociation of penicilloic acid was monitored.

The most popular enzyme electrode is the glucose oxidase electrode. Bourdillon et al.[68], for instance, described such an electrode based on the covalent linkage of glucose oxidase onto a modified rotating glassy carbon electrode. Oxygen, one

of the substrates in the reaction, can be electrochemically regenerated according to the reaction:

$$O_2 + \text{glucose} \xrightarrow{GOD} \text{gluconic acid} + H_2O_2$$

$$H_2O_2 \xrightarrow{\text{electrochemically}} O_2 + 2e^- + 2H^+$$

Hence, the enzyme activity is controlled by the electrochemical regeneration of oxygen in the diffusion layer. The H_2O_2 produced could be oxidised at the electrode in the potential range +0.70 - +1.00 V (vs SCE) without adverse effects to the enzyme. De Alwis et al.[69] used an immunological reaction to reversibly immobilise glucose oxidase onto the support packing of a reactor. This reactor was coupled to an FIA system and offers a flowing system with an easily regenerated reactor for the determination of glucose. The enzyme immobilisation involved different reaction sequences. The enzyme was covalently attached to an antibody and was passed through a packed-bed reactor to which the antigen was already bound. A second method involved the immobilisation of a monoclonal anti-enzyme antibody which was used to immobilise the enzyme. The advantage of this second procedure was that it could be adapted to a system where more than one type of enzyme was immobilised.

To achieve electron transfer between some enzymes and the electrode, mediators had to be employed. These are usually small electroactive molecules that shuttle electrons efficiently between the electrode and enzyme. Many mediators used in biosensor technology today are based on ferrocene and

its derivatives. In the amperometric glucose oxidase electrode described by Cass et al.[70], a substituted ferrocene, ($Fecp_2R$), mediated the electron transfer between the enzyme and the graphite electrode. The ferricinium ion replaced oxygen as the enzyme cofactor and can be regenerated at the electrode:

$$\text{Glucose} + GOD_{(ox)} \longrightarrow \text{Gluconolactone} + GOD_{(red)}$$

$$GOD_{(red)} + 2Fecp_2R^+ \longrightarrow GOD_{(ox)} + 2Fecp_2R + 2H^+$$

$$2Fecp_2R \rightleftharpoons 2Fecp_2R^+ + 2e^-$$

Similar systems have been reported for D-galactose, glycolate and L-amino acids[71].

1.3.3. IMMUNOSENSORS

An antibody, being a protein, has in an aqueous environment a net charge associated with it, the polarity and magnitude of which depends on the isoelectric point of that protein and on the ionic composition of the solvent. The antigen, which in this case is also a protein, is also charged, and following interaction, the resulting complex has a net charge different to that of either of its precursors.

Janata[72] has exploited this to develop an immunoelectrode for yeast manaan using the lectin concanavilin A. Concanavilin A is not an antibody, but was used here as a test system, as it complexes certain polysaccharides in the same manner as true

antibodies. Concanavilin A was covalently attached to a PVC membrane deposited on a platinum wire. The surface charge of the polymer solution interface should be dependent on the net charge of the immobilised protein. The immunochemical reaction takes place at this interface and hence changes the surface charge. This system worked satisfactorilly and has also been applied to other antibody-antigen systems.

A major application of immunosensors has been the detection and quantification of the hormone, human chorionic gonadotropin (hCG). This hormone is an important diagnostic measure of pregnancy.

Yamamoto et al.[73] have described an immunoelectrode for hCG by exploiting the potential changes arising from the antibody-antigen interaction occuring on the immunologically reactive surface. A titanium wire was chemically activated with cyanogen bromide and then treated with a solution of hCG (or anti-hCG if an antigen electrode was being prepared). A similarly activated titanium wire, coated with urea instead of hCG, was used as a reference electrode. The electrode potential of the antibody electrode changed as soon as the antiserum was added, due to charge transfer and the orientational changes of dipoles in both of the reactants caused by hydrogen bonding or electrostatic interactions. This electrode could be regenerated by treatment with acid and reacting with a fresh hCG solution.

In a subsequent paper[74], the electrode was used to detect the levels of hCG in urine. All the samples tested, even those from men and non-pregnant normal women, gave rise to some shift in potential. However, when the sample solution was replaced

by buffer, the potentials returned to their normal value except in the case of urine from pregnant women. The non-specific response, due to adsorption of some components of urine, would suggest that some modification of the surplus active site deactivation step and the use of a very high purity antibody would be required for a more sensitive and reliable electrode.

Antibody-selective membrane electrodes, selective for the hapten dinitrophenol and for bovine serum albumin were described by Solsky and Rechnitz[75]. The antibodies were coupled to an ion carrier, dibenzo-18-crown-6[76], and immobilised onto a suitable membrane. The observed potentiometric effects were directly due to the interaction of the antibody in the sample solution to the antibody conjugated to the ion carrier.

Field effect transistors have played an important role in biosensor work. For instance, Collins and Janata[77] have investigated the use of a Wasserman membrane[78] on a chemically sensitive field effect transistor (CHEMFET)[79] as an immunosensor. The CHEMFET "senses" changes in charge and permits direct measurements of polarised or non-polarised membrane/solution interfaces. It was suggested that the ionic nature of proteins may be observed potentiometrically by one of two paths: the adsorbed charge may be detected directly by means of the polarised membrane surface, or the effect of adsorption might be coupled to the membrane mixed potential via membrane ion exchange currents. The experimental evidence provided by this work pointed to the latter, and showed that the primary response was non-specific due to interfering buffer ions.

Direct detection of an immunochemical reaction, and a study of the interaction kinetics was reported by Bataillard et al.[80]

using capacitance measurements on α-fetoprotein and IgE antigens. A silicon/silicon dioxide/immobilised Ab/electrolyte hetero-structure was immersed in a solution containing the antigen. The binding of the antigen to the surface immobilised antibody induced a change in the capacitance, and the resulting potential change led to a shift in the capacitance/voltage curve. The increase in thickness of the dielectric layer caused a decrease in the capacitance which may be related directly to the size of the molecule. These probes were found to have a working lifetime of greater than 18 months, are simple to use and easily regenerated.

1.3.4. Bioaffinity Probes

The "bioaffinity probe" is probably the most recent development in biosensor technology. Ikariyama has described a "unique biosensing method" using a molecular complex receptor of low affinity combined with an enzyme amplification technique[81]. Avidin forms a very stable complex with biotin (vitamin H). It also, however, binds similar compounds, such as 2-[(4-hydroxyphenyl)azo]benzoic acid (HABA) and lipoic acid to form meta-stable complexes. When such a complex is exposed to biotin, it dissociates to form the more stable avidin-biotin complex. The dissociation of the metastable complex receptor and the resulting formation of a stable complex depends on the determinant, i.e. biotin, concentration. Catalase was used as the enzyme amplifier and a Clark-type oxygen probe was used as the sensor. Measurements in the 10^{-7} - 10^{-9} mg/l range were found to be possible. This scheme is illustrated in Figure 1.6.

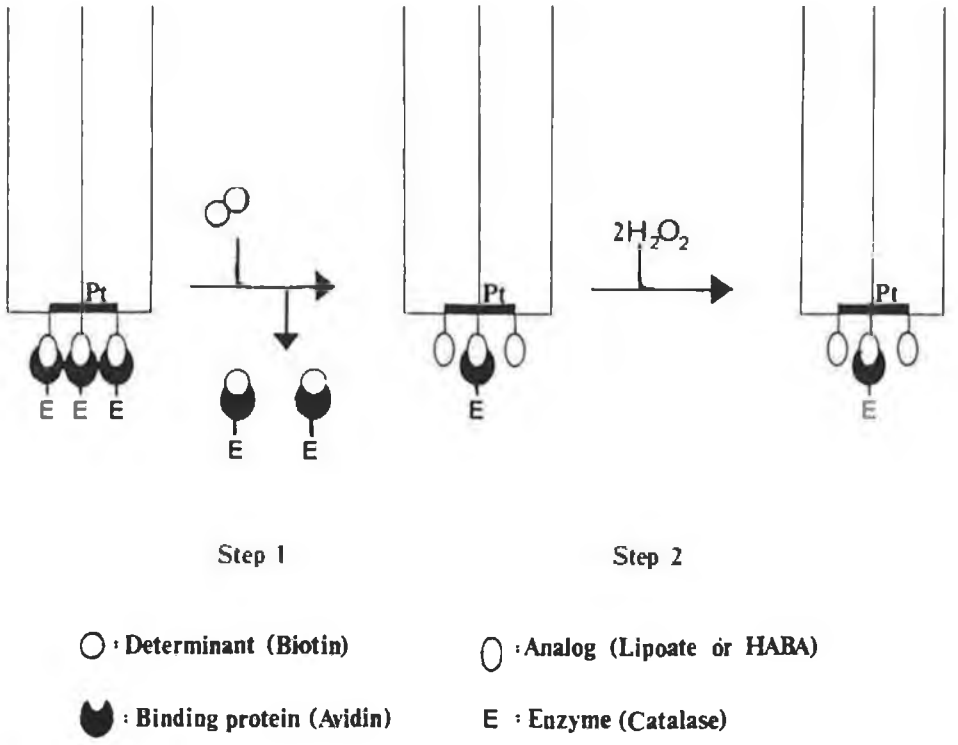

Figure 1.6. Schematic representation of a bioaffinity sensor. A molecular complex of low affinity is employed as a receptor. The first step is the biosensing of biotin, the remaining molecular complex is sensitively detected by enzyme amplification.

1.4. REFERENCES

1. Darwin,C., "Economy of Nature", (London, 1887).
2. Heyrovsky,J. and Babicka,J., Coll. Czech. Commun., 2(1930)370.
3. Herles,F. and Vancura,A., Rozpr. II. tr Ces. akad. (1932)42, Bull. Intern. de l'Acad. des Sc. de Boheme (1932).
4. Brdicka,R., Coll. Czech. Commun., 5(1933)112.
5. Brdicka,R., Coll. Czech. Commun., 8(1936)366.
6. Yalow,R.S. and Berson,S.A., J. Clin. Invest., 39(1960)1157.
7. Boitieux,J.L., Desmet,G. and Thomas,D., Clin. Chim. Acta., 88(1978)329.
8. Laurell,C-B., Scand. J. Clin. Lab. Invest., 29(1972)21.
9. Heineman,W.R., Anderson,C.W. and Halsall, H.B., Science., 204(1979)865.
10. Wehmeyer,K.R., Doyle,M.J., Halsall,H.B. and Heineman,W.R., Methods. Enzymol., 92(1983)433.
11. Alam,I.A. and Christian,G.D., Anal. Lett., (1982)1449.
12. Doyle,M.J., Halsall,H.B. and Heineman,W.R., Anal. Chem., 54(1982)2318.
13. Doyle,M.J., Halsall,H.B. and Heineman,W.R., Anal. Chem., 56(1984)2355.
14. Wehmeyer,K.R., Halsall,H.B. and Heineman,W.R., Clin. Chem. 31(1985)1546.
15. Wehmeyer,K.R., Halsall,H.B., Heineman,W.R., Volle,C.P. and Chen,I., Anal. Chem. 58(1986)135.

16. Jenkins,S.H., Heineman,W.R. and Halsall,H.B., Anal. Biochem., 168(1988)292.

17. Tang,H.T., Lunte,C.E., Halsall,H.B. and Heineman,W.R., Anal. Chim. Acta., 214(1988)187.

18. McNeil,C.J., Higgins,J.J. and Bannister,J.V., Biosensors 3(1987/88)199.

19. Walker,P.J. and King,E.J., Biochem. J. 47(1950)93.

20. King,E.J. and Nicholson,T.F. Biochem. J. 33(1959)1182.

21. Rosen,I. and Rishpon,J., J. Electroanal. Chem., 258(1989)27.

22. Laval,J.M. and Bourdillon,C.B., J. Electroanal. Chem., 152(1983)125.

23. Weetal,H.H. and Hotaling,T., Biosensors 3(1987/88)57.

24. Robinson,G.A., Hill,H.A.O., Philo,R.D.,Gear,J.M., Rattle,S.J. and Forest,G.C., Clin. Chem. 31(1985)1449.

25. Weber,S.G. and Purdy,W.C., Anal. Lett. 12(1979)1.

26. Moiroux,J. and Elving,P.J., Anal. Chem., 50(1978)1056.

27. Eggers,H.M., Halsall,H.B. and Heineman,W.R., Clin. Chem., 28(1982)1848.

28. Van Weeman,B.K. and Shuvrs,A.H.W.M., Febs. Lett. 15(1971)232.

29. Wright,D.S., Halsall,H.B. and Heineman,W.R., in "Electrochemical Immunosensors in Immunological Analysis" ed. Ngo,T.T., (Plenum Press, New York, 1987).

30. Erni,F., Keller,H.P., Morin,C. and Schmitt,M., J. Chromatogr., 204(1981)65.

31. Broyles,C.A. and Rechnitz,G.A., Anal. Chem., 58(1986)1241.

32. Kuan,S.S. and Guilbault,G.G., in "Electrochemical Immunosensors in Immunological Analysis" ed. Ngo,T.T.,(Plenum Press, New York, 1987).

33. Yuan,C-L.,Kuan,S.S. and Guilbault,G.G., Anal. Cham., 53(1981)190.

34. Sittampalam,G. and Wilson,G.S., Anal. Chem., 55(1983)1608.

35. de Alwis,W.U-. and Wilson,G.S., in "Electrochemical Immunosensors in Immunological Analysis" ed. Ngo,T.T.,(Plenum Press, New York, 1987).

36. Ngo,T.T., Bovaird,J.H. and Lenhoff,H.M., Appl. Biochem. Biotechnol., 11(1985)63.

37. Ngo,T.T., in "Electrochemical Immunosensors in Immunological Analysis" ed. Ngo,T.T.,(Plenum Press, New York, 1987).

38. Boitieux,J.L., Groshemy,R., Thomas,D. and Ergan,F., Anal. Chim. Acta., 197(1987)299.

39. Aizawa,M., Morioko,A., Suzuki,S. and Nagamura,Y., Anal. Biochem., 94(1970)22.

40. Aizawa,M., Morioko,A. and Suzuki,S., Anal. Chim. Acta.,115(1980)61.

41. Aizawa,M., in "Electrochemical Immunosensors in Immunological Analysis" ed. Ngo,T.T.,(Plenum Press, New York, 1987).

42. Solsky, R.L., Anal. Chem., 60(1988)109R.

43. Moody,G.J. and Thomas,J.D.R., Ion-Sel. Elec. Rev., 6(1984)209.

44. Oesch,U., Ammann,D.D. and Simon,W., Clin. Chem., 32(1986)1448.

45. Monroe,D., Immunoassay. Technol., 2(1986)57.

46. Keating,M.Y. and Rechnitz,G.A., Anal. Chem., 56(1984)801.

47. Boitieux,J.L., Desmet,G. and Thomas,D., Clin. Chem., 25(1979)318.

48. Boitieux,J.L., Desmet,G. and Thomas,D., Clin. Chim. Acta., 88(1978)329.

49. Nagy,G., Von Storp,L.H. and Guilbault,G.C., Anal. Chim. Acta., 66(1973)443.

50. Boitieux,J.L., Lemay,C., Desmet,G. and Thomas,D., Clin. Chim. Acta., 113(1981)175.

51. Broyles,C.A. and Rechnitz,G.A., in "Electrochemical Immunosensors in Immunological Analysis" ed. Ngo,T.T., (Plenum Press, New York, 1987).

52. Keating,M.Y. and Rechnitz,G.A., Anal. Lett., 18(1985)1.

53. Fonong,J. and Rechnitz,G.A., Anal. Chem., 56(1984)2586.

54. Meyerhoff,M.E. and Rechnitz,G.A., Anal. Biochem., 95(1979)483.

55. Gebauer,C.R. and Rechnitz,G.A., Anal. Biochem., 124(1982)338.

56. Gregoriadis,G., Trends. Biotechnol., 3(1985)235.

57. Freytag,J.W. and Litchfield,W.J., J. of Immuno. Meth., 70(1984)139.

58. Shiba,K., Watanabe,T., Umezawa,Y., Fujiwara,S. and Momoi,H., Chem. Lett., 2(1980)155.

59. Kannuck,R.M., Bellama,J.M. and Durst,R.A., Anal. Chem., 60(1988)142.

60. Umezawa,Y., Sofue,S.and Takamoto,Y., Anal. Lett.,15(1982)135.

61. Haga,M., in "Electrochemical Immunosensors in Immunological Analysis" ed. Ngo,T.T.,(Plenum Press, New York, 1987).

62. Czban.J.D., Anal. Chem., 57(1985)345A.

63. Nagy,G. and Pungor,E., Bioelectrochem. Bioenerg., 20(1988)1.

64. Thompson,M. and Krull,J.J., in "Electrochemistry, Sensors and Analysis" eds. Smyth,M.R. and Vos,J.G., (Elsevier, Amsterdam, 1986).

65. Uchiyama,S. and Rechnitz,G.A., J. Electroanal. Chem., 222(1987)343.

66. Bowers,L.D., Anal. Chem., 58(1986)513A.

67. Frew,J.E. and Hill,H.A.O., Anal. Chem., 59(1987)933A.

68. Bourdillon,C., Bourgeois,J.P. and Thomas,D., J. Am. Chem.Soc., 102(1980)4231.

69. de Alwis,W.U., Hill,B.S., Meiklejohn,B.I. and Wilson G.S., Anal. Chem., 59(1987)2688.

70. Cass,A.E.G., Davis,G., Francis,G.D., Hill,H.A.O., Aston,W.J., Higgins,J.J., Plotkin, E.V., Scott,L.D.L. and Turner,A.P.F., Anal. Chem., 56(1984)667.

71. Gough,D.A., Lucisano,J.Y. and Tse,P.H.S., Anal. Chem., 57(1985)2351.

72. Janata,J., J. Am. Chem. Soc., 97(1975)2914.

73. Yamamoto,N., Nagasawa,Y., Sawi,M., Sudo,T. and Tsubomura,H., J. Immunol. Methods. 22(1978)309.

74. Yamamoto,N., Nagasawa,Y., Shuto,S., Tsubomura,H., Sawi,M. and okumura,H., Clin. Chem., 26(1980)1569.

75. Solsky,R.L. and Rechnitz,G.A., Science. 204(1979)1309.

76. Peterson,C.J., J. Am. Chem. Soc. 89(1967)7017.

77 Collins,S. and Janata,J., Anal. Chim. Acta., 136(1982)93.

78. Aizawa,M., Kato,S. and Suzuki,S., J. Membr. Sci. 2(1977)25.

79. Janata,J. and Huber,R.J., in "Ion Selective Electrodes in Analytical Chemistry. Vol.2" ed. Freiser,H., (Plenum Press, New York, 1980)

80. Bataillard,P., Gardies,F., Jaffrezic-Renault,N., Martelet,C., Colic,B. and Mandrand,B., Anal. Chem., 60(1988)2374.

81. Ikariyama,Y., Furuki,M.and Aizawa,M., Anal. Chem., 57(1985)496.

CHAPTER 2

THEORY

2.1. VOLTAMMETRIC METHODS

2.1.1. Introduction

Voltammetry is the name given to a group of electroanalytical techniques where the current is measured as a function of potential applied to a working electrode with respect to a reference electrode. A third electrode, the auxiliary or counter electrode, is used to complete the circuit. The current of analytical interest is called the faradaic current which arises from a heterogeneous electron transfer between the electrode and a redox species, resulting in the oxidation or reduction of that species.

Jaroslav Heyrovsky developed the first voltammetric technique, i.e. polarography, in the early 1920s[1], for which he was subsequently awarded the Nobel prize in chemistry in 1959. A reproducible current-voltage curve called a polarogram was produced using a dropping mercury electrode (DME) as the working electrode, and the term "polarography" today is confined to those voltammetric techniques utilising this particular electrode. In the direct current (DC) polarographic technique developed by Heyrovsky, a constant potential ramp was applied to the DME, resulting in current potential curves such as those shown in Figure 2.1.

In the early 1970s, voltammetry enjoyed a general revival as an important analytical technique after almost two decades when it had been largly superceded by spectroscopic and chromatographic techniques. During this time, however, many significant advances had been made in the development of the technique,

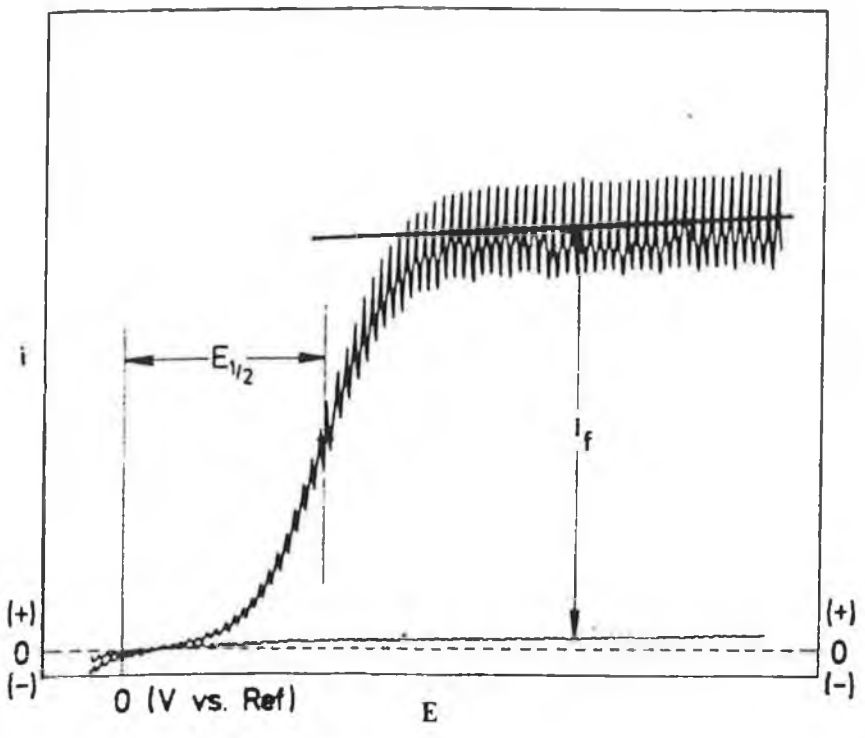

Figure 2.1. A typical DC polarogram. $E_{1/2}$ is the half wave potential and i_f is the current due to a faradaic process.

such as the advent of pulse methods[2,3] which served to greatly increase the sensitivity of the technique.

Today, voltammetry is recognised as a "powerful analytical tool that offers sub part per million sensitivity with low cost instrumentation"[4].

The following sections shall deal with the theory of electrolysis, some fundamental concepts of voltammetry and a description of the techniques used in this work.

2.1.2. Basic Features of the Electrochemical Process

2.1.2.1. Mass Transfer

Mass transfer of the electroactive species of interest to the electrode surface plays a major role in electrochemical dynamics. There are three modes of mass transfer: (i) diffusion, a spontaneous process where the species of interest moves under the influence of a concentration gradient; (ii) migration, where movement is effected under the influence of an electrostatic potential gradient; and (iii) convection, where movement is influenced by stirring or temperature gradients in solution[5]. These modes may be mathematically described (in one dimension along the x-axis, where x is the distance from the electrode surface) by the Nernst-Planck equation:

$$J(x,t) = -D(\partial C(x,t)/\partial x) - zF/RT\ DC(x,t)$$
$$(\partial \phi(x,t)/\partial x) + C(x,t)\ v_x(x,t) \qquad 2.1$$

where J is the flux, or mass transport (mol cm^{-2} s^{-1}), D is the diffusion coefficient (cm^2s^{-1}), C is the concentration (mol dm^{-3}), ϕ is the electrostatic potential, v_x is the hydrodynamic velocity and z is the ionic charge[7]. The flux is proportional to the slope of the concentration gradient, the electrostatic potential profile and the hydrodynamic velocity profile. These three modes of mass transfer all contribute to the instantaneous current, which is given by:

$$i(t) = nFAD\ (\partial C(x,t)/\partial x|_{x=0}) \qquad 2.2$$

where n is the number of electrons involved in the electrode process, and A is the electrode area. For equation 2.2 to be valid, the mass transfer contributions from migration and convection must be eliminated. The effect of migrational mass transfer is effectively eliminated by the addition of an excess of supporting electrolyte ions which then carry practically the entire charge within the solution. Convectional mass transfer is avoided by keeping the solution quiescent. The flux is then entirely diffusion dependent. Convection, however, is desirable in some techniques, such as stripping voltammetry, which is discussed in section 2.1.5.

2.1.2.2. The Electrode Process

The overall rate of a heterogeneous electrochemical reaction is determined by the transfer of the electroactive species to the electrode (as outlined above) and the charge transfer at the electrode/electrolyte interface[7]. If one considers a typical

redox process, such as:

$$O + ne \rightleftharpoons R$$

the conversion of O to R involves the following steps:

(i) diffusion of O from the bulk solution to the electrode surface;

(ii) electron transfer at, or close to, the electrode surface to form R; and

(iii) diffusion of R from the electrode surface back into the bulk solution.

In addition to the above steps, many homogeneous chemical reactions, such as the rearrangment of species or their interaction with some other solution components, may precede or follow the heterogeneous electrode process. Other heterogeneous processes, such as adsorption or desorption of products or reactants, also contribute to the overall reaction.

2.1.2.3. Faradaic and Capacitance Currents

The total current resulting from an electrochemical process is a combination of currents resulting from both faradaic and non-faradaic processes[8].

$$i_t = i_f + i_{nf} \qquad 2.3$$

where i_t is the total current obtained, i_f is the faradaic current and i_{nf} is the sum of contributions to the current from non-faradaic processes. The faradaic current results from the oxidation or reduction of the electroactive species of interest. The magnitude of this current is determined by the technique used, mass transfer, the area of the electrode, the applied potential and whether the electrolysis is limited by diffusion, electron transfer, chemical kinetics or adsorption. The main non-faradaic current is the capacitive (or charging) current (i_c) which is due to the recharging of the double layer following some disturbance such as potential change, or, as in the case of a DME, a change in the electrode area. For a DME this may be described mathematically by the equation:

$$i_c = 0.0057\ C_{dl}(E_{max}-E)m^{2/3}t^{-1/3} \qquad 2.4$$

where C_{dl} is the capacitance of the double layer ($\mu F\ cm^{-2}$), E_{max} is the electrocapillary maximum, m is the mercury flow (mgs^{-1}) and t is the drop time (s). The charging of the double layer is analogous to the charging of a capacitor, to which the double layer is often compared. A typical polarogram is shown in Figure 2.1. to illustrate the nature of these currents. In voltammetric studies it is only the faradaic current that is of analytical interest.

2.1.2.4. <u>The Double Layer</u>

The area of the electrode/electrolyte interface is broadly defined as the "electrical double layer". It is a region of

very high potential gradient (typically 10^6 V/cm), and within which electron transfer takes place. Although research is continuing into the structural and kinetic details of this phenomenon, there are widely accepted models of the structure of the double layer such as that illustrated in Figure 2.2., which considers a positively polarised metal electrode (e.g. mercury) and an aqueous electrolyte such as sodium fluoride[9]. The case of a simple model neglecting specific adsorption is shown in Figure 2.2a. At the electrode surface there is a layer of solvent molecules orientated with respect to their dipole moments. Next to this, aligned along the plane of closest approach (distance x_2 from the electrode) are a layer of solvated F^- ions, through the centre of which runs the Helmholtz plane. It is at the distance of closest approach that the charge transfer reactions are proposed to occur. On the solution side of the Helmholtz plane there is an inhomogeneous distribution of anions and cations called the diffuse layer made up of an inhomogeneous distribution of anions and cations. The double layer thickness is negligible by comparison to the thickness of the diffusion layer (δ), and may be safely ignored when considering most mass transfer applications. It is, however, very important in situations involving adsorption or when using non-aqueous media.

2.1.2.4.1. Adsorption Phenomena

Where there is specific adsorption of one or both ions of the electrolyte, the model proposed most frequently is based upon the hypothesis that ions which have sufficiently strong

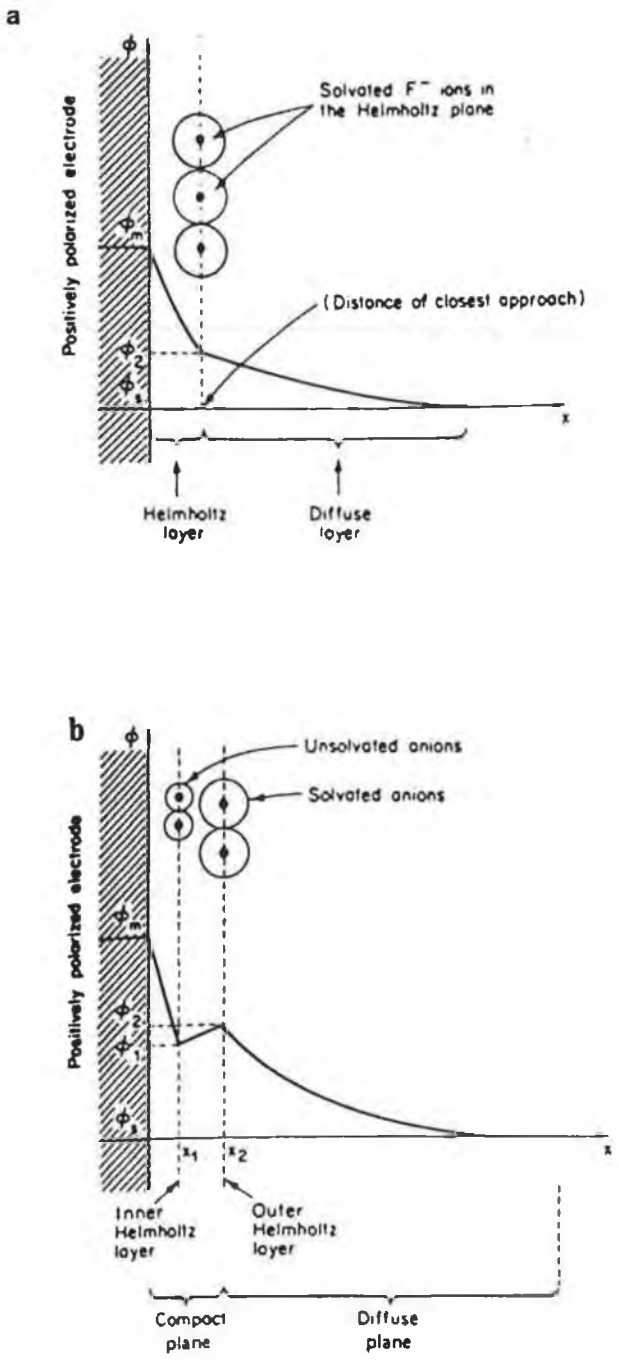

Figure 2.2. schematic representation of the double layer and change of potential with distance from the electrode. (a) in the absence of specific adsorption, (b) in the case of specific adsorption of the anion.

interaction with the electrode surface can approach this surface to within a distance x_1, illustrated in Figure 2.2.b, and the solvation shell disappears or is deformed. This plane is now known as the inner Helmholtz plane (IHP). The ions not specifically adsorbed (which retain normal solvation shells), approach the outer Helmholtz plane (OHP) or Gouy plane. This region, bounded by the OHP is the compact, rigid "Stern" layer. The diffuse layer behaves as an "ionic atmosphere" in which the potential drops to ϕ_s, its value in the bulk solution.

Neutral molecules may also be adsorbed, particularly if they have a dipole moment. The surface concentration of the adsorbed species is denoted by Γ(moles cm^{-2}) and, since not all of the solvent molecules are usually displaced, $\Gamma$is less than the maximum value theoretically possible, Γ_m. The Lanqmuir isotherm is frequently used to describe the relationship between $\Gamma$and Γ_m;

$$\Gamma = \Gamma_m \, C_o/(C_o + a) \qquad 2.5$$

when C_o is the concentration of dissolved substance and a is a constant characteristic of this compound. Γ_m is also dependent on the electrode potential.

For a mercury electrode, the interfacial tension, ρ, which is dependent upon adsorption, is easily measured. The interfacial tension varies considerably with the electrode potential and may be illustrated by an electrocapillary curve, which is parabolic in shape. In the presence of an adsorbate, the parabolic curve flattens out.

The presence of adsorbed molecules at the electrode surface also affects the charge density. If the adsorption equilibrium is reached, this charge is related the variation of interfacial tension by the Lippmann equation:

$$\rho = -\partial\gamma/\partial E \qquad 2.6$$

Reorientation of adsorbed molecules has also been detected using such measurements[10].

2.1.3. Electroanalytical Techniques

2.1.3.1. Cyclic Voltammetry

Cyclic voltammetry is one of the most extensively used techniques for obtaining qualitative information about electrochemical reactions. The technique was developed by Matheson and Nichols[11] In the late 1950's. It is an important tool for the rapid determination of formal potentials, detection of chemical reactions preceeding or following electron transfer, and studying electron transfer kinetics.

The technique involves cycling the potential of the working electrode with respect to a reference electrode (such as Ag/AgCl). The working electrode potential is scanned linearly between an initial potential, E_i, and a switching potential, E_λ, in a quiescent solution and measuring the resulting current. The waveform applied to the working electrode is shown in Figure 2.3., and a typical response of a reversible redox couple during a single cycle is shown in Figure 2.4.

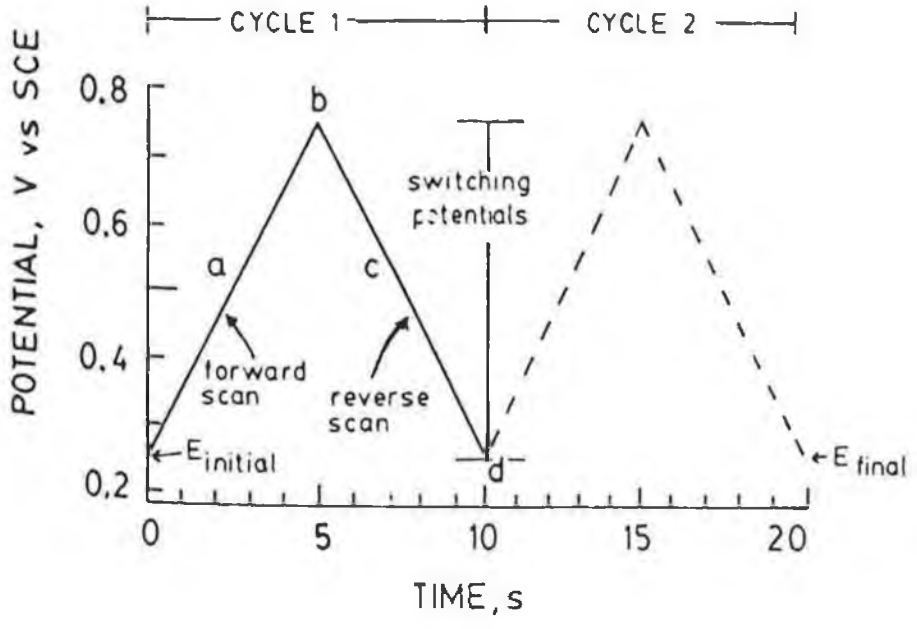

Figure 2.3. A typical potential-time excitation signal for cyclic voltammetry

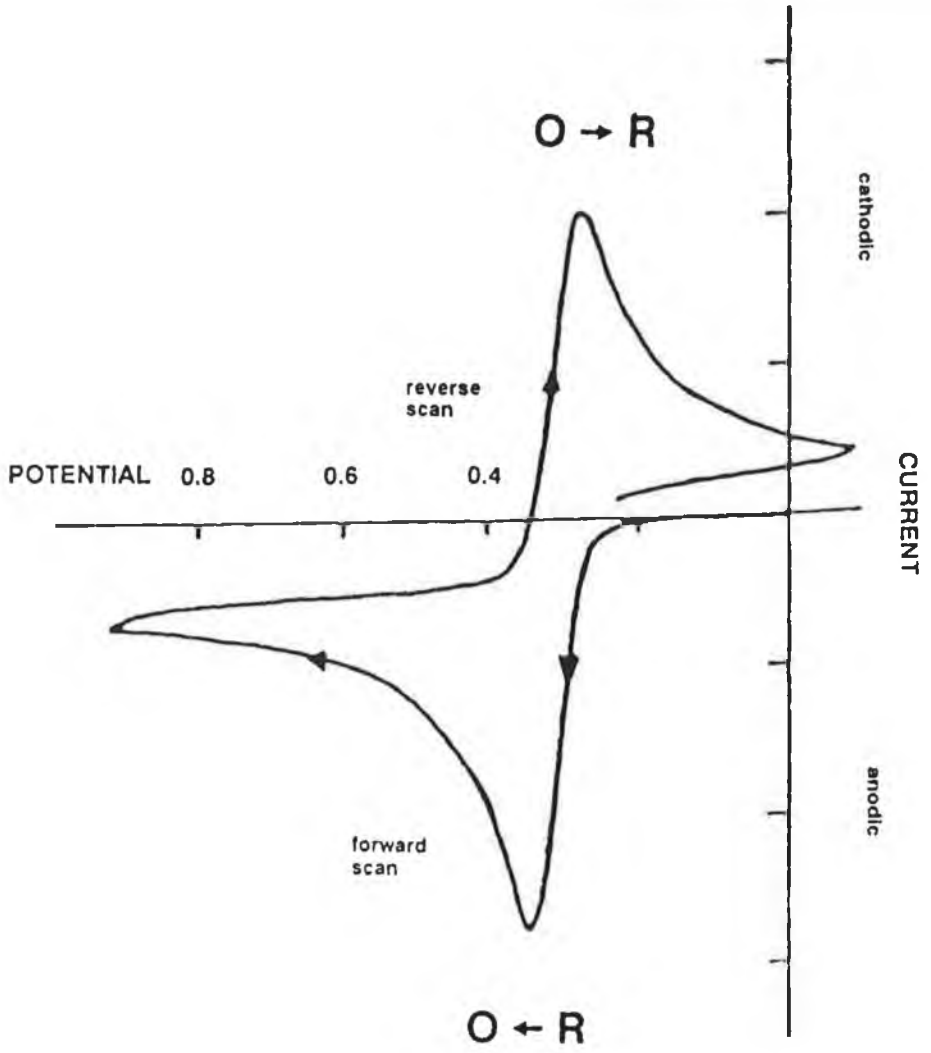

Figure 2.4. A typical cyclic voltammogram for a reversible redox process.

The cyclic voltammogram is characterised by several important parameters:

(i) the cathodic peak potential, E_{p_c}, and anodic peak potential, E_{p_a}; and

(ii) the cathodic (i_{p_c}) and anodic (i_{p_a}) peak currents.

The peak current, i_p, depends on the amount of electroactive species reaching the working electrode surface and on the rate of the electron transfer reaction. For a reduction process, the forward rate constant, k_f, may be described as:

$$k_f = k^o \exp(-\alpha nF/RT(E-E^{o'})) \qquad 2.7$$

where $E^{o'}$ is the formal reduction potential, α the transfer coefficient, and k^o is the electron transfer rate constant.
The oxidation process may be described using a backward rate constant, k_b, given as :

$$k_b = k^o \exp(1-\alpha nF/RT(E-E^{o'})) \qquad 2.8$$

For a reversible (or Nernstian process) the anodic and cathodic peaks are related through:

$$\Delta E = E_{p_a} - E_{p_c} = 59.1/n \text{ (mV)} \qquad 2.9$$

Under these conditions, the electron transfer is fast enough to

maintain an equilibrium between the oxidised and reduced forms of the species at the electrode surface.

At a given potential, the equilibrium ratio at the electrode surface is described by the Nernst equation:

$$E = E^{o'} + RT/nF \ln ([R]/[O])_{x=0} \qquad 2.10$$

When the electron transfer reaction is not fast enough to maintain this equilibrium between the oxidised and reduced species, the process is considered irreversible. Under these conditions the separation between the anodic and cathodic peaks is increased to >59/n mV.

The peak current (i_p) is described by the following equation:

$$i_p = k_{RS}\, n^{2/3}\, A\, D^{1/2}\, C^o\, v^{1/2} \qquad 2.11$$

where k_{RS} is the Randles-Sevčik constant, C^o is the bulk concentration and v is the scan rate. From this we can see that the peak current is proportional to the bulk concentration C^o and the square root of the scan rate, i.e. $v^{1/2}$.

2.1.4. Pulse Techniques

Pulse techniques became more widely available in the late 1960's with the introduction of the operational amplifier-based instruments by Princeton Applied Research Corporation. These techniques had originally been developed by Barker[12] resulting from his work on square wave polarography.

There are two important sources of current that result from

pulse application: (i) the faradaic current, which is proportional to the concentration of electroactive species in the solution; and (ii) the charging current that is required to charge the electrode double layer. The charging current, i_c, which flows at the electrode in response to a potential pulse, decays exponentially while the faradaic current decays at a much slower rate, as shown in Figure 2.5. If the current is measured at the end of the pulse, i_c will be negligible relative to the faradaic current. The decay of i_c may be described mathematically:

$$i_c = (\Delta E/R)\ e^{-(t_m/RC_{dl})} \qquad 2.12$$

where ΔE is the pulse amplitude, R is the uncompensated cell resistance, t_m is the time elapsed following the pulse application and C_{dl} is the double layer capacitance.

2.1.4.1. Normal Pulse Voltammetry

In normal pulse voltammetry (NPV) a series of pulses of increasing amplitude are applied to the electrode as illustrated in Figure 2.6. The normal pulse current on the diffusion current plateau (i_{NPV}) is described by the Cottrell equation[13]:

$$i_{NPV} = nFAD^{1/2}C^o/(\pi t_m)^{1/2} \qquad 2.13$$

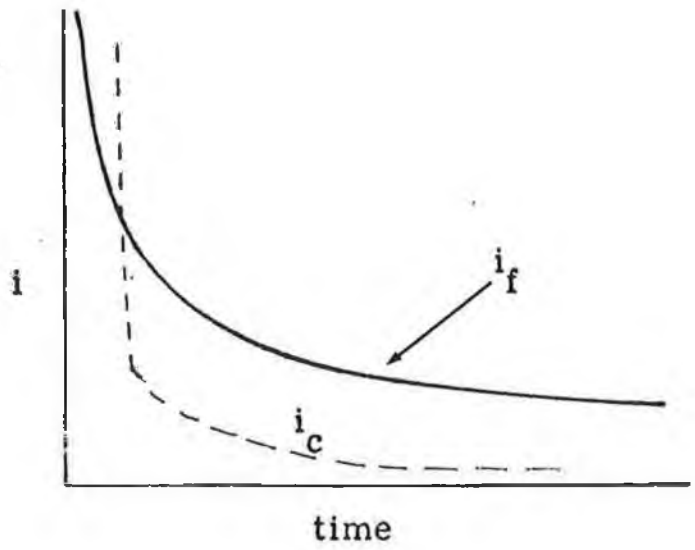

Figure 2.5. The decay of the Faradaic (i_f) and charging (i_c) currents in pulse voltammetry.

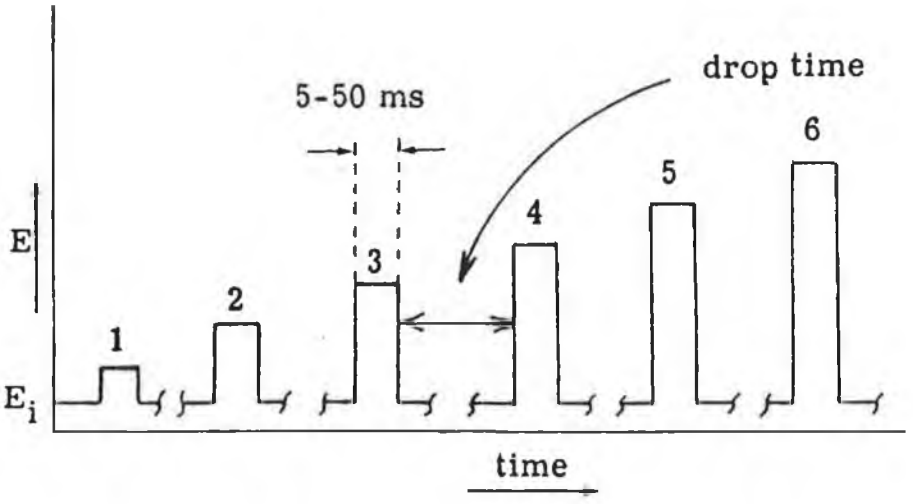

Figure 2.6. Typical excitation signal for normal pulse voltammetry.

where:

$$t_m = t - \partial t/2 \qquad 2.14$$

where t is the pulse width and ∂t is the sample width (illustrated in Figure 2.6.).

It may be seen from equation 2.13 that i_{NPV} is directly proportional to concentration and decreases as $t_m^{-1/2}$. This means the measurement time should be small enough to maximise the signal, yet large enough to allow the charging current to decay to a negligible value.

2.1.4.2. Differential Pulse Voltammetry

In differential pulse voltammetry (DPV)[14], pulses of equal amplitude are superimposed on a linear DC voltage ramp as illustrated in Figure 2.7.(a). The current is sampled immediatly prior to the pulse application and again just before the end of the pulse. The difference between these currents is plotted against the applied potential resulting in a peak-shaped response as illustrated in Figure 2.7. (b). The potential scan rate is usually slow so that the ramp potential does not change significantly during the pulse lifetime.

In a differential pulse experiment it is the difference current (Δi) which is measured:

$$\Delta i = i(E_1+\Delta E) - i(E_1) \qquad 2.15$$

where E_1 is the electrode potential. The difference current

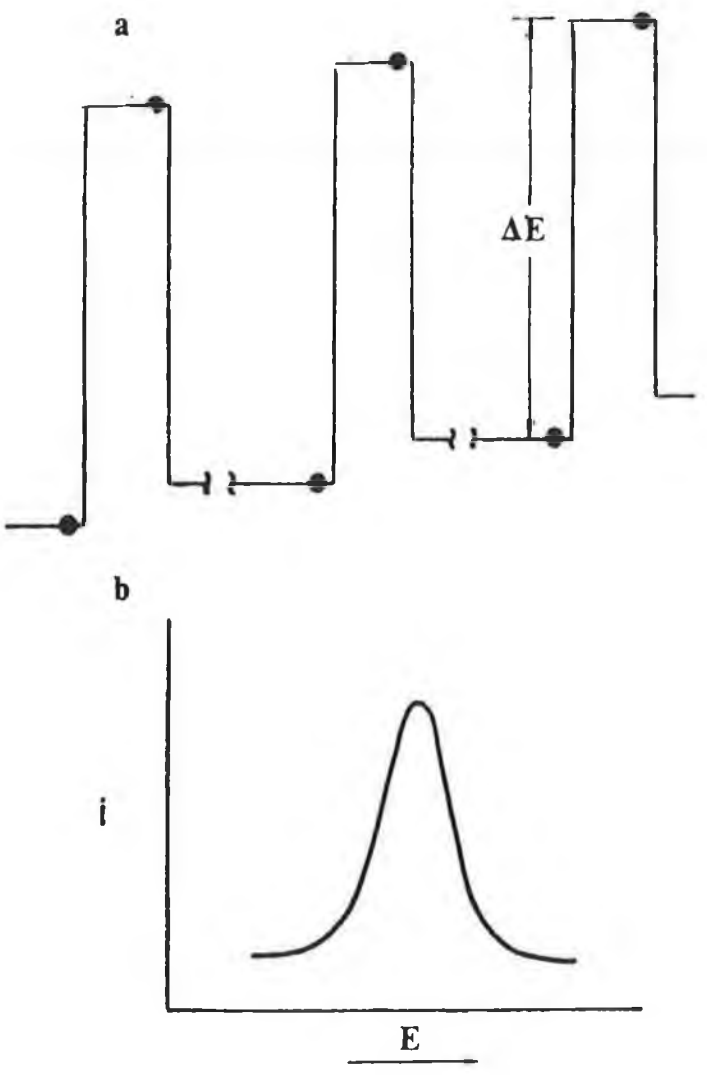

Figure 2.7. (a) Typical excitation signal for differential pulse voltammtery. (b) Typical differential pulse voltammogram.

is related to the diffusion current (i_d) through the expression:

$$i/i_d = (\sigma^2-1)/(\sigma^2+\epsilon)\ (1+\epsilon) \qquad 2.16$$

where:

$$\epsilon = e^{+nF/RT(E-E_{1/2})} \qquad 2.17$$

and:

$$\sigma = e\ (-nF/RT\,\Delta E/2) \qquad 2.18$$

Since $\Delta i\ (E_1)/i_d$ is at a maximum at E_p it can be shown by differentiation that:

$$i_{DPV} = i_{NPV}(\sigma-1)/(\sigma+1) \qquad 2.19$$

In addition:

$$E_p = E_{1/2} - \Delta E/2 \qquad 2.20$$

Therefore the procedure for calculating i_{DPV} is to calculate i_{NPV} and apply equation 2.19.

The ratio $(\sigma-1)/(\sigma+1)$ depends on the number of electrons transferred and the pulse amplitude and is always less than 1. For small values of ΔE this ratio may be approximated by:

$$(\sigma-1)/(\sigma+1) = nF/RT\,\Delta E/4 \qquad 2.21$$

From equation 2.21 it may be seen that for small pulse amplitudes an increase in ΔE will increase i_{DPV}, but at larger pulse amplitudes (>100 mV) the sensitivity is not further increased. Also the ratio increases linearly with increasing n, implying that DPV is a very sensitive technique for reactions involving a large number of electrons transferred.

2.1.5. Stripping Analysis

2.1.5.1. Introduction

The first application of a "stripping" method of analysis came from the work of Zbinden[15] who in 1931 attempted to measure copper electrogravimetrically by plating it onto a platinum electrode. The small amount which was electrochemically plated could not at that time be weighed accurately, so instead a quantitative measurement was made of the current consumed during the electrochemical stripping of the copper from the electrode. It was not until the late 1950's, with the introduction of the hanging mercury drop electrode (HMDE) by Kemula, that the technique attained popular recognition and could be used for sub-ppb determination of metals such as cadmium[16]. At that time, however, a very long deposition time (60 min) was required for this determination. During the 1960's, more sensitive voltammetric techniques (such as DPV) were being developed, and the stripping voltammetric technique was combined with these new wave forms to give a very sensitive and rapid technique applicable to a wide variety of analytical problems[17].

Stripping analysis to-day has the lowest detection limit of any commonly used electoanalytical technique. The technique is capable of simultaneous multi-element determination and the instrumentation is relatively inexpensive. Its remarkable sensitivity may be attributed to an effective preconcentration step and advanced measurement procedures. The preconcentration step enhances the faradaic current relative to the charging

current, which remains at that value associated with the method of measurment chosen. All stripping analysis techniques have three steps: (i) the preconcentration (or deposition) step, which involves the electrolytic deposition of a small portion of the analyte in solution into (or onto) a stationary electrode such as a HMDE; (ii) an equilibration step and (iii) the stripping of the deposit from the electrode. The resulting electrochemical signal is used to determine the concentration of each analyte species in the sample.

2.1.5.2. Linear Scan Stripping Voltammety

Anodic stripping voltammetry (ASV) is the technique used primarily for the determination of heavy metals[18]. A variety of electrodes have been used in association with this technique, including carbon, gold and platinum. However, mercury, in the form of the HMDE or stationary mercury drop electrode (SMDE) or the thin film mercury electrode (TFME), is still the most common electode material used with the technique.

In ASV, the preconcentration step is achieved by cathodic deposition at a controlled potential for a given period of time. The metal ions reach the electrode surface by both diffusion and convection (achieved by either stirring the solution or rotating the electrode), and are reduced and concentrated as amalgams in the Hg electode:

$$M^{n+} + Hg + ne^- \longrightarrow M(Hg)$$

The sensitivity and precision of this technique are dependent

on the effectiveness of the hydrodynamics, which controls the amount of metal plated during the deposition step. The concentration of analyte deposited is governed by Faradays law:

$$C^a = i_L\ t_d/n\ FV_{Hg} \qquad 2.22$$

where C^a is the concentration of metal in the amalgam, i_L is the current, and V_{Hg} is the volume of the mercury. Under the forced convection conditions used in the technique, both diffusion and convection contribute to the deposition current. Convection maintains the analyte concentration in the bulk solution uniform to a distance δ from the electode, where δ is the thickness of the diffusion layer. Within the diffusion layer there is a concentration gradient, and here the ion movement is controlled exclusively by diffusion. The stripping current (i_L) is proportional to the slope of the concentration profile at the electrode surface:

$$i_L = nFADC^o/\delta \qquad 2.23$$

Where δ is related to the convection rate (U) through:

$$\delta = K/U^{\alpha} \qquad 2.24$$

where K and α are constants depending on flow regime and the electrode geometry.

The stripping step must be performed in a quiescent solution; hence there is a rest (or equilibration) period between plating and recording the voltammogram. During this equilibration

period (typically 30 s for a HMDE), electodeposition (now exclusively diffusion controlled) continues. This results in a non-zero intercept in the peak current vs. deposition time plot.

The stripping step then consists of scanning the potential anodically. When the potential reaches the standard potential of a metal-metal ion couple, the metal is reoxidised and the metal ion returns back into solution:

$$M(Hg) \longrightarrow M^{n+} + ne^{-}$$

The resulting current is proportional to the concentration of that metal in or on the electrode and therefore to the bulk concentration.

There are a variety of measurement techniques that may be combined with the stripping technique, including linear scan, differential pulse, staircase and square-wave voltammetry.

To obtain an accurate measurement of the faradaic current, the background current, i_b, which is unrelated to the stripping reaction of interest, must be eliminated. the background current is given by:

$$i_b = i_c + i_f, \qquad 2.25$$

where i_c is the charging current and i_f' is the background component associated with redox reactions of impurities or decomposition of electrolyte. The faradaic background component is composed of currents that limit the working potential range, e.g. the oxidation of mercury at about +0.25 V

vs SCE, hydrogen evolution current resulting from the reduction of hydrogen ions; and the reduction of dissolved oxygen. Differential pulse stripping voltammetry is perhaps the most widely used stripping mode, and is designed to compensate for the charging current (section 2.1.2.3.). In addition to the gain in sensitivity offered by the DPV technique, a gain in the overall signal to background ratio occurs because some of the metal ions stripped from the electrode during the life time of the pulse are replated into (or onto) the electrode during the period between pulses. The same material is then stripped and reduced many times resulting in an amplification effect. Hence, a shorter pulse duration results in a higher sensitivity.

The stripping peak current at the HMDE derived by Lund and Onshus[19] is given by:

$$\Delta i_p = Kn^2 r \Delta E U^{1/2} t_d C^o \qquad 2.26$$

This equation is valid only for small pulse amplitudes (less than 100 mV). The peak potential is given by:

$$E_p = E_{1/2} - 1.1\ RT/nF \qquad 2.27$$

This equation assumes equal diffusion coefficients for the reduced and oxidised forms and ignores sphericity effects. The main disadvantage of this technique lies in the long analysis times, due to deposition plus the relatively slow scan rate needed for DPV. It is also susceptible to interferences by surface active materials (contributing to i_f' which may

affect the rate of the electrode reaction.

2.1.5.3. Adsorptive Stripping Voltammetry

Adsorptive stripping voltammetry (AdSV) is based on preconcentration by adsorptive accumulation at the electrode surface[20]. The concentrated surface species retains its electochemical characteristics and therefore may be quantified using a sensitive voltammetric technique such as DPV.

The adsorption of organic species onto the electrode has traditionally been regarded as a problem, limiting the usefullness of voltammetric measurements. However, it is now widely known that the adsorptive accumulation of organic molecules, or species of biological interest, enhance the sensitivity for their measurement.

In this technique, the adsorptive accumulation step is governed by diffusion of the species to the electrode surface. The equation for these conditions was proposed by Koryta[21]:

$$M_{max} = 7.36 \times 10^{-4} D^{1/2} t^{1/2} C \qquad 2.28$$

Where C is the concentration of the surface active compound, of which M_{max} (moles cm^{-2}) fully cover the electrode surface in time, t. As for ASV, the adsorption of the species of interest depends on its concentration in solution, the deposition time and the process of mass transfer to the electrode. The deposition time is critical in AdSV, as the stripping signal does not increase linearly with time beyond the complete drop coverage value. As the accumulation rate is

governed by mass transport, various forms of forced convection such as stirring or rotation are employed during the accumulation step, followed by an equilibration period of about 15 seconds. The voltammetric measurment is made in a quiescent solution.

Parameters such as accumulation potential, electrolyte composition, electrode material, temperature and pH, also affect the accumulation of surface active species onto the electrode and need to be optimised to achieve maximum sensitivity. Varying these parameters has been known to enhance selectivity. Stara and Kopanica have used accumulation potential to discriminate against interferences in the determination of thiourea in urine[22]. It is possible to enhance the stripping signal by using diluted supporting electrolyte, and Wang and Freiha[23] have described a strategy called adsorptive transfer stripping voltammetry (also discussed by Palacek[24]) that involves carrying out the stripping step in a simple electrolyte solution as opposed to the complex matrix from which the species of interest was adsorbed.

2.2. Liquid Chromatography with Electrochemical Detection

2.2.1. High Performance Liquid Chromatography

High performance liquid chromatography (HPLC) was developed in the mid 1960's, and has made a significant contribution to pharmaceutical, biochemical, clinical and environmental analysis. It is a powerful analytical method capable of separating complex mixtures of components in relatively fast analysis times. The technique is very well documented in the literature[25,26].

2.2.2. Requirements of a Detector for HPLC

The detection systems employed in HPLC are based on instrumentation designed to measure a particular physical or chemical property of a solute in an eluent that flows from a chromatographic column.

The function of any detector employed in HPLC is to monitor the concentration or amount of the sample components eluted from the column. The following detector requirements are important[27]: (i) the capability to detect 1 part of solute in 10 parts eluent (larger concentrations will overload a standard analytical column); (ii) no remixing of components as they pass through the detector; (iii) a wide linear dynamic range; (iv) low drift and noise; (v) a fast response time; (vi) insensitive response to pulsation and changes in flow rate or temperature; (vii) insensitive response to eluent composition

(important where gradient elution is performed); and (viii) ease of operation and reliability.

2.2.3. Electrochemical Detectors

The coupling of liquid chromatography with electrochemical detection (LCEC) offers a selective and sensitive tool for the determination of a wide variety of analytes. The technologies are very compatible, and in combination yield important advantages for a number of trace determinations. The modern interest in LCEC was stimulated by application of the technique to studies on aromatic metabolism in the mammalian central nervous system. The technique is now commonplace in many clinical, biochemical and pharmaceutical laboratories. The major advantages offered by the system are: (i) high selectivity; (ii) low limits of detection; and (iii) low cost.

2.2.4. Fundamental Principles of Electrochemical Detection with HPLC

Electrochemical detectors operated in the amperometric mode measure the current (resulting from a faradaic process) produced under the influence of a fixed applied potential. This potential is determined from the limiting plateau of a hydrodynamic voltammogram (HDV). This is obtained from the measurement of currents produced by an eluting species at a range of fixed potentials. The potential chosen must be in the region where the analyte is electroactive and free from interference. The measured voltammetric signal depends upon

the hydrodynamic parameters of the measuring system and the kinetics are determined by the mass transfer process.

2.2.5. Mass Transfer Under Hydrodynamic Conditions[28]

The rate of a heterogeneous chemical reaction, such as the electode process, is governed by the rate of the slowest step, often due to mass tansport. The kinetics of the reaction in stirred solution are complex. The Nernst theory describes a thin layer of static liquid adjacent to the electrode surface, of thickness δ, called the diffusion layer[29]. Next to this, the species of interest is transported by convection. In the diffusion layer the concentration gradient is linear, hence the mass flux (J) of the component taking part in the heterogeneous reaction can be given by:

$$J = DA(C^O - C^S)/\delta \qquad 2.29.$$

where C^S is the concentration of the species at the electrode surface. Although this assumption has not been upheld by experimental observations (which have shown the diffusion layer is not static nor is the concentration gradient linear), the equation is still being used. Equation 2.29 relates a decrease in δ to an increase in mass flow.

Equation 2.30 describes the concentration distribution relating to a heterogeneous chemical reaction:

$$\partial C_i/\partial t = \nabla(D_i \nabla C_i) - V\nabla C_i + z_i F \nabla(U_i C_i \nabla\phi) + R_i \qquad 2.30$$

where C_i is the concentration of species i, z_i is the number of charges transported by i, U is the ionic mobility and ϕ is the strength of the ionic field. This relationship was derived from Levich's theory that states "the transport of a solute in a liquid is governed by two quite different mechanisms. First, there is molecular diffusion as a result of concentration differences; second, solute particles are entrained by the moving liquid and are transported with it. The combination of these two processes is called convective diffusion of a solute in a liquid."[30] Both processes play significant roles and hence both are considered in the description of mass flux. The first term in the relationship relates to the concentration gradient (transport by diffusion), the second term relates to the macroscopic flow velocity (transport by convection), the third term relates to mass transport due to migration, and the fourth is the rate of the homogeneous chemical reaction.

2.2.6. Electrodes

There are a large number of working electrodes to which the Levich theory has been applied, e.g. tubular, rotating discs, conical microelectrodes, DME's etc. One of the most common designs in commercial LCEC systems is the thin layer cell as shown in Figure 2.8.

2.2.6.1. Thin Layer Electrodes

In the application of the Levich theory to thin layer

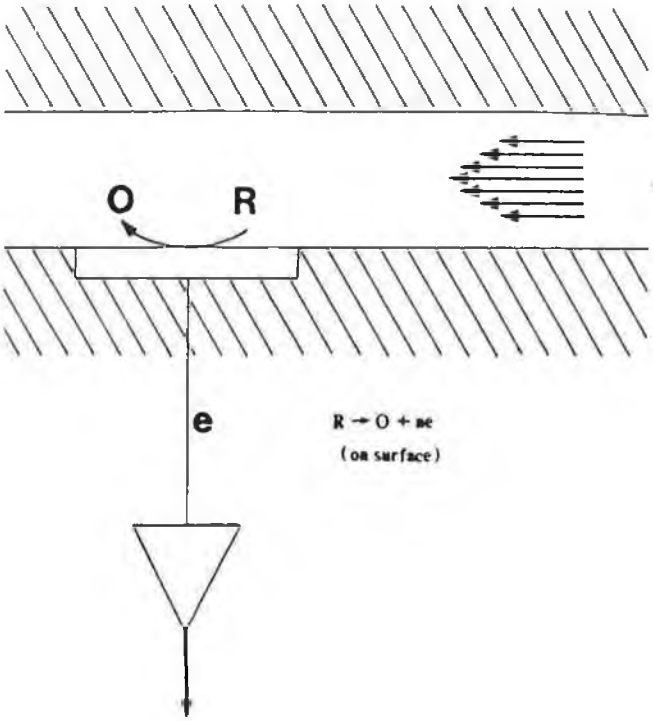

Figure 2.8. schematic diagram of a thin layer cell used as aa amperometric detector in LCEC. R is the reactant and O is the oxidised product.

electrodes, the following assumptions were made: (i) that the flow velocity (v) is laminar in the vicinity of the plate; and (ii) that the length (h) and the width (b) of the plate are much greater than the thickness of the hydrodynamic boundary layer[30]. The following relationship was obtained for i_L, the limiting current:

$$i_L = 0.63\ nFD^{2/3}v_k^{-1/6}bh^{1/2}v^{1/2}C \qquad 2.31.$$

where v_k is the kinematic viscosity, and v the solution flow rate. This equation was later experimentally verified and applied to both laminar and turbulent conditions[31,32].

2.2.7. Mobile Phase

The mobile phase chosen for LCEC must (as with other voltammetric electrolyte solutions) be conductive to maintain good potential control[33]. The mobile phases used with reversed-phase or ion exchange chromatography are often suitable because of their polar nature, and usually an electrolyte concentration from 0.01 to 0.1 M is sufficient. To avoid interference from the reduction of oxygen, the mobile phase should be purged with an inert gas prior to entering the LC system.

2.3. THEORY OF ENZYME KINETICS

2.3.1. Introduction

Enzymes may be described as "real" catalysts as they directly enhance the rate of a specific reaction that would otherwise occur only very slowly, without changing the equilibrium point of that reaction or being changed or used up in the process.
Unlike most organic reactions, such as nucleophilic substitution, which exhibit a linear dependance of rate on the concentration of at least one of the reactants, enzyme-catalysed reactions usually exhibit a non-linear dependence on the concentration of the reactant or substrate (S).

2.3.2. Mechanism

The general mechanism for an enzyme catalysed reaction is given by:

$$E + S \rightleftharpoons ES \longrightarrow E + P$$

which was proposed by Michaelis and Menten (based on earlier work by Brown and Henri) in 1913[34,35,36]. The first step (i.e. the formation of the enzyme-substrate complex) is a relatively fast reversible reaction; the second step (the breakdown of the complex to a product (P) and free enzyme (E)) is much slower and, therefore, the rate determining step.
At any point in the reaction the enzyme is present in two

forms: (i) as part of the enzyme-substrate complex; or (ii) as free enzyme. The reaction rate will be at a maximum when all or most of the enzyme is present in the complexed form, i.e. when the substrate is in excess. At these very high substrate concentrations, the enzyme forms a product and then immediately combines with another substrate molecule. A steady state is achieved in which the enzyme is always saturated with substrate and the reaction rate is at a maximum.

2.3.3. Determination of Enzyme Kinetic Constants

The equation described by Michaelis and Menten[36], i.e.

$$V_o = V_{max}\,[S]/(K_M + [S]) \qquad 2.32$$

is an algebraic expression describing the shape of the relationship between the substrate concentration and the reaction rate and is illustrated in Figure 2.9. From this curve, V_{max} and K_M may be estimated where V_{max} is the maximum velocity obtained, K_M (the Michaelis-Menten constant) is the concentration of the substrate at which the enzyme reaches half-maximum velocity, and V_o is the velocity obtained at substrate concentration [S]. Each enzyme has a characteristic K_M value for a given substrate. The activity of the enzyme (the rate of product turnover per mg of enzyme) is calculated from this data and quoted in international units (IU). By international agreement, 1 unit of enzyme activity is defined as that amount of an enzyme causing transformation of 1 μM of substrate per minute, at 25^{o}C, under optimal conditions

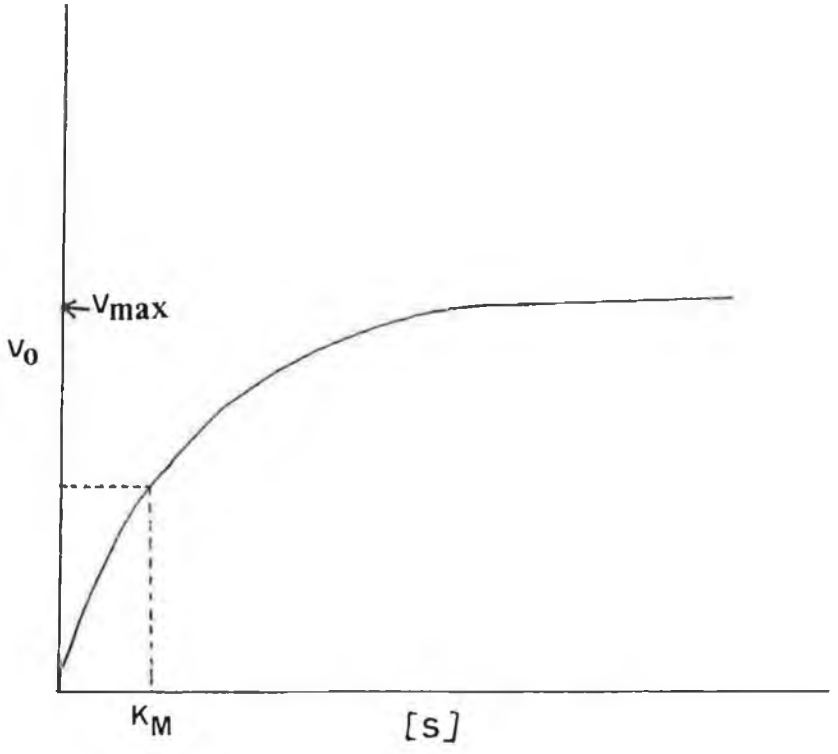

Figure 2.9. Plot of initial rate vs substrate concentration for a reaction obeying the Michaelis-Menton equation.

of measurement. The specific activity is the number of units generated by 1 mg of enzyme:

$$1\ IU = [P]\ (\mu M)/\ E\ (mg)\ min \qquad 2.33$$

An alternative method of determining K_M and V_{max} is the double reciprocal plot described by a transformation of the Michaelis-Menten equation, and was first used by Lineweaver and Burk:[37]

$$1/V_o = K_M/V_{max}\ [S] + 1/V_{max} \qquad 2.34$$

As may be seen from Figure 2.10.(a), K_M and V_{max} may be read directly from this plot.

Multiplying both sides of this equation by [S], equation 2.35

$$[S]/V_o = K_M/V_{max} + [S]/V_{max} \qquad 2.35$$

is obtained. This equation, first described by Hanes[38], is illustrated in Figure 2.10.(b), where a graph of $[S]/V_o$ vs [S] is plotted, yielding a straight line with slope $1/V_o$ and intercepts of K_M/V_{max} on the y-axis and $-K_M$ on the x-axis.

A third linear transformation of the Michaelis-Menten equation is obtained by multiplying both sides of equation 2.34 by V_oV_{max} and rearranging to give:

$$V_o = V_{max} - K_M\ V_o/[S] \qquad 2.36$$

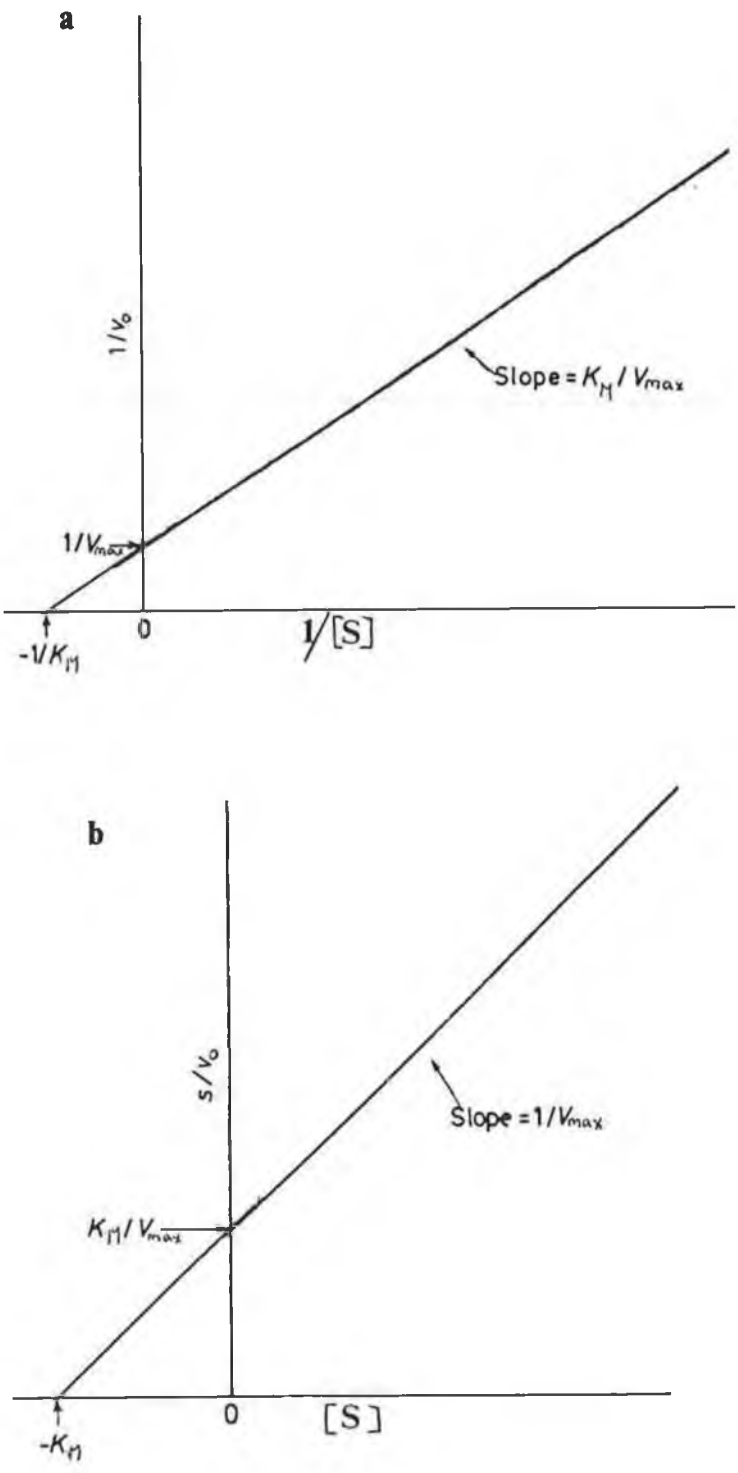

Figure 2.10. (a) The Lineweaver-Burk plot of $1/V_o$ against $1/[S]$. (b) The Hanes plot of $[S]/V_o$ against $[S]$.

On plotting V_o against $V_o/[S]$, a straight line is obtained with slope $-K_M$, which intercepts on the y-axis at V_{max} and the x-axis at V_{max}/K_M. This plot is known as the Eadie-Hofstee plot[39,40].

An alternative direct linear plot was described by Eisenthal and Cornish-Bowden in 1974[41]. The Michealis-Menten equation was rearranged to show the dependence of V_{max} on K_M through:

$$V_{max} = V_o + V_o/[S]\ K_M \qquad 2.37$$

and the resulting plot is illustrated in Figure 2.11. The substrate concentration (treated as a constant for the purposes of this plot) is plotted as a negative value on the x-axis and is joined to its experimentally obtained velocity value on the y axis by a straight line. This line describes all possible sets of values for K_M and V_{max} that satisfy these values of S_i and V_i, where V_i is the velocity corresponding to the substrate concentration S_i. If a second line were drawn for a second experimental observation (S_j,V_j), there would be only one set of values for K_M and V_{max} that satisfy both observations i.e. the cross-over point. This may be determined mathematically from:

$$V_{ij} = S_i - S_j/(S_i/V_i) - (S_j/V_j) \qquad 2.38$$

$$K_{ij} = V_j - V_i/(V_i/S_i) - (V_j/S_j) \qquad 2.39$$

where V_{ij} and K_{ij} are the values for V_{max} and K_M

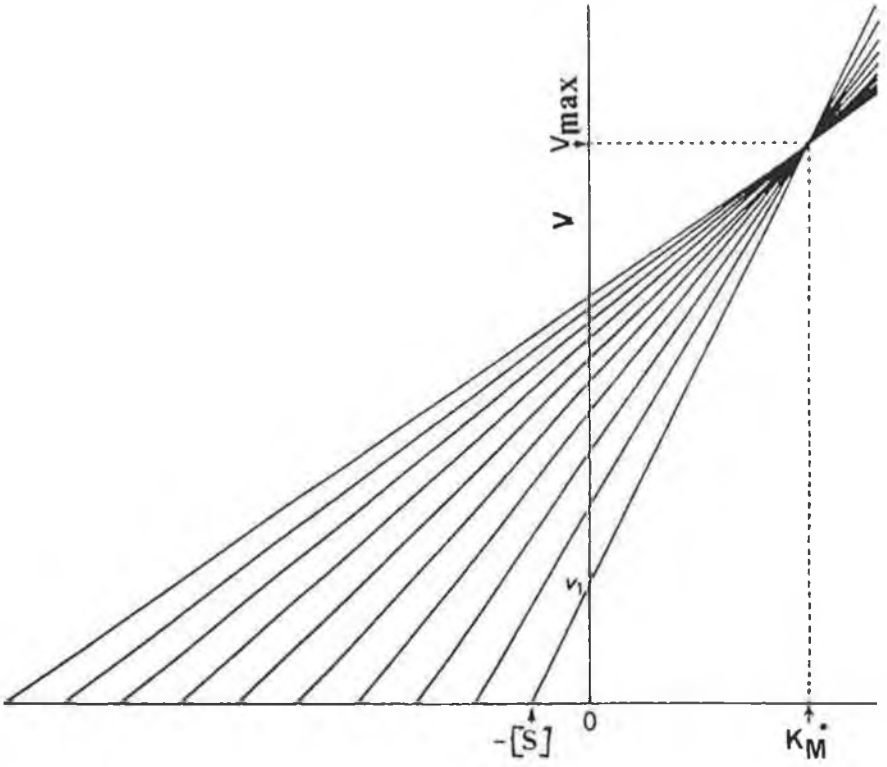

Figure 2.11. Direct Linear plot of V_{max} against K_M. Each line represents one observation and is drawn with intercepts $-[S]$, on the abscissa and V_o on the ordinate. The crossover point gives the coordinates for the values K_M and V_{max}.

represented by the cross-over point (figure 2.11). In a real experiment, the crossover point for a number of observations would be less well defined than that illustrated in Figure 2.11; hence the median is chosen. For this plot, the choice of the median value is more accurate than the arithemetic mean as it is insensitive to extreme values which may occur for some of the lines which run almost parallel on approaching the maximum velocity.

2.3.4. Treatment of Error

Although it is algebraically correct to rearrange the Michaelis-Menten equation for a theoretical curve to a linearised form such as the Lineweaver-Burk equation, this manipulation is not appropriate when analysing experimental data where there is inevitably some experimental error. The equation:

$$V_o = [V_{max}\ [S]/(K_M + [S])]\ (1 + e) \qquad 2.40$$

is more appropriate for the analysis of experimental results where e is the experimental error[42]. This has been illustrated in Figure 2.12 where (a) is a kinetic curve assuming constant error in rate measurement. When this curve is transformed to a linear plot as in (b) and (c), the error distribution is distorted. An understanding of these problems is important when analysing experimental data. Weighting of the original data is invalidated once the data has been transformed.

These problems may be overcome by using: (i) the direct linear

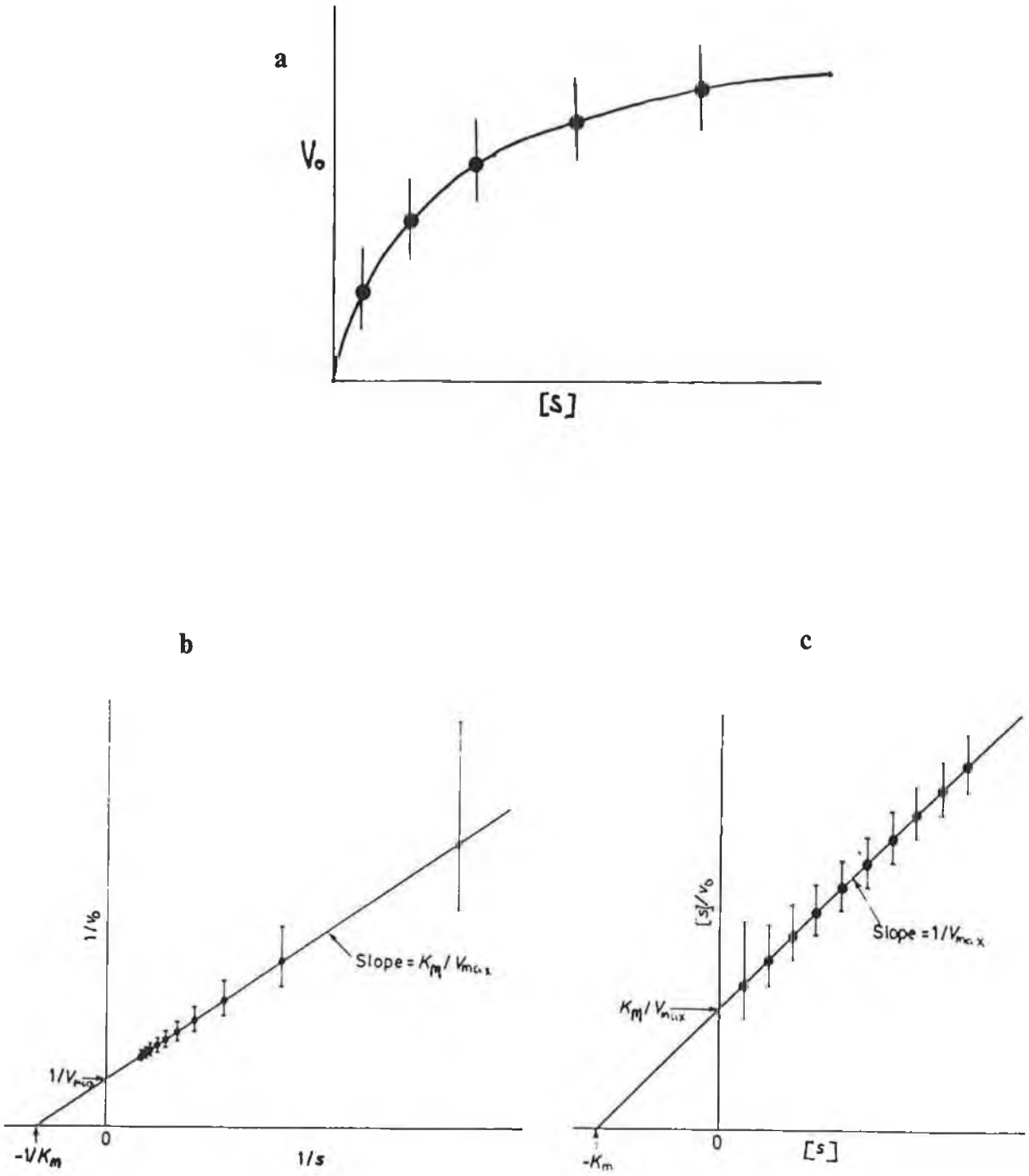

Figure 2.12. (a) Enzyme kinetic data assuming random error. (b) and (c) linear transformation of data illustrating the effect of such a transformation on random error.

method (described in section 2.3.3.); or (ii) a non-linear regression of the Michaelis-Menten equation.

2.3.5. Effect of pH

Enzymes exhibit a pH dependency, as shown in Figure 2.13[43], depending on whether proton-donating, or proton-accepting, groups at the catalytic site are in their required state of ionisation[44]. Ionisable groups in proteins include C-terminal groups (pK_a=3.4), and histidine (pK_a=6.3) and tyrosine (pK_a=9.6) residues.

In the model proposed by Michaelis[43], only two ionisable groups are considered and the enzyme may be represented as a dibasic acid. The proton may be considered as a modifier, an activator or inhibitor that binds to the protein without the steric effects of larger modifiers.

The effect of pH on enzymes is very complex, yet in most cases relatively easy to control. Hence it plays a vital role in elucidating the structure and function of enzymes. Studies of pH may also be used to determine the chemical mechanism of enzyme catalysed reactions.

2.3.6. Effect of Temperature

The relationship of enzyme activity to temperature is illustrated in Figure 2.14. The temperature dependence of V_{max} at lower temperatures is described by the Arrhenius equation:

$$\log_{10} V_{Max} = -E_a 2.3R\ 1/T + \text{constant} \qquad 2.41$$

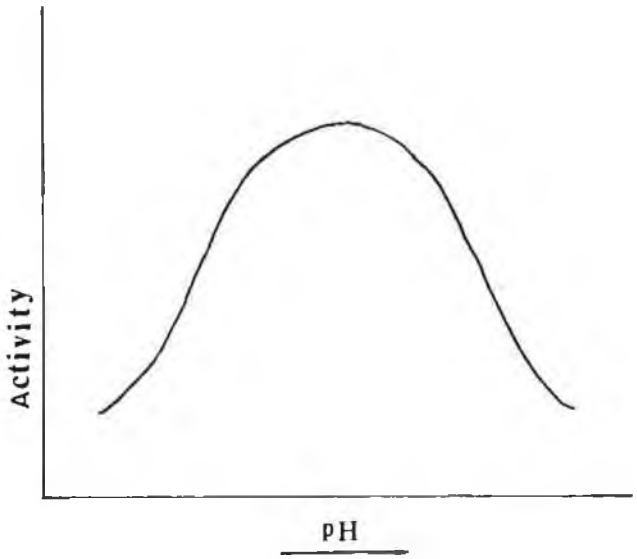

Figure 2.13. Effect of pH on enzyme activity.

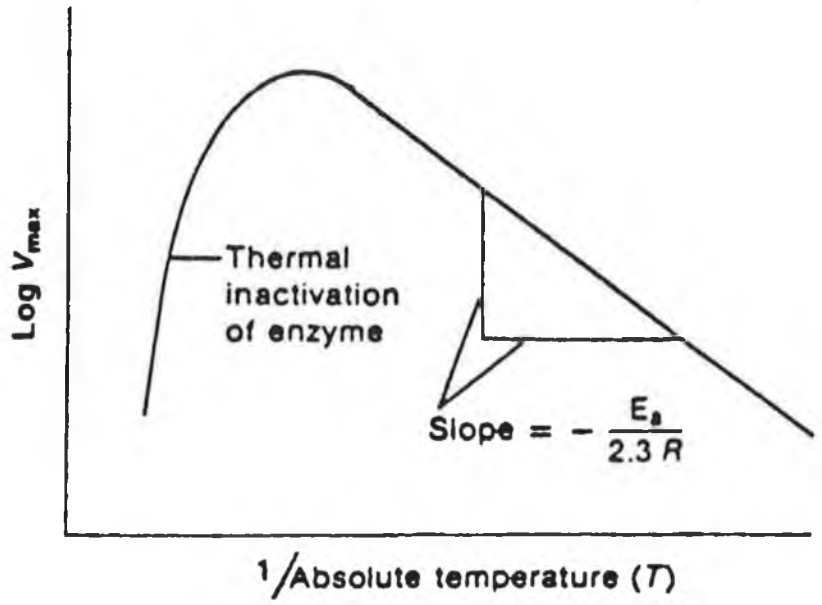

Figure 2.14. Effect of temperature on enzyme activity.

where E_a is the Arrhenius activation energy, R is the gas constant and T is absolute temperature[45].

At higher temperatures (>physiological temperature of 37°C) most enzymes would denature giving a lower activity than would have been predicted.

2.3.7. Inhibitors and Activators

Enzyme inhibitors are compounds that prevent or decrease the rate of an enzyme-catalysed reaction when present in the reaction mixture[42]. Inhibition can occur in a variety of ways. An irreversible inhibitor may combine with the enzyme and completely destroy its catalytic activity. A reversible inhibitor may change the catalytic profile of the enzyme on combining with the enzyme.

Conversely, an activator is a compound that increases the catalytic activity of the enzyme. The most important activation is that called "compulsory activation" where without the activator the free enzyme has no activity and does not bind the substrate.

2.4. THEORY OF ENZYME IMMUNOASSAY

2.4.1. Immunoassay

Immunoassay techniques have, since the early work of Yalow and Berson[46], been applied to many analytes of biological and clinical significance. As an analytical technique it has many advantages[47]. It may, in principle, be applied to any analyte. The technique is very sensitive, and assays for amounts as low as 10^{-18} mol have been reported[48]. It is also potentially even more sensitive. The analyte need not be pretreated and the design of the assay facilitates simple automation.

The immunoassay itself is a technique that exploits an antibody as an analytical reagent capable of detecting and quantifying an analyte that possesses the chemical structure toward which the antibody-binding site is directed. This immunochemical reaction is one of the most selective chemical reactions known; its high selectivity allows assays in complex biological media with little interference. Antibodies are serum proteins called immunoglobulins which are produced as a result of infection (or immunisation) of a host by a foreign body (called an antigen). The antibody structure and immunological reaction are outlined in chapter 4.

The sensitivity of any immunoassay depends primarily on the type of label used. Labels used to date have included: radioisotopes, fluorigenic substrates, chemiluminescent markers, liposomes, metal atoms and stable free radicals.

2.4.1.1. Radioimmunoassay

Radioisotopic tracers such as Iodine^{125} are still popular labels as they allow highly sensitive assays. These may be divided into radioimmunoassay (RIA), where the analyte is labelled, and immunoradiometric assay (IRMA) where the antibody is labelled[49].

Alternatives to radiolabelling are constantly being sought and methods such as fluorescent labelling, electrochemical immunoassay and particularly enzyme labels are becoming increasingly more popular.

2.4.1.2. Enzyme Immunoassay

The enzyme label is the most widely used of alternative labels to RIA and is a very powerful amplification system. There are many reviews of the technique[50-53]. Any EIA is based on two reactions: the immunological binding of the antibody to its antigen and the enzymatic signal indicating that the immunological reaction did or did not take place.

The sensitivity of EIA depends on the detection system, the most common of which is spectrophotometry. The sensitivity of the assay is limited by the limit of detection for that technique used to quantify the substrate to product reaction of the enzyme. Detection techniques applied to EIA include fluorimetry, luminescence measurements, and electrochemical techniques, reviewed in chapter 1.

EIA first became feasible when a system for coupling enzymes to antibodies was developed by Avrameas et al [54]. They are now

applied to a huge variety analytes, including drugs[55], immunoglobulins[56], vitamins[57] and microorganisms[58].

Enzyme immunoassays may be divided into heterogeneous or homogeneous assays. In a heterogenous assay after incubation of the antibody and antigen, the resulting complex is separated from the free antibody (or antigen). The signal from the complexed enzyme-labelled antigen (or antibody) does not differ from that of the free enzyme-labelled antigen (or antibody) and, if not separated, would lead to interference. The most common separation system involves a solid phase (such as a polystyrene well or tube), first described by Engval and Perlman[59]. An example of this system, an enzyme-linked immunosorbent assay (ELISA), is illustrated in Figure 2.15 Separation of the bound and free labelled antigen (or antibody) may also be achieved by precipitating the immune complex.

In a homogeneous assay, such as the enzyme-multiplied immunoassay technique (EMIT), illustrated in Figure 2.16., a separation step is not necessary. The enzyme-coupled antigen (or antibody) exhibits a change in activity on reaction with the antibody (or antigen), and therefore the signals, being different, will not interfere. Normally the activity of the marker enzyme is reduced as a consequence of steric hindrance and limited substrate access.

A comparison of EMIT and ELISA techniques is outlined in Table 1[60]. ELISA is usually more sensitive and capable of assaying larger molecules, such as other proteins.

EIA may also be divided into competitive or non-competitive assays. The former is based on the competitive equilibrium between an excess of labelled and unlabelled antigen for a

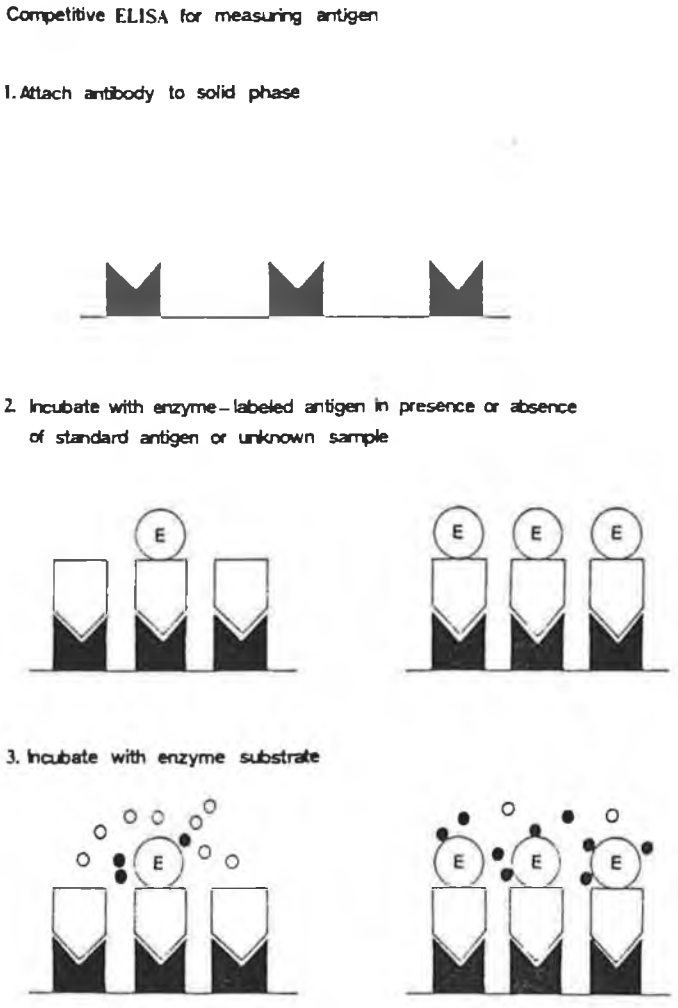

Figure 2.15. Competitive ELISA for measuring antigen.

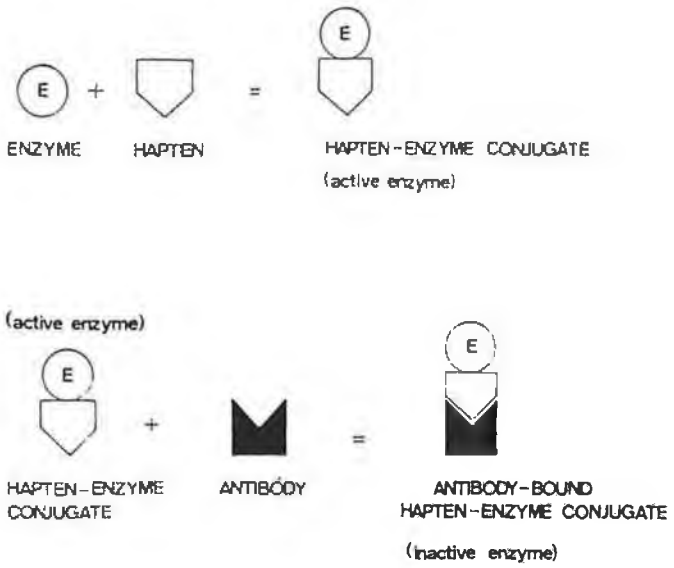

Figure 2.16. A typical enzyme multiplied immunoassay technique (EMIT).

ELISA	EMIT
Heterogeneous assay	Homogeneous assay
Separation step required	Separation step not required
Washing steps required	Washing steps not required
Slower than EMIT	Faster than ELISA
Greater sensitivity than EMIT	Lesser sensitivity than ELISA
Measures large molecules	Measures small molecules
Solid phase assay	Liquid phase assay

Table 2.1. A comparison of EIA procedures.

limited amount of highly specific antibody:

$$Ab + Ag + Ag^* \rightleftharpoons AbAg + AbAg^*$$

In a non-competitive assay, the antigen to be measured reacts with the antibody bound to a solid phase and the binding of the enzyme-labelled antibody is measured. The sandwich ELISA technique, illustrated in Figure 2.17, is an example of such an assay.

The quality of an EIA depends on many factors, including the suitability of the enzyme label, the purity of the antigen or hapten used for immunisation, the specificity of the antibody produced and its immobilisation to the solid phase. The purity of the antigen or hapten used for immunisation (now called an immunogen, defined as a substance that induces an immune response) is of vital importance when a polyclonal antisera is used. The response induced by traces of very immunogenic impurities may exceed the required immunogenic responce. It is also important that the host has not already developed an immunity toward the analyte. The application of monoclonal antibodies (MAbs)[61] to EIA has lead to the development of very sensitive immunoassays, supplying a solution of identical antibodies. However, disadvantages include the reduced affinity of MAbs to high molecular weight proteins, and the fact that such antibodies (with a single specificity) could not be used in a non-competitive sandwich assay if the antigen had only one binding site (toward which the MAb was directed)[62].

The choice of binding to the solid phase is important, as the bound protein must retain its immunoreactivity. Also, the bond

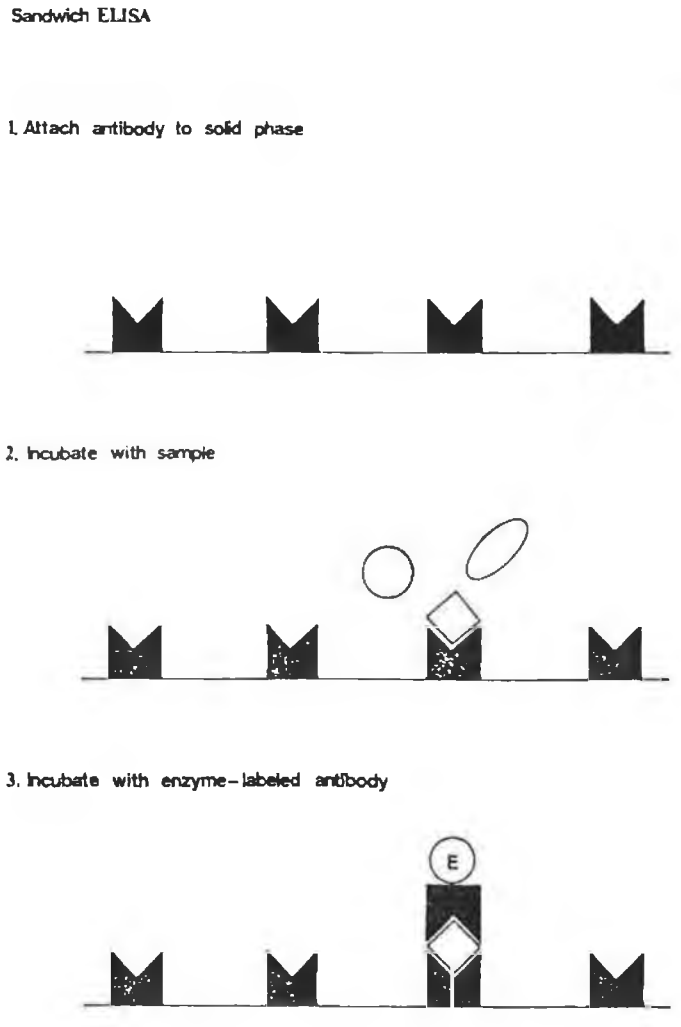

Figure 2.17. A typical sandwich ELISA technique.

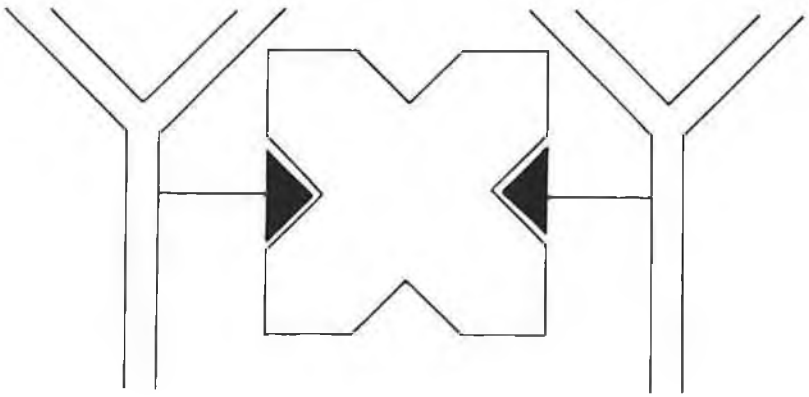

Figure 2.18. Avidin (or streptavidin) as a bridging molecule between two biotinylated immunoglobulin molecules.

2.5. REFERENCES

1. Heyrovsky, J., Chem. Listy., 16(1192)256.
2. Barker, G.C., F.Z. Anal. Chem., 176(1960)79.
3. Parry, E.P. and Osteryoung, R.A., Anal. Chem., 36(1964)1366.
4. Whitteker, J.W., Chan, C. and Levine, S.L., Am. Lab. 15(1983)79.
5. Maloy, J.T., J. Chem. Educ., 60(1983)285.
6. Bard, A.J. and Faulkner, L.R., "Electrochemical methods: Fundamentals and applications"., (Wiley, New York, 1980).
7. Crow, D.R. and Westwood, J.V., Q. Rev., 19(1965)57.
8. Bond, A.M., "Modern Polarographic Methods in Analytical Chemistry"., (Marcell Dekker, New York, 1980)
9. Cauquis, G., in "Organic Electrochemistry: an introduction and a guide," eds. Baizer, M.M. and Lund, H., (Marcel Dekker Inc. New York & Basel 1983).
10. Damaskin, B.A., Electrochim. Acta., 9(1964)231.
11. Matheson, L.A. and Nichols, N., Trans. Electrochem. Soc. 73(1938)193.
12. Barker, G.C., Z. Anal. Chem. 173(1960)79.
13. Parry, E.R. and Osteryoung, R.A., Anal. Chem., 36(1964)1366.
14. Osteryoung, J. and Hasabe, K., Review of Polraography (Japan) 22(1976)1.
15. Zbinden, C., Bull. Soc. Chim. Biol., 13(1931)35.
16. Demars, R.D., Shain, I., Anal. Chem., 29(1957)1825.
17. Nurnberg, H.W., Pure. Appl. Chem., 54(1982)859.

18. Wang, J., "Stripping Analysis: Principles and applications," (VCH Deerfield Beach, FL. 1985).

19. Lund, W. and Onshus, D., Anal. Chim. Acta., 86(1976)109.

20. Smyth, W.F., in "Electrochemistry: Sensors and analysis"., eds. Smyth, M.R. and Vos, J.G., (Elsvier, amsterdam, 1986).

21. Koryta, J., Coll. Czech. Chem. Comm., 18(1953)206.

22. Stara, V. and Kopanica, M., Anal. Chim. Acta., 159(1984)105.

23 Wang, J. and Freiha, B.A., Anal. Chem., 56(1984)849.

24. Palecek, E. and Postbieglova, I., J. Electroanal. Chem., 214(1986)359.

25. Karger, B.L., Snyder, L.R. and Horvath, C., "An Introduction to Separation Science," (J. Wiley and Sons, New York 1973).

26. Poole, C.F. and schuette, S.A., "contemporary Practise of Chromatography" (Elsiver, Amsterdam 1984).

27. White, P.C., Analyst., 109(1984)677.

28. Pungor, E., Feher, Z. and Varadi, M., CRC Crit. Rev. Anal. Chem., 9(1980)97.

29. Nernst, W., Z. Phys. Chem. (Leipzig)., 47(1904)52.

30. Levich, V.G., "Physicochemical Hudrodynamics," (Prentice-hall, Englewood Cliffs NJ. 1962).

31. Trumpher, G. and Zeller, H., Helv. Chim. Acta. 34(1951)952.

32. Wrangless, G. and Nilsson, O., Electrochim. Acta., 7(1962)121.

33. Kissenger, P.T., in "Laboratory Techniques in Electranalytical Chemistry," eds. Kissenger, P.T. and Heineman, W.R., (Marcel Dekker Inc. New York and Basel, 1984).

34. Brown, A.J., J. Chem. Soc. Trans., 61(1892)369.

35. Henri, V., Cr. Hebd. Acad. Sci. (Paris) 135(1902)916.

36. Michealis, L. and Menton, M.L., Biochem. Z. 49(1913)333.

37. Lineweaver, H. and Burk. D., J. Amer. Chem. Soc., 56(1934)658.

38. Hanes, C.S., Biochem, J., 26(1932)1406.

39. Eadie, G.S., J. Biol. Chem., 146(1942)85.

40. Hofstee, R.H.J., J. Biol. Chem., 199(1952)357.

41. Eisenthal, R. and Cornish-Bowden, A., Biochem. J., 139(1974)715.

42. Cornish-Bowden, A., "Fundamentals of Enzyme kinetics," (Butterworths and Co. ltd. London, 1979).

43. Michaelis, L. and Davidshon, H., Biochem. Z. 35(1911)386.

44. Tipton, K.F. and Dixon, H.B.F., Methods Enzymol. 63(1979)183.

45. Arrhenius, Z., Z. Physik. Chem., 4(1889)226.

46. Yalow, R.S. and Berson, S.A., Nature., 184(1959)1648.

47. Blake, C. and Gould, B.J., Analyst., 109(1984)533.

48. Jenkins, S.H., Heineman, W.R. and Halsall, H.B., Anal. Biochem., 168(1988)xxx.

49. Van-Vunakis, H., Methods. Enzymol., 70(1980)201.

50. Kurstak, E., Bulletin of the world health organisation., 63(1985)793.

51. Oellerich, M., J. Clin .Chem. Clin. Biochem., 22(1984)895.

52. Monroe, D., Anal. Chem., 56(1984)921A.

53. Yolken, R.H., Rev. infect. dis., 4(1982)35.

54. Avramaes, S., Immunochemistry., 5(1969)43.

55. Asselin, W.M., Leslie, J.M. and McKinley, B., J. Anal. Toxicol. 12(1988)207.

56. Brennand, D.M., Danson, M.J. and Hough, D.W., J. Immunol. Methods., 93(1986)9.

57. Hashida, S., Ishikawa, E., Mohri, Z., Nakanishi, T., Noguchi, H. and Murakami, Y., Endocrinol. Jpn., 35(1988)171.

58. Merson, M.H., Sack, R.B., Islam, S., Saklayen, G., Huda, N., Hug, I. Zulich, A.W., Yolken, R.H., Kapikian, A.Z., J. Infect. Dis., 141(1980)702.

59. Engval, E. and Perlman, P., Immunochemistry., 8(1971)871.

60. Kohler, G. and Milstein, C., Nature., 256(1975)495.

61. Kemeny, D.M. and Challacombe, S.J., Immunol. Today., 7(1986)67.

62. Graves, H.C.B., J. Immunol. Methods. 111(1988)167.

63. Tijssen, P., "Practise and Theory of Enzyme Immunassays"., (Elsevier Amsterdam 1985).

CHAPTER THREE

OPTIMISATION OF THE BUFFER CONDITIONS FOR THE ALKALINE PHOSPHATASE-CATALYSED HYDROLYSIS OF p-AMINOPHENYLPHOSPHATE TO p-AMINOPHENOL FOR USE IN ELECTROCHEMICAL IMMUNOASSAY

3.1. INTRODUCTION

In the search for an alternative to radiolabelling as a method of detection for immunoassay, enzyme-labelled immunoassay (EIA)[1] has emerged as a very popular choice for diagnostic assay systems (discussed in chapter 2).

The enzyme label is exploited as an amplification factor of the labelled molecule. The conversion of many molecules of substrate by a single molecule of enzyme results in an amplification effect that increases the detectability of the labelled molecule. This is known as an activity amplification (AA) assay which has a theoretical limit of detection of one molecule!

Sensitive immunoassays require a highly purified enzyme with a high substrate to product turnover and a low detection limit for the reaction product. The properties of an ideal enzyme label[2] are: (i) high enzyme activity at low substrate concentrations (low K_M); (ii) the enzyme must be stable and active at the pH required for good antibody-antigen binding; (iii) that it may be detectable by an accurate and sensitive assay method; (iv) reactive groups present through which the enzyme may be covalently linked (e.g. to the antibody or antigen) with minimum loss of activity; (v) the enzyme-labelled conjugate must be stable under normal assay and storage conditions; (vi) substrates and cofactors must be safe to handle; and (vii) enzyme must be available in a soluble highly purified form at low cost.

Lysozyme[3] was the first enzyme used for homogeneous EIA and the reaction product was detected by turbidimetry. Today, the

most important enzyme labels are alkaline phosphatase[4,5], peroxidase[6,7] and galactosidase[8,9].

3.1.1. Alkaline Phosphatase as an Enzyme Label

Alkaline phosphatase has been used as a label for numerous enzyme immunoassays since the work of Engvall et al.[10], and its use has been reviewed by Miedema et al.[11]

This enzyme and its conjugates are stable, and its substrates are not hazardous. Calf intestinal alkaline phosphatase is particularly useful as a label because of its high specific activity relative to alkaline phosphatase from other sources.

As a label, the enzyme must be crosslinked to the protein (immunoglobulin etc.) and still retain its activity. An overview of such crosslinking techniques has been included in a review by Blake and Gould[1], and a useful paper on the glutaraldehyde method of coupling alkaline phosphatase to antibodies, antigens and haptens has been reported by Ford et al.[12]

Alkaline phosphatase is the enzyme label used for a competitive heterogeneous enzyme immunoassay for the heart drug, digoxin, developed by Wehmeyer et al.[13] (reviewed chapter 1). The enzyme amplification, combined with the excellent sensitivity of electrochemical detection, yields a potentially highly sensitive immunoassay[14].

3.1.2. Choice of substrate

Spectrophotometric techniques have hitherto been the most

popular means of detection used for EIA[15]. Hence, the substrates that yield products suitable for spectrophotometric determination are well documented in the literature and have been optimised for detection with this procedure. Most of these substrates are commercially available at suitable levels of purity. The commercial availability of the compound is a very important factor in the choice of substrate. However, some commercial preparations of substrates have been found to contain impurities including orthophosphoric acid [16] and inhibitors of the enzyme alkaline phosphatase[17]. Impurities may be due to spontaneous hydrolysis during storage or inadequate purification during synthesis.

The compounds phenylphosphate and p-nitrophenylphosphate (PNPP) (both optimised as alkaline phosphate substrates for detection by spectrophotometric methods) were found to be suitable for immunoassay with electrochemical detection by Heineman, Halsall and co-workers[18]. The respective products, i.e. phenol and p-nitrophenol, could both be oxidised at the glassy carbon electrode. However, both products required high potentials for oxidation, and phenol was found to foul the working electrode at concentrations greater than 40μM[19,20].

p-aminophenylphosphate (PAPP) was investigated as an alternative substrate for electrochemical immunoassay by Tang et al[9]. In this work, the buffer conditions for the activity of alkaline phosphatase with respect to PAPP were optimised for detection by LCEC. The product of the enzymatic hydrolysis of PAPP, i.e. p-aminophenol, is easily oxidised and does not foul the electrode, even at concentrations as high as 0.1 mM.

3.1.3. Mechanism of the Action of Alkaline Phosphatase

The mode of action of alkaline phosphatase on the substrate PAPP is a transphosphorylation reaction to form PAP, and is an example of a classical Michaelis-Menten enzyme-catalysed reaction. The products of the enzyme-catalysed reaction on the phosphate substrate are the parent acid (orthophosphoric acid) and an alcohol (p-aminophenol). Work has been done on elucidating the mechanism of the enzymatic hydrolysis of the monoesters of ortho-phosphoric acid, since Martland and Robison[21] first demonstrated that alkaline phosphatase could catalyse the synthesis of phosphate esters as well as causing their hydrolysis. This was later confirmed by Meyerhof and Green[22], and Morton[23,24].

The experimental conditions for this reaction are as important as the choice of substrate. The rate of the reaction outlined below also depends on the stoichiometry of the phosphoprotein, which is affected by experimental conditions, and is dependent on the source of the alkaline phosphatase. The effect of pH on the reaction catalysed by mammalian alkaline phosphatase was studied by Morton[24,25,26] who found that both transphosphorylation and hydrolysis rates decrease on lowering the pH of the reaction medium. At pH's greater than pH 8.0 the phosphate ester is in its dianionic form. At pH 4.0 it is a monoanion and at pH's less than 0.5 it is a free acid (Figure 3.1.). The effect of temperature on enzyme reactions has been discussed in section 2.1.3.

The presence of a phosphate acceptor in the reaction media greatly enhances the rate of the reaction. Hydroxylated

a

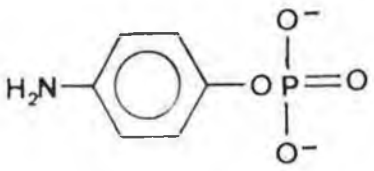

b

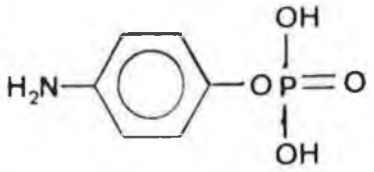

c

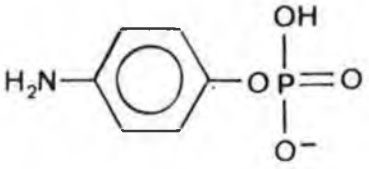

Figure 3.1. Predominant acid-base forms of the phosphate ester at: (a) > pH 8.0, (b) < pH 0.5, (c) pH 4.0.

solvents, particularly alcohols, accept inorganic phosphate thus enhancing the formation of new phosphate esters.

3.1.3.1. Proposed Reaction Mechanism:

The following mechanism has been outlined by McComb et al[27]. and is illustrated here modified for the substrate PAPP:

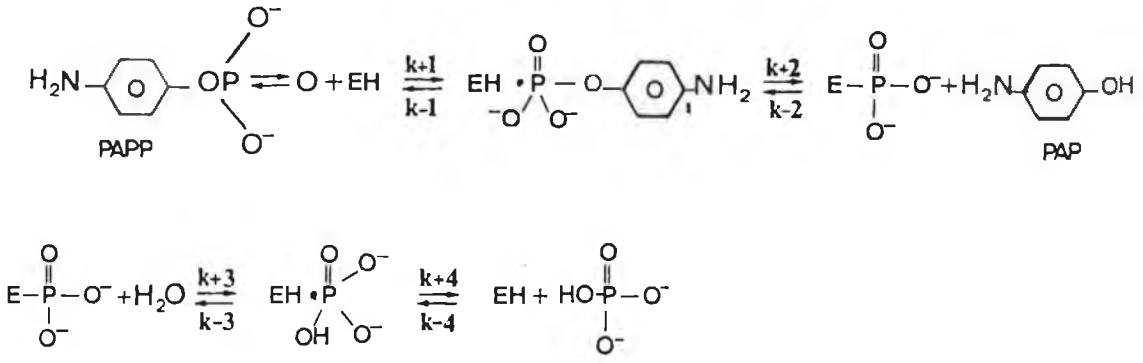

In the first step, the enzyme binds non-covalently to the substrate forming an enzyme-substrate complex. This complex then breaks down to give p-aminophenol and a phosphoprotein intermediate is formed[16], where the enzyme is covalently bound to the phosphate. It has been suggested[28] that this bond forms at the active site of the enzyme. The phosphoprotein intermediate is then converted to a non-covalent complex, with the equilibrium depending on the pH of the reaction medium. Under normal assay conditions, the pH is around pH 9.0. At this pH the non-covalent complex is more stable and the reaction continues to the right where it is terminated by the release of the enzyme and orthophosphate. This reaction may proceed in either direction. Under normal

assay conditions, where inorganic phosphate is not present and the substrate is in excess, the free enzyme combines with another substrate molecule and drives the reaction to the right.

3.1.4. Reaction Media

The choice of the reaction medium is of vital importance to the rate of the enzyme-catalysed reaction. Many of the buffers cited in the literature have inhibitory effects on the reaction and yet are still frequently used.

Inorganic phosphate is a major inhibitor of alkaline phosphatase activity. Many enzyme immunoassays use phosphate buffered saline (PBS) which contains a relatively high amount of inorganic phosphate, some of which may remain in the wells of the microtitre plate or other reaction tubes after washing step, thus affecting the assay.

Of the buffers discussed in this work, two are known to have inhibitory effects. Glycine was first cited as an inhibitor in 1946 by Bodansky[29,30,31]. This effect may be due to the chelation of group II metals (known activators of alkaline phosphatase) by amino acids[32,33] and some amino alcohols. Glycine is also a non-hydroxylated compound, and therefore does not accept phosphate. Ammonium carbonate has also been reported as a weak inhibitor of alkaline phosphatase[34].

Tris, ethanolamine and other amino alcohols have been cited as good phosphate acceptors[35,36,37]. The structure of the amino alcohol is important, because, to support transphosphorylation, the amino group must be in close proximity to the hydroxyl group.

3.2. EXPERIMENTAL

3.2.1. Materials

The enzyme used was calf intestinal alkaline phosphatase obtained from Boehringer Mannheim. The commercial preparation (10 mg/ml protein concentration) was stored in 30 mM triethanolamine buffer, pH 7.0, containing 3.0 M NaCl at less than $0^{o}C$. 1.0 mM $MgCl_2$ and 0.1 mM $ZnCl_2$ were added to the preparation as enzyme cofactors. This enzyme had a reported activity of greater than 2500 IU assayed in a 1.0 M diethanolamine buffer, pH 9.8 at $37^{o}C$ using PNPP as a substrate. 10 µl of this solution was diluted into 10 ml of a 0.1 M phosphate buffer, pH 7.0, and stored in borosilicate glass at less than $0^{o}C$.

The phosphate buffer was prepared using dipotassium hydrogen phosphate and potassium dihydrogen phosphate with 0.1% (w/v) sodium azide and 0.15 M NaCl in deionised water.

The substrate PAPP was prepared by hydrogenation of PNPP by the method of Dereimer and Meares[38]. The resulting product was washed with absolute ethanol and characterised by nuclear magnetic resonance spectroscopy (NMR).

Ammonium carbonate was prepared with ammonium chloride and sodium bicarbonate, obtained from Fischer Scientific, and adjusted to pH 9.0 with NaOH. $MgCl_2$ was added as an activator to a final concentration of 1.0 mM with respect to Mg^{2+} ions.

Trishydroxymethylaminomethane (tris) and glycine were also obtained from Fischer Scientific and the pH adjusted with HCl

to pH 9.0. These buffers also contained 1.0 mM Mg^{2+} ions. 2-ethylaminoethanol (EAE) was obtained from the Aldrich Chemical Company Inc. and the pH adjusted to 9.8 with acetic acid. Diethanolamine (DEA) was also obtained from Aldrich and was adjusted to pH 9.0 with acetic acid.

3.2.2. Methods

A hydrodynamic voltammogram was recorded to find the optimum potential at which to study the oxidation of the substrate PAPP under the conditions outlined.

Separation was achieved on a 10 cm Brownlee reverse phase C_8-column using a mobile phase of 0.1 M ammonium acetate, pH 5. The injection loop had a capacity of 20 µl, the flow rate was 1 ml/min and the chart speed was 0.5 cm/min.

A calibration curve for the product PAP was also prepared under these conditions. The rate of decay of substrate was explored in some of the buffers by making a series of injections of a solution of the substrate dissolved in the buffer of interest over a period of time and assaying for any product formed by non-enzymatic hydrolysis using LCEC.

In every procedure outlined, a fresh solution of substrate was prepared prior to analysis. For the study of the enzyme activity, two assay procedures were used and compared. These are described in the following sections.

3.2.2.1. Assay A

A series of substrate concentrations were prepared in the

buffer of interest and aliquoted into polypropylene tubes, which were kept at room temperature. Each tube was spiked with the enzyme solution (also prepared in the buffer under study) and the tube was gently shaken ten times to ensure mixing of the enzyme and substrate solutions. The incubation was timed precisely and the solution was injected into the LCEC system exactly two minutes after the enzyme had been added.

The incubation period (two minutes) was kept short so as not to allow any non-enzymatic hydrolysis of the substrate or oxidation of the product. An average value was taken over four injections and a blank was run in duplicate.

3.2.2.2. Assay B

The substrate and enzyme solutions were prepared, as for assay A, except that all solutions were kept in a 25°C water bath to prevent any temperature fluctuations. Instead of incubating all enzyme substrate mixtures for the same time and calculating the velocity from the amount of product formed, three short incubation times were chosen: i.e. 1.0, 1.5 and 2.0 minutes. The amount of product formed was plotted against the incubation time and the velocity was calculated from the slope.

Data was analysed using a program (appendix 1), based on the direct linear plot described by Eisenthal and Cornish-Bowden[39], outlined in chapter 2, as well as using the commercially available "Enzfitter" program[40], based on non-linear regression analysis of the Michaelis-Menten equation[41].

3.2.3. Apparatus

A Bioanalytical systems model 400 HPLC system with an electrochemical detector was used. The cell was a thin layer cell with a glassy carbon working electrode embedded flush with the face of the teflon cell block; a silver/silver chloride reference electrode was located separately downstream and the stainless steel mount was used as a counter electrode. Chromatograms were recorded on an x-t recorder.

3.3. RESULTS AND DISCUSSION

3.3.1. Calibration of PAP

The optimum oxidation potential for the detection of PAP in ammonium acetate buffer mobile phase, pH 5.0, was determined from the hydrodynamic voltammogram illustrated in Figure 3.2. A potential of +0.35 V was chosen for further study. It has been reported[19] that PAPP is electroactive at potentials greater than +0.66 V; hence the product may be detected without interference from the substrate. This reference[19] also reports oxidation potentials of potential interferences present in the biological matrix such as ascorbic acid, uric acid and hydrogen peroxide, all oxidised at potentials greater than +0.40 V.

A typical calibration curve for PAP solution in water is shown in Figure 3.3. This line can be represented by the equation:

$$i(nA) = 31.5\ C(\mu M) - 2.43 \qquad 3.1.$$

and was used to determine the amount of product formed in the enzyme reaction. From this, the enzyme activity was calculated in international units.

3.3.2. Studies in Ammonium Carbonate Buffer System

The enzyme activity of alkaline phosphatase for the substrate PAPP in 0.1 M ammonium carbonate buffer, pH 9.0, was determined using assay A. This buffer system was included in the

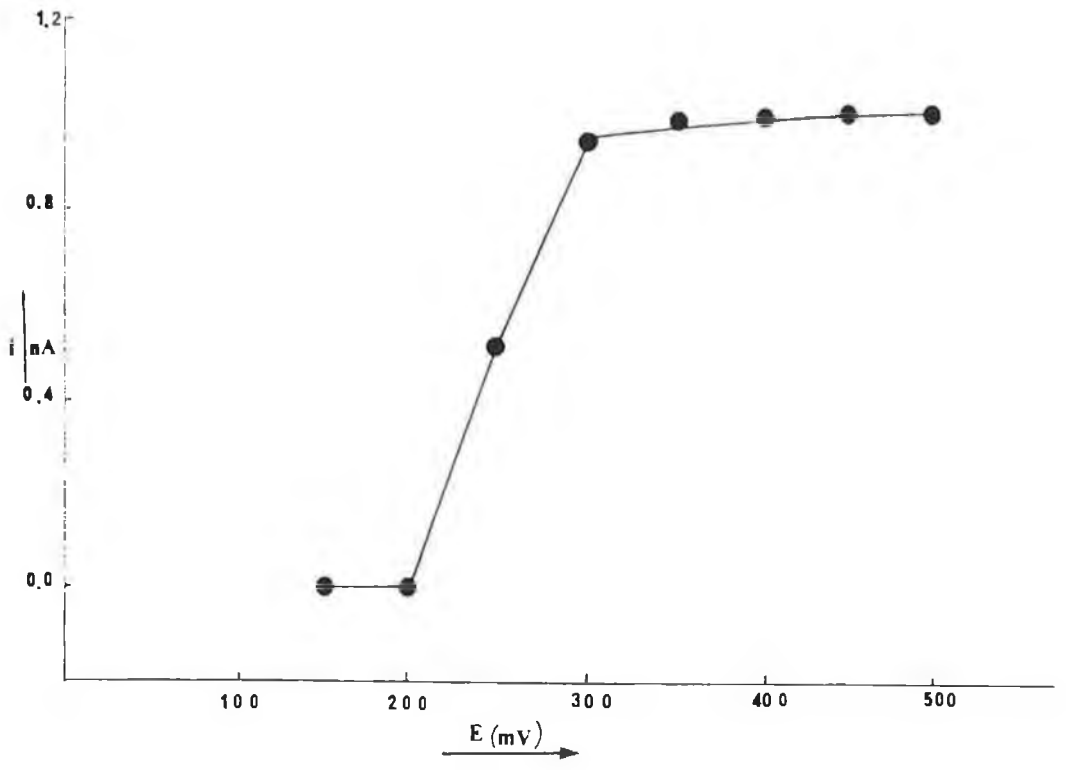

Figure 3.2. Hydrodynamic voltammogram of PAP in 0.1 M ammonium acetate mobile phase, pH 5.0.

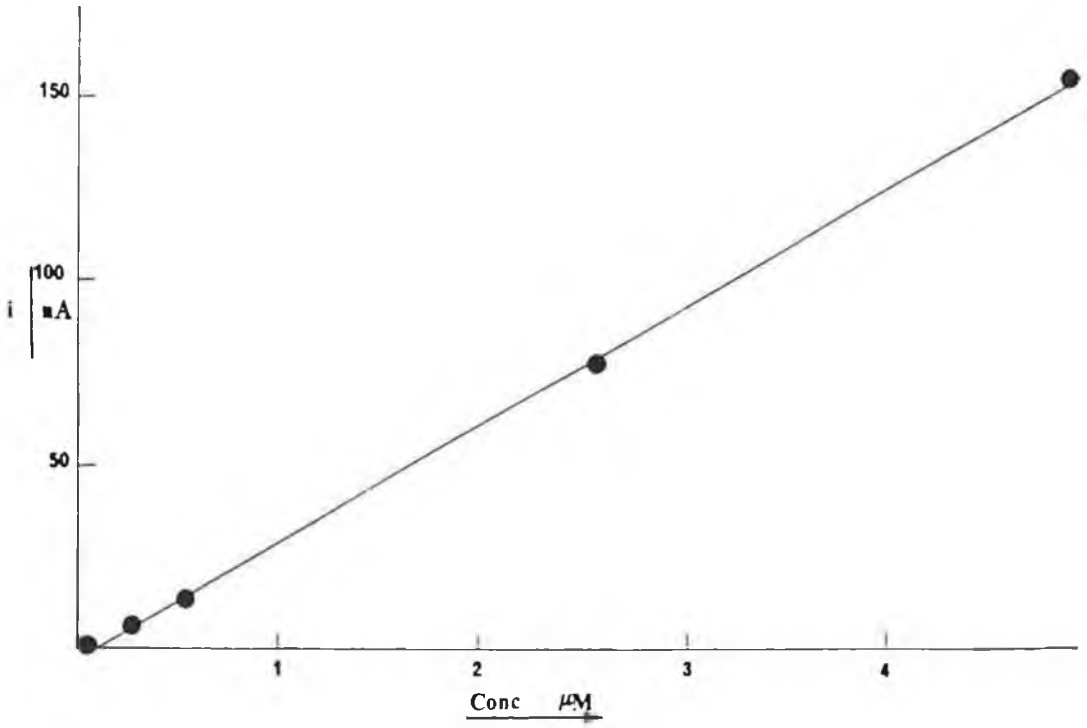

Figure 3.3. Calibration curve for a solution of p-aminophenol in water.

comparison study, as it was the system initially chosen in the development of this new substrate[19]. Although ammonium carbonate has been reported as a weak inhibitor of alkaline phosphatase[34], it is still used for studies involving alkaline phosphatase reported in the literature[42,43].

The stability of the substrate in ammonium carbonate has been described elsewhere, and the half-life of the substrate under these conditions is reported to be 7 days[19]. Nevertheless, all solutions were prepared fresh daily.

The enzyme in the ammonium carbonate buffer system gave rise to a comparable activity to that previously reported for this substrate (PAPP)[19], approximately 620 IU. The K_M value of 0.15 mM calculated by the method of Eisenthal and Cornish-Bowden[39], was comparable to the previously published value of 0.16 mM calculated by the method of Lineweaver and Burk[19]. Table 3.1. shows replicate sets of data (a and b) used to construct the substrate concentration vs. velocity curve described by the Michealis-Menten equation (Figure 3.4.), and the direct linear plot, as described by Eisenthal and Cornish-Bowden (Figure 3.5.). The velocity, in µM/min, has been obtained from average peak heights of PAP detected after a 2 minute incubation of enzyme and substrate using assay method A.

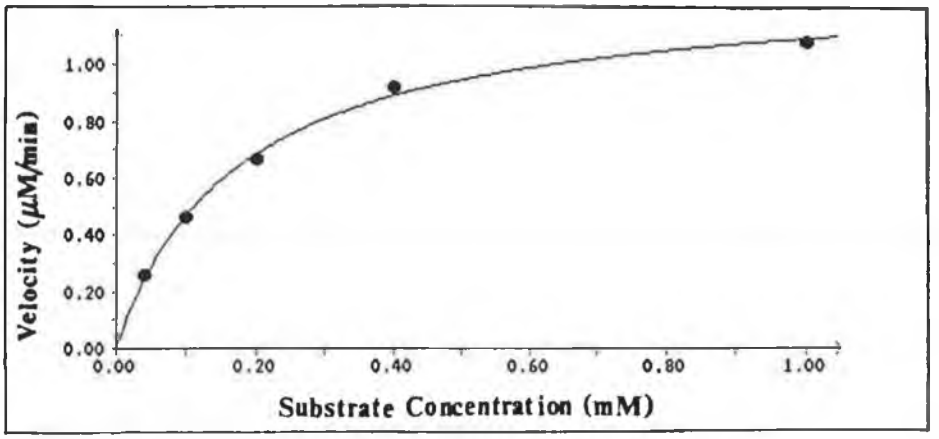

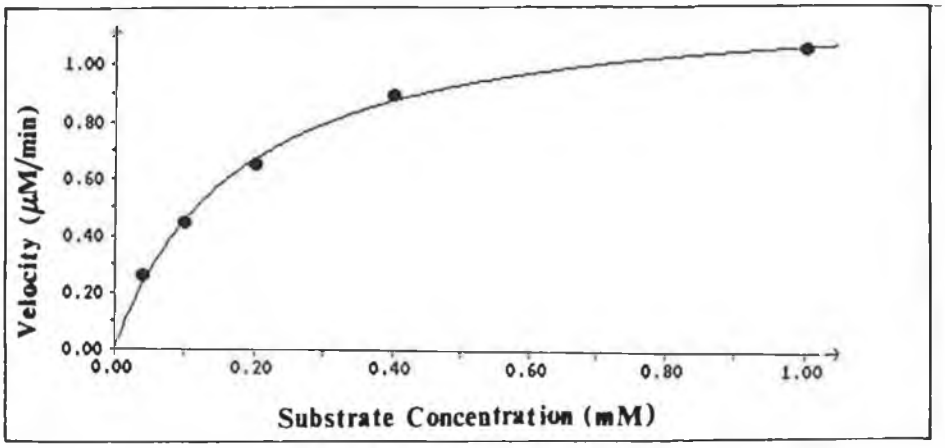

Figure 3.4. Plots of initial velocity vs. substrate concentration for the alkaline phosphatase catalysed hydrolysis of PAPP in ammonium carbonate buffer, using assay A.

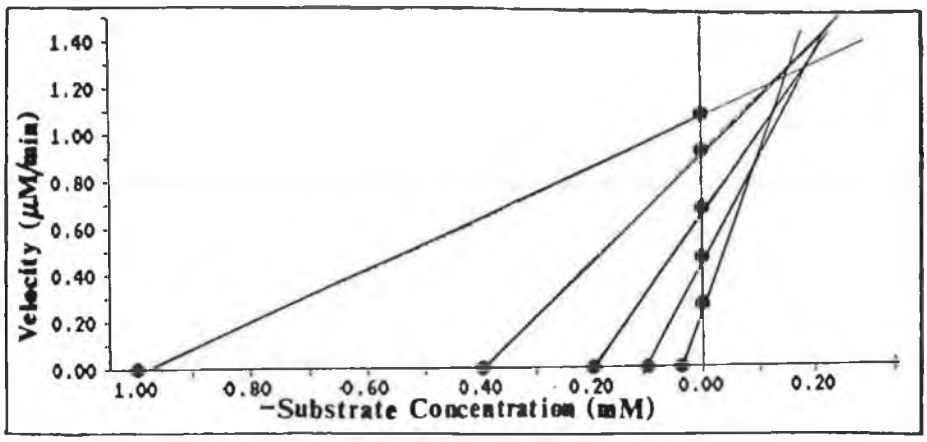

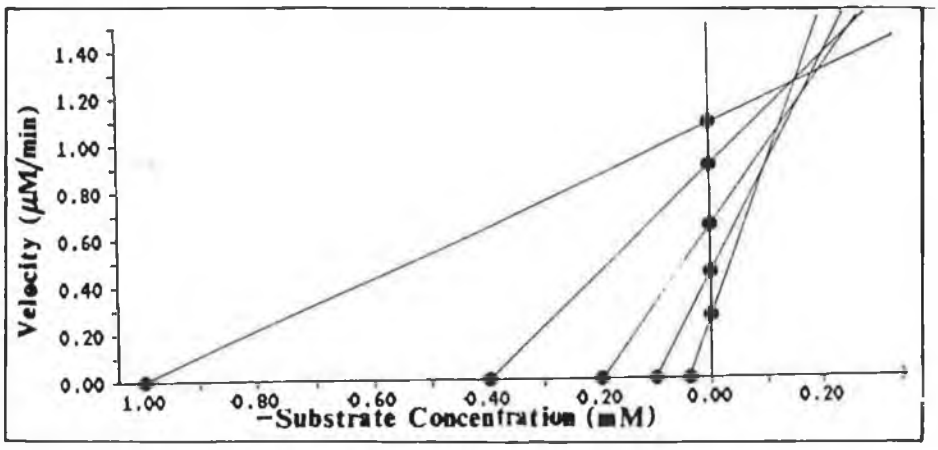

Figure 3.5. Direct linear plots of initial velocity vs. negative substrate concentration for the alkaline phosphatase catalysed hydrolysis of PAPP in ammonium carbonate buffer, using assay A.

TABLE 3.1. Substrate concentration vs. reaction velocity, for replicate sets of data a and b, in ammonium carbonate buffer system.

SUBSTRATE CONCENTRATION (mM)	VELOCITY (μM/min) a	b
1.00	1.07	1.08
0.40	0.92	0.90
0.20	0.68	0.65
0.10	0.46	0.45
0.04	0.26	0.26

a K_M = 0.17 mM V_{max} = 1.24 μM/min

b K_M = 0.15 mM V_{max} = 1.24 μM/min

3.3.3. Studies in Glycine Buffer System

The stability of PAP was tested in a 0.1 M glycine buffer, pH 9.0 This stability of PAP in glycine over a thirty minute period is illustrated in Figure 3.6. From this graph it can be seen that PAP is very stable in this buffer system, and this study also indicates that electrode fouling by the product does not occur at these concentrations. However, if the solution was left overnight, an average decrease of 22% was found in the signal. Hence, the solution was freshly prepared prior to each assay.

However, the substrate PAPP was found to degrade in the buffer by up to 10% over a one hour period. This was compensated for

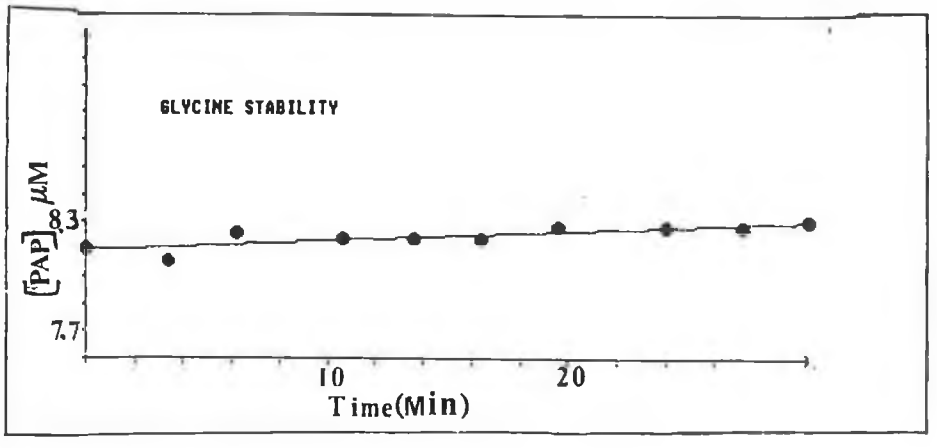

Figure 3.6. The stability profile of the enzymatic reaction product, PAP, in 0.1 M glycine buffer.

by subtracting an average blank for each series of substrate concentrations.

The results of the enzyme assay in the glycine buffer using assay A are shown in Table 3.2.

TABLE 3.2. Substrate concentration vs. reaction velocity, for replicate sets of data a and b, in a glycine buffer system.

SUBSTRATE CONCENTRATION (mM)	VELOCITY (µM/min) a	b
1.85	1.06	1.21
1.48	1.05	1.18
0.74	1.02	1.18
0.37	1.01	1.16
0.15	0.94	1.12

a K_M = 0.02 mM V_{max} = 1.26 µM/min

b K_M = 0.02 mM V_{max} = 1.15 µM/min

It has been recommended that a substrate concentration range from five times to one fifth of the estimated K_M value be used in the study. However, the velocities obtained for each substrate concentration were found to be very similar, which seems to indicate that the incubation period was too long and the velocities obtained were those approaching the maximum. This may be seen clearly from the concentration vs. velocity curves in Figure 3.7. and the direct linear plot in Figure 3.8.

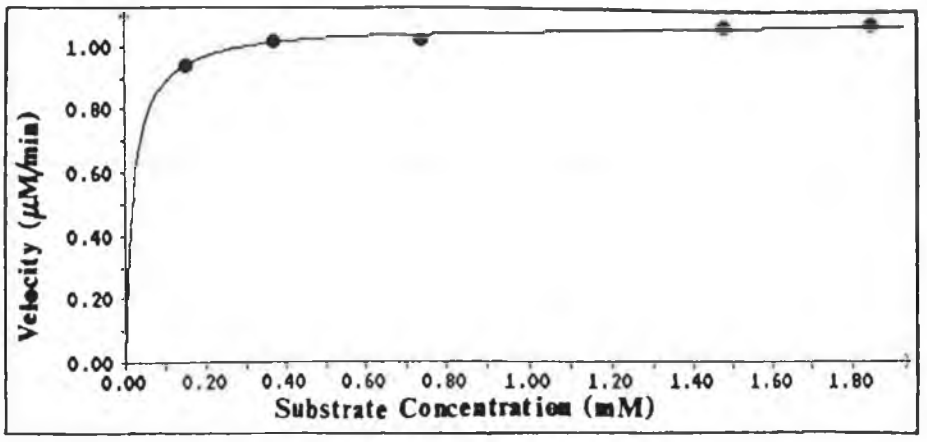

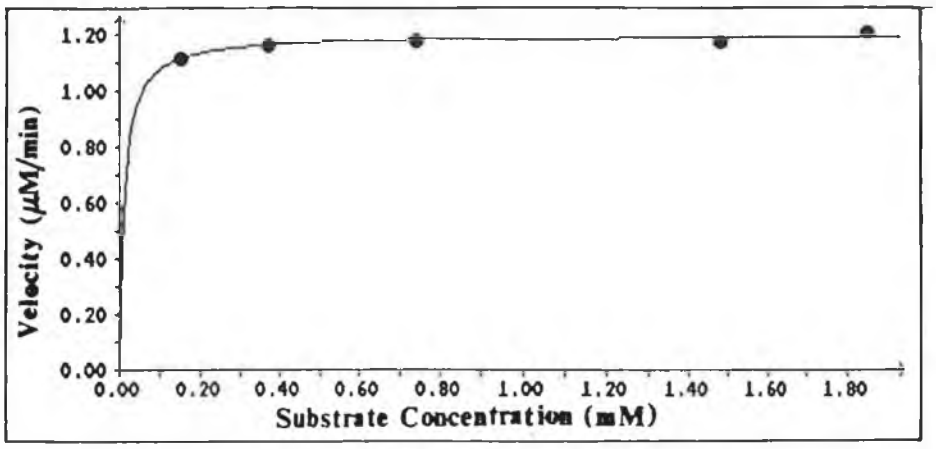

Figure 3.7. Plots of initial velocity vs. substrate concentration for the alkaline phosphatase catalysed hydrolysis of PAPP in glycine buffer, using assay A.

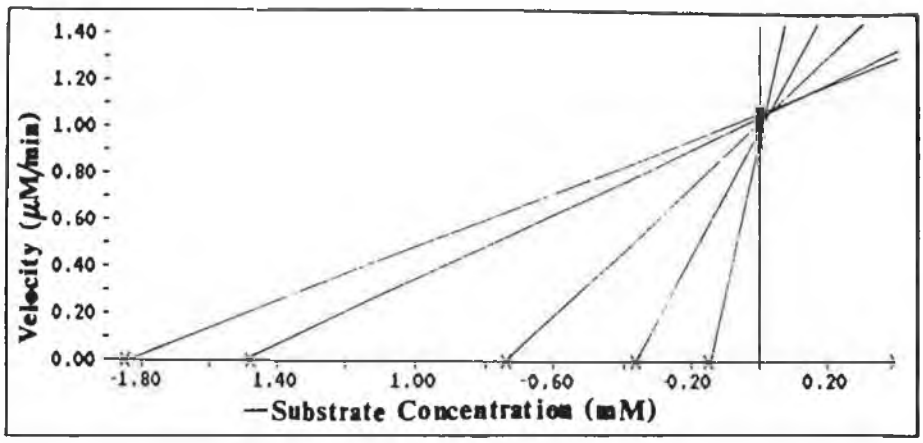

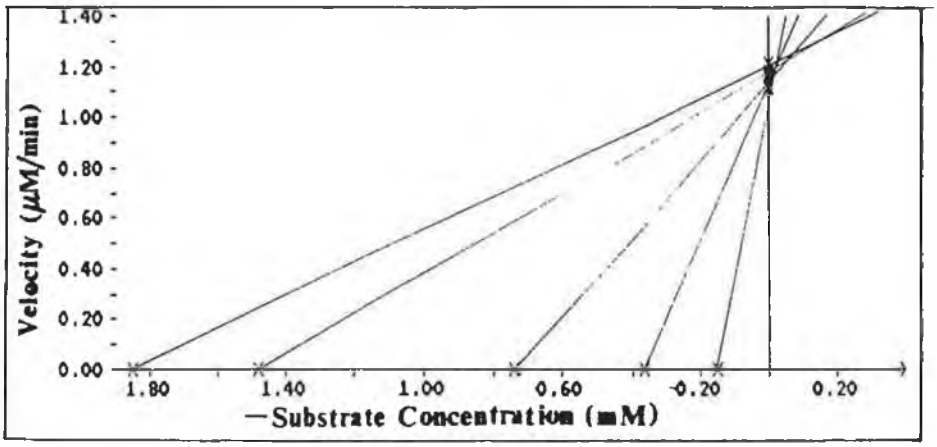

Figure 3.8. Direct linear plots of initial velocity vs. negative substrate concentration for the alkaline phosphatase catalysed hydrolysis of PAPP in glycine buffer, using assay A.

an incubation period of less than one minute is not practical with the detection system used in this study. For a more accurate estimation of K_M a wider range of substrate concentrations should be used. However, the method is valid to obtain the value for V_{max} (that is then used to calculate the enzyme activity) and an average enzyme activity of approximately 560 IU is obtained, which is within the range reported by Sigma (i.e. 500 to 700 IU), for the activity of calf intestinal alkaline phosphatase using the substrate PNPP.

It has been noted in the literature that increased concentrations of glycine causes a marked decrease in the enzyme activity of alkaline phosphatase from beef kidney[44] and human serum[45]. This was verified for calf intestinal alkaline phosphatase, since on increasing the buffer concentration to 0.5 M a decrease in activity was found. A 0.1 M concentration of glycine was therefore used as it gives rise to an acceptable activity for the enzyme and still retains its buffering capacity.

Glycine has been used as a buffer for activity studies on alkaline phosphatase (bovine intestinal mucosa) by Sigma using the substrate PNPP. At 25°C, activities between 500 and 700 IU have been reported, and under the same conditions, but at 37°C, the activity increased to 1000-1500 IU. In the same assay, using diethanolamine (DEA) as a buffer, an activity of 1000-1500 IU was reported at 25°C.

3.3.4. Studies in Diethanolamine (DEA) Buffer System

DEA has been reported to enhance transphosphorylation and has

been described as an ideal buffer for alkaline phosphatase by Hausman et al.[36] It was recommended in 1970, by the German Enzyme Commission, as the buffer to be used for reference serum alkaline phosphatase assays.

DEA has been used in a buffer system to assay calf intestinal alkaline phosphatase by Boehringer Mannheim and Sigma. The activity of 1000-1500 IU mentioned in the previous section was obtained using a 1.0 M buffer at pH 9.8, with 0.5 mM MgCl included as an activator. At a temperature of 37°C, Sigma have reported that the activity increases to between 2000 and 3000 IU, which is in agreement with Boehringer Mannheim who reported an activity of greater than 2500 IU for the hydrolysis of PNPP by calf intestinal alkaline phosphatase.

Using assay A, the values in Table 3.3. for PAPP were obtained and are illustrated in Figures 3.9. and 3.10.

TABLE 3.3. Substrate concentration vs. reaction velocity, for replicate sets of data a and b, in a DEA buffer system.

SUBSTRATE CONCENTRATION (mM)	VELOCITY (μM/min) a	b
1.00	1.06	1.00
0.40	0.91	0.87
0.20	0.66	0.67
0.10	0.42	0.45
0.04	0.23	0.26

a K_M = 0.18 mM V_{max} = 1.26 μM/min

b K_M = 0.15 mM V_{max} = 1.15 μM/min

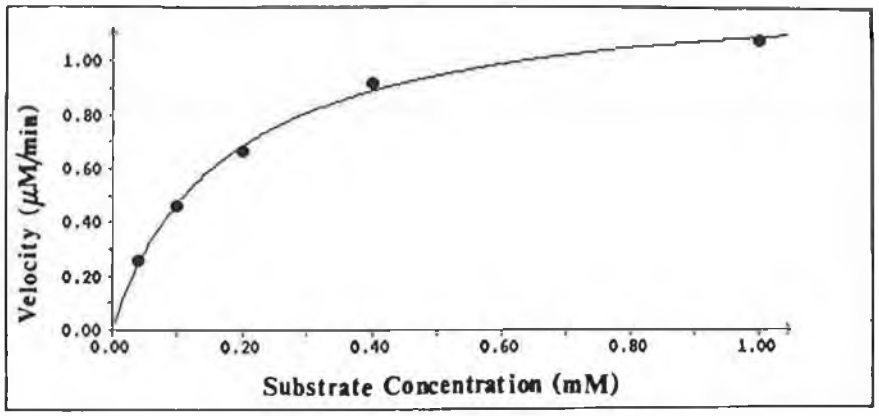

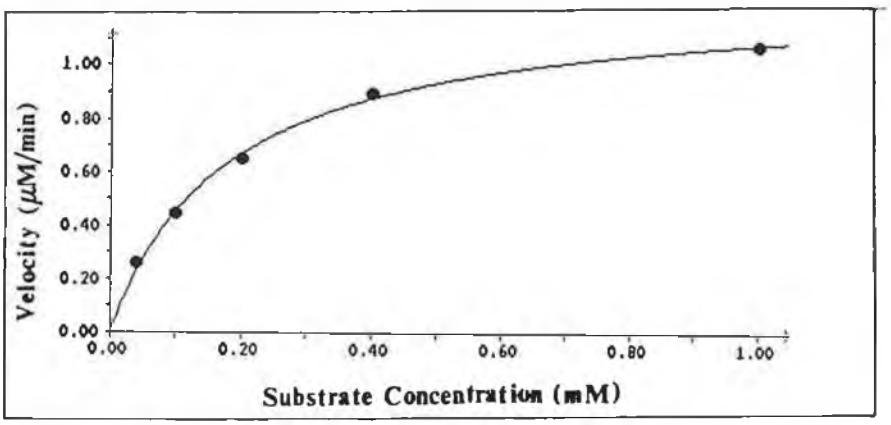

Figure 3.9. Plots of initial velocity vs. substrate concentration for the alkaline phosphatase catalysed hydrolysis of PAPP in DEA buffer, using assay A.

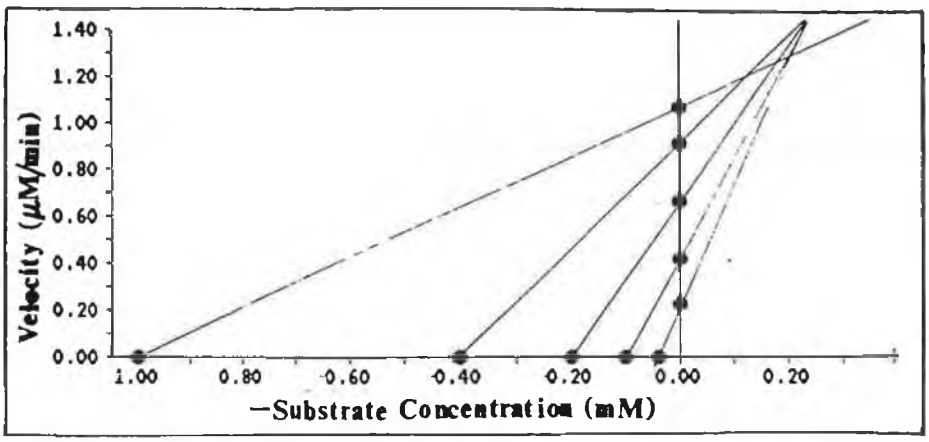

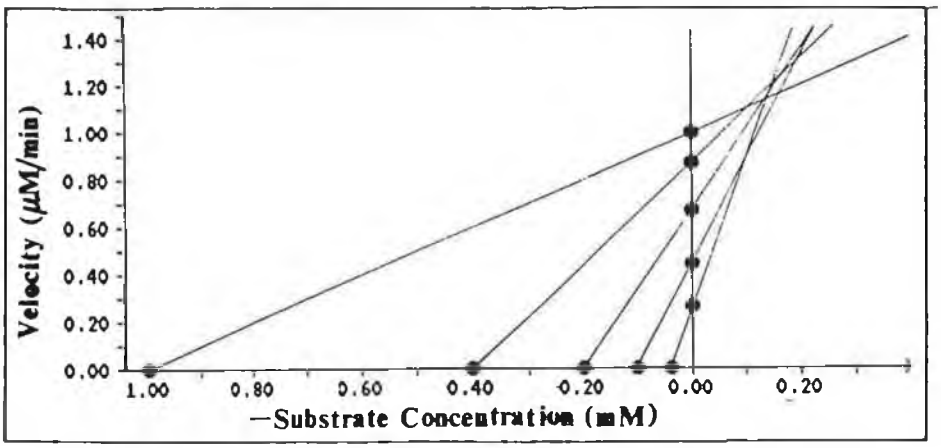

Figure 3.10. Direct linear plots of initial velocity vs. negative substrate concentration for the alkaline phosphatase catalysed hydrolysis of PAPP in DEA buffer, using assay A.

In this comparison study, an enzyme activity for DEA buffer using PAPP was found to be approximately 600 IU. This is much lower than that reported by Boehringer Mannheim or Sigma. However, the conditions were slightly different in that an 0.1 M buffer at pH 9.0 was used with a smaller concentration of activator (Mg^{2+} ions) present. In this study, the activator was added to the buffer and not to the enzyme preparation, so that for this comparison study it was only the buffer composition that was varied. $MgCl_2$ was found not to dissolve in DEA or EAE (2-ethylaminoethanol) without resulting in cloudiness (which may have damaged the LC system). The enzyme activity in these buffers (EAE and DEA) were compared with only the concentration of activator that had been added to the commercial preparation of the enzyme present. A study designed to illustrate the effect of extra $MgCl_2$ added to the buffer as an enzyme cofactor was carried out in tris buffer (section 3.3.7.1.).

3.3.5. Studies in Tris Buffer System

Tris (trishydroxymethylaminomethane or tham) is known to be a good phosphate acceptor[46] and is widely used as a buffer system for alkaline phosphatase. A 1.0 M solution of tris adjusted to pH 9.0 with HCl, was used and contained $MgCl_2$ as a cofactor. A preliminary study showed that a concentration of tris of 1.0 M resulted in a higher activity (1000 IU) than a concentration of 0.5 M (approximately 800 IU) or 0.05 M (approximately 400 IU). The results for this system using assay A are shown in Table 3.4. and Figures 3.11. and 3.12.

TABLE 3.4. Substrate concentration vs. reaction velocity, for replicate sets of data a and b, in a tris buffer system.

SUBSTRATE CONCENTRATION (mM)	VELOCITY (μM/min) a	b
1.00	1.61	1.53
0.40	1.41	1.19
0.20	0.93	0.84
0.10	0.60	0.54
0.04	0.17	0.27

a K_M = 0.24 mM V_{max} = 2.06 μM/min

b K_M = 0.25 mM V_{max} = 1.90 μM/min

It is interesting to note the variation of optimum buffer concentrations reported in the literature. Malamy et al.[47] used a 1.0 M tris buffer, pH 10.8, for their study on alkaline phosphatase with PNPP as a substrate, whereas Kulys et al.[48] reported a decrease in activity of immobilised alkaline phosphatase for PNPP on increasing the buffer concentration. The results obtained here show an increase in enzyme activity on increasing buffer concentration and are thus in agreement with observations made by McComb and Bowers[49] in a study using PAPP as the substrate. Dayan and Wilson[46] have reported an increase in the amount of product (PNP), from the hydrolysis PNPP using alkaline phosphatase from Escherichia coli, on increasing the concentration of tris. In studies of

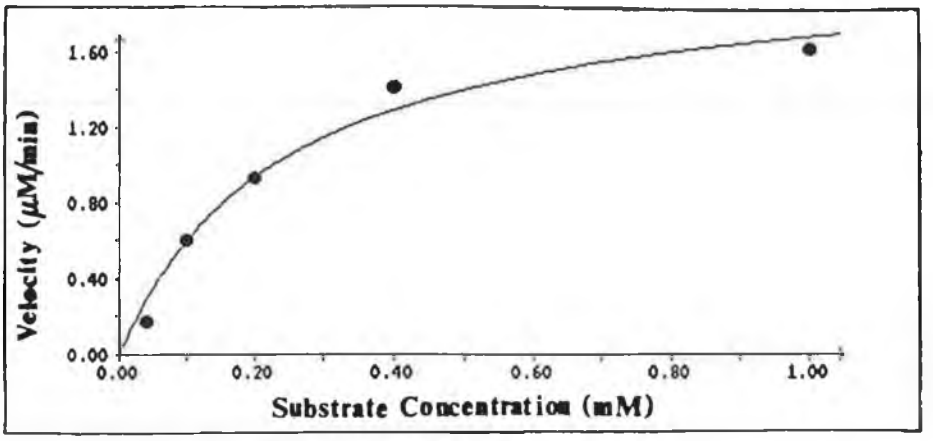

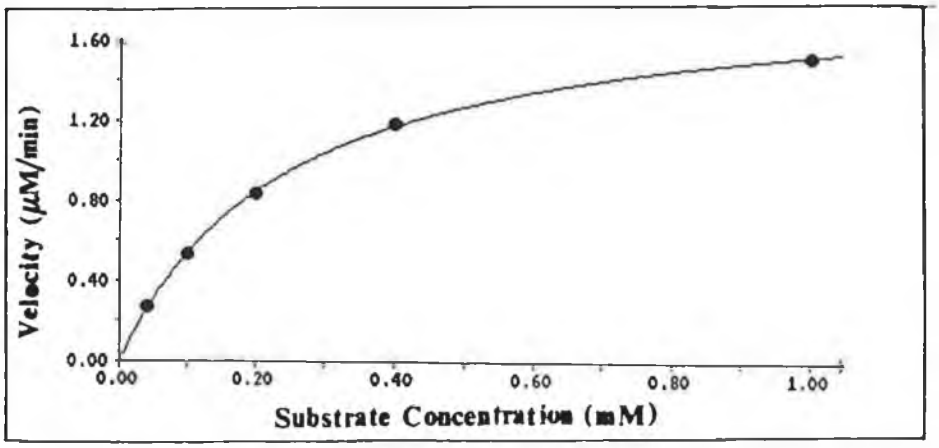

Figure 3.11. Plots of initial velocity vs. substrate concentration for the alkaline phosphatase catalysed hydrolysis of PAPP in tris buffer, using assay A.

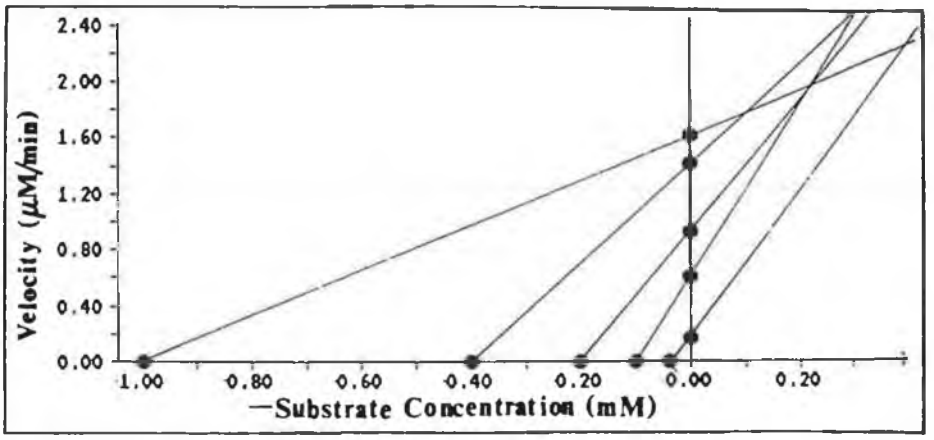

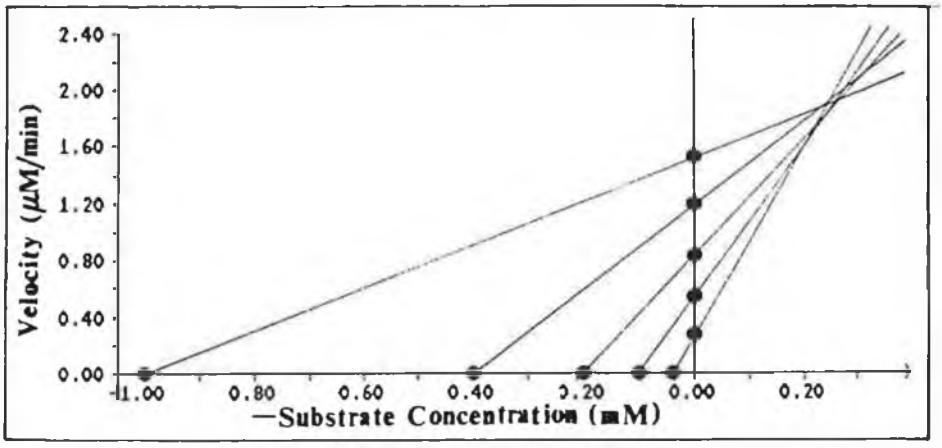

Figure 3.12. Direct linear plots of initial velocity vs. negative substrate concentration for the alkaline phosphatase catalysed hydrolysis of PAPP in tris buffer, using assay A.

human serum alkaline phosphatase activity using PNPP, tris concentrations from 0.01 M[12] to 1 M[47] are frequently cited.

3.3.6. Studies in Ethylaminoethanol (EAE) Buffer System

PAPP was found to be relatively stable in a 0.45 M EAE buffer, pH 9.0. The increase in the background level of PAP was only about 3% over two hours. The degradation of PAP was also studied, and even at a low buffer concentration (such as 0.045 M) the decay was quite considerable, being as much as 13% in an 11 minute period.

Using assay method A, irreproducible results for activity were obtained for a 0.45 M EAE buffer system, pH 9.8, ranging from approximately 1200 to 3000 IU. A plot of product formed (by enzymatic hydrolysis) vs. time is shown in Figure 3.13., which shows a considerable lag phase (relative to the incubation time used in the assay). Taking both this lag phase and the stability of PAP in this buffer system into consideration, an alternative assay (assay B) was developed as described in section 3.2.2.2.

3.3.7. A Comparison of EAE and Tris Buffer Systems

Tris and EAE exhibited the highest activities of those systems described above. A comparative study of these buffer systems was therefore carried out. Assay B was used as the assay procedure.

A new stock of enzyme was used for this part of the study prepared and stored as described in section 3.2.1.

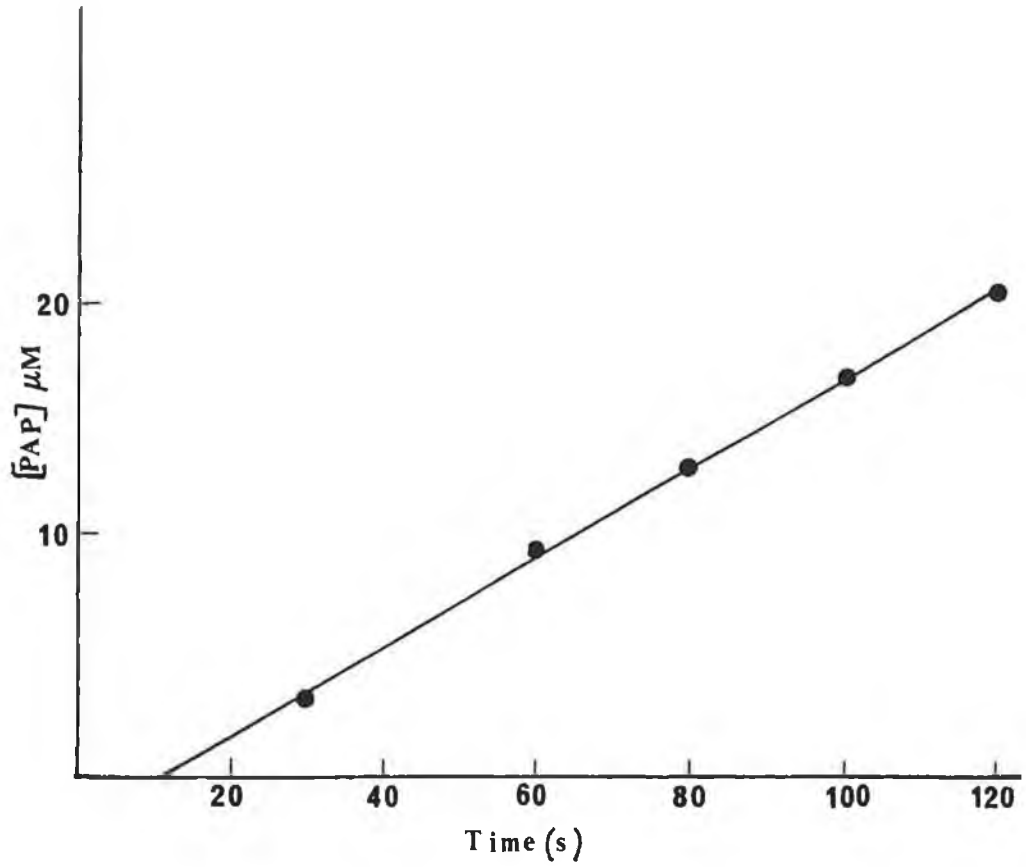

Figure 3.13. Plot of PAP concentration vs. time in EAE buffer for the alkaline phosphatase catalysed hydrolysis of PAP.

3.3.7.1. Study of Tris Buffer System Using Assay B

In the study reported in section 3.3.6. using assay method A, the enzyme exhibited a higher activity with a greater concentration of tris in the reaction media. However, the enzyme immunoassay for which this system was being optimised requires a buffer concentration of 0.1 M. A comparison of assay methods A and B was therefore made using a 0.1 M tris buffer, pH 9.0., at 25°C.

The data obtained using assay A has been tabulated in Table 3.5. and that obtained using assay B has been tabulated in Table 3.6. and the resulting plots are shown in Figures 3.14. and 3.15.

Table 3.5. Substrate concentration vs. velocity, for replicate sets of data a and b, in a tris buffer system using assay method A.

SUBSTRATE CONCENTRATION (mM)	VELOCITY µM/min a	b
0.50	3.66	3.49
0.30	3.41	3.07
0.10	2.39	2.12
0.05	0.66	1.38
0.01	0.44	0.34

a K_M = 0.09 mM V_{max} = 4.39 µM/min

b K_M = 0.12 mM V_{max} = 4.27 µM/min

The high values for maximum velocity (4.39 and 4.27 μM/min) are due to the fact that twice the amount of enzyme was used in this assay as used for the others reported in this work. This has been accounted for, in the calculations for enzyme activity and thus, may be compared with the other results reported.

Table 3.6. Substrate concentration vs. reaction velocity, for replicate sets of data a and b, in a tris buffer system using assay B.

SUBSTRATE CONCENTRATION (mM)	VELOCITY (μM/min) a	b
0.20	1.76	1.52
0.10	1.55	1.17
0.06	1.19	0.94
0.01	0.39	0.36
0.005	0.22	0.22

a K_M = 0.045 mM V_{max} = 2.15 μM/min

b K_M = 0.034 mM V_{max} = 1.68 μM/min

The activities obtained using assays A and B are similar, approximately 1000 IU. The advantage of assay B over assay A is that it may be used for systems where there is a lag or burst phase as it does not assume a (0,0) point. It has previously been mentioned that the enzyme was supplied with a small amount of activator present in the commercial preparation. To see how much the addition of more $MgCl_2$ to

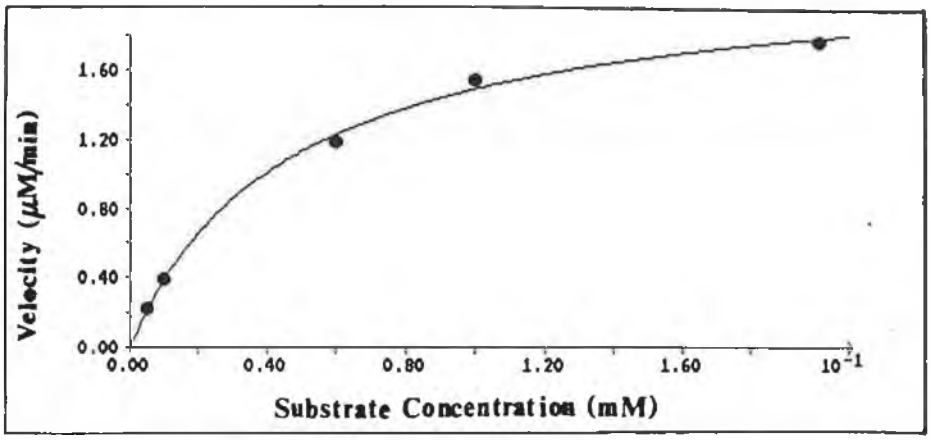

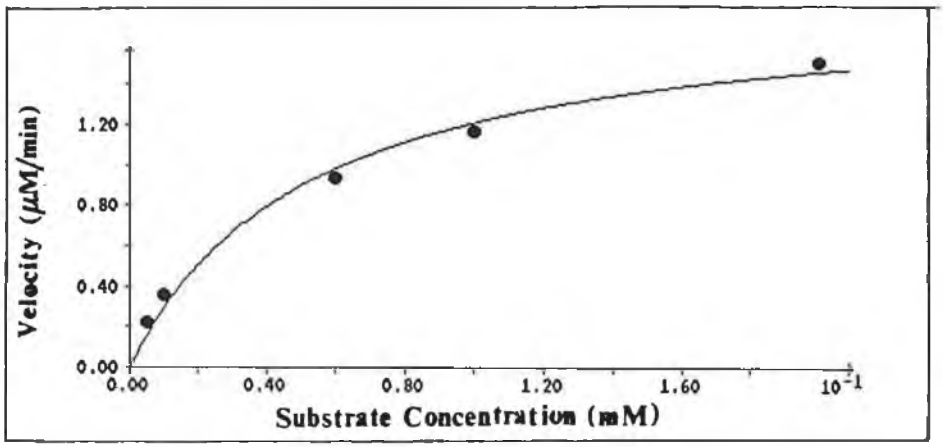

Figure 3.14. Plots of initial velocity vs. substrate concentration for the alkaline phosphatase catalysed hydrolysis of PAPP in tris buffer, using assay B.

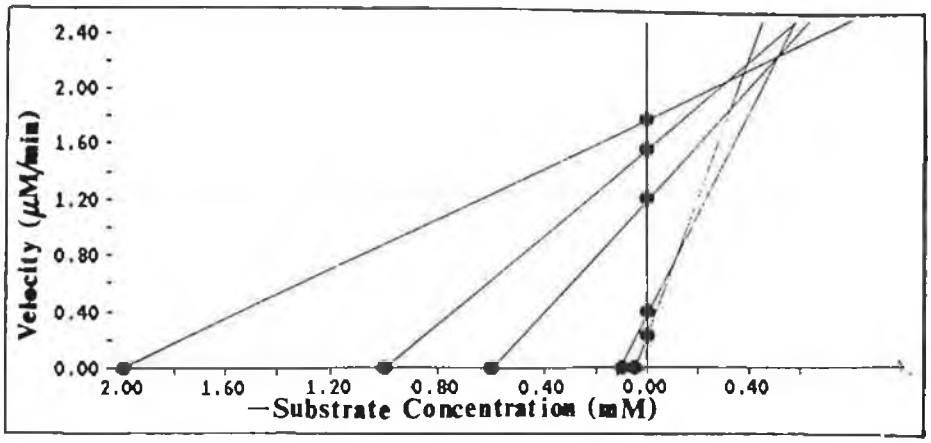

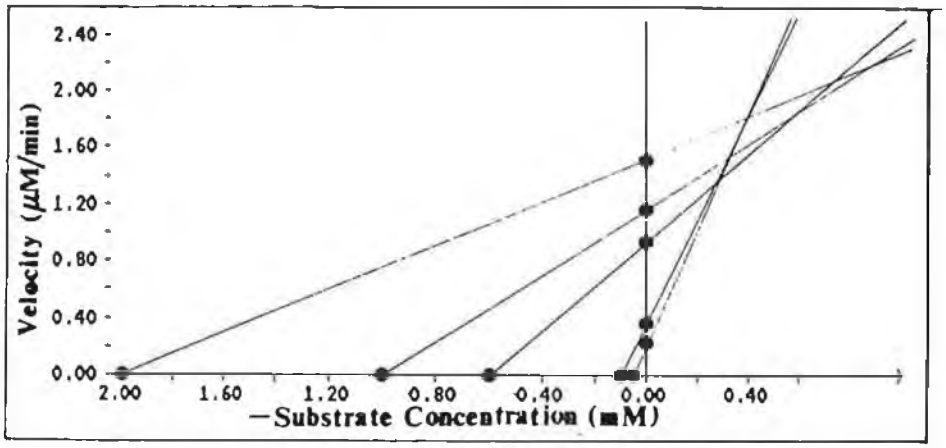

Figure 3.15. Direct linear plots of initial velocity vs. negative substrate concentration for the alkaline phosphatase catalysed hydrolysis of PAPP in tris buffer, using assay B.

the buffer actually enhanced the enzyme activity, a trial assay using tris buffer (0.1 M, pH 9.0) was run without the addition of the activator. A very slight decrease in activity was noted almost within the range of experimental error (10%).

3.3.7.2. Study of Ethylaminoethanol Buffer System using Assay B

The optimum pH determined for alkaline phosphatase activity for PAPP in EAE buffer was pH 9.8 (Figure 3.16.) and the best buffer concentration was determined to be in the range 0.15 M to 0.2 M.

From the data collected using assay method B, the concentration of product formed was plotted against the incubation time and the reaction velocity determined from the slope of this line. The increase in velocity with increasing substrate concentration is illustrated in Figure 3.17. The data obtained is tabulated in Table 3.7. below and is illustrated in Figures 3.18. and 3.19.

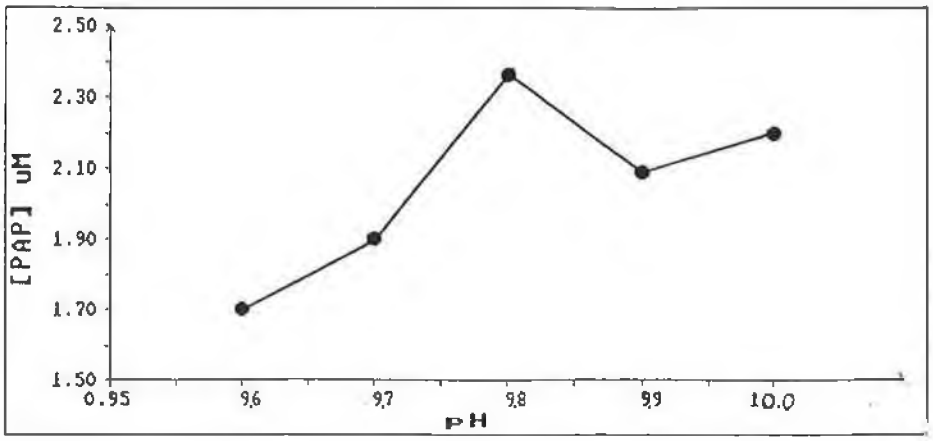

Figure 3.16. The effect of pH on the activity of alkaline phosphatase on the substrate PAPP, in an EAE buffer system.

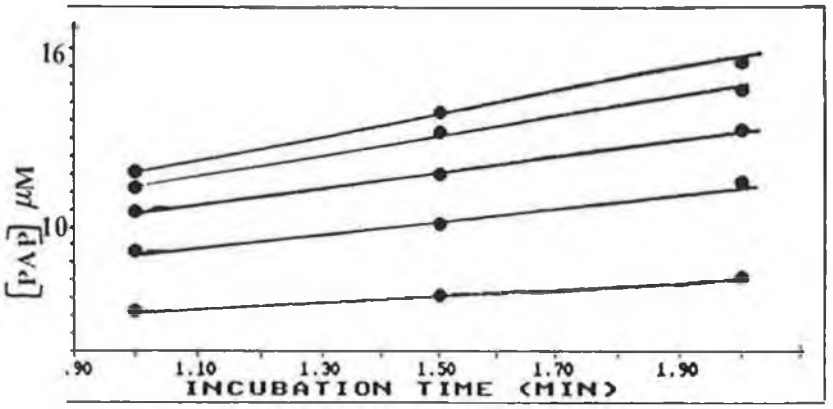

Figure 3.17. Plot of product formed (uM) vs. incubation time (min), illustrating the increase of initial velocity (determined from the slope of the line), with increasing concentration.

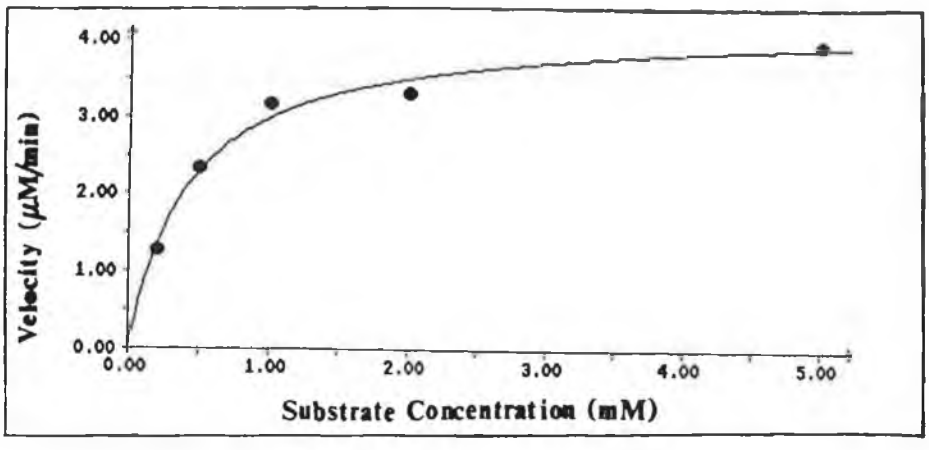

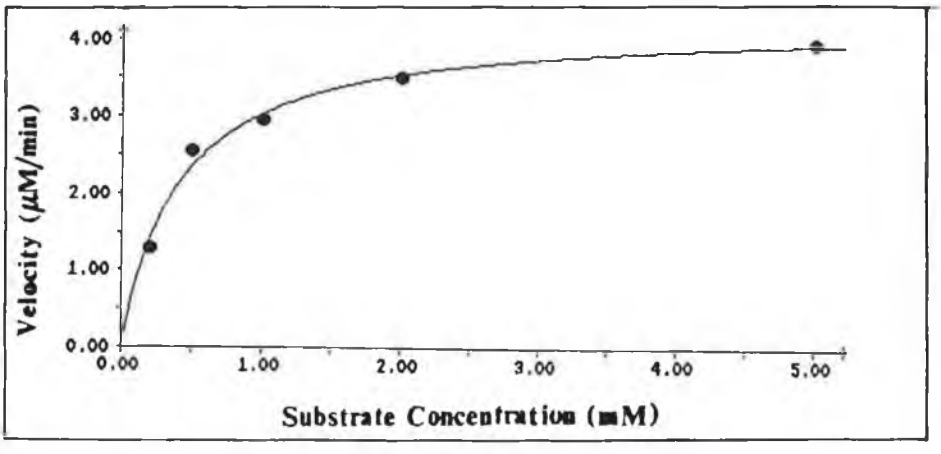

Figure 3.18. Plots of initial velocity vs. substrate concentration for the alkaline phosphatase catalysed hydrolysis of PAPP in EAE buffer, using assay B.

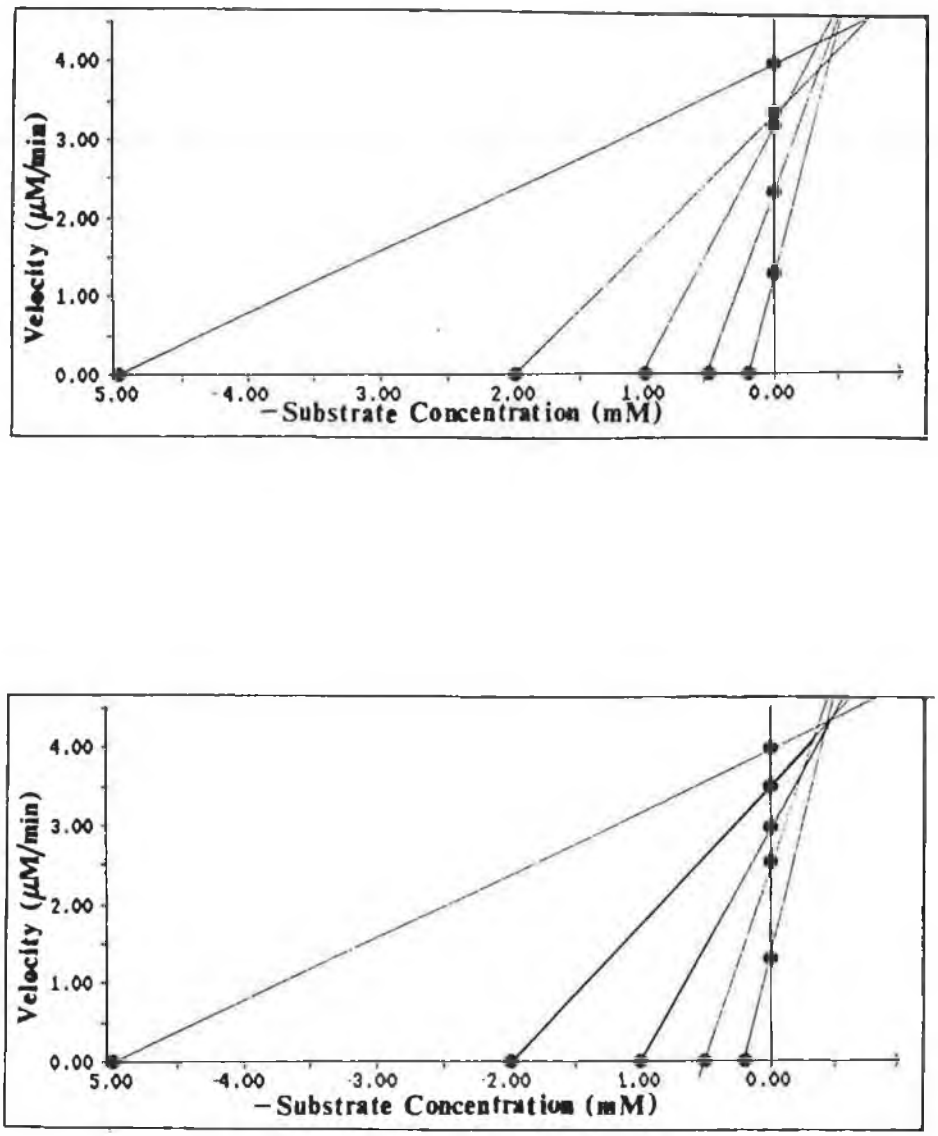

Figure 3.19. Direct linear plots of initial velocity vs. negative substrate concentration for the alkaline phosphatase catalysed hydrolysis of PAPP in EAE, using assay B.

TABLE 3.7. Substrate concentration vs. reaction velocity, for replicate sets of data a and b, in an EAE buffer system using assay B.

SUBSTRATE CONCENTRATION (mM)	VELOCITY (μM/min) a	b
5.00	3.95	3.97
2.00	3.32	3.50
1.00	3.17	2.96
0.50	2.33	2.55
0.20	1.28	1.30

a K_M = 0.45 mM V_{max} = 4.30 μM/min

b K_M = 0.46 mM V_{max} = 4.33 μM/min

3.38. Conclusion

The relative activities of alkaline phosphatase in all of the buffer systems were determined and the two buffers providing the greatest enzymatic activity were compared using assay method (B). Ethylaminoethanol and diethanolamine were used without the addition of group II metal ions as activators, as experimental problems with solubility were encountered. However, it has been reported that the addition of group II ions to chelating buffer systems such as glycine markedly enhances the activity. This effect is not as noticeable in

buffers such as DEA[51], implying that the comparison between the buffers, with and without the addition of extra $MgCl_2$, is valid.

The K_M and activities obtained for each assay system are shown in Table 3.8. It may be seen that the K_M varies considerably (and independently of V_{max}) depending on the buffer used, indicating that reaction conditions as well as substrate and the source of the enzyme determine the value for K_M as well as enzyme activity.

The reproducibility of V_{max} values within the the buffer systems was not ideal (but within $\pm$10% for most systems, Tris was 15%). This may be due to slight electrode fouling by the assay matrix or impurities that may be present in the substrate preparation. This substrate is not as yet commercially available, and although it is carefully prepared and stored, it may not as yet be pure enough for such sensitive measurements. The electrochemical detection system for this assay is a sensitive, clean and reproducible technique. The coefficient of variation within a replicate set of samples was never more than 5%. Another major advantage of this system was that the reaction was not terminated artificially (e.g by addition of trichloroacetic acid) but could instead be injected directly into the injection system which avoided the extra step of terminating the reaction.

From this work it may be seen that EAE is the buffer system that supports the highest enzyme activity. This buffer has some disadvantages however, the lifetime of the PAP in the buffer (section 3.3.6.) should be considered when choosing a buffer for immunoassay. EAE is also toxic at high

concentrations and caution must be taken when handling the substance. Tris, although not supporting as high an activity for the enzyme action on PAPP, is readily available and is a well documented buffer for use in immunoassays involving alkaline phosphatase.

		Direct Linear Method.		Non-Linear Regression.	
BUFFER		K_M (mM)	ACTIVITY (μM/min)	K_M (mM)	ACTIVITY (μM/min)
Ammonium Carbonate	a:	0.17	620	0.17	630
	b:	0.15	620	0.18	640
Glycine	a:	0.02	535	0.02	530
	b:	0.02	600	0.01	600
DEA	a:	0.18	630	0.19	640
	b:	0.15	575	0.15	580
Tris	a:	0.05	1075	0.05	1100
	b:	0.04	840	0.05	930
EAE	a:	0.45	2150	0.42	2115
	b:	0.46	2165	0.40	2125

Table 3.9. A table of K_M and enzyme activity for each of the buffer systems investigated, determined by the direct linear method[39] and non-linear regression[40].

3.4. APPENDIX A

Program to analyse kinetic data by the method of Cornish-Bowden.

```
10 REM cornish-bowden
20 DIM Y(10)
30 DIM X(10)
40 DIM S(5)
50 DIM V(5)
60 CLS
70 PRINT "DIRECT LINEAR ANALYSIS FOR ENZYME KINETICS"
80 PRINT ""
90 PRINT "       BASED ON THE METHOD OF"
100 PRINT ""
110 PRINT "    EISENTHAL AND CORNISH-BOWDEN"
120 PRINT ""
130 PRINT ""
135 INPUT "Title for data";T$
136 PRINT ""
140 PRINT "Enter substrate concentration"
150 FOR LOOP=1 TO 5
160 INPUT S(LOOP)
170 NEXT LOOP
180 PRINT ""
190 PRINT "Enter velocity"
200 FOR LOOP=1 TO 5
210 INPUT V(LOOP)
220 NEXT LOOP
230 CLS
240 N=1
250 I=1
260 FOR J=2 TO 5
270 GOSUB 1000
280 N=N+1
290 NEXT J
300 N=5
310 I=2
320 FOR J=3 TO 5
330 GOSUB 1000
340 N=N+1
350 NEXT
360 N=8
370 I=3
380 FOR J=4 TO 5
390 GOSUB 1000
400 N=N+1
410 NEXT
420 N=10
430 I=4
440 J=5
450 GOSUB 1000
460 PRINT "For the data ";T$
470 PRINT "sub";"  Vel"
490 FOR LOOP=1 TO 5
500 PRINT S(LOOP);V(LOOP)
510 NEXT LOOP
520 PRINT ""
530 PRINT "ESTIMATED VALUES FOR ..."
540 PRINT ""
550 PRINT "    Km";"           Vmax"
570 FOR LOOP=1 TO 10
580 PRINT X(LOOP),Y(LOOP)
590 NEXT LOOP
600 END
1000 Y(N)=(S(I)-S(J))/((S(I)/V(I))-(S(J)/V(J)))
1010 X(N)=(V(J)-V(I))/((V(I)/S(I))-(V(J)/S(J)))
1020 RETURN
```

3.5. REFERENCES

1. Gould, B.J., Anal. Proc., 24(1987)136.
2. Blake, C. and Gould, B.J., Analyst., 109(1984)533.
3. Rubenstein, K.E., Schneider, R.S. and Ulman, E.F., Biochem. Biophys. Acta., 47(1972)848.
4. Hansen, S.I. and Holm, J. Anal. Biochem., 172(1988)160.
5. Brennand, D.M., Danson, M.J. and Hough, D.W., J. Immunol. Methods., 93(1986)9.
6. Maciewicz, R.A. and Eitherington, D.J., Biochem. Soc. Trans., 16(1988)812.
7. Ferrante, A., Rowen-Kelly, B., Beard, L.J. and Maxwell, G.M., J. Immunol. Methods., 93(1986)207.
8. Stults, C.L.M., Wilbur, B.J. and Macher, B.A., Anal. Biochem., 174(1988)151.
9. Blake, C., Al-Bassam, M.N., Gould, B.J., Marks, V., Bridges, J.W. and Riley, C., Clin. Chem., 28(1982)1469.
10. Engvall, E. and Perlman, P., Immunochemistry, 8(1971)871.
11. Miedema, K., Boelhovwer, J. and Otten, J.W. Clin. Chim. Acta., 40(1972)187.
12. Ford, D.J., Radin, R. and Pesce, A.J., Immunochemistry., 15(1978)237.
13. Wehmeyer, K.R., Halsall, H.B., Heineman, W.R., Volle, C.P. and Chen, I.W., Anal. Chem. 58(1986)135.
14. Jenkins, S.H., Heineman, W.R. and Halsall, H.B., Anal. Biochem., 168(1988)292.
15. Chui, S.H., Wan, K.C., Lam, C.W.K. and Lewis, W.H.P., Clin. Chem., 35(1989)1770.

16. Salomon, L.L., James, J. and Weaver, P.R., Anal. Chem., 36(1964)1162.

17. Bowers, G.N.,Jr., McComb, R.B. and Horder, M., in "Expansion Scientifique Francais," ed. Siest, G. (paris 1976).

18. Wehmeyer, K.R., Halsall, H.B. and Heineman, W.R., Clin. Chem., 31(1985)1546.

19. Tang, H.T., Lunte, C.L., Halsall, H.B. and Heineman, W.R., Anal. Chim. Acta., 214(1988)187.

20. Rosen, I. and Rishpon, J., J. Electroanal. Chem., 258(1989)27.

21. Martland, M. and Robison, R., Biochem. J., 21(1927)665.

22. Meyerhof, O. and Green, H., J. Biol. Chem., 183(1950)377.

23. Morton, R.K., Nature., 172(1953)65.

24. Morton, R.K., Biochem. J., 70(1958)139.

25. Morton, R.K., Discuss. Faraday. Soc., 20(1955)149.

26. Morton, R.K., Biochem. J., 70(1958)134.

27. McComb, R.B., Bowers, G.N., Jr. and Posen, S., "Alkaline Phosphatase," (Plenum press, New York and London 1979).

28. Barman, T.E. and Gutfreund, H., Biochem. J., 101(1966)460.

29. Bodansky, O., J. Biol. Chem., 114(1936)273.

30. Bodansky, O., J. Biol. Chem., 115(1936)101.

31. Bodansky, O., J. Biol. Chem., 165(1946)605.

32. Albert, A., Biochem. J., 47(1950)531.

33. Perkins, D.J., Biochem. J., 51(1952)487.

34. Aebi, H. Abelin, I., Helv. Chim. Acta., 31(1948)1943.

35. Garen, A. and Levinthal, C., Biochim. Biophys. Acta. 38(1960)470.

36. Hausamen, T.U., Helger, R., Rick, W. and Gross, W., Clin. Chim. Acta. 15(1967)241.

37. Turner, B.M., Methods. Enzymol., 121(1986)848.

38. DeReimer, L.H. and Meares, C.F., Biochemistry., 20(1981)1606.

39. Eisenthal, R. and Cornish-Bowden, A., Biochem. J., 139(1974)715.

40. Leatherbarrow, R.J., "Enzfitter" (Elsevier Science Publisher BV, Amsterdam, 1987).

41. Michaelis, L. and Menton, M.L., Biochem. Z., 49(1913)33.

42. Rouslahti, E., Viotila, M. and Engvall, E., Methods. Enzymol., 84(1982)3.

43. Klotz, J., Methods. Enzymol., 84(1982)194.

44. Babson, A.L., Greeley, S.J., Coleman, C.M. and Philips, G.E., Clin. Chem., 12(1966)482.

45. Bowers, G.M.,Jr. and McComb, R.B., Clin. Chem., 12(1966)70.

46. Wilson, I.B., Dayan, J. and Cyr, K., J. Biol. Chem., 239(1964)4182.

47. Dayan, J. and Wilson, I.B., Biochim. Biophys. Acta., 81(1964)620.

48. Malamy, M. and Horecker, B.L., Methods. Enzymol., 9(1966)639.

49. Kulys, J.J., Jasaitis, J.J. and Razumas, V.J., Bioelectrochem. Bioenerg., 16(1986)205.

50. Mc.Comb, R.B. and Bowers,G.N. Jr., Clin. Chem. 18(1972)97.

51. Bergmeyer, H.-U., Gawehn, K. and Grassl, M., in "Methods of Enzymatic Analysis," ed. Bergmeyer, H.-U. (Acedemic press New York 1974).

CHAPTER FOUR

A Study of the Adsorptive Voltammetric Behaviour of Immunoglobulin G and Anti-Immunoglobulin G, and Application to Studies of their Interaction in Vitro

4.1. INTRODUCTION

The monitoring of the immunological reaction using electrochemical techniques is beginning to have far-reaching effects in the field of non-isotopic immunoassay, (discussed in chapter 1), and in the development of immunoselective electrodes[1]. With the exception of the pH and ion selective electrodes, electroanalytical techniques have not been popular tools among clinical chemists. However, as more and more electrochemically-based biosensors become available and new research into immunosensors is undertaken, this situation is rapidly improving.

To fully exploit the direct electrochemical detection of immunochemical reactions one must first understand the nature of the electrochemical response that is characteristic of these proteins. Factors that influence this response include the presence of electroactive groups within the protein structure, such as the disulphide linkages, the conformation of the protein at the electrode surface, and its adsorption profile.

4.1.1. The Immune System

The antibody-antigen interaction is one of the more important aspects of the immune system in all vertebrates. The two major classes of immune response are: (i) humoral antibody response; and (ii) cell-mediated immune response. It is the former response that involves the antibody-antigen interaction. Antibodies are produced by B-lymphocytes (a type of white blood cell) which are stimulated by the introduction of a foreign

body into the system. This foreign body is called an "antigen" and is capable of inducing an immune response. Some molecules are too small, however, to induce an immune response, and will do so only if attached to a large carrier molecule. Such molecules are called haptens. The antibodies circulate in the blood stream and bind specifically to those antigens that induced their production. If, for example, the antigen was a bacterial cell, upon binding to the antigen, the antibody may activate a serum protein called a complement (C) which starts a series of events resulting in lysis of the cell thus destroying the antigen.

4.1.2. Antibody Structure

An immunoglobulin (Ig) is a Y-shaped glycoprotein present in the serum and tissue fluids of all mammals. It consists of four polypeptide chains[2,3], two of which are identical heavy and two identical light chains. These chains are linked by covalent disulphide bonds, and other non-covalent forces such as hydrogen bonding help to maintain the molecule in its proper conformation. In higher mammals there are five distinct classes of immunoglobulin: IgG, IgA, IgM, IgD and IgE. These classes differ on the basis of charge, size, amino acid composition and carbohydrate content. IgG is the major immunoglobulin found in human serum, and accounts for 70-75% of the total immunoglobulin content. There are four subclasses within the IgG class, due to differences in the IgG heavy chain (γ) structure. A typical structure for an IgG molecule is illustrated in Figure 4.1.

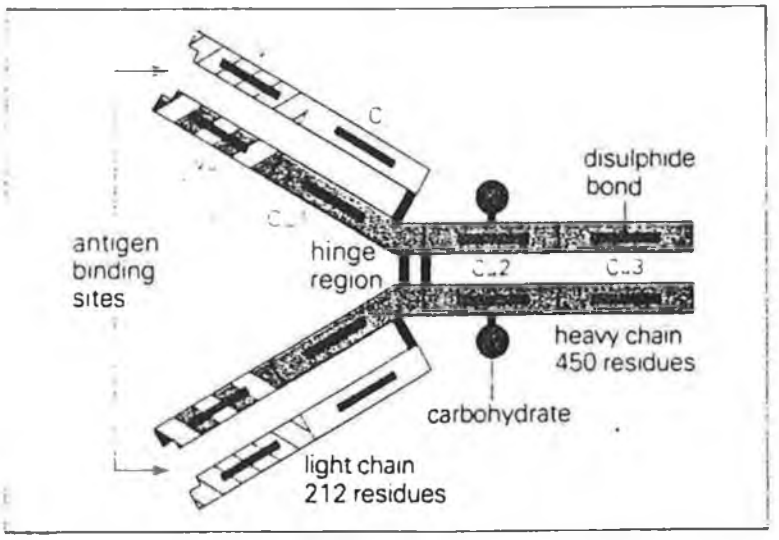

Figure 4.1. The basic structure of IgG. The unit consists of two identical light polypeptide chains and two identical heavy polypeptide chains, linked together by disulphide bonds.

The heavy chains are made up of around 450 amino acid residues (with a relative molecular mass of 50,000-77,000, depending on the subclass), whereas the light chains contain about 212 residues (approximate relative molecular mass = 25,000). The light chain may exist in two distinct forms: kappa (κ-type) and lambda (λ-type), which may be distinguished by their behaviour as antigens. The light chain also consists of two distinct regions: the carboxy terminal half (C_L) of the chain is constant in its amino acid sequence whereas the amino terminal half of the chain (V_L) is more variable in its amino acid sequence. There are two intrachain disulphide bonds within the light chain structure, each bond enclosing a peptide loop consisting of 60-70 amino acid residues forming a globular structure called a "domain". Similarly, there are four such bonds in the heavy chain.

IgG also consists of about 2%-3% carbohydrate which is covalently attached to asparagine (or in some cases serine or threonine) residues in the heavy chain. The functions of the carbohydrate are threefold:

(i) to facilitate secretion from the lymphocyte;
(ii) to enhance solubility; and
(iii) to protect the immunoglobulin from degradation.

There is a "hinge" region near the interchain disulphide links, which consists of a large number of proline residues. This flexible portion allows the "arm", or Fab region, of the molecule to rotate around an angle of greater than 100°. This flexibility accounts for the molecule's ability to bind to

two sites on the same antigen. Also the "looseness" of the protein folding in this region renders the molecule sensitive to attack by specific proteolytic enzymes.

The effect of the proteolytic enzymes, pepsin and papain on the molecule is illustrated in Figure 4.2. Papain produces two identical Fab (fragment antigen binding) fragments and one F_c portion (so called because it crystallises on isolation). On digestion with pepsin, the molecule cleaves into two portions: a $F(ab')_2$ fragment which retains the antibody binding sites, enabling it to still crosslink antigens and hence cause precipitation of the antibody-antigen complex in solution, and the remainder of the molecule which is broken down into smaller fragments.

The antibody-binding site is located in the Fab region of the molecule and is composed of the hypervariable region of both the heavy and light chains. These form a cleft into which the specific antigen determinant fits to make contact with the molecule. The F_c region mediates important functions of IgG such as complement fixation, monocyte binding and placental transmission.

4.1.3. Antibody-Antigen Interaction

The structure of an antibody molecule is very important in relation to its function to bind an antigen. Within the variable regions of the light chain, there are short polypeptide segments which show exceptional variability and are called "hypervariable regions". These are also sometimes referred to as "complementarity determining regions" (CDR) and

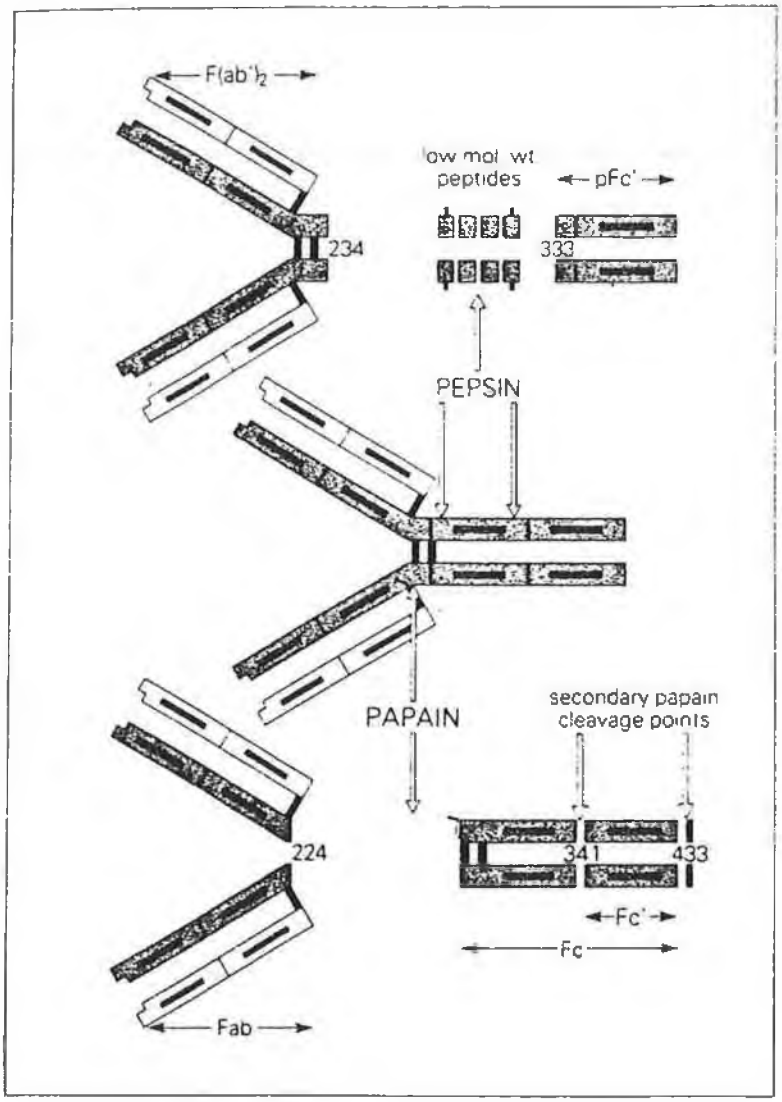

Figure 4.2. The effect of the proteolytic enzymes, pepsin and papain, on the antibody, and the antigen binding fragments produced.

are generally accepted to be directly involved in the antigen binding site.

The reaction between an antibody and its antigen take place at this binding site, where the antigenic determinant fits into the hypervariable "cleft" at the site and makes contact with 10 to 12 amino acid residues. The intermolecular forces that stabilise the antibody-antigen (Ab-Ag) complex are the same as those involved in the stabilisation of the protein structure itself. They include hydrogen bonding, where the amino- or hydroxyl groups are the major hydrogen donors, and hydrophobic interactions, where the non-polar side chains of some amino acids, such as leucine, interact with each other to ensure the exclusion of water. Van der Waals and London dispersion forces also contribute to a lesser extent. Ionic interactions, such as the attraction of $R-COO^-$ for $^+NH_3-R$, also contribute, but are not as important as the other forces for stabilisation. Another important contribution is the steric factor which arises from interpenetration of electron clouds, i.e. if the electron cloud shapes are complimentary, the steric repulsive forces will be low and the antibody will have a high affinity for that antigenic determinant. Conversely, a non-homologous determinant will have a non-complimentary electron cloud and therefore the repulsion forces will be greater, resulting in a lower affinity[4]. "Affinity" is the term used to describe the strength of binding at a single antigen binding site. Naturally occuring antigens are multivalent and are bound by a multivalent antibody. The combined binding site affinities in this case is termed "avidity".

4.1.4. Direct Electrochemical Studies of the Antibody-Antigen Interaction.

The first report in the literature of a direct electrochemical measurement of an antibody-antigen interaction was by B. Breyer and J.J. Radcliff in a letter to Nature in 1951[5]. They prepared an azoprotein by coupling egg albumin with diazotized para-aminobenzoic acid and raised an antibody against this in rabbits. A DC polarographic wave between -0.24 and -0.44 V vs SCE was obtained for the azo-protein and on addition of the specific antisera, the wave height decreased in size. If a non-specific serum was added to the solution of azoprotein it acted as a normal diluent. In a subsequent paper[6], the authors discussed how the formation and composition of the antibody-antigen complex (in the presence of excess antigen) can be readily studied by polarography, under near physiological conditions.

Fontaine et al.[7,8] have carried out extensive studies on the electrochemistry of the various subclasses of the immunoglobulin molecule. The direct electrochemical study of proteins in general is discussed more fully in chapter 6.

Kano et al.[9] have used the Brdicka current to directly monitor the interaction between human IgG and sheep anti-human IgG by polarography. This current was first reported in the early 1930's by Brdicka[10]. On studying the reduction of trivalent cobalt compounds at the DME in solutions of cobaltamines, Brdicka observed an unexpected phenomenon on the current-voltage curve in the presence of proteins. The current was a polarographic catalytic hydrogen evolution current

produced by proteins containing -SH and/or S-S groups in the presence of cobalt.

Using DC and DP polarography, Kano and coworkers[9] obtained a well defined protein wave for IgG (and anti-IgG) in terms of the Brdicka current. This current, at -1.35 V (vs SCE), increased linearly with the addition of IgG (or anti-IgG) up to about 10^{-8}M. If, however, a solution of IgG was added to the cell containing anti-IgG, the current obtained was smaller than that obtained for the sum of the currents for IgG and anti-IgG. This was explained as being due to the inaccessibility of some of the disulphide linkages for reduction due to the formation of the IgG-anti-IgG complex. This group used this reaction to determine the dissociation constants of this immunological complex. This method combined with DPP allows detection of IgG down to $5x10^{-10}$ M. The direct titration of IgG with anti IgG was also carried out at -1.28 V (vs SCE).

Rodriguez-Flores and Smyth[11] have used the technique of adsorptive stripping voltammetry (AdSV) to study the interaction of the globular protein, human serum albumin (HSA) with anti-HSA. Both proteins gave rise to two cathodic peaks at the HMDE, at -0.28 V and -0.55 V (vs Ag/AgCl) for HSA and at -0.26 V and -0.55 V (vs Ag/AgCl) for anti-HSA. On addition of anti-HSA to a solution of HSA in the electrochemical cell, a small increase in the first cathodic peak was observed; however, the second peak decreased linearly with respect to the amount of antibody added. On addition of non-specific anti-sera, such as anti-mouse IgG, no decrease in the second cathodic peak was seen; instead, the normal current increase

that would be expected on the addition of non-specific protein was seen.

Borrachera et al.[12] have monitored the interaction of the immunoglobulin IgE with its antibody (anti-IgE). The peak potentials of -0.20 V and -0.51 V found for IgE agree with those obtained for IgG in this work, and the peak decrease for the second cathodic peak was similar to that obtained in this work on addition of anti-IgE to IgE. However, the results were not completely analagous to those obtained in this work for the reaction of mouse IgG and anti-mouse IgG, as there was no decrease noticed in the first cathodic peak (-0.2 V vs Ag/AgCl) for IgE, as there was for IgG.

The main objective of this chapter is to report on the adsorptive stripping voltammetric behaviour of two immunoglobulins, namely mouse immunoglobulin G (IgG) and its specific antibody, anti-mouse IgG (raised in a donkey), and to report on the direct electrochemical detection of the interaction of these immunoglobulins <u>in vitro</u>.

4.2. EXPERIMENTAL

4.2.1. Reagents

All reagents used were of analytical reagent grade and solutions were prepared in water obtained by passing distilled water through a Waters Milli-Q water purification system. An 0.1 M phosphate buffer was prepared using sodium di-hydrogen orthophosphate (Reidel de Haen) and disodium hydrogen orthophosphate (May and Baker), and the pH was adjusted to pH 7.4 with NaOH. Oxygen-free nitrogen (IIG) was passed through a vanadous chloride scrubbing system before being used to deoxygenate the sample solution.

0.02 M phosphate buffered saline (PBS), pH 7.0, was prepared as for phosphate buffer above, except 9 g l^{-1} NaCl was added. For electrophoresis, the resolving gel was made up of 9.9 ml acrylamide stock solution, 15.0 ml of 0.75 M tris buffer with 0.2% sodium dodecyl sulphate (SDS) adjusted to pH 8.8 with 1 M HCl, 15 ml of (N,N,N',N',-Tetramethylethylenediamine) TEMED, 1.5 ml 1% ammonium persulphate and 5.1 ml of water. The stacking gel was prepared with 2 ml of acrylamide stock solution, 10 ml of 0.25 M tris with 0.2% SDS adjusted to pH 6.8 with 1 M HCl, 5 ml of TEMED , 0.5 ml of 1% ammonium persulphate and 8 ml of water. Both of these solutions were degassed before use.

The sample for electrophoresis was prepared in 100 ml of 0.0625 M tris buffer with 2% SDS adjusted to pH 6.8 with 1 M HCl, 10% (v/v) glycerol, 5% (v/v) 2-mercaptoethanol and 0.1 ml of 1% bromophenol blue. The electrode buffer was 0.025 M with

respect to tris buffer, 0.192 M with respect to glycine buffer, 0.1% with respect to SDS and was adjusted to pH 8.3 with 1 M HCl.

Mouse IgG was obtained from Sigma and the antibody to this was raised in a donkey according to the method of Dwyer et al[13]. The serum (taken from a donkey innoculated with mouse IgG) was purified according to the procedures outlined in 4.2.3. below.

4.2.2. Apparatus

A Waters Model 6000A HPLC pump was operated in conjunction with a Waters Protein Pak 300 SW gel filtration column for HPLC separations. Detection was carried out using a Waters Model 440 absorbance detector. Adsorptive stripping voltammograms were obtained using a Princeton Applied Research Corporation (PARC) Model 264 polarographic analyser, combined with a PARC Model 303 mercury electrode system, containing a platinum counter electrode and a Ag/AgCl reference electrode, a PARC Model 305 magnetic stirrer and an Omnigraph Model 2000 X-Y recorder. A PARC Model 175 Universal Programmer was coupled to this system for cyclic voltammetry.

The absorbances from the Bradford protein assay were read on a Biotex EL-307 ELISA (Enzyme Linked Immunosorbent Assay) reader.

4.2.3. Protein Purification

The donkey anti-mouse IgG (anti-IgG) was purified from donkey serum using the procedures outlined below. The proteins were separated on the basis of size (gel-filtration), charge (sodium

dodecyl sulphate polyacrylamide-gel (SDS-PAGE) electrophoresis[14]) and specific affinity, (affinity chromatography[15]).

The purified protein was then stored at <4°C, and if frozen was aliquoted to avoid denaturation as a result of freeze thawing.

4.2.3.1. Ammonium Sulphate Precipitation

Ammonium sulphate precipitation is a salt precipitation procedure which causes the precipitation of a crude fraction of immunoglobulins from crude sera. This fraction is relatively free of albumin, one of the major contaminating proteins in serum.

The donkey serum was diluted 1:2 with a 0.14 M saline solution. Saturated ammonium sulphate (SAS) was added dropwise to make a final concentration of 45%. The solution was centrifuged at 1000 g and washed in 45% SAS and centrifuged again. The precipitate was then dissolved in 0.02 M phosphate buffered saline (PBS) to a total volume equivalent to the original. This precipitation procedure was repeated using 40% SAS and the resulting precipitate was dissolved in a minimum volume of saline. This fraction contains crude immunoglobulin and was dialysed overnight at 4°C against PBS. The stirred solution was changed at least three times until no more salt was detected (compared to a $BaCl_2$ standard). The anti-serum was further purified for specific immunoglobulins using affinity chromatography.

4.2.3.2. Affinity Chromatography

Affinity chromatography was employed using an immunoadsorbent containing CNBr activated Sepharose with 10 mg ml^{-1} pure mouse IgG. The column capacity was 1 ml. Before use the column was washed with 0.02 M PBS until no trace of protein was detected with the modified Bradford assay. Fractions were collected at one ml intervals and stored at <4°C for the protein assay. The fraction containing crude anti-serum was then introduced onto the column and 0.02 M PBS was added to remove any unbound protein. The dissociating buffer (0.1 M glycine/HCl, pH 2.5) was then added, allowed to elute to the end of the column, then the flow was stopped for 15 minutes. The specific anti-mouse antibodies were then eluted with 0.1 M glycine/HCl. The column was regeneratd with 0.1 M tris/HCl, pH 8.0 and 0.1 M sodium acetate, pH 4.0. The pH of each fraction was adjusted to pH 8.0 with solid tris and analysed using the modified Bradford assay, for protein content.

4.2.3.3. Modified Bradford Assay

Standards of bovine serum albumin (BSA) in the range 0.0 to 0.5 $mgml^{-1}$ were prepared in 0,02 M PBS. The assay was performed using a microtitre plate, 200 µl of a 1:4 dilution of "Bradfords reagent" was first dispensed into a series of wells. 10 µl of the standards or sample was then added and mixing was acheived by moving the covered plate gently backwards and forwards on the bench. After a certain time (between 5 and 60 min) the absorbance was recorded at 600 nm

using the ELISA reader and the protein concentration was determined. This assay was performed in duplicate. The pure anti-IgG fraction was then characterised using HPLC and SDS-PAGE electrophoresis[15].

4.2.3.4. Sodium Dodecyl Sulphate Polyacrylamide Gel Electrophoresis

The SDS-PAGE gel was prepared using a vertical mould and the resolving gel described in section 4.2.1. The resolving gel was allowed to polymerise for two hours before being overlaid with a stacking gel. The mould was then left to stand overnight. To begin the separation, the electrophoresis tank was filled with two litres of electrode buffer. 400 ml of this buffer was then added to the upper reservoir and the cooling water applied. The samples and standards were boiled with sample buffer for two minutes and 25 µl of sample added to the appropriate well. The gel was set into the tank and a constant current of 50 µA applied for approximately one hour and forty minutes. The gel was then removed from the tank, fixed for one hour, stained for two hours, and then destained overnight.

4.2.3.5. High Performance Liquid Chromatography

The fraction containing the anti-mouse IgG was also characterised by high performance liquid chromatography (HPLC). The protein sample was first dissolved in potassium phosphate buffer, pH 7.0. The sample was then injected onto a Waters Protein Pak 300SW column using a flow rate of 0.5 ml

min^{-1}. Detection was acheived using an ultra-violet detector set at 280 nm.

4.2.4. Voltammetric Procedures

Before each voltammetric investigation, the electrolyte (phosphate buffer) was purged with oxygen-free nitrogen for not less than 8 minutes. On addition of sample, the solution was purged for a further 30 seconds. Care was taken to avoid frothing the protein solution which may cause denaturation of the protein.

The potential was then set at the optimum accumulation potential (E_{acc}) for the optimum accumulation time (t_{acc}) with stirring at 400 rpm. The stirring was then stopped automatically and after a 15 second equilibration time, the potential scan was initiated.

After working with protein, the system was cleaned extensively with dilute nitric acid to remove any protein that may have adsorbed onto the glass or plastic components of the system, such as the capillary or stirring bar etc., as this would cause major contamination in the next experiment.

4.3. RESULTS AND DISCUSSION

4.3.1. Immunoglobulin Purification

A typical affinity chromatogram for the isolated anti-mouse IgG is shown in Figure 4.3. The first set of peaks are due to any immunoglobulins present in the serum that do not have binding sites specific for mouse IgG. Non-specific proteins, such as albumin, were extracted by ammonium sulphate precipitation. The peak, obtained between fraction numbers 43-47, is due to the fraction containing the specific anti-mouse immunoglobulin. The fraction containing pure immunoglobulin was then characterised by SDS-PAGE electrophoresis and HPLC, as described in the Experimental section.

The SDS-PAGE electrophoretic gel is represented in Figure 4.4. (the original is not a permanent record). The pure standard immunoglobulin (a) has two bands: one, representing the heavy chain portion of the molecule(h) and the other representing the light chain portion (l). The crude serum (b) contains more bands due to the many other protein species normally present. It may be seen that after purification, the sample, (c), shows only two bands, those of pure IgG.

The HPLC chromatogram of a pure immunoglobulin standard and the affinity purified anti-serum are compared in Figure 4.5. It may be seen that the isolated anti-mouse IgG is very pure with no contaminating peaks.

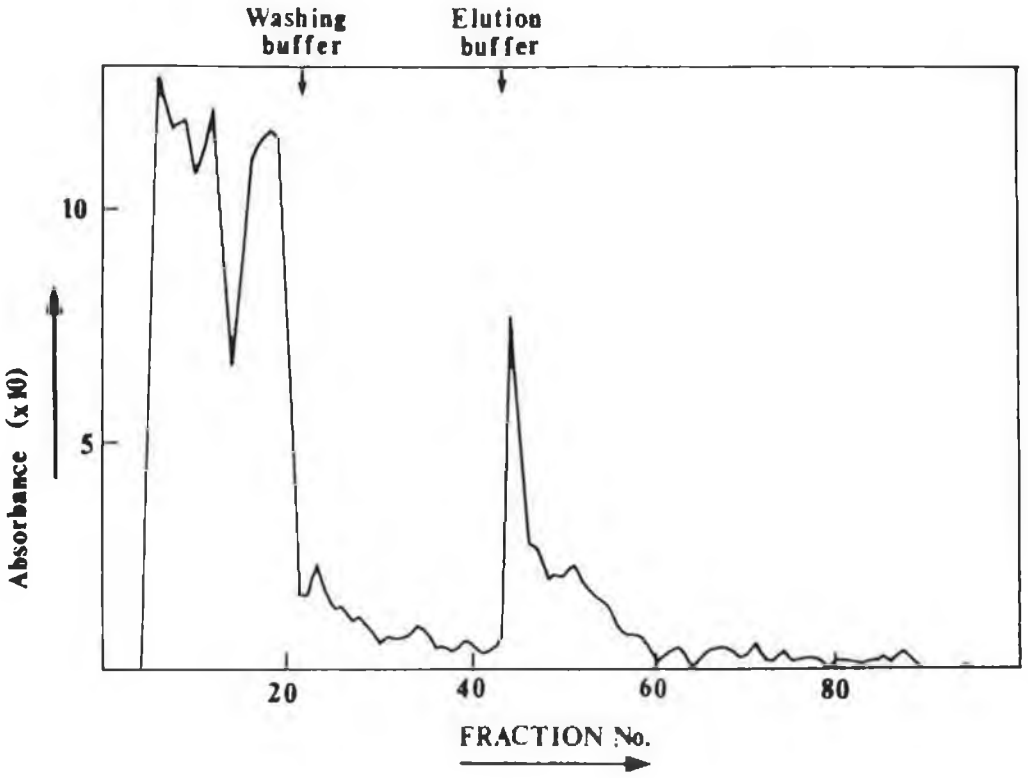

Figure 4.3. A typical affinity chromatogram for the isolation of anti-IgG from donkey serum, absorbance was measured at 600 nm.

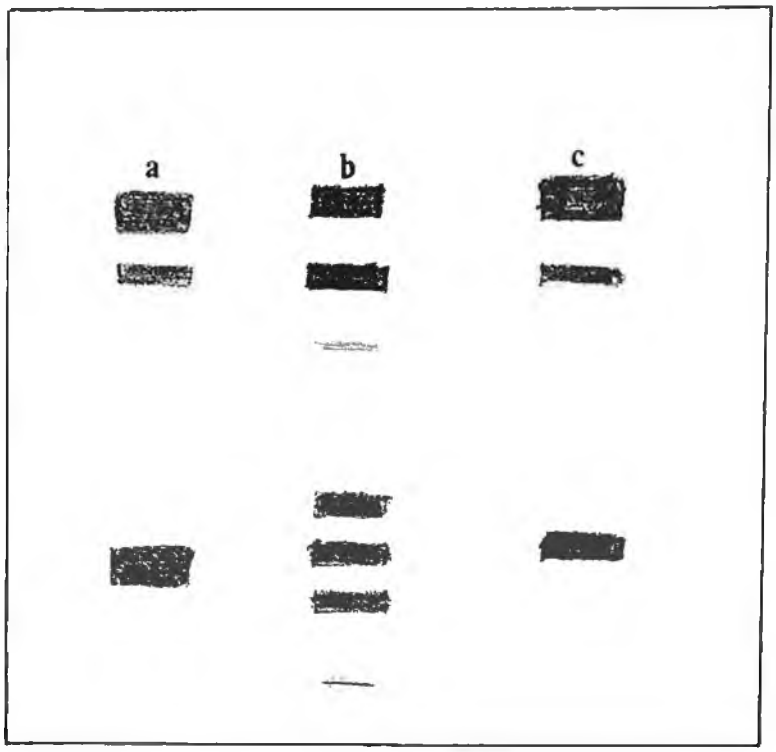

Figure 4.4. A representation of separation on an SDS-PAGE electrophoresis gel, showing: (a) the immunoglobulin standard bands; (b) the crude serum; and (c) the affinity purified sample.

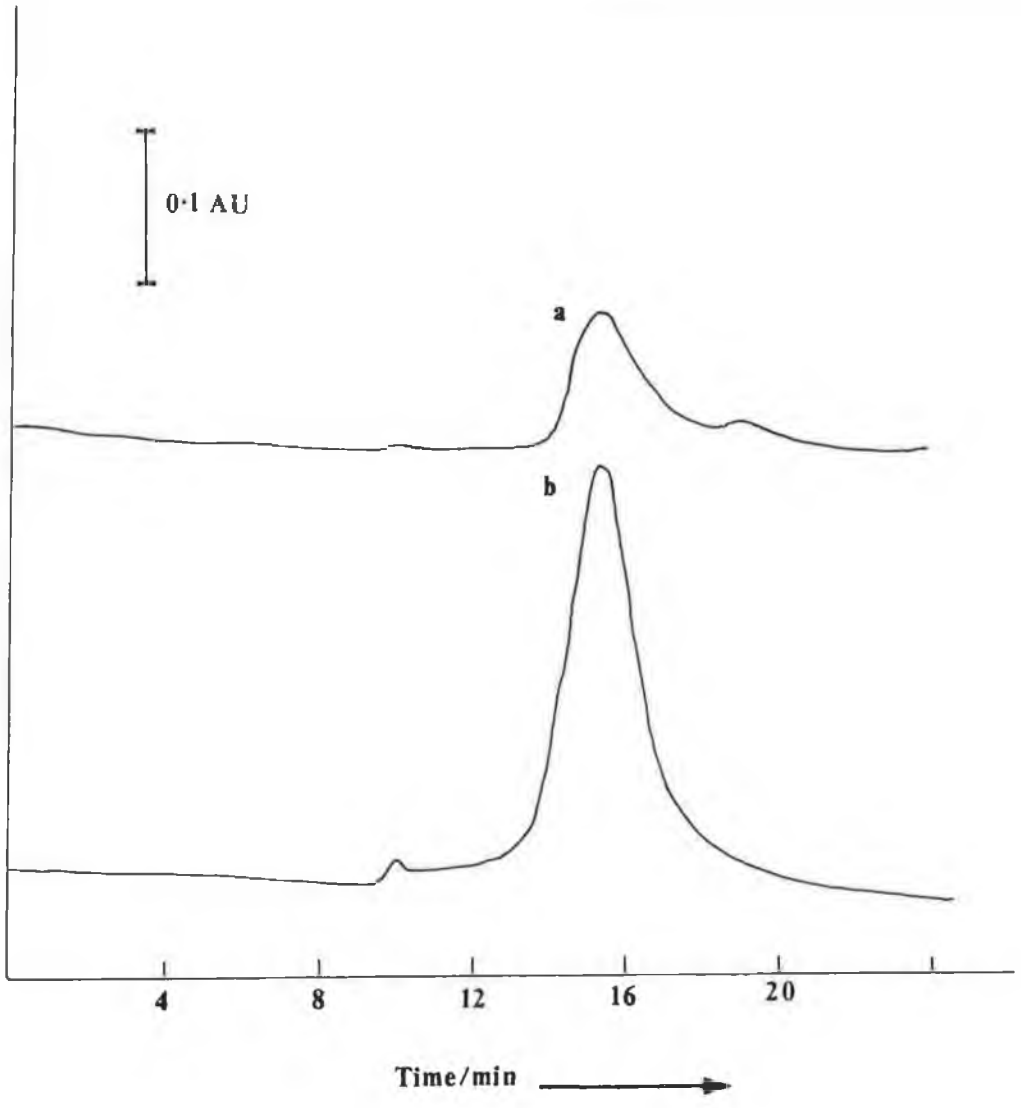

Figure 4.5. An HPLC trace of (a) standard immunoglobulin and (b) affinity purified antiserum.

4.3.2. Adsorptive Stripping Voltammetry of Immunoglobulin Species

4.3.2.1. Adsorptive Stripping Voltammetry of Mouse IgG

A typical adsorptive stripping voltammetric scan of 2 mg l^{-1} mouse IgG is shown in Figure 4.6. This was obtained using an accumulation potential of 0.0 V and a scan rate of 10 mVs^{-1}. From this it can be seen that there are two peaks, the first peak (A) at -0.25 V and the second peak (B) at -0.56 V. Both peak currents were found to increase in size on increasing concentration. The conditions for the analysis of mouse IgG were optimised as in Table 4.1. with respect to accumulation time, accumulation potential and scan rate.

Both the currents of peak A and peak B increase with respect to increasing accumulation time. The increase in peak B, illustrated in Figure 4.7, was linear with a correlation coefficient of 0.9948 and a slope of 8.25×10^{-2} nAs^{-1}, the slope of peak current vs accumulation time for peak A was 6.22×10^{-2} nAs^{-1} and had a correlation coefficient of 0.9854.

The peak current of both peaks varied considerably with respect to accumulation potential. Peak B gave rise to the highest peak currents when accumulated for 400 seconds at +0.10 V and at +0.05 V. Peak A, however, gave rise to the highest peak currents when accumulated at 0.0 V and +0.05 V. An accumulation potential of +0.05 V was chosen to continue the study as it gave a good response for both peaks. The optimum accumulation potential may depend on the net charge of the molecule that is to be adsorbed. This is determined from the

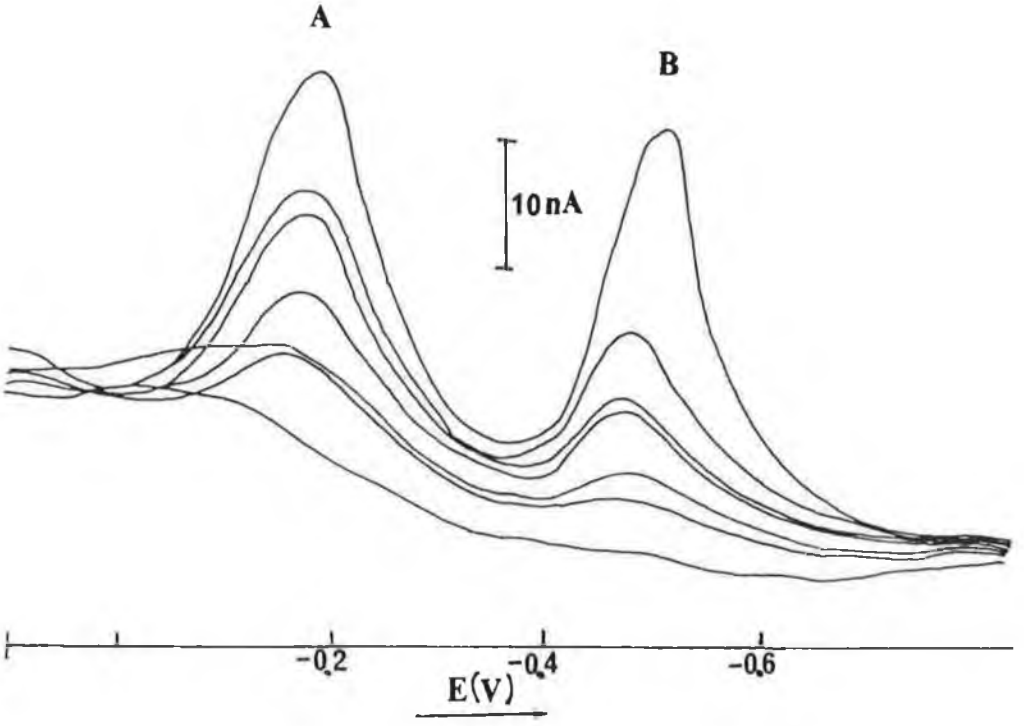

Figure 4.6. A typical adsorptive stripping voltammogram of 2 mg l^{-1} mouse IgG.

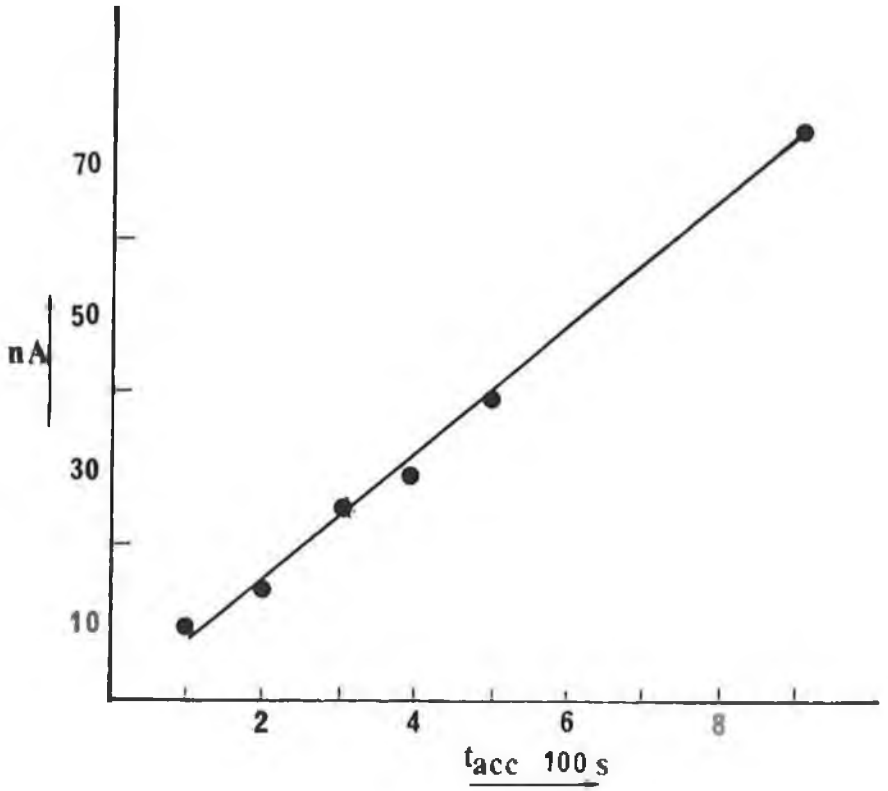

Figure 4.7. A graph of the increase in peak current of peak B for mouse IgG with increasing accumulation time.

isoelectric point (P_i) (as discussed in chapter 5). The isoelectric point for IgG from polyclonal sera was not available, as there is quite a range of IgG subclasses with a range of isoelectric points, the P_i of the IgG solution therefore may range aross the pH scale.

Table 4.1.

Influence of accumulation potential, accumulation time and scan rate on peak potentials and peak currents of peaks A and B of mouse IgG.

			Peak A		Peak B	
t_{acc} s	E_{acc} V	v mV s^{-1}	i_p nA	$-E_p$ V	i_p nA	$-E_p$ V
100	0.00	10	14.0	0.23	9.0	0.56
200	0.00	10	17.0	0.25	14.0	0.56
300	0.00	10	26.0	0.25	23.0	0.56
400	0.00	10	38.0	0.25	27.0	0.56
500	0.00	10	41.0	0.25	38.0	0.56
900	0.00	10	62.0	0.25	74.0	0.56
400	0.10	10	29.0	0.24	29.0	0.56
400	0.05	10	38.0	0.25	29.0	0.56
400	-0.05	10	23.0	0.25	16.0	0.57
400	-0.10	10	8.0	0.26	8.0	0.60
400	0.00	2	19.0	0.20	4.0	0.57
400	0.00	5	27.0	0.25	12.0	0.60
400	0.00	20	23.0	0.27	24.0	0.56

The effect of scan rate on the current response was also investigated. Both peaks gave rise to a high current response at a scan rate of 10 mVs^{-1} which was chosen for the rest of the study. The accumulation time, however, may be varied. Although greater sensitivity is acheived with longer accumulation times, this in turn leads to a longer analysis time. An accumulation time of 400 s was chosen for this study as it combines sensitive conditions with a practical analysis time. A linear calibration curve was obtained for mouse IgG in the concentration range 1.0 to 10.0 mgl^{-1} and had a slope of 17 nA l mg^{-1}.

4.3.2.2. Adsorptive Stripping Voltammetry of Anti-Mouse IgG

The adsorptive stripping voltammetric behaviour of anti-mouse IgG under the conditions optimised for mouse IgG above, is illustrated in Figure 4.8. A 1.0 mgl^{-1} solution of the immunoglobulin gave rise to two peaks: peak A at -0.23 V and peak B at -0.53 V which (as for mouse immunoglobulin) both increased in size on increasing concentration. The same optimum conditions were obtained for anti-mouse IgG as for mouse IgG. A plot of the increase in peak current with respect to increasing accumulation time is illustrated in Figure 4.9. The first portion of the graph was found to be linear with a slope of 4.3 x 10^{-2} nAs^{-1} and a correlation coefficient of 0.9969. The peak currents reached a limiting value at accumulation times of 500 s or longer. Peak A obtained for anti-mouse IgG was not as well defined as that for mouse IgG. In fact, at accumulation times of up to 300 s, it was barely

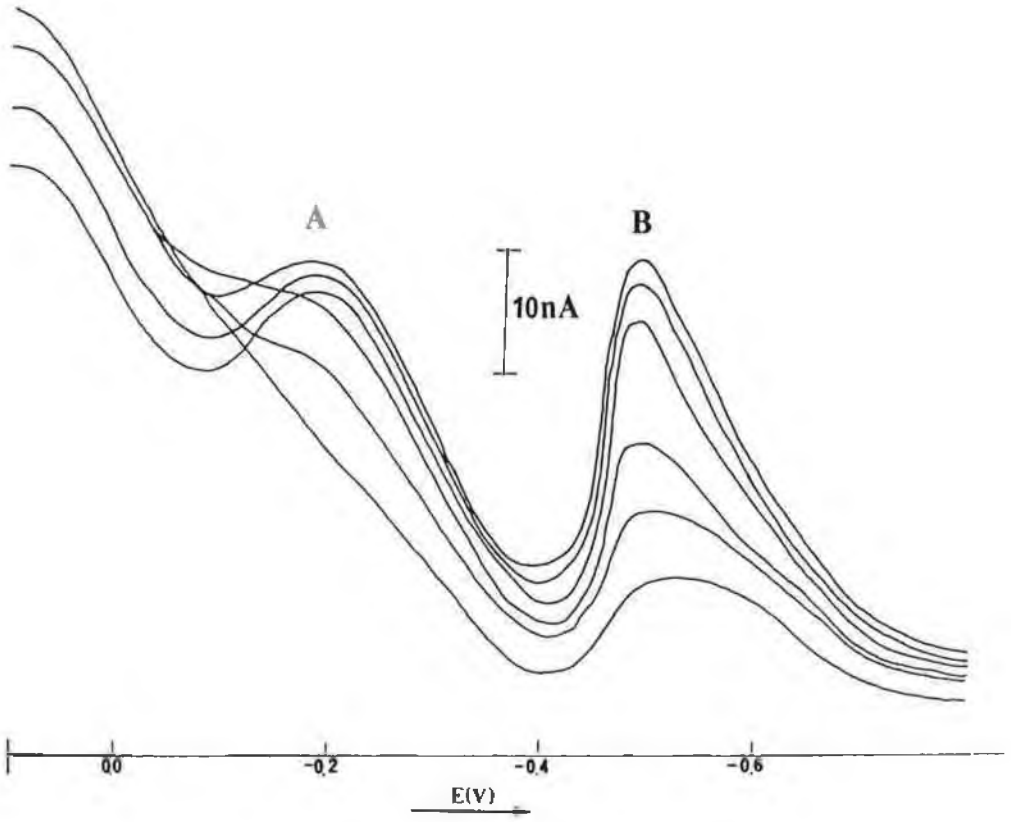

Figure 4.8. A typical adsorptive stripping voltammogram of 1 $mgml^{-1}$ anti-mouse IgG.

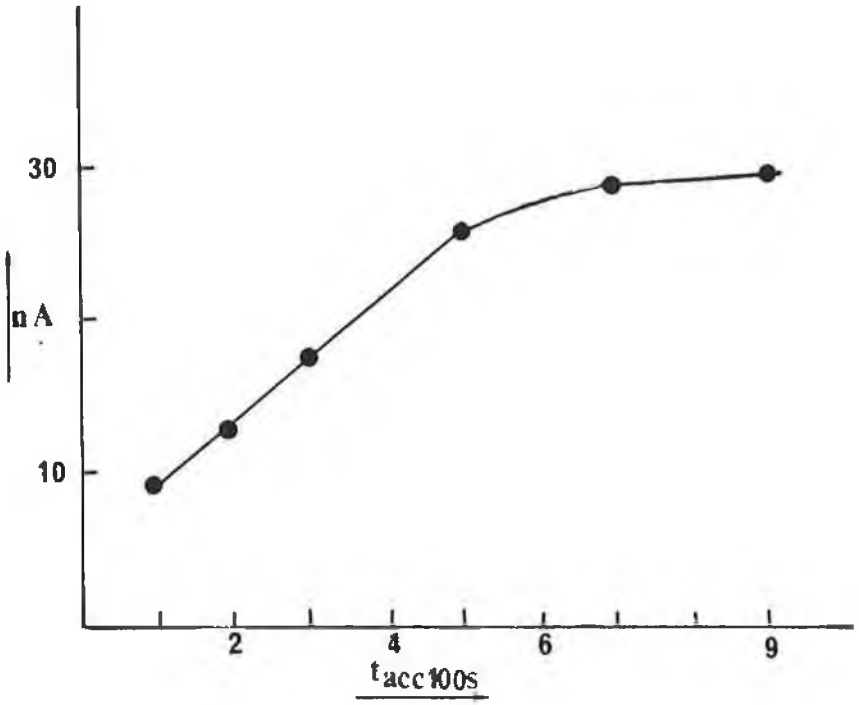

Figure 4.9. A graph of the increase in peak current of peak B for anti mouse IgG with increasing accumulation time.

discernable from the background. A linear calibration plot for peak B, using an accumulation time of 400 s, was obtained between 1 and 10 mg ml^{-1} with a slope of 16 nA l mg^{-1}.

4.3.2.3. Interaction of Mouse IgG with Anti-Mouse IgG

The reaction of mouse IgG with anti-mouse IgG was then monitored directly in solution by adsorptive stripping voltammetry using the conditions optimised above. In this case, however, an accumulation time of 50 seconds was used to decrease the time of analysis and to minimise any possible denaturation of the immunoglobulin-anti-immunoglobulin complex at the electrode surface.

The differential pulse adsorptive stripping voltammetric behaviour of increasing concentrations of mouse immunoglobiln in the concentration range 2.0-8.0 mg l^{-1} is shown in Figure 4.10. (b-e). When anti-mouse IgG was added, at concentrations of 1.0 to 6.0 mg ml^{-1}, to a solution of 8.0 mg l^{-1} mouse IgG, the peak currents of both the cathodic peaks A and B decreased. This is illustrated in Figure 4.11. where it may be seen that the decrease in peak B was linear with respect to the concentration of anti-mouse IgG, whereas the decrease in peak A exhibits two linear portions in the plot.

To verify that this reaction was due to the specific affinity of anti-mouse IgG to mouse IgG, anti-human serum albumin (anti-HSA) was added. This caused an increase in the peak currents at -0.25 V and -0.55 V, as would have been expected if no interaction was occurring between the two proteins in solution.

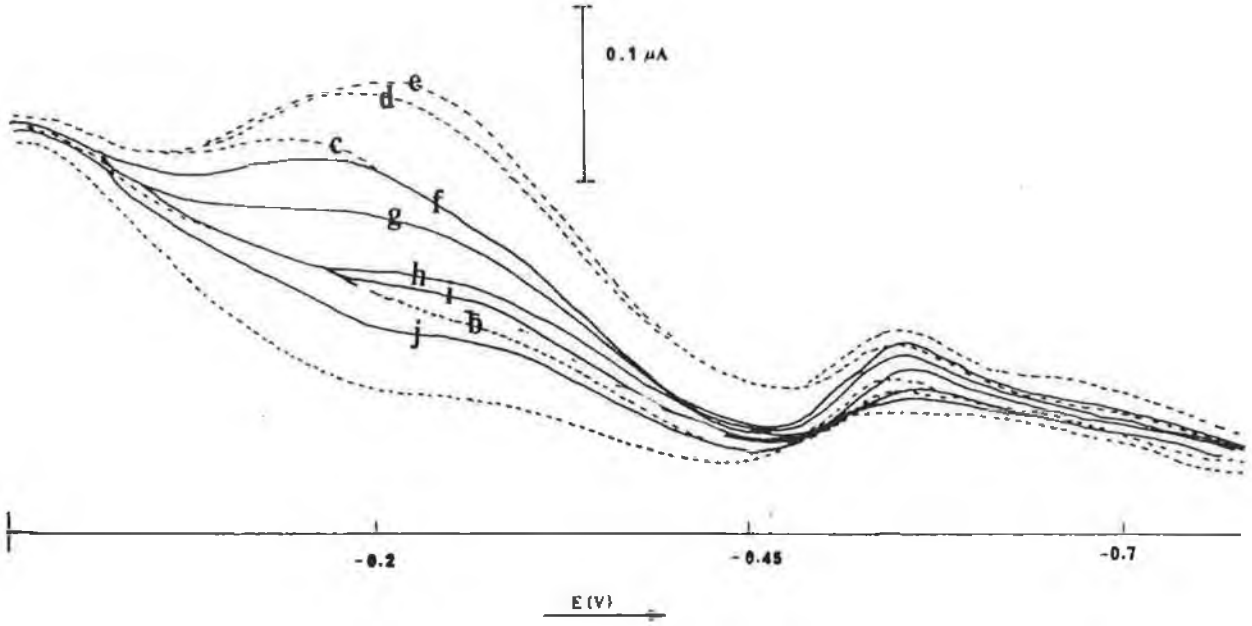

Figure 4.10 The effect of adding anti-IgG to a solution of IgG. The broken lines (b-e) represent increasing concentrations, to 8.0 mg l^{-1}, of IgG. The unbroken lines (f-j) represent the addition of anti-serum, 1.0-6.0 mg l^{-1}.

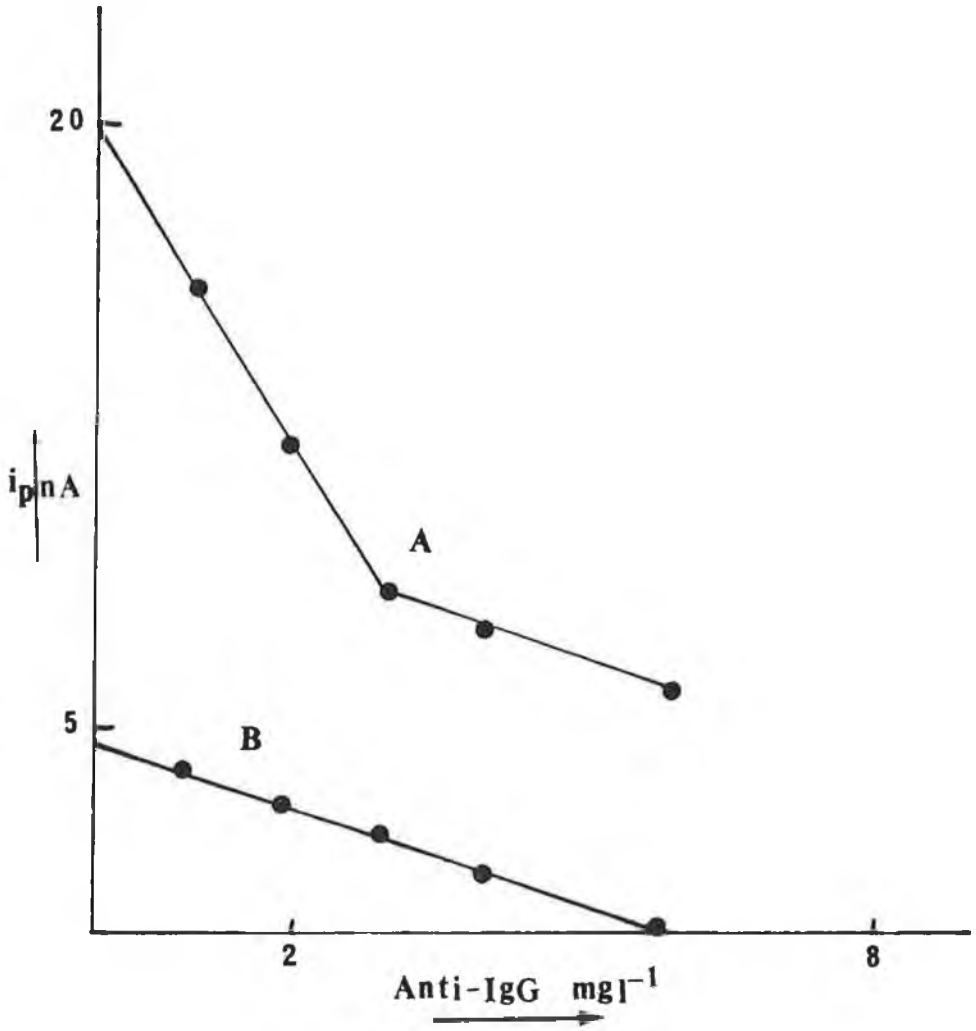

Figure 4.11. A graph of the decrease in peak current of peak A and peak B of mouse IgG with increasing concentration of anti-mouse IgG.

This data was compared to a study of HSA and anti-HSA by Rodriguez Flores and Smyth[11]. The adsorptive stripping voltammetric behaviour of anti-HSA gave rise to two peaks similar to those obtained for IgG; a peak at -0.23 V and at -0.53 V. This is not surprising, as anti-HSA, being an antibody, would have a similar make-up and conformation as the antibodies studied in this work. HSA also gave rise to two peaks, the first at around -0.48 V and the second at -0.65 V. HSA in the presence of anti-HSA gave rise to two peaks, similar to those for anti-HSA above. As greater concentrations of anti-HSA were added to a solution of HSA there was a linear decrease in the second cathodic peak at -0.53 V. There was no coccomitant decrease in the peak at -0.23 V; in fact there was a small increase which reached a limiting value after the addition of 4.0 mg l^{-1} anti-HSA. Rodriquez Flores et al. also studied the effect of the interaction of concanavalin A and mannose on the adsorptive stripping voltammetric behaviour of concanavalin A[16]. This protein also gave rise to two peaks, one at -0.21 V and a second at -0.53 V. The binding of mannose with the protein gave rise to a linear increase in the second peak, at -0.53 V, but had no effect on the peak at -0.21 V.

It may be seen that the behaviour of the peak A of IgG is not analagous to that reported for the corresponding peaks of the proteins anti-HSA and concanavalin A. However, the lack of linearity of peak A with respect to increasing accumulation time and its non-linear decrease on interaction with antibody would indicate that peak A is not useful analytically, and that the behaviour of peak B only is indicative of what is occurring

in the cell. Subsequent studies, using the conditions optimised for the Fab fragments and proteins (discussed in chapter 5) gave rise to a clear well defined "analytical wave" in the region of peak B and a small wave in the region of peak A, that did not vary with respect to increasing accumulation time, etc. Further work on the characterisation of these peaks is described in the following chapters.

4.4. REFERENCES

1. Ngo,T.T., " Electrochemical sensors in immunological analysis", (Plenum press, New York, 1987).
2. Porter,R.R., Scientific American,(1967)81.
3. Porter,R.R., Science, 180(1973)81.
4. Steward,M.W., "Antibodies: Their structure and function", (Chapman and Hall, London, New York, 1984).
5. Breyer,B. and Radcliff,F.G., Nature, 167(1951)79.
6. Breyer,B. and Radcliff,F.G., Austral. J. exp. Biol. 31(1953)167.
7. Fontaine,M., Rivat,C., Ropartz,C. and Caullet,C., Bull. Soc. Chim. Fr.,11(1974)1513
8. Fontaine,M., Rivat,C., Ropartz,C., and Caullet,C., Ann. Inst. Pasteur, Paris, 120(1971)313.
9. Kano,K., Ikeda,T. and Senda,M., Agric. Biol. Chem.,5(1983) 1043.
10. Brdicka,R., Coll. Czech. Comm, 5(1933)112.
11. Rodriguez Flores, J. and Smyth, M.R., J. Electroanal. Chem., 235(1987)317.
12. Borrachera,A., Rodriguez,J., Vinagre,F. and Sanchez,A., Analyst. 113(1988)1795.
13. Dwyer, G., Gilvary, U., Carty, P., O'Kennedy, R. and Thomas, R.D., Biochem. Soc. Trans., 15(1987)293.
14. Laemmli, U.K., Nature., 227(1979)680.
15. Axen, R., Porath, J. and Ernback, S., Nature., 214(1967)1302.
16. Rodriguez Flores, J., O'Kennedy, R. and Smyth, M.R., Analyst., 113(1988)525.

CHAPTER FIVE

ADSORPTIVE VOLTAMMETRY OF IMMUNOGLOBULIN FRAGMENTS, AND OF THE GLOBULAR PROTEINS AVIDIN AND STREPTAVIDIN

5.1. Introduction

In an attempt to understand the nature of the electrochemical response exhibited by typical immunoglobulin molecules (as reported in chapter 4), two different strategies were employed. In the first one, the molecule was digested enzymatically to yeild the Fab and $F(ab')_2$ antigen binding fragments. In the second part, two globular proteins were studied: avidin, a glycoprotein with one disulphide bond; and streptavidin, a protein of similar structure but with no carbohydrate or sulphur-containing residues. Each of these proteins are important molecular recognition systems in their own right, and each has been exploited in immunoassay systems.

5.1.2. Antigen Binding Fragments

The proteolytic cleavage of IgG and the structure of the resulting fragments has been described in the preceding chapter. These fragments, which retain most of the properties of the intact molecule, are in some cases preferred over the whole molecule for enzyme immunoassay. Fab fragments produce a lower background in sandwich assays and decrease non-specific adsorption of rheumatoid factors. As the conjugated anti-IgG usually recognises the Fc fragment only, both IgG and Fab fragments from the same serum may be used in different layers of an immunoassay without interference. The major disadvantage of these fragments is loss of avidity. De Alwis and Wilson have recently demonstrated the use of Fab fragments for a rapid heterogeneous competitive electrochemical immunoassay for IgG

in the picomolar range[1].

5.1.3. Avidin and Streptavidin

One of the more important non-immunological molecular recognition systems exploited in immunoassay is the avidin-biotin (or the similar streptavidin-biotin) system. Avidin accounts for 0.05% of egg white protein. It was first noticed in 1898 that uncooked egg white was toxic[2] and resulted in what appeared to be a vitamin deficiency[3]. It was later discovered that avidin, first purified in 1942, did in fact bind biotin (vitamin H), preventing its absorption from the intestine, or in the case of microorganisms from the surrounding growth medium, thus conferring antibacterial properties on avidin. Streptavidin was discovered in culture filtrates of streptomyces avidinii by Chaiet and Wolf[4], and was found to exhibit the same biotin binding properties as avidin, although it has not yet been used as widely as avidin. In recent years, these proteins have been exploited to devise powerful and widely applicable tools for biochemistry, microbiology and clinical chemistry. The applications of this system has included antigen localisation, protein blotting immunotherapy, bioaffinity sensors, and particularly immunoassay.

5.1.3.1. The Avidin-Biotin Complex in Bioanalytical Applications

Numerous strategies have been outlined in the literature for

applying avidin-biotin technology to a range of bioanalytical applications. Such strategies have been summarised in a recent review by Welchek and Bayer[5]. The use of the avidin-biotin system in immunoassay is still in the development stages, but the majority of applications have involved enzyme-linked immunoassay. Labelling is usually achieved either by using an appropriate avidin-conjugated group or using native avidin followed by reaction with a biotinylated molecule as illustrated in Figure 5.1.[6]

This latter labelling technique was used by Guesdon et al.[7] Biotin was covalently attached to a range of proteins, antibodies, antigens and enzymes; the effect of the labelling procedure on the activity of the protein was established and the system was then applied to two different assay procedures. The first was called the "bridged avidin-biotin technique" (BRAB), in which four steps were used to quantify an immobilised antigen, i.e. human IgE. The immobilised antigen was incubated with: (i) biotin-labelled antibody; then (ii) with avidin; then (iii) with biotin-labelled enzyme (horseradish peroxidase); and finally (iv) the enzyme activity was measured. The second method described was applied to the detection and quantification of bovine serum albumin and was called the "labelled avidin-biotin technique" (LAB). In this procedure, biotin-labelled antibody and enzyme-labelled avidin were used. The labelled antibody was allowed to react with the antigen and after washing, the enzyme-labelled avidin was added. After incubation and a further washing step, the enzyme activity was measured. Both techniques were found to be very specific. Although the LAB procedure was less time-consuming,

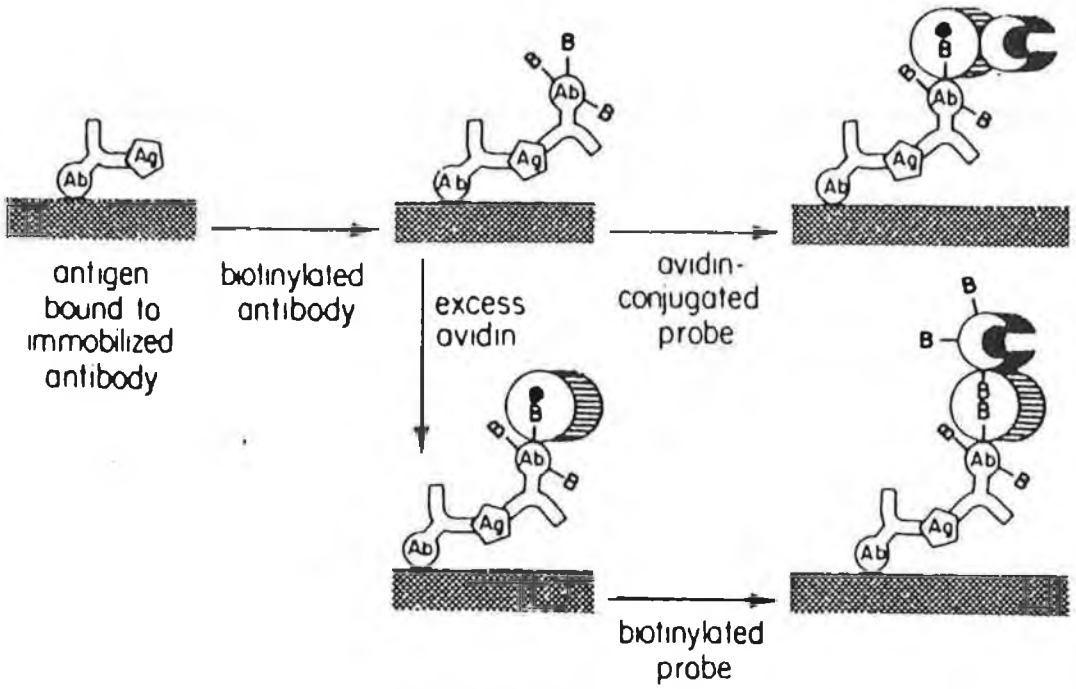

Figure 5.1. An enzyme immunoassay using a biotinylated second antibody. The signal is achieved either by using an appropriate avidin-conjugated reporter group or employing native avidin followed by a biotinylated marker.

the BRAB procedure was more sensitive and had the added advantage of only involving a biotin conjugation procedure, thus avoiding protein-protein conjugation, as such high molecular weight conjugates are undesirable.

Schray and Niedbala[8] exploited the avidin-biotin system in a dual solid-phase enzyme immunoassay (DSPEIA). This technique relies on the partitioning of an enzyme-biotin conjugate (biotin-glucose-6-phosphate dehydrogenase-antibody) between two solid phases, i.e. polystyrene latex bound avidin and polystyrene latex bound antigen. On binding to the bound antigen, the activity of the conjugated enzyme is unaffected, whereas binding to the bound avidin inhibits the enzyme activity. The assay is based on competition between the conjugate and analyte antibody for the bound antigen. This assay was used to detect and quantify rabbit IgG. This technique combined the solid phase characteristics of heterogeneous EIA, with inactivation of enzyme upon complexation, as found in homogeneous EIA.

An enzyme-linked ligand sorbent assay for the quantification of folates in biological fluids was developed by Hansen and Holm[9] as an alternative to currently available radiosotopic methods. The folate extracted from blood samples competed with folate bound to immobilised BSA for binding sites on biotinylated folate binding protein (FBP). The biotinylated FBP was detected after binding of an avidin-alkaline phosphatase conjugate. This procedure is illustrated in Figure 5.2. A new and interesting strategy using avidin-biotin coupling as a general method for preparing enzyme-based fibre-optic sensors was devised by Luo and Walt[10]. Three

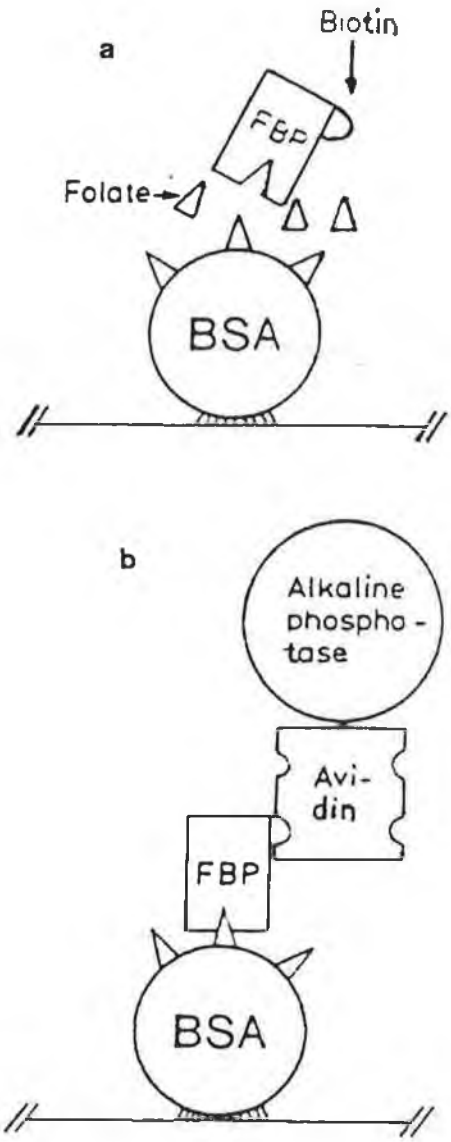

Figure 5.2. An enzyme-linked ligand sorbent assay for quantitation of folates. (a) Folates extracted from biological fluids and folate complexed to BSA on microtiter plates compete for binding to biotinylated folate binding protein (FBP). (b) Biotinylated FBP bound to immobilised folate is detected after binding of avidin conjugated to alkaline phosphatase.

different sensors, capable of detecting penicillin, organic esters and urea were described. Normally, such a sensor is comprised of a thin layer of polymer containing an immobilised enzyme and an indicator that responds to the analyte concentration as a consequence of the enzyme catalysed reaction. In this case, the enzyme was attached to the sensor via a biotin-avidin-biotin link. The advantages of the method included the retention of enzyme activity that is sometimes lost during physical entrapment, the diffusion barrier is kept to a minimum (as the enzymes bind to the polymer, only where the pore size is large) and that the derivatised enzyme is strongly bound to the fibre due to the high stability of the avidin-biotin interaction.

5.1.3.2. Structure of Avidin

Avidin is a basic glycoprotein made up of four identical subunits, with a relative molecular mass of approximately 67,000. Each subunit has 128 amino acid residues, including two cysteine residues and terminating with alanine at the $-NH_2$ end of the polypeptide chain[11]. Each subunit also contains about six units of mannose and three units of glucosamine. The oligosaccharide portion of the molecule is linked through one of its acetylglucosamine residues to the amino acid asparagine (Asn). The molecule contains only one intrachain disulphide bond[12]. Avidin is a very stable protein, its conformation is not sensitive to changes in temperature, pH or ionic strength. There is also little change effected in its structure when biotin is bound. It has an

isoelectric point (P_i) of 10.5.

5.1.3.3. Structure Of Streptavidin

Streptavidin is very similar in structure to avidin, and is also made up of four subunits. There are, however, important differences that distinguish these two proteins; streptavidin has no associated carbohydrate residues and is completely devoid of sulphur-containing amino acids[13], such as cysteine and methionine, both of which are found in avidin. Streptavidin is also very stable, the $-NH_2$ and -COOH terminal portions of the molecule are flexible, and the core is folded compactly. The relative molecular mass of streptavidin is approximately 60,000 and it has a P_i in the range 7.2-7.5.

5.1.3.4. Structure and Function of Biotin

Although avidin binds to other biological molecules (such as lectins) via its carbohydrate moiety[14], its most important binding reaction is that with biotin. Streptavidin has a similar affinity for biotin. Biotin is a small, water soluble vitamin with a relative molecular mass of 244, and its structure is shown in Figure 5.3. In nature, biotin has an enzymatic role as the coenzyme responsible for the transfer of carbon dioxide in carboxylation reactions. It can be easily conjugated to a wide selection of biological molecules, using various activated forms such as N-hydroxysuccinimidobiotin, which is used to conjugate biotin to immunoglobulins[15]. Biotinylation of antibodies can be achieved to a high degree

a

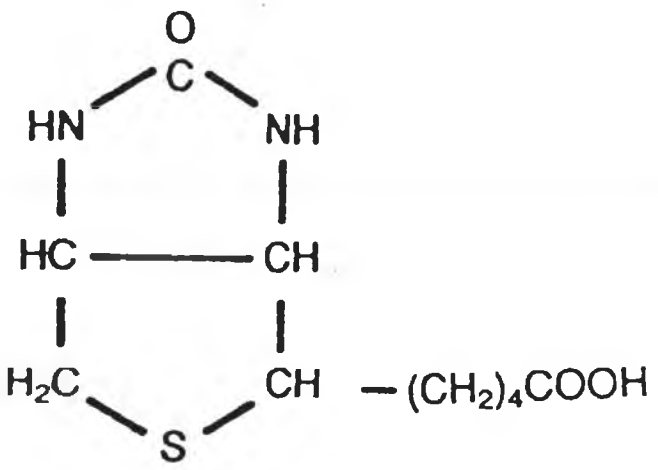

b

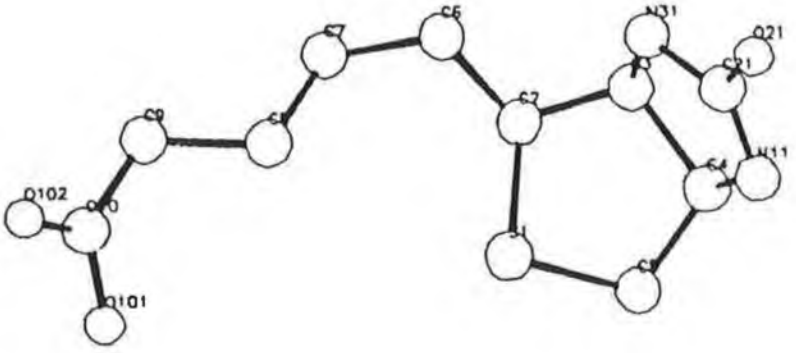

Figure 5.3. (a) The structure of biotin showing a "vertical" arrangement of the two rings. (b) The structure of biotin as obtained from crystallographic data.

without damage to the antigen binding ability or other physical properties.

5.1.3.5. Binding Reactions of Avidin and Streptavidin

The dissociation constants for both avidin and streptavidin bound to biotin is of the order of 10^{-15} M. The interaction of avidin and biotin is primarly of a non-covalent nature with all parts of the biotin molecule contributing to the interaction. Many analogues or small molecules, such as urea, glycol etc., may be bound or compete in the interaction. Although the action of avidin and biotin has been known for a long time[16], the mechanism has not been illucidated in any great detail. However, it is known that the imidazolone portion of the biotin molecule must be intact for strong binding; the rest of the molecule may be used for coupling to other proteins. It has been suggested that three or four tryptophan residues in each subunit interact directly with biotin, and a single subunit of lysine is implicated as being nearby[16]. A single subunit of avidin or streptavidin will still bind biotin, but to a lesser extent[17]. The biotin binding sites are deep within the avidin structure. The carboxyl group of the valeric acid of bound biotin lies approximately 0.8 - 0.9 nm beneath the Van der Waals surface of the molecule, and this engulfment of the biotin molecule may contribute in part to the high affinity. The complex of one biotin molecule per subunit of avidin is stable over a wide range of pH and temperature.

The binding sites are arranged so that two sites are close

together, but each pair of sites can only bind one biotinylated protein (due to steric hindrance). Since there are two pairs of sites, the avidin molecule is capable of acting as a binding agent between two biotinylated proteins.

5.2. EXPERIMENTAL

5.2.1. Reagents

All reagents used were of analytical reagent grade and solutions were prepared in water obtained by passing distilled water through a Waters Milli-Q water purification system. 0.1 and 0.01 M phosphate buffers were prepared as described in chapter 4, and the pH was adjusted to pH 7.4 with 0.5 M NaOH. Fab fragments were prepared as described below, whereas $F(ab')_2$ fragments were obtained from the Sigma Chemical Co. Affinity-purified avidin D was obtained from Vector Laboratories and affinity-purified streptavidin was obtained from the Sigma Chemical Co.. Both proteins were reconstituted in 0.1 M sodium bicarbonate solution. Biotin and biotin-conjugated goat anti-mouse IgG were obtained from the Sigma Chemical Co.

5.2.2. Apparatus

The apparatus used for the voltammetric measurements in this work have been described previously; except in this case, cyclic voltammograms were recorded using a PARC model 264A polarographic analyser.

5.2.3. Methods

5.2.3.1. Enzymatic Cleavage of Immunoglobulin G

Two methods were used to cleave the donkey anti-mouse IgG into Fab fragments. The first involved the use of mercuripapain and cysteine following the method of Hudson and May[18], whereas the second involved the use of mercuripapain and iodoacetamide following the method of Mishell and Shiigi.[19]

Method 1

The concentration of the immunoglobulin fraction was determined using the modified Bradford assay (described in chapter 4) prior to digestion. Cysteine and EDTA were added to the IgG solution to a final concentration of 0.01 M and 0.002 M respectively, before 1 mg of mercuripapain was added for every 100 mg of IgG. The solution was digested at 37°C for four hours, stirring regularly, and the digest was dialysed against PBS overnight at 4°C.

Method 2

The immunoglobulin fraction was dialysed against 0.1 M phosphate buffer containing 4×10^{-3} M EDTA overnight at 4°C, then brought to a final concentration of 0.01 M with 2-mercaptoethanol. An amount of mercuripapain equivalent to 2% of the weight of protein was added, and the solution was flushed with nitrogen, sealed and digested at 37°C for four

hours, stirring regularly. The reaction was stopped by adding 50 µl of 0.3 M iodoacetamide in 1 M tris-HCl, pH 8.0, per ml of protein, and the mixture was placed in an ice-bath for 30 min. The sample was dialysed against PBS at 4°C overnight. The IgG fraction was then subjected to affinity chromatography, as described in chapter 4, to elute any non-specific protein and the Fc portion which has no binding capacity. The fraction was found to contain some undigested IgG and this was removed using gel filtration.

5.2.3.2. Gel Filtration

The column used was packed with 1 g of Sephadex G-75 swollen in 40 ml of PBS. The samples were concentrated to approximately 0.5 ml using polyethylene glycol (PEG) 6000 . 100 µl of sample with 200 µl of phenol red and 100 µl blue dextran (to determine the column volume and void volume respectively) were applied to the column. The column was washed with PBS at a flow rate of 4 $mlhr^{-1}$ and 1 ml fractions were retained for protein determination.

The Fab fragments were characterised using SDS-PAGE electrophoresis and HPLC as described in chapter 4.

5.2.3.3. Voltammetric Analysis

5.2.3.3.1. Procedures

The voltammetric measurments were carried out using the procedures outlined in chapter 4. Modifications of the above

procedures included silanising the sample cell and regularly changing the reference electrode sleeve, so as to avoid adsorption of the protein which would cause contamination in subsequent measurements. All potentials are quoted in V vs. Ag/AgCl.

5.3. RESULTS AND DISCUSSION

5.3.1. Preparation and voltammetric investigation of immunoglobulin fragments

5.3.1.1. Preparation and Purification of Fab Fragments

Three protocols combining various digestions with purification steps were compared. The three protocols were:

Protocol 1: digestion Method 1 followed by affinity chromatography and Sephadex G-75 gel filtration;

Protocol 2: digestion Method 1 followed by Sephadex G-75 gel filtration;

Protocol 3: digestion Method 2 followed by with Sephadex G-75 gel filtration.

The elution profile for the affinity column using protocol 1 is illustrated in Figure 5.4. The Fab fragments, which retain their binding capacity for mouse IgG, would be expected to be in the first fraction after the application of eluting buffer. However, this fraction was found to contain only pure undigested whole anti-IgG, as detected by HPLC. The Fab fragments had eluted at an earlier stage. This was due to the slight loss of avidity of the fragments for the anti-serum bound to the column. Therefore, in the presence of a large amount of undigested IgG, the whole molecule would compete for sites on the column. Hence it is important to separate on the

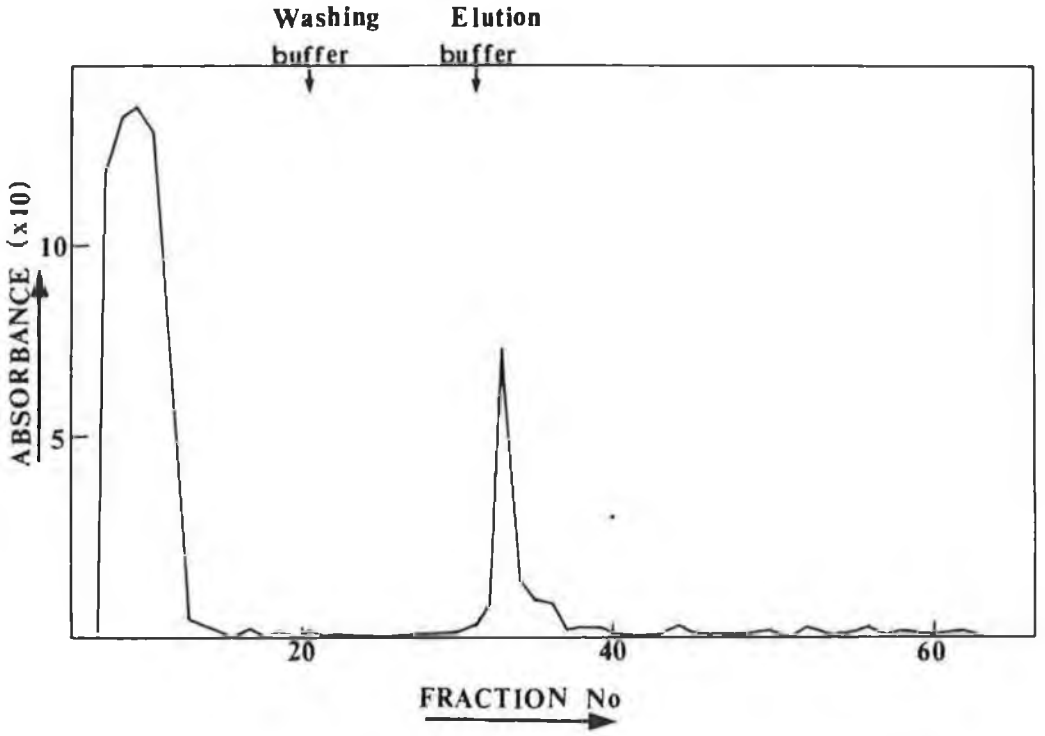

Figure 5.4 The elution profile for the affinity chromatographic procedure used for the purification of Fab fragments. Absorbance was read at 600 nm.

Sample	Total Protein mg	% Yield
Donkey serum	670	100
Precipitated protein	218	32.6
One:		
Digested protein applied to affinity column.	37.8	-
Concentrated fractions from affinity column applied to gel filtration.	13.0	34.4
Fab fragment.	1.85	(i) from gel = 14.2% (ii) from digested IgG = 4.9%
Two:		
Concentrated digested method one IgG applied to gel filtration.	4.66	-
Fab fragment.	0.88	(i) from digested IgG = 18.9%
Three:		
Concentrated digested IgG (method 2) applied to gel filtration.	1.02	-
Fab fragment	0.20	(ii) from digested IgG = 19.6%

Table 5.1. A table of the yield of Fab fragments from the three protocols used in this study: i.e. 1, 2, and 3. Presented as total protein (mg) and as a percentage yield of the original serum.

basis of size first and then affinity.

The comparitive protein yields of all three experiments are shown in Table 5.1. It is clear that the second digestion method[19] followed directly by gel filtration gives the highest yield of digested material, and that affinity chromatography resulted in quite a large loss of fragments. The large amount of undigested material suggests that the incubation times were too short in both methods. Enough pure Fab fragments (verified by HPLC) were obtained, however, to continue with the electrochemical study.

HPLC was found to be a very useful and reproducible technique for the detection of digested and undigested material. The Fc fragment was seen to crystallize out of solution leaving a pure fraction of Fab fragments.

The HPLC profile of purified donkey anti-mouse IgG is shown in Figure 5.5.a. This protein was shown to have an average retention time of 15 minutes. The HPLC profile of the solution after the digestion procedure, containing both undigested IgG and the Fab fragments, is shown in Figure 5.5.b. where it can be seen that these species have average retention times of approximately 15 minutes and 19 minutes respectively.

5.3.1.2. Cyclic Voltammetry of the $F(ab')_2$ Fragments

The cyclic voltammetric behaviour of $F(ab')_2$ fragments is illustrated in Figure 5.6. This study was made at the HMDE with a medium drop size (of area 0.016 cm^2) in 0.1 M phosphate buffer, pH 7.4. In each case 20 µl of the 0.5 mg/ml stock solution of $F(ab')_2$ fragments was added to 10 ml of

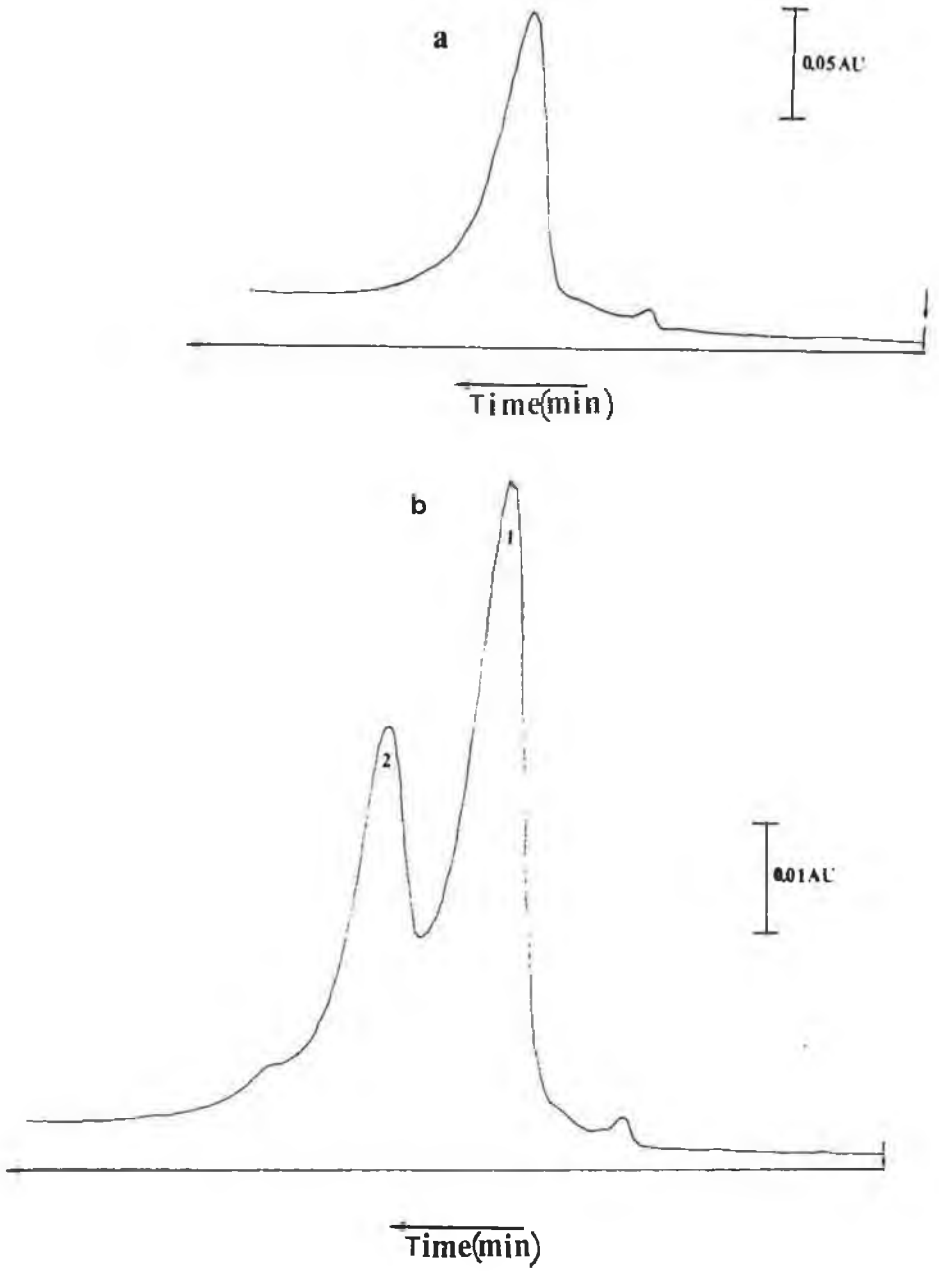

Figure 5.5. HPLC profile of (a) purified anti-mouse IgG and (b) the solution after digestion with papain. Peak 1 represents undigested IgG and peak 2 represents the resulting Fab fragments. Conditions: Flow rate 0.5 ml/min; chart speed 5 mm/min; UV detection at 280 nm.

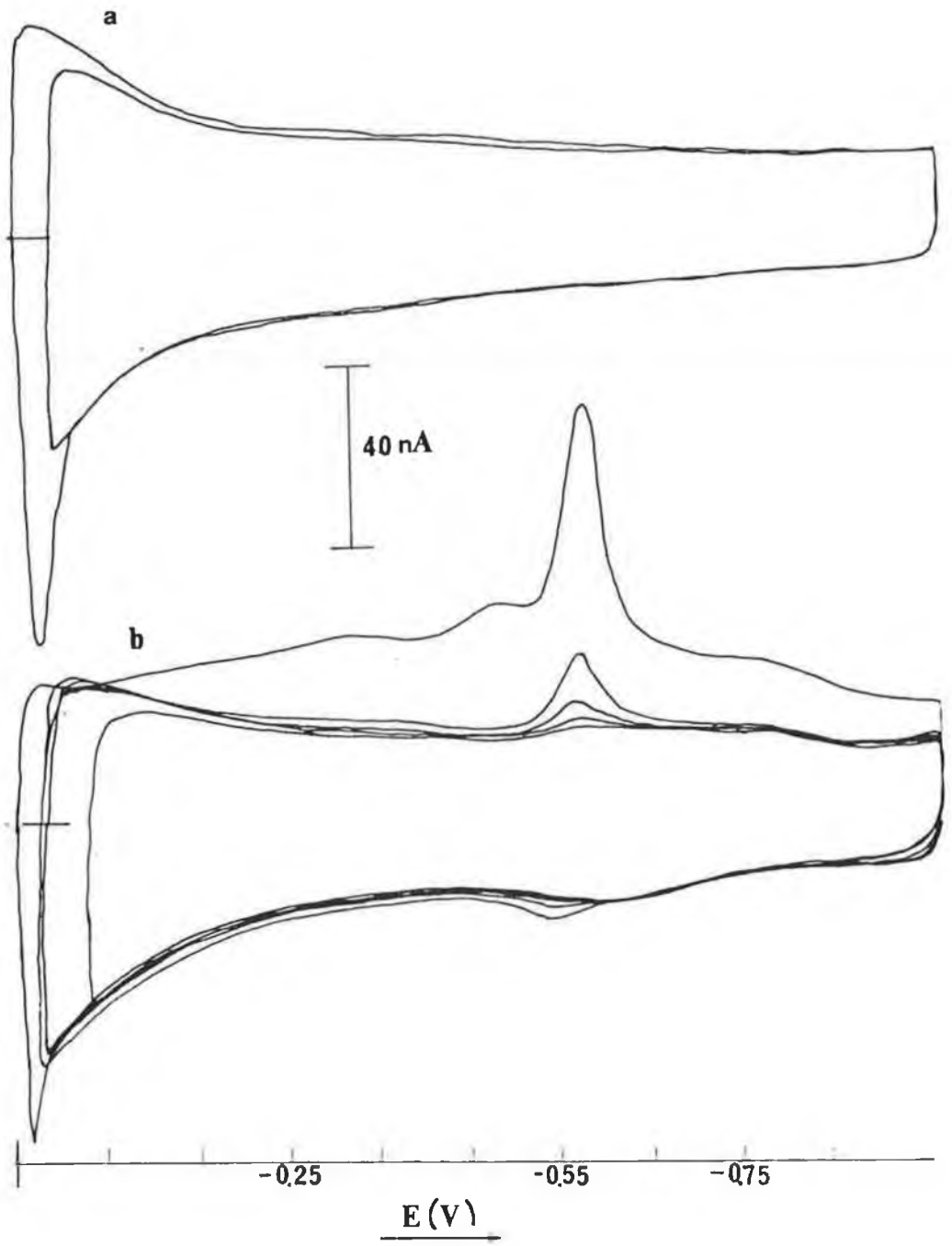

Figure 5.6. Cyclic voltammetric behaviour of $F(ab')_2$ fragments in 0.1 M phosphate buffer at the HMDE. Repetitive scans; (a) without accumulation and (b) with 1000 s accumulation. Conditions: E_{start} +0.05 V; scan rate 200 mV/s.

electrolyte.

In both cases, the potential was scanned from +0.05 V to -1.00 V. It may be seen from Figure 5.6.a. that without any accumulation time, no peak was evident in either the cathodic or anodic direction, whereas in Figure 5.6.b., with an accumulation of 1000 s, there was a large cathodic peak at -0.56 V (peak B) and a small pre-peak at -0.47 V. On the reverse scan, a small peak was evident at -0.55 V with no apparent pre-peak.

Repetitive scans showed a very significant decrease in the size of peak A with the disappearance of the pre-peak by the second scan. The anodic peak exhibited similar behaviour. This indicates that the electrochemistry depends primarily on transport to and adsorption onto the electrode surface before any response is evident.

5.3.1.3. Adsorptive Stripping Voltammetry of the $F(ab')_2$ Fragments

As carried out for the study of the immunoglobulins in chapter 4, the working parameters for adsorptive stripping voltammetry were optimised with respect to accumulation potential, accumulation time, pulse amplitude and scan rate. The results of this study are tabulated in Table 5.2.

The main cathodic peak (peak B) at -0.525 V and a small peak (peak A) at -0.265 V may be clearly seen in the differential pulse voltammogram shown in Figure 5.7., using an accumulation potential of +0.05 V, a scan rate of 10 mV/s and an accumulation time of 800 s. The effect of varying the

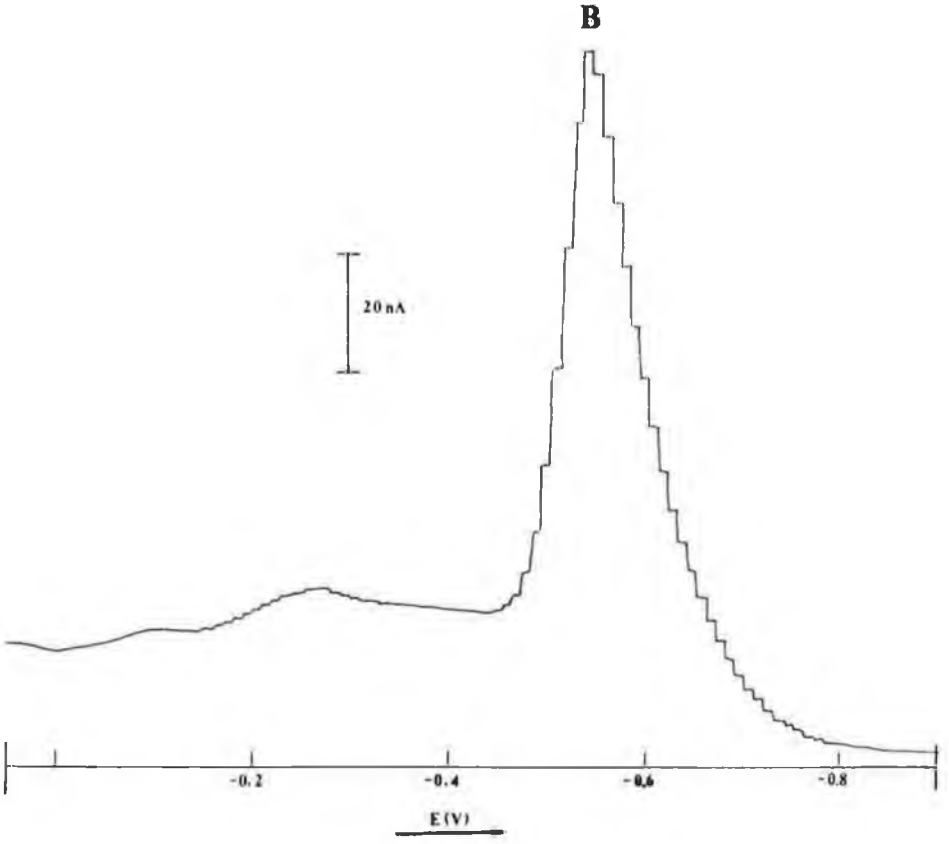

Figure 5.7. A typical differential pulse adsorptive stripping voltammogram of $F(ab')_2$ fragments in 0.1 M phosphate buffer. Conditions: E_{acc} +0.05 V; scan rate 10 mV/s; t_{acc} 800 s.

				Peak A		Peak B	
t_{acc} (s)	E_{acc} (V)	ν (mV s^{-1})	ΔE (mV)	i_p (μA)	E_p (V)	i_p (μA)	E_p (V)
200	−0.10	5	50	—	—	0.019	−0.525
200	−0.05	5	50	—	—	0.019	−0.525
200	0.00	5	50	—	—	0.024	−0.525
200	+0.05	5	50	—	—	0.026	−0.525
200	+0.10	5	50	—	—	0.031	−0.525
200	+0.15	5	50	—	—	0.031	−0.525
200	+0.20	5	50	0.003	−0.175	0.028	−0.525
100	+0.05	5	50	—	—	0.014	−0.55
200	+0.05	5	50	—	—	0.018	−0.55
300	+0.05	5	50	0.008	−0.23	0.022	−0.56
400	+0.05	5	50	0.004	−0.23	0.024	−0.56
500	+0.05	5	50	0.006	−0.22	0.026	−0.56
600	+0.05	5	50	0.007	−0.21	0.027	−0.56
700	+0.05	5	50	0.007	−0.21	0.028	−0.56
800	+0.05	5	50	0.009	−0.21	0.029	−0.56
200	+0.05	5	25	—	—	0.019	−0.53
200	+0.05	5	100	—	—	0.019	−0.48
200	+0.05	20	50	—	—	Badly defined	
200	+0.05	50	50	—	—	Badly defined	

Table 5.2. Adsorptive stripping voltammetric data for $F(ab')_2$ fragments of anti-mouse IgG.

accumulation time on the peak currents may be seen in Figure 5.8. The increase in current response with increasing accumulation time was found to be linear for peak B and reaches a plateau at around 500 s. The linear portion has a slope of 4.72×10^{-2} nA/s and a correlation coefficient of 0.9987. An increase was also apparent with respect to increasing accumulation time for the pre-peak, A.

The effect of varying the accumulation potential on the adsorptive voltammetric behaviour of $F(ab')_2$ fragments may be seen in Figure 5.9. Peak B was well defined using accumulation potentials in the range -0.05 V to +0.20 V, but the peak currents were found to be higher at the more positive potentials, decreasing again at those accumulation potentials greater than +0.20 V. The large initial peak at around +0.15 V was also present in the background electrolyte scan. Although the best current response was achieved by using an accumulation potential of +0.15 V, the accumulation potential chosen for this study was +0.05 V, as it gave both a well defined peak and would allow comparison with the earlier immunoglobulin work.

The two stirring rates offered by the PARC model 305 stirrer were compared, and the rate of 400 rpm was chosen as the more suitable, since the higher rate of 700 rpm resulted in a dramatic decrease in current due to the unsuitable adsorption conditions. Of the scan rates offered, both 5 and 10 mVs^{-1} gave rise to well defined peaks; a rate of 10 mV/s was chosen to minimise analysis time. The effect of pulse amplitude on the current response is shown in Figure 5.10. The increase in current response was found to be linear with increasing pulse amplitude. The peak potentials, however, shifted to more

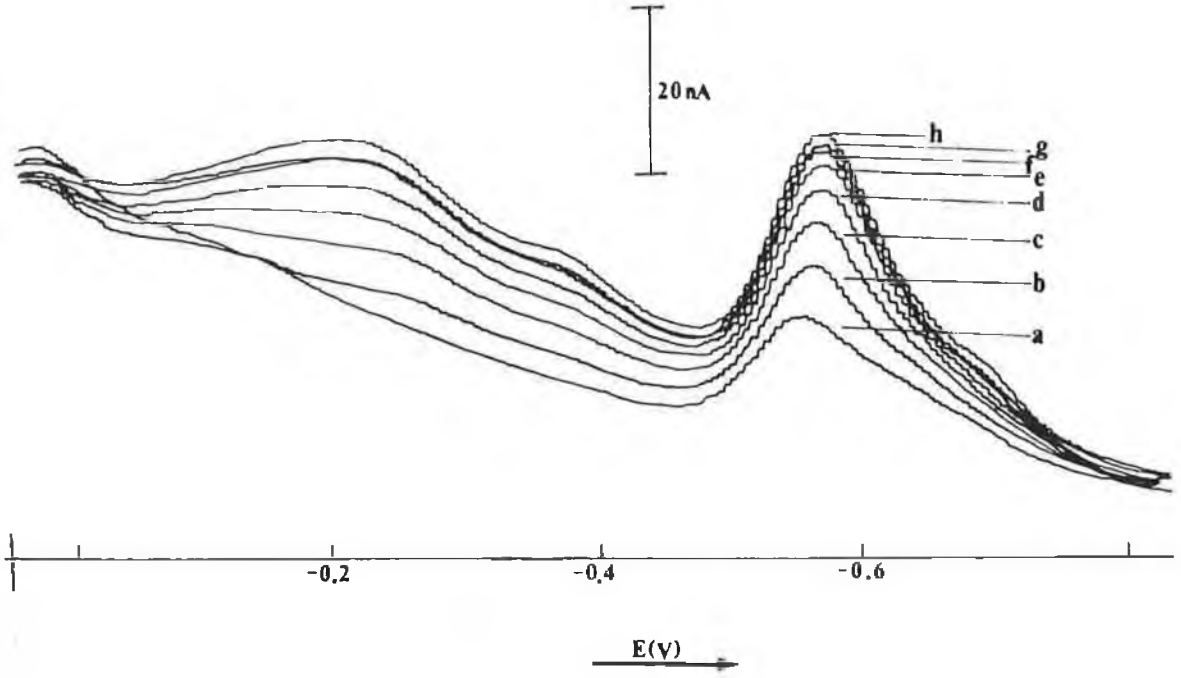

Figure 5.8. Effect of accumulation time on the differential pulse voltammetric behaviour of $F(ab')_2$ fragments in 0.1 M phosphate buffer. Conditions: E_{acc} +0.05 V; scan rate 5 mV/s; pulse amplitude 50 mV; t_{acc} (a) 100 s, (b) 200 s, (c) 300 s, (d) 400 s, (e) 500 s, (f) 600 s, (g) 700 s, (h) 800 s.

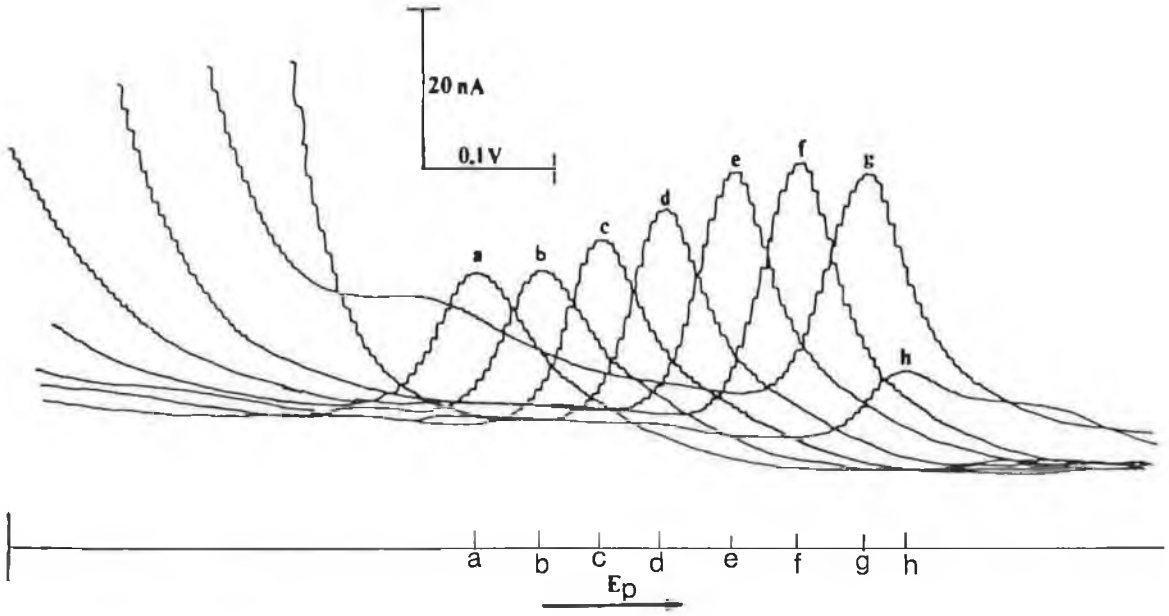

Figure 5.9. Effect of varying accumulation potential on the differential pulse adsorptive stripping behaviour of $F(ab')_2$ fragments in 0.1 M phosphate buffer. In each case the starting potential(E_{acc}) is different. Conditions: E_{acc} (a) -0.1 V, (b) -0.05 V, (c) 0.0 V, (d) +0.05 V, (e) +0.1 V, (f) +0.15 V, (g) +0.2 V, (h) +0.25 V; scan rate 10 mV/s; pulse amplitude 50 mV; t_{acc} 200 s.

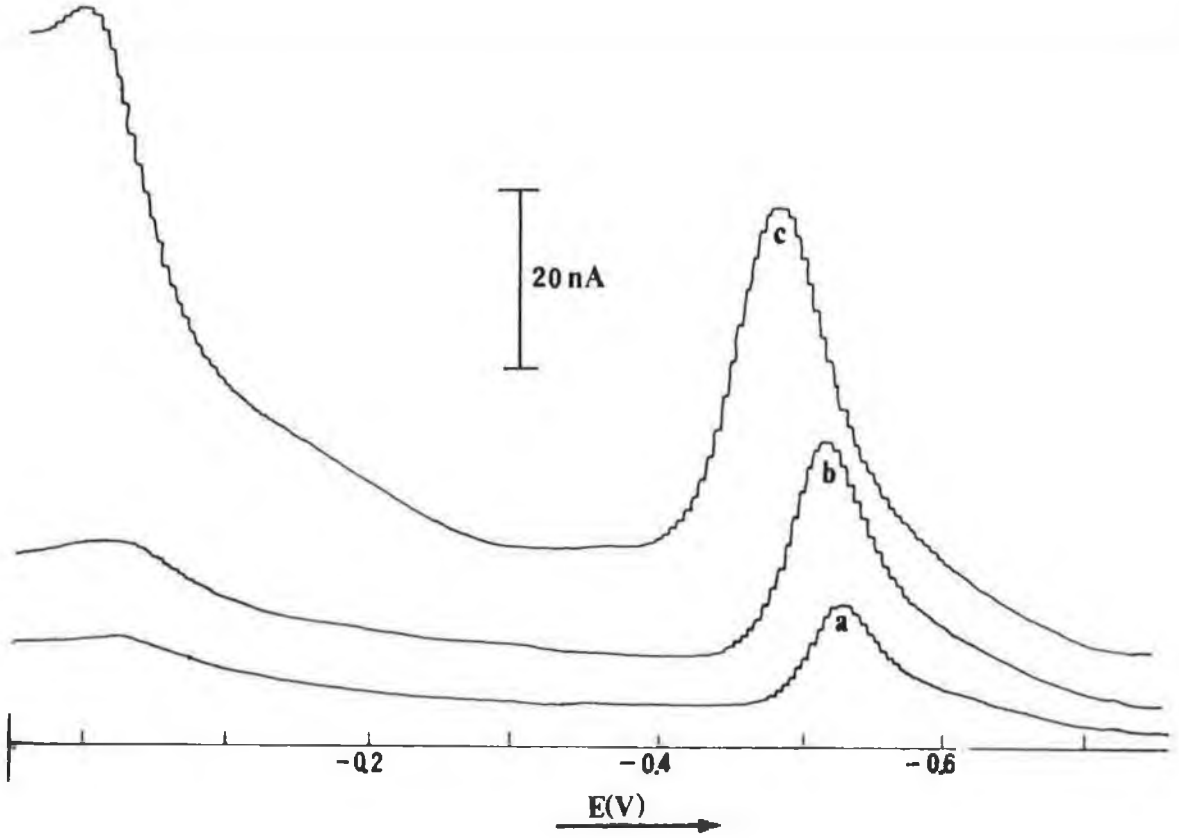

Figure 5.10. Effect of varying pulse amplitude on the differential pulse adsorptive voltammetric behaviour of $F(ab')_2$ fragments in 0.1 M phosphate buffer. Conditions: E_{acc} +0.05 V; scan rate 10 mV/s; pulse amplitude (a) 25 mV, (b) 50 mV, (c) 100 mV; t_{acc} 200 s.

negative values with decreasing pulse amplitude, a phenomena often seen in such studies. The pulse amplitude chosen was 50 mV, as it gave a well defined peak and allowed comparison with the IgG studies in chapter 4. A medium drop size (of area 0.016 cm^2) was chosen for the same reasons. Peak B was found to be suitable for the construction of a calibration curve for the $F(ab')_2$ fragments over a concentration range 0.25 to 1.50 mg/l, which is illustrated in Figure 5.11. The slight levelling of the curve at approximately 1.0 mg/l is probably due to complete drop coverage. The slope of the linear portion of the curve was 10.4 $nAmg^{-1}l$, and had a correlation coefficient of 0.9912.

5.3.1.4. The Effect of Electrolyte Concentration on the Voltammetric behaviour of the Fab Fragments

The Fab fragments were found to exhibit similar differential pulse adsorptive stripping voltammetric behaviour to the $F(ab')_2$ fragments. The Fab fragments exhibited two cathodic peaks at -0.215 V (peak A) and at -0.55 V (peak B). The effect of decreasing electrolyte concentration on the current response of cathodic peak B for these Fab fragments was investigated. In all of the studies involving the $F(ab')_2$ fragments, the same electrolyte concentration (0.10 M) was used. In order to study the effect of a lower electrolyte concentration, a comparison of the effect of varying drop size on the peak current was carried out for concentrations of 0.1 M and 0.01 M buffer. It may be seen from Figure 5.12. that the lower electrolyte concentration yields a better defined peak with a

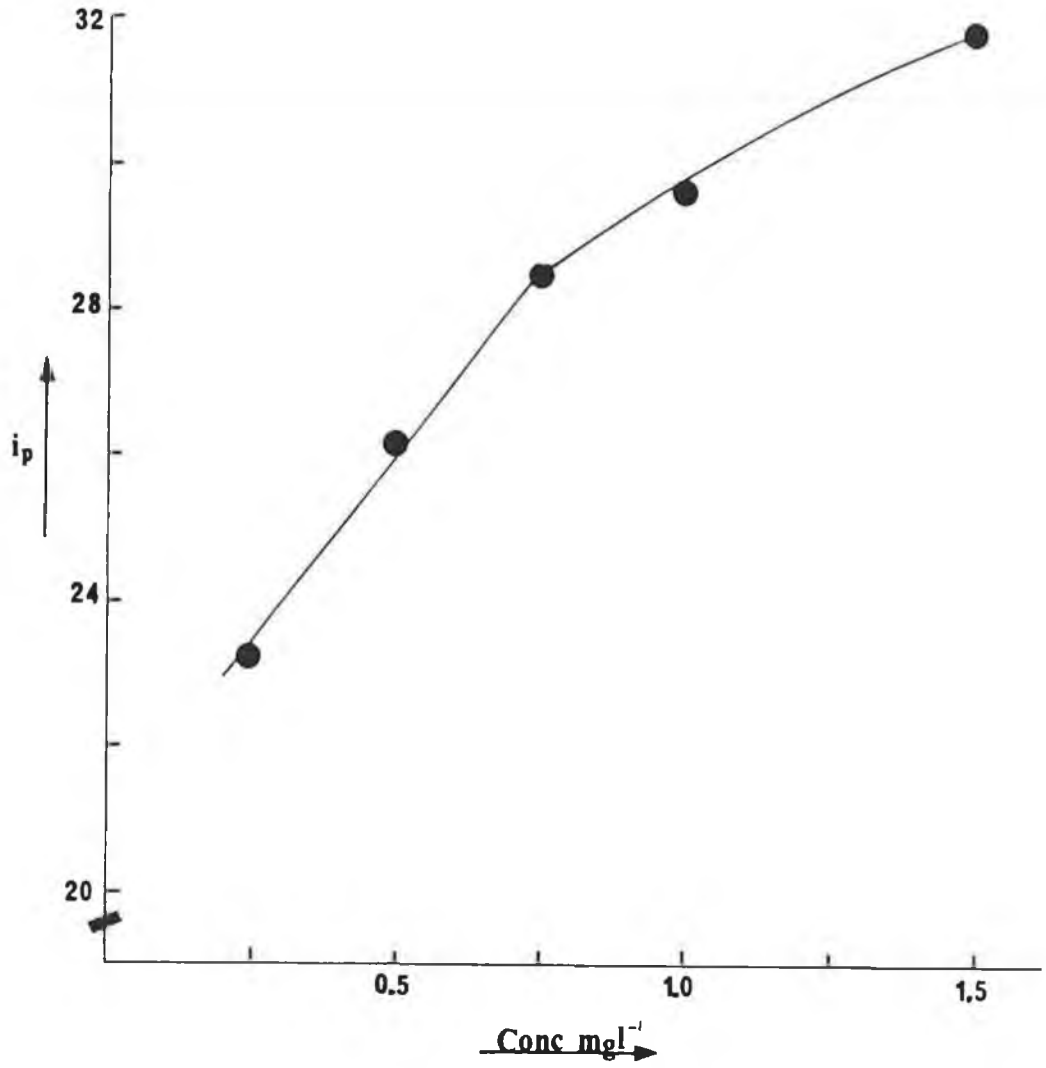

Figure 5.11. Graph of the increase in current of peak B on increasing concentration of $F(ab')_2$ fragments. Conditions: E_{acc} +0.05 V; scan rate 5 mV/s; pulse amplitude 50 mV; t_{acc} 300 s.

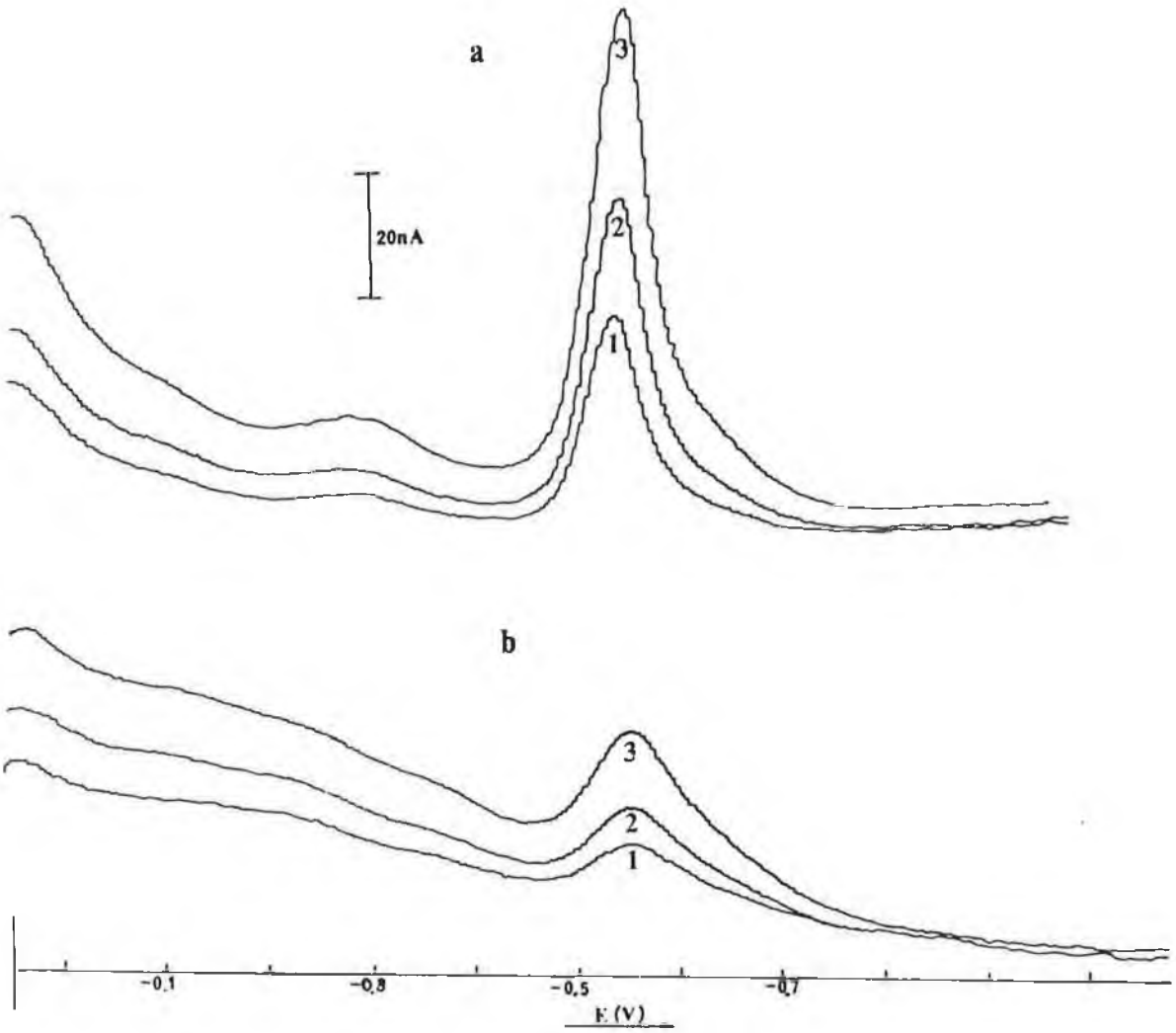

Figure 5.12. Effect of varying drop size, (1) 0.01 cm^2, (2) 0.016 cm^2, (3) 0.025 cm^2, on the peak currents of cathodic peak B of Fab fragments in (a) 0.01 M phosphate buffer and (b) in 0.1 M phosphate buffer, pH 7.4.

peak current increase compared to the identical scan at the higher electrolyte concentration.

Copeland et al.[20] have demonstrated that anodic stripping voltammetric measurements of heavy metals exhibit peak current decreases at lower electrolyte concentrations. This can be counteracted, however, by using microelectrodes. However on studying the adsorptive stripping voltammetry of organic compounds such as riboflavin using conventional electrodes, Wang et al.[21] noticed that in lower electrolyte concentrations an improved response was obtained. It has been suggested, in a study of the CV and DP voltammetric behaviour of reactants adsorbed at the electrode surface by Brown and Anson[22], that the intentional addition of external uncompensated resistance when using DPV leads to significant increases in the sensitivity.

From this study it would seem that Fab and $F(ab')_2$ fragments give rise to the same voltammetric behaviour as the intact immunoglobulin molecule. The similarity of the behaviour of the single Fab fragment, although not ruling out contribution from the Fc portion of the molecule, indicates that the primary and secondary structures (ie. the amino acid residues structure and sequence) contribute to the voltammetric response of the protein. This is discussed further in chapter 6. In this next section, proteins with a different conformation to the immunoglobulin molecule have been investigated.

5.3.2. Voltammetric Investigation of Streptavidin and Avidin

5.3.2.1. Adsorptive Voltammetric Study of Streptavidin

The adsorptive stripping voltammetric behaviour of streptavidin was optimised, using a similar procedure to that used for the intact immunoglobulin study, discussed in chapter 4. Throughout this study, a phosphate buffer concentration of 0.01 M was used, as preliminary studies had indicated that, as for the Fab fragments, a less concentrated electrolyte solution resulted in an enhanced peak current. From the cyclic voltammogram illustrated in Figure 5.13., the main peak (peak B) may be seen at -0.53 V, which is similar to that obtained for both the intact immunoglobulin molecules and the Fab and $F(ab')_2$ fragments. In this scan the protein was accumulated without electrolysis. The decrease in the size of peak B on repetitive scans indicated that, as before, the analytical peak is dependent on adsorptive accumulation at the electrode surface. The small pre-peak (at -0.36 V), was also evident (to a lesser degree) in the background electrolyte scan, this was found to decrease in subsequent scans but at a slower rate than peak B. The effect of pulse amplitude and drop size on the current of peak B may be seen in Figure 5.14. Although a pulse amplitude of 100 mV resulted in a greater peak current, the peak was not as well defined as that with a pulse amplitude of 50 mV, which was used for the rest of the study. For the investigation into the effect of varying the drop size on the peak size and shape of peak B, a pulse of 100 mV was used and

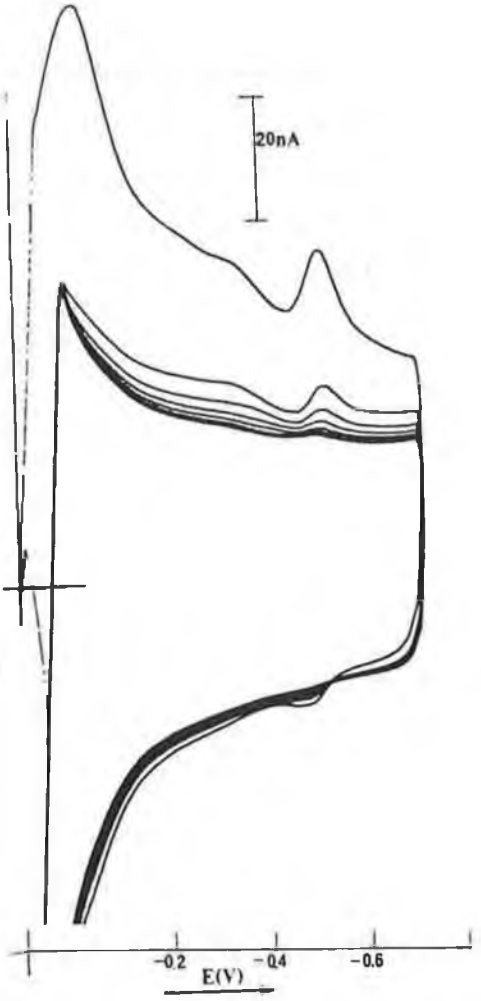

Figure 5.13. A cyclic voltammogram of streptavidin accumulated under conditions of no electrolysis, in 0.01 M phosphate buffer. Conditions: E_{start} +0.1 V; t_{acc} 500 s; scan rate; 500 mV/s; pulse amplitude 100 mV.

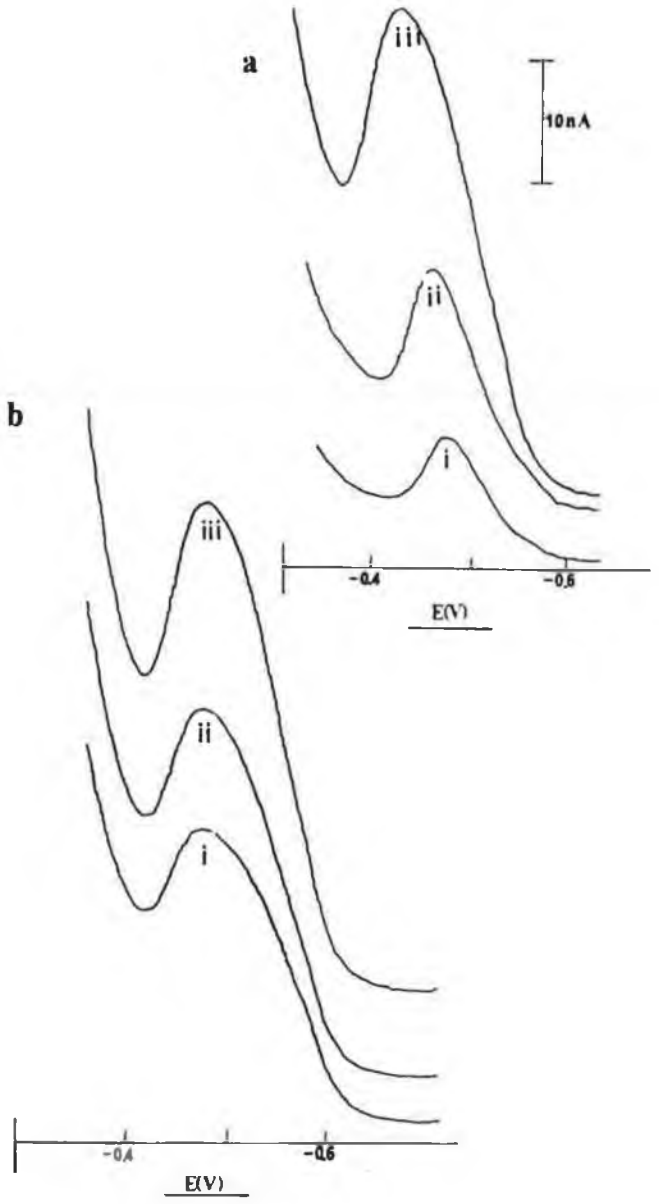

Figure 5.14. (a) The effect of varying pulse amplitude on the differential pulse adsorptive stripping voltammetric behaviour of streptavidin in 0.01 M phosphate buffer. (i) 25 mV; (ii) 50 mV; (iii) 100 mV. (b) The effect of varying drop size. (i) 0.01 cm^2; (ii) 0.016 cm^2; (iii) 0.025 cm^2. Conditions: E_{acc} +.01 V; scan rate 5 mV/s; t_{acc} 600 s.

resulting in broad, badly defined peaks for each scan regardless of drop size. Although a large drop size was used throughout the study of pulse amplitude, a medium drop size was chosen for the rest of study to minimise the accumulation of mercury at the bottom of the cell.

The optimum accumulation potential for the accumulation of streptavidin under electrolysis was found to be +0.1 V (Figure 5.15.). Streptavidin, however, gave rise to a much larger current response (approximately a 60% increase) when the accumulation was carried out without electrolysis (Figure 5.16.). Streptavidin has an isoelectric point near neutral pH; hence it is very slightly positive at pH 7.4, which would explain its preferential adsorption to an uncharged electrode (i.e. without electrolysis) than to a positively charged surface. The increase in the current of peak B was linear with respect to both accumulation time and concentration until complete drop coverage was reached. The effect of increasing the accumulation time on the peak current of peak B is illustrated in Figure 5.17. The relationship between the increasing accumulation time and the current was linear, with a slope of 8.95×10^{-2} nAs^{-1} and a correlation coefficient of 0.9965. A large drop size was used to facilitate the use of longer accumulation times for this study. The effect of increasing streptavidin concentration on the current of peak B is illustrated in Figure 5.18. This calibration curve has a plateau starting at around 1 mg/ml implying that the drop was completely covered. The linear portion of the curve had a slope of 54.6 nA/mgl^{-1} and a correlation coefficient of 0.9993. This study was undertaken using a medium drop size;

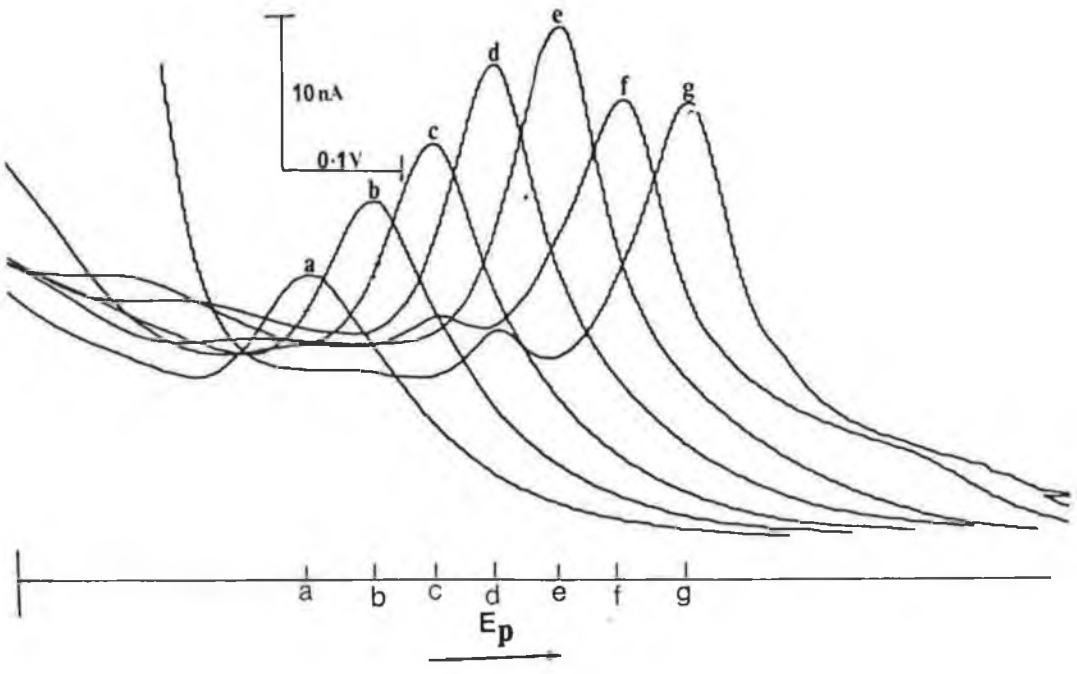

Figure 5.15. Effect of varying accumulation potential on the differential pulse adsorptive stripping voltammetric behaviour of streptavidin in 0.01 M phosphate buffer. Conditions: E_{acc}; (a) -0.10 V (b) -0.05 V (c) 0.00 V (d) +0.05 V (e) +0.10 V (f) +0.15 V (g) +0.20 V; scan rate 5 mV/s; pulse amplitude; 25 mV; t_{acc} 200 s; drop size 0.016 cm^2.

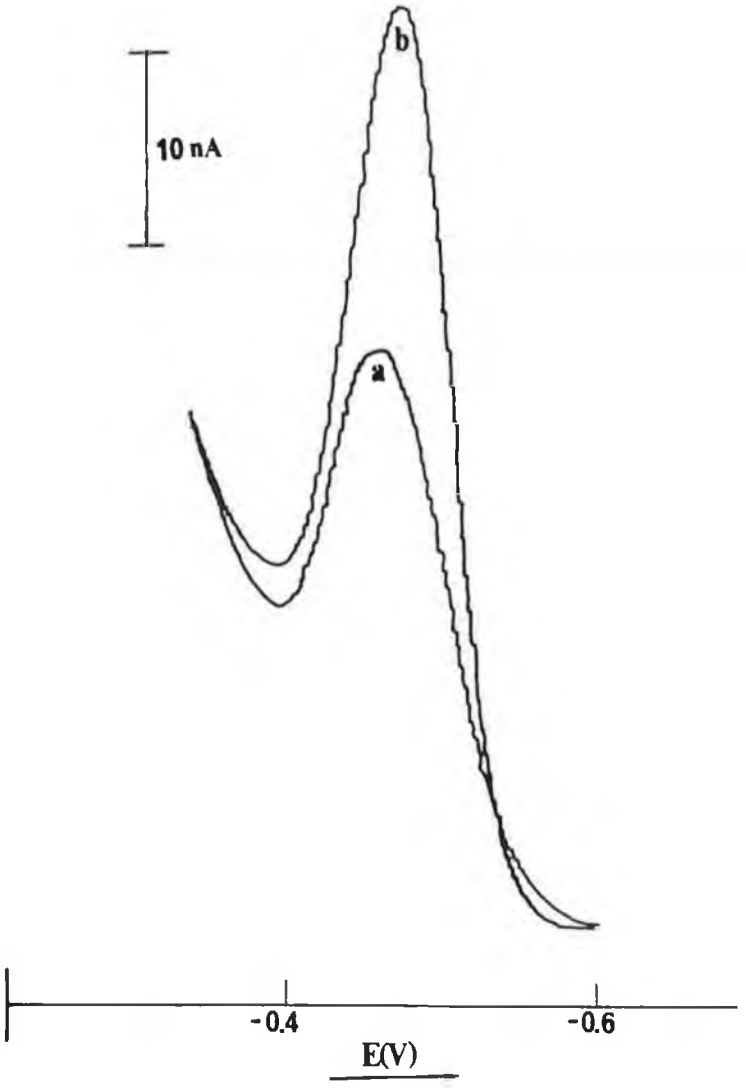

Figure 5.16. Differential pulse adsorptive stripping voltammogram of streptavidin in 0.01 M phosphate buffer: (a) under conditions of electrolysis, E_{acc} +0.1 V; (b) without electrolysis. Conditions: scan rate 5 mV/s; pulse amplitude 100 mV/s; t_{acc} 500 s; drop size 0.025 cm^2.

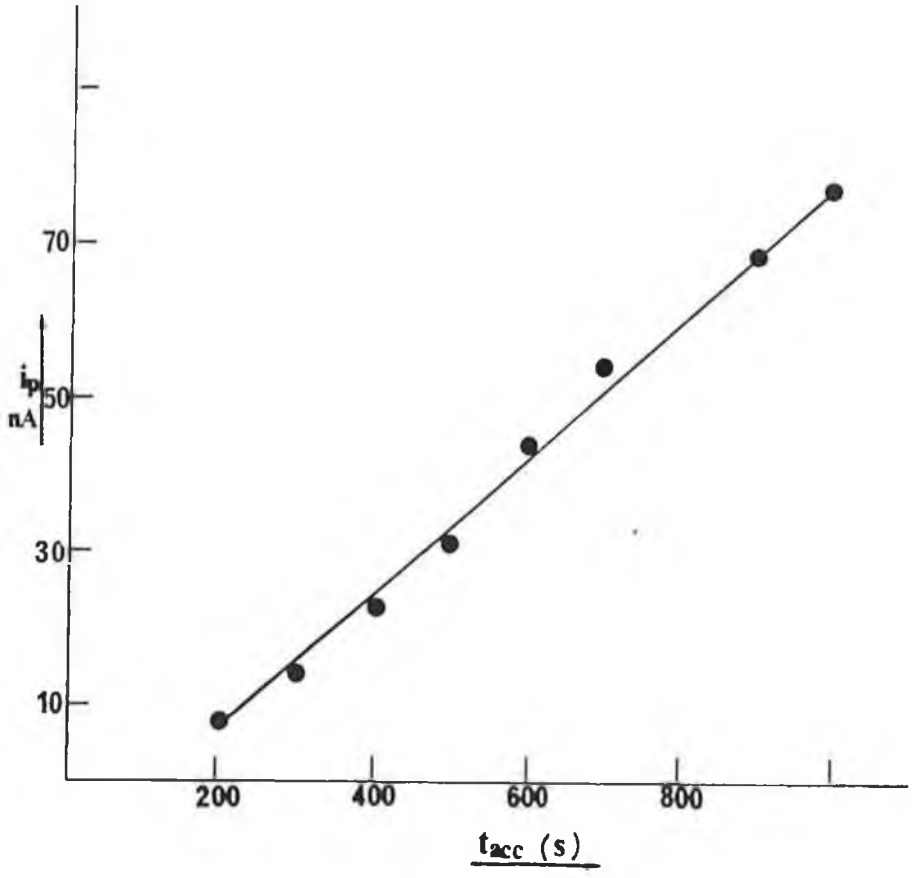

Figure 5.17. Graph of increase in peak current of streptavidin with increasing accumulation time.

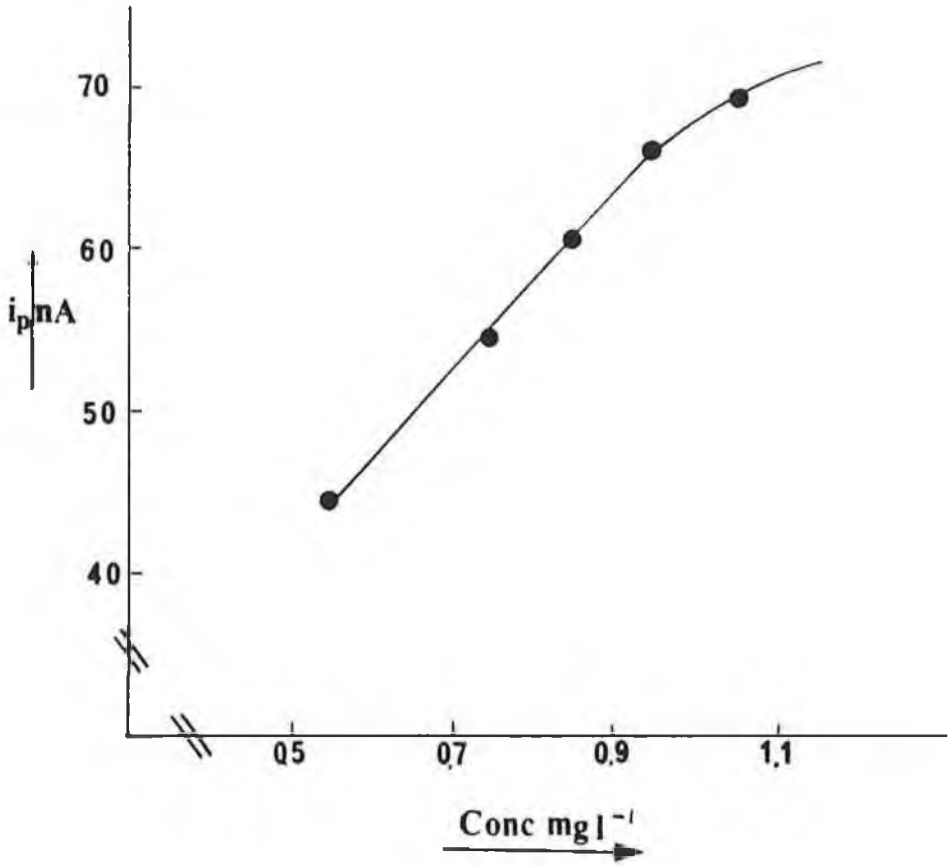

Figure 5.18. Graph of increase in peak current of peak B with increasing concentration of streptavidin.

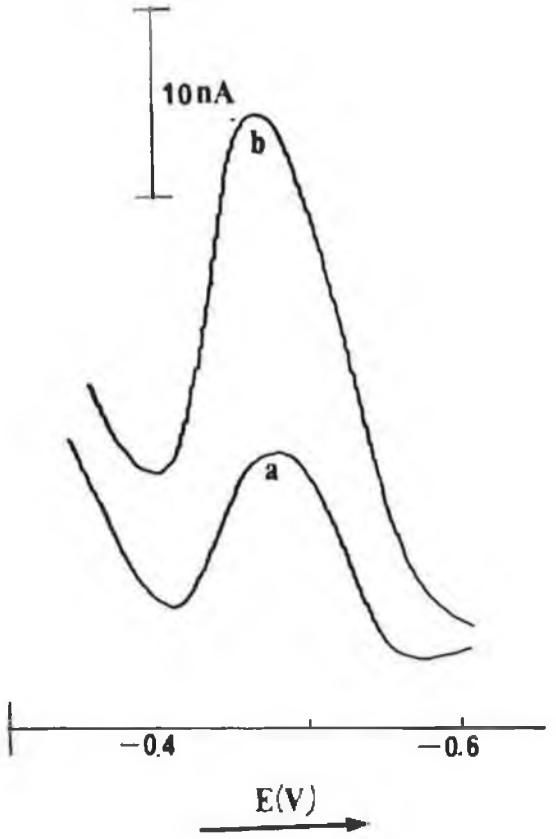

Figure 5.19. Effect of varying electrolyte concentration on the current response of a 1.18 x 10^{-8} solution of avidin: (a) 0.1 M phosphate buffer; (b) 0.01 M phosphate buffer.

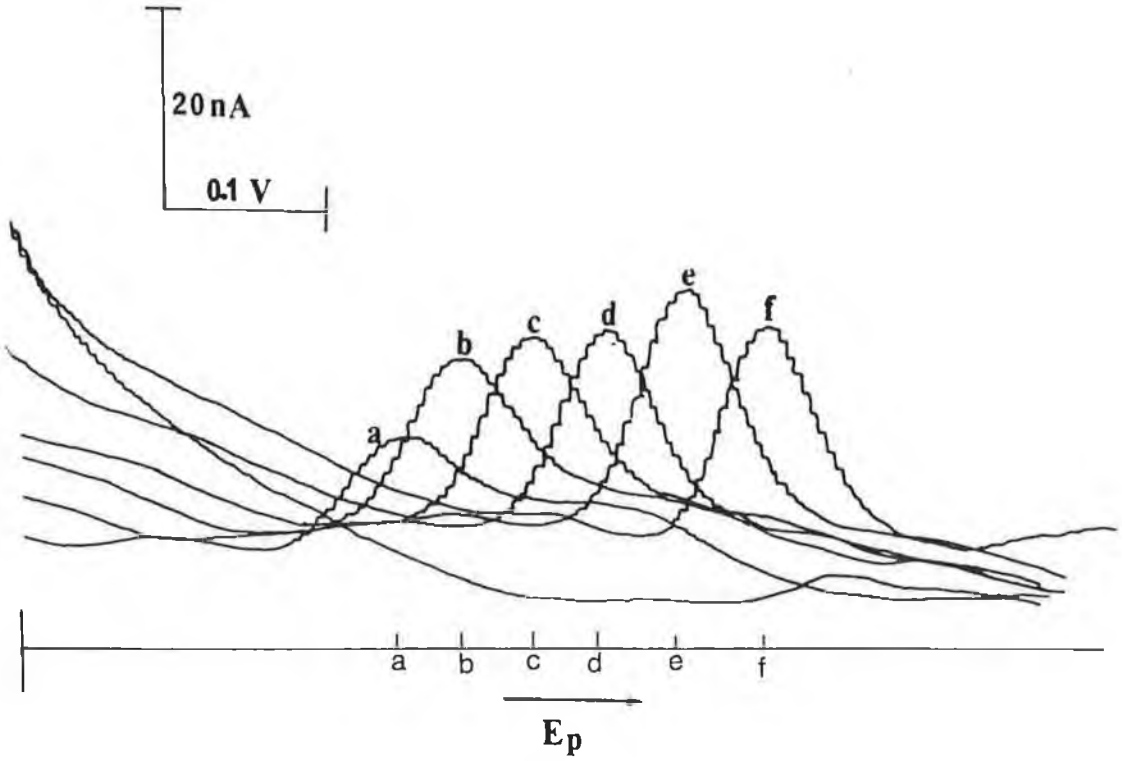

Figure 5.21. Effect of varying accumulation potential on the differential pulse adsorptive stripping voltammetric behaviour of avidin in 0.01 M phosphate buffer. Conditions: E_{acc} (a) -0.10 V; (b) -0.05 V; (c) 0.0 V; (d) +0.05 V; (e) +0.10 V; (f) +0.15 V; scan rate 5 mV/s; pulse amplitude 50 mV; drop size 0.016 cm^2; t_{acc} 300 s.

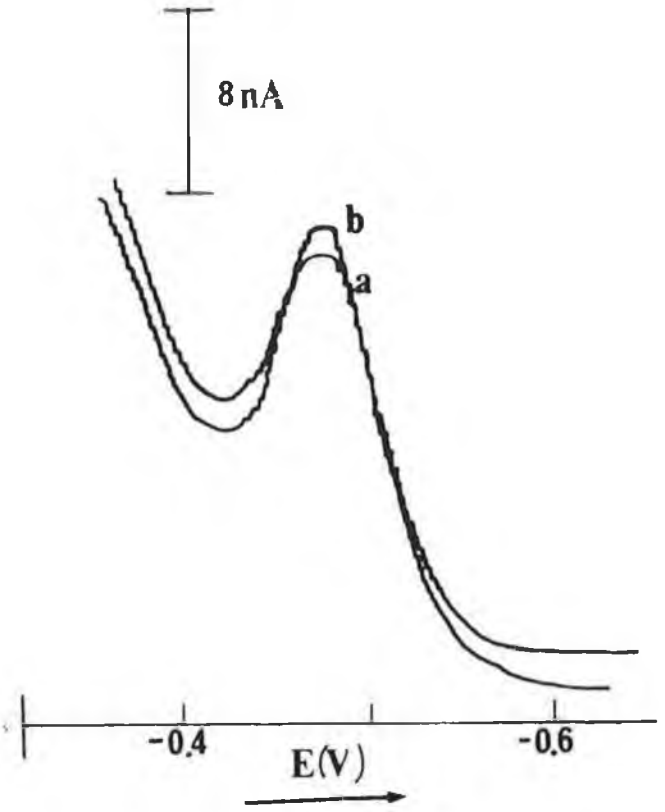

Figure 5.22. Differential pulse adsorptive stripping voltammogram of avidin in 0.01 M phosphate buffer: (a) under conditions of electrolysis, E_{acc} +0.10 V; (b) without electrolysis. Conditions: scan rate 5 mV/s; pulse amplitude 100 mV; drop size 0.025 cm^2; t_{acc} 400 s.

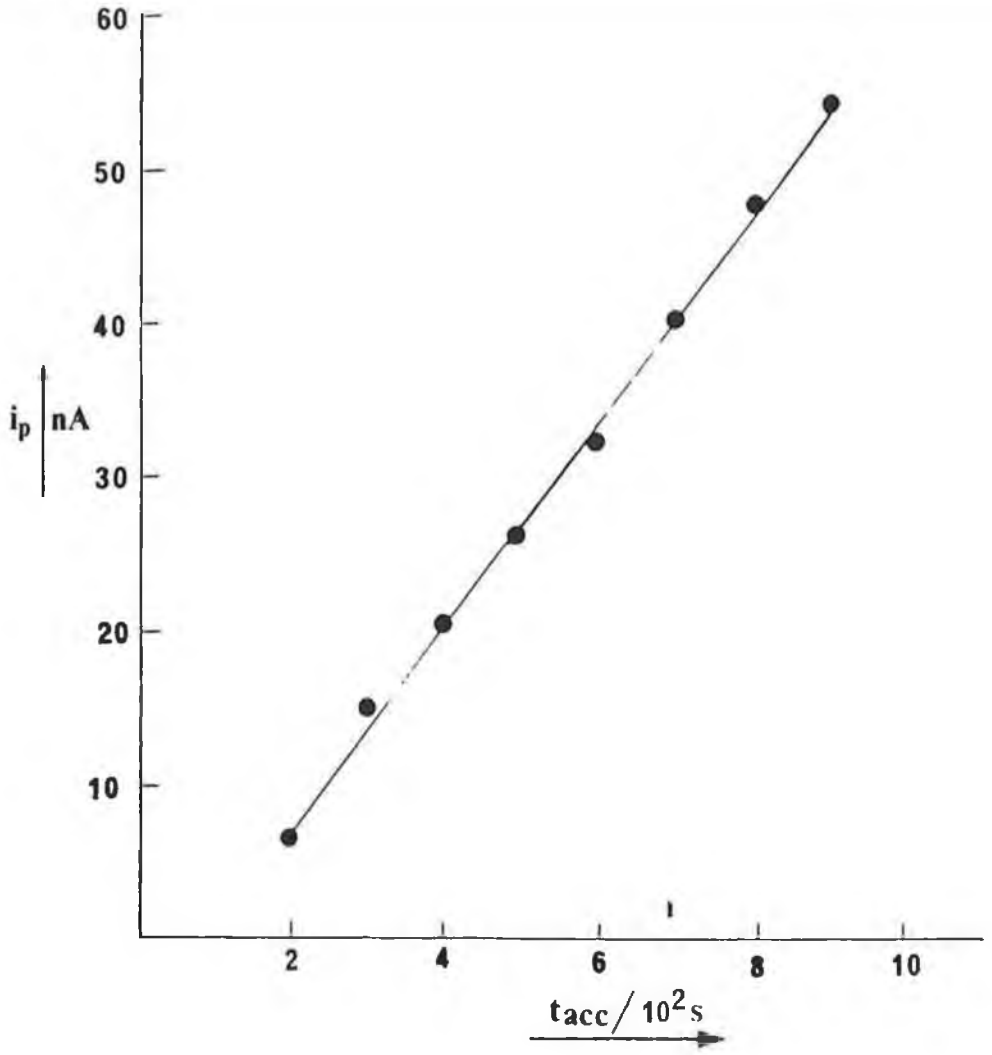

Figure 5.23. Graph of increase in peak current of avidin with increasing accumulation time.

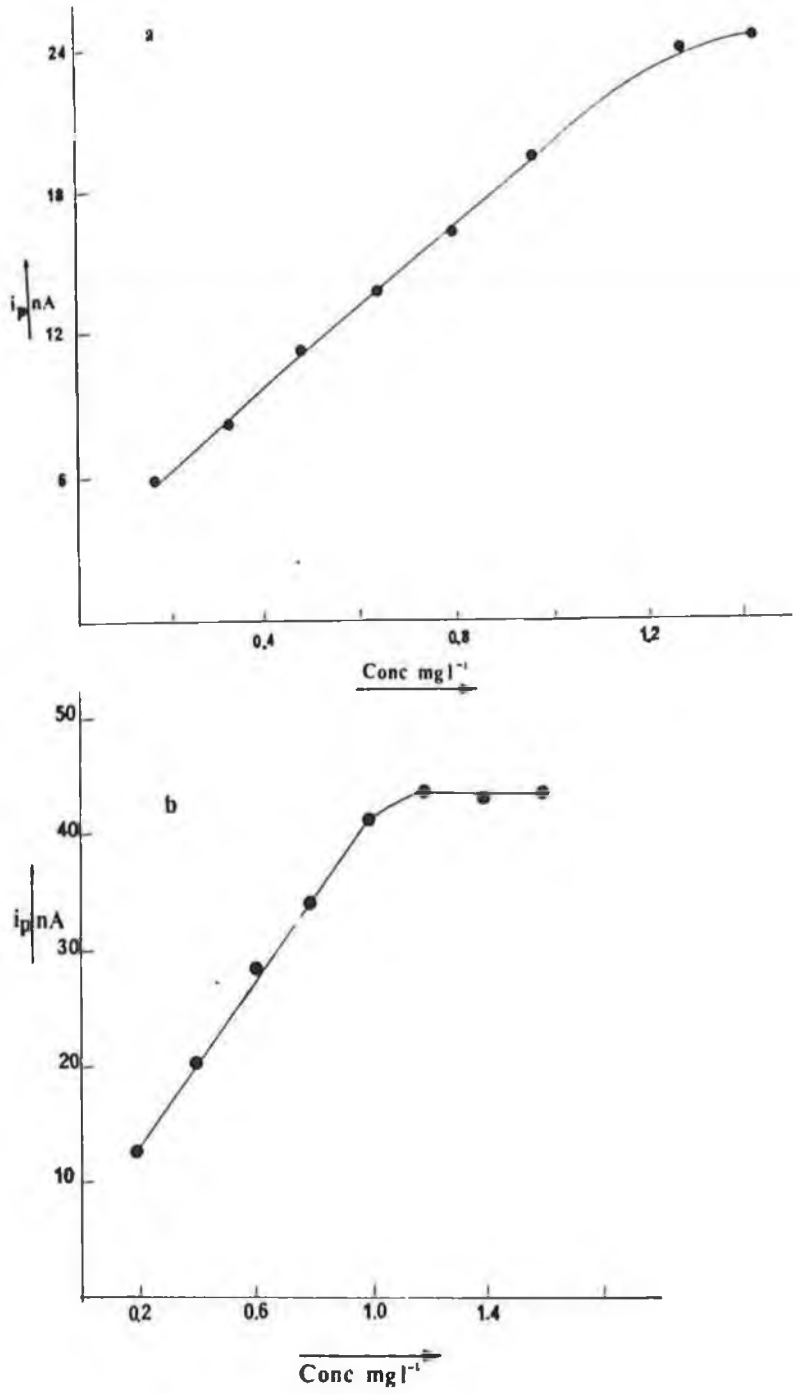

Figure 5.24. Graphs of increase in peak current with respect to increasing concentration of avidin: (a) pulse amplitude 50 mV; (b) pulse amplitude 100 mV.

5.3.2.3. Interaction of Avidin and Streptavidin with Biotin

The addition of biotin to a solution of avidin was found to have a negligible effect on the voltammetric response of the protein, as can be seen in Figure 5.25. As biotin binding alone had no effect on the electrochemical response of the protein, the interaction of both avidin and streptavidin with a larger molecule, ie. biotinylated anti-mouse IgG, raised in a rabbit, was investigated.

A calibration curve for avidin was constructed, and as expected, the current increased with increasing concentration, to a concentration of 1.12×10^{-8} M ($1\ mgl^{-1}$) represented by peaks (a) to (d) in Figure 5.26. Peak (e), (represented by a dotted line) represents the current response on addition of 3.1×10^{-9} M (0.5 mg/l) biotinylated anti-mouse IgG, where a large increase in the protein peak, from 13 to 23 nA, was observed. With subsequent additions of more avidin to the solution of avidin and biotinylated IgG, to a final avidin concentration of 1.8×10^{-8} M ($1.6\ mgl^{-1}$), represented by peaks f-h, there was a slight increase in the current response. This was not as significant as the current response obtained for the first four additions of avidin to the cell, as it had probably reached complete drop coverage. On addition of a further aliquot of biotinylated IgG to the cell (peak i), bringing the total IgG concentration to 6.2×10^{-9} M (1 mg/l), another large current increase from 27 to 35 nA was obtained. There was certainly no decrease in the avidin signal as a result of binding to the IgG molecule via the biotin link, which would indicate that the inavailability of the proteins

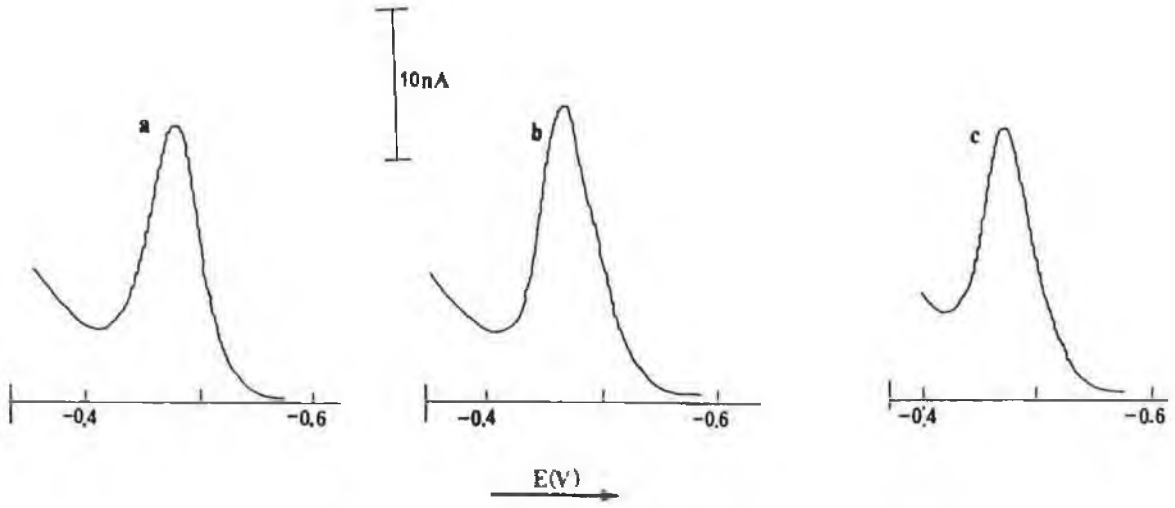

Figure 5.25. Effect of increasing concentrations of biotin on the peak current response of a 3.3 x 10^{-8} M solution of avidin in 0.01 M phosphate buffer. (a) without biotin. (b) 1.6 x 10^{-6} M biotin. (c) 6.5 x 10^{-6} biotin. Conditions: E_{acc} +0.10 V; scan rate 5 mV/s; pulse amplitude 100 mV; drop size 0.025 cm^2; t_{acc} 200 s.

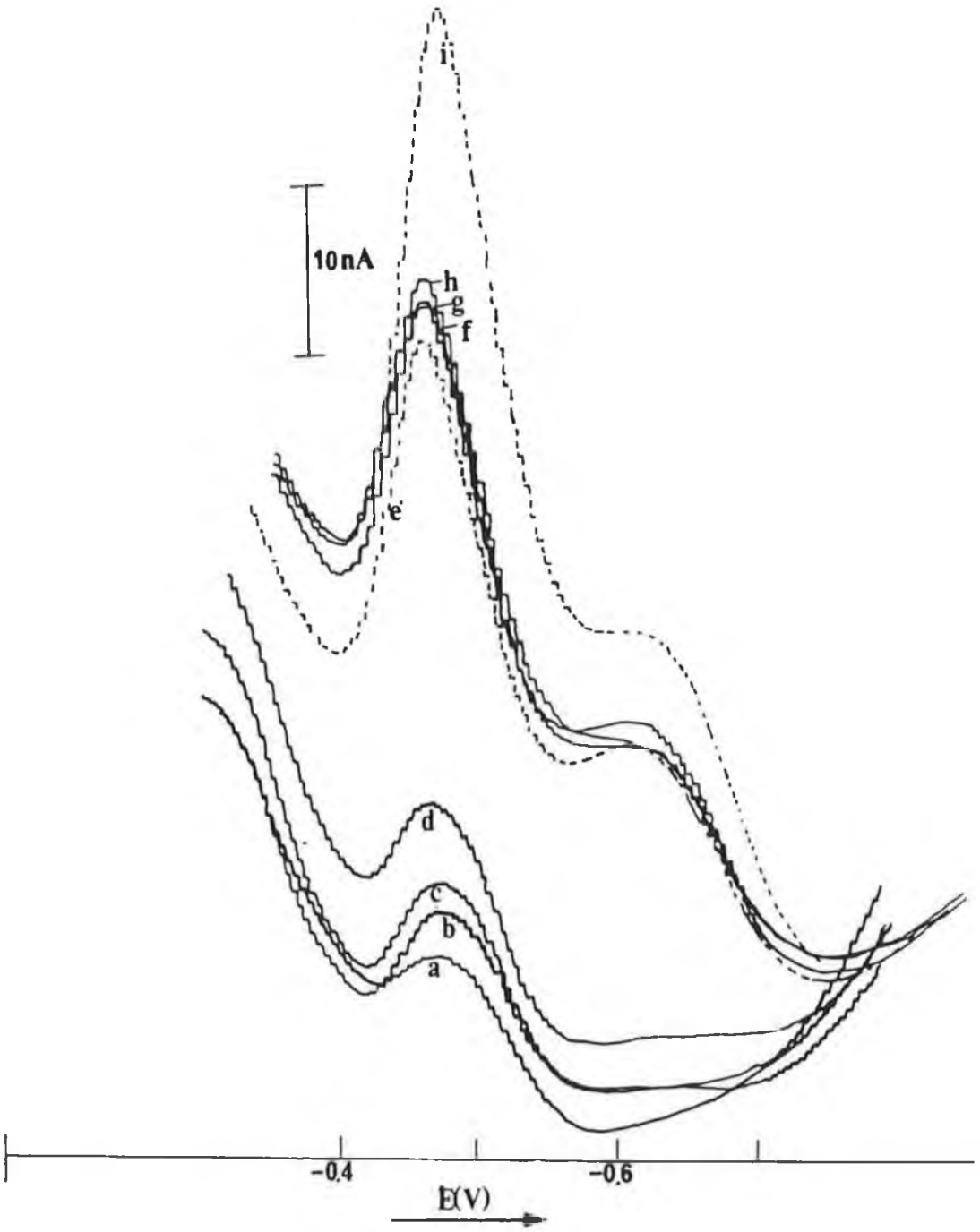

Figure 5.26. Effect of addition of biotinylated rabbit anti-mouse IgG on the peak current response of avidin in 0.01 M phosphate buffer. Conditions: E_{acc} +0.10 V; scan rate 5 mV/s; pulse amplitude 100 mV; drop size 0.025 cm^2; t_{acc} 400 s.

binding site did not affect its adsorption to the electrode or its electrochemical response. It would seem however, from the fact that the increase in current response with increasing concentration of avidin after the biotinylated IgG had been added was very slight (if not negligible), and that the peak due to protein increased after complete drop coverage, by avidin, that there was some competition for adsorption sites on the electrode between the two protein molecules. The current response of the immunoglobulin molecule was not inhibited by its specific binding to avidin, as it had been by the specific interaction with its antibody, mouse-IgG, as discussed in chapter 4. The interaction of the immunoglobulin with avidin occurs at a different site on the immunoglobulin molecule, ie. at the -COOH portion of the F_c fragment, as opposed to the $-NH_2$ terminal at the antigen binding site. This would suggest that the antigen binding sites may have something to do with the adsorption of the molecule on the electrode surface.

There is an interesting incidence of an appearance of a new peak at -0.625 V (peak C) with the addition of the biotinylated IgG. This may be more clearly seen in Figure 5.27., which illustrates an alternative approach to verify the previous phenomena.

In this study, streptavidin, which has the same effect as avidin, was used to illustrate the case. A calibration curve was prepared for biotinylated-IgG. The peaks represented by unbroken lines in Figure 5.27. correspond to the increasing concentration of biotinylated-IgG (to 1.25 mg/l). On addition of 0.9 mg/l of streptavidin there was an increased response, represented by a broken line, as would be expected on addition

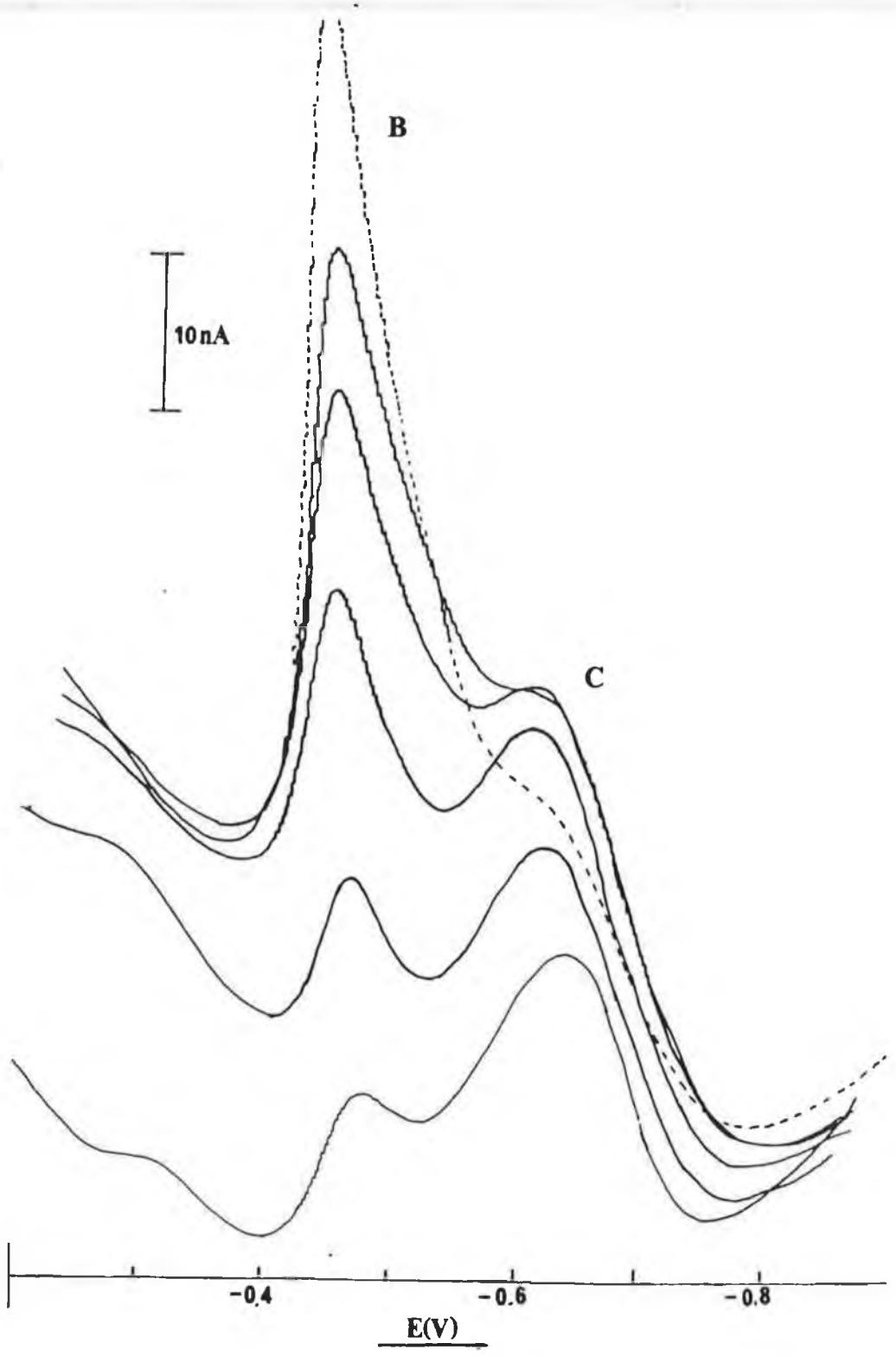

Figure 5.27. Effect of addition of streptavidin on the differential pulse adsorptive stripping voltammetric behaviour of biotinylated rabbit anti-mouse IgG. Streptavidin is represented by the dashed line. Conditions: E_{acc} +0.10 V; scan rate 5 mV/s; pulse amplitude 100 mV; drop size 0.025 cm^2; t_{acc} 200 s.

of non-specific protein. It may be seen that there is no decrease in the cathodic peak at -0.50 V for biotinylated-IgG on addition of the specific binding protein. This is more clearly illustrated in Figure 5.28., where the current response is plotted against the concentration of protein in mg/l. The plot is linear as would be expected for increasing protein concentration. The last point represents the response due to the addition of streptavidin and is identical to that that would be expected for the addition of 0.9 mg/l of IgG. It may be seen from Figure 5.27. that a there is a second peak (peak C) at -0.625 V. This peak was not seen for either of the immunoglobulins or fragments previously studied. This peak does not, however, increase relative to the peak at -0.50 V and is clearly affected by the addition of biotinylated-IgG. The height of peak C seems to decrease as the concentration of immunoglobulin is increased. Such a relationship may be clearly seen in Figure 5.29. where the current response of peak C is plotted against the concentration of biotinylated-IgG. The graph is linear until this peak becomes a shoulder at a concentration level of 1.25 mg/l and eventually disappears. This phenomena may be due to the adsorption profile of the protein and will be discussed further in chapter 6.

5.3.3. Conclusion

From the above work it may be seen that the proteins studied give clear well defined analytical peaks that may be used for quantitative work, as they produce reproducible calibration curves from which an unknown concentration may be estimated.

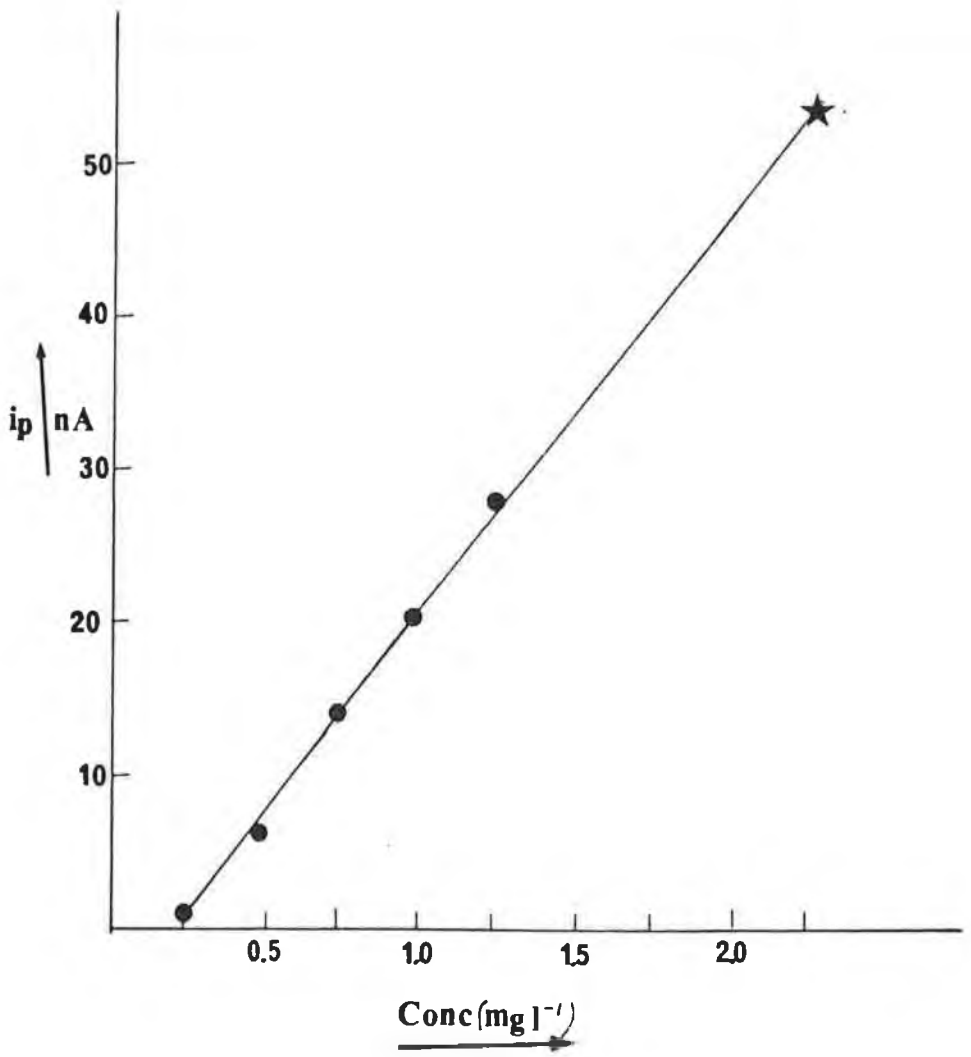

Figure 5.28. Graph of increase in the current response of peak B of biotinylated-IgG with (●) increasing concentration of biotinylated IgG and (★) with the addition of streptavidin.

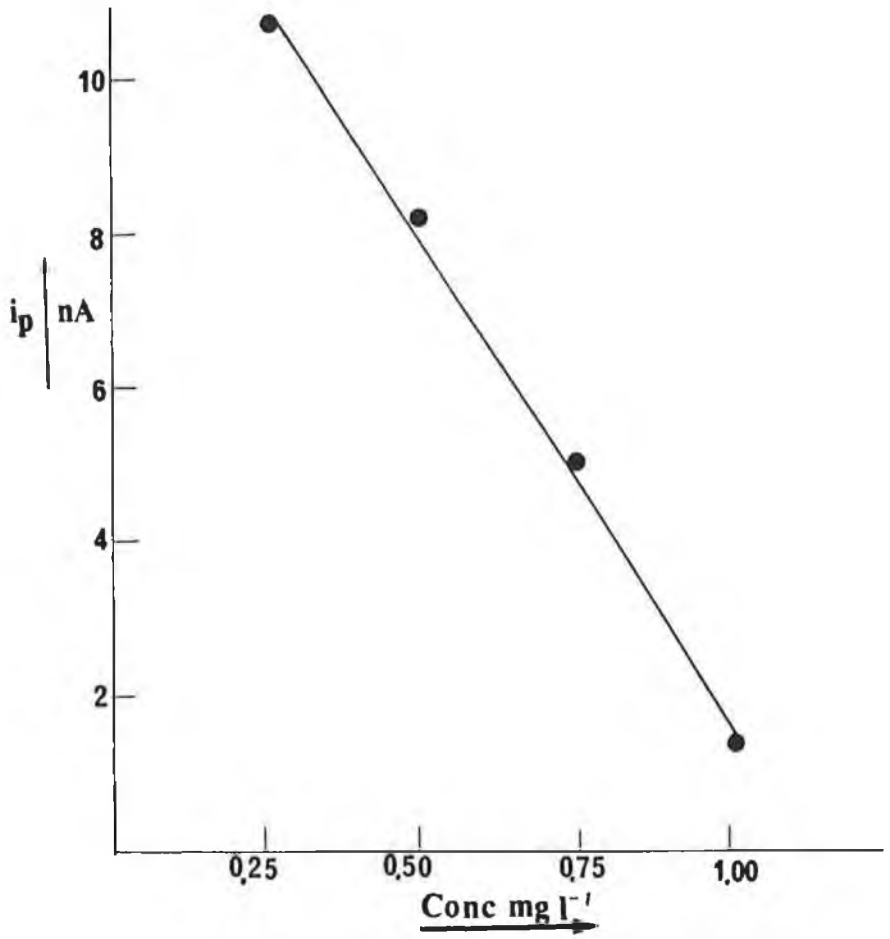

Figure 5.29. Graph of decrease in peak current of peak C of biotinylated IgG with increasing concentration of biotinylated IgG.

However, this is only possible in pure solutions, as all of the proteins studied in this work, regardless of structure and amino acid sequence, give rise to similar response characteristics. This response may still be exploited analytically if not in the clinical sample. The assay of the immunological reaction described in chapter four has been used to assay for immunological activity of labelled IgG (Ryan, E., Vos, J.G. and O'Kennedy, R., personal correspondance). In the following chapter, possible suggestions as to the nature of the electrochemical response of such proteins is more fully discussed.

5.4. REFERENCES

1. De Alwis, V. and Wilson, G.S., Anal. Chem., 59(1987)2786.
2. Steinitz, F., Arch. Gesamte. Physiol., 72(1898)75.
3. Parsons, H.T. and Kelly, E., Amer. J. Physiol., 104(1933)150.
4. Chaiet, L. and Wolf, F.J., Arch. Biochem. Biophys., 106(1964)1.
5. Wilchek, M. and Bayer, E.A., Anal. Biochem., 171(1988)1.
6. Kohen, F., Amir-Zaltsman, Y., Strasburger, C.J., Bayer, E.A. and Wilchek, M., in "Complementary immunoassays" ed. Collins, W.P., (Wiley, New York, 1987).
7. Guesdon, J.-L., Ternynck, T. and Avrameas, S., J. Histochem. Cytochem., 27(1979)1131.
8. Schray, K.J and Niedbala, R.S., Anal. Chem., 60(1988)353.
9. Hanson, S.I. and Holm, J., Anal. Biochem., 172(1988)160.
10. Luo, S. and Walt. D.R., Anal. Chem., 59(1987)1.
11. Green, N.M., Biochem. J., 89(1963)609.
12. Green, N.M., Biochem. J., 96(1964)16c.
13. Pahler, A., Hendrickson, W.A., Gawinowicz Kolks, M.A., Argarana, C.E. and Cantor, C., J. Biol. Chem., 262(1987)13933.
14. Green, N.M. and Toms, E.J., Biochem. J., 118(1970)67.
15. Bayer, E.A., Skutelsky, E. and Wilchek, M., Meth. Enzymol. 62(1979)308.
16. Green, N.M., in "Advances in Protein Chemistry" ed. Anson, M.L. and Edsell, J.T., (Acedemic Press, New York, 1975).
17. Green, N.M. and Toms, E., Biochem. J., 133(1973)687.

18. Hudson, L. and May, F.C., "Practical Immunology", (Blackwell Scientific Publications, Boston, 1980).

19. Mishell, B. and Shigi, S., "Selected Methods in Cellular Immunology" (WH Freeman and Co., San Francisco, 1980).

20. Copeland, T.R., Christe, J.H., Skogerboe, R.K. and Osteryoung, R.A., Anal. Chem., 45(1973)995.

21. Wang, J. and Farias, P.A.M., J. Electroanal. Chem. 182(1985)211

22. Brown, A.P. and Anson, F.C., Anal. Chem. 49(1984)1589.

CHAPTER 6

DIRECT VOLTAMMETRIC DETECTION OF PROTEINS

6.1. INTRODUCTION

In the two preceding chapters, the voltammetric behaviour of analytically important binding proteins has been investigated. All of the proteins studied are important in immunoassay procedures, and an understanding of their electrochemical behaviour is vital at a time when electrochemical technologies are becoming of greater importance in biosensor technology.
During this work, it became apparent that there was no satisfactory explanation for the electrochemical behaviour of proteins that do not contain a prosthetic group. In the following chapter, an attempt has been made to add some fresh evidence, and to try to explain the behaviour of the proteins chosen.

6.2. PROTEIN STRUCTURE

The word "protein" covers a multitude of complex macromolecules, with very different structures and functions. Proteins such as collagen (which is fibrous and has very high tensile strength) are the major components of cartilage and tendons, whereas proteins such as enzymes are highly specialised and designed to catalyse chemical reactions occurring in the body. All proteins, regardless of function, shape or activity, are built from a set of twenty basic amino acids. All amino acids (except for glycine) have an asymmetric carbon (α-carbon) atom to which is bonded a hydrogen atom, a carboxyl group, an amino group and an "R" group, as illustrated in Figure 6.1. These amino acids join together via a

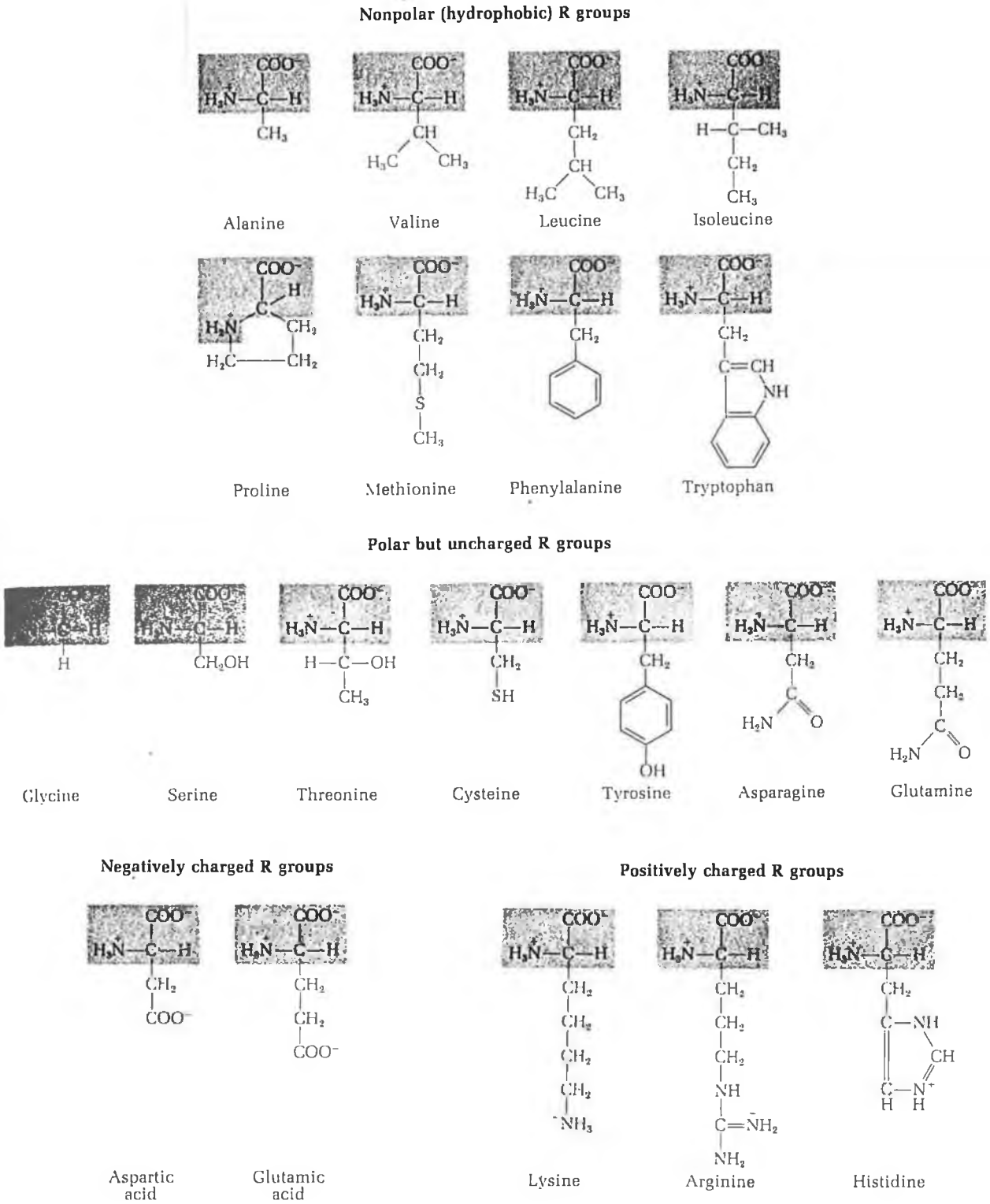

Figure 6.1. Structure of the twenty amino acids in proteins. The unshaded portion of the molecule represents the "R" group.

substituted amide linkage called a peptide bond:

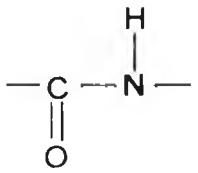

The amino acid residue at that end of the peptide which has a free α-amino group is termed the "amino terminal residue", and at that end containing the free carboxyl group is termed the "carboxyl-terminal residue". It is the particular sequence of amino acids (i.e. its secondary structure) that gives each protein its unique biological activity. Some proteins contain chemical groups other than amino acids and are called "conjugated proteins". These non-amino acid parts of the protein are called "prosthetic groups" and can be anything from a carbohydrate residue (hence, glycoprotein) to a metal ion (hence, metalloprotein). If a protein has one polypeptide chain it is called an "oligomeric protein", but most have more than one chain with anything from 100 to 2000 amino acid residues. The polypeptide chains are further folded and stabilised to form a three dimensional protein structure. In this work, globular proteins were of interest; these, as a class, are more complex than fibrous proteins and have a far greater variety of biological functions. The three dimensional structure of the protein is necessary, for example, for antigen binding sites of the immunoglobulin studied in chapter 4, the substrate binding site of the enzyme alkaline phosphatase in chapter 3, or the biotin binding sites of avidin and streptavidin in chapter 5. The compact folding of the polypeptide chain into its spherical or globular shape is

called the "tertiary structure". Four different forces help to stabilise the structure of proteins:

(i) hydrogen bonding between 2 groups of residues in adjacent loops of the chain;
(ii) ionic attractions between oppositely charged R groups;
(iii) hydrophobic interactions; and
(iv) covalent cross linkages.

The native protein may undergo denaturation if heated, exposed to extremes of pH or when it is adsorbed at a surface. Although the secondary structure remains intact the polypeptide chains unfold. As the tertiary structure is dictated by the amino acid residue sequence, folding is predetermined by certain residue positions, such as cystine residues at crosslinking points; therefore in some cases, denaturation is reversible if the environmental conditions are returned to normal. This process is called "renaturation".

6.3. ELECTROCHEMICAL CLASSIFICATION OF PROTEINS

Berg[2] has classified proteins into three groups from an electrochemical point of view:

(i) proteins yielding catalytic double waves after complexation;
(ii) proteins with prosthetic groups;
(iii) proteins with disulphide-thiol groups.

Before electron exchange occurs, the protein must adsorb onto the electrode surface, which is bound to have an important influence both on the protein itself (in terms of activity, such as enzymes in biosensor technology) and on its electrochemical behaviour[3]. Thus the adsorption profile of the protein must also be taken into consideration.

6.3.1. Proteins Yielding Catalytic Double Waves After Complexation

The first report of catalytic hydrogen waves was made by Heyrovsky and Babicka in the early 1930's. They were exploring a phenomena of a "peculiar wave" on current-voltage curves due to solution of human serum reported by Herles and Vancura[4]. A polarographic wave occurring before that due to sodium or ammonium ions (and thus called "presodium waves") was found to depend upon the simultaneous presence of ammonium ions and serum in solution[5]. A wave called the "albumin wave" appeared at -1.60 V (vs SCE) due to the addition of an aqueous solution of flour to a solution containing lithium chloride, hydrochloric acid and ammonium chloride. Similar responses were obtained using human serum and diluted egg white etc.[4] Brdicka could detect proteins containing cystine in the presence of cobalt ions by catalytic hydrogen deposition[6,7]. The explanation[2] given was that the RSH or RS^- groups complexed with cobalt, which then catalysed hydrogen evolution before the complex was decomposed into a cobalt amalgam and RSH or RS^-. This wave was found to be dependent on concentration and could therefore be exploited for quantitative analytical

measurements. A recent example of the use of the Brdicka current was to monitor the immunological interaction of human IgG and anti-human IgG by Kano et al[8]. Two proteins that do not contain any cysteine residues, i.e. myoglobin and subtilisin BPN, were studied by Senda et al[9]. Although myoglobin gave rise to a Brdicka current which was attributed to the presence of its heme group, subtilisin BPN did not.

6.3.2. Proteins with Prosthetic Groups

There are a huge variety of proteins with prosthetic groups that have been studied electrochemically. The electron transfer properties of these proteins are of vital importance in the electron transport chain of the body[1]. The respiratory chain of mitochondria contains a large number of electron-carrying transfer proteins that act in sequence to transfer electrons from substrates to oxygen. In electrochemical terms, these proteins are often called redox proteins and include flavoproteins and hemeproteins e.g. cytochromes etc. The electrochemistry of cytochromes, and particularly of cytochrome C, has been very well documented[10,11], as has hemeproteins[12]. In an important recent review of the direct electrochemistry of redox proteins by Armstrong et al[10]., the authors summarised the importance of a thorough understanding of the electrochemistry of redox proteins in three main points: (i) that the "marriage between electrode materials and biological macromolecules that bear highly specific modes of catalytic or sensory action is highly desirable", (ii) that such studies yield important information

about thermodynamic and kinetic properties, and (iii) that such electron transfer may only be studied after the problems associated with adsorption have been overcome. The information gained from studies of macromolecular interfaces is thus very useful to the electrochemist.

These points are valid also to electrochemical studies of simple "unconjugated" proteins that do not contain a prosthetic group. In particular, concerning the latter point, the information gained from studies on the adsorption of redox proteins is vital to the understanding of all biological macromolecule electrochemistry.

6.3.3. Proteins with Disulphide-Thiol Groups

It is an understanding of the electrochemical behaviour (particularly voltammetric) of these proteins that is important to this work. The disulphide bond in a protein comes from the interaction of two cysteine residues to form cystine as illustrated in Figure 6.2.

Proteins containing this disulphide bond adsorb strongly at the mercury electrode, and the electrochemistry of disulphide-containing proteins and of cysteine and cystine is very well documented[13,14,15]. Cyclic voltammograms for a 4.6 x 10^{-4} M solution of cystine in a 0.1 M phosphate buffer at pH 7.4, pre-equilibrated for 60 s at open circuit are illustrated in Figure 6.3[16]. At open circuit, the electrode was at its "abandoned potential" which was determined to be -0.32 V (vs. SCE). The main cathodic wave was found at -0.53 V (vs. SCE) and was a symmetrical wave characteristic of an

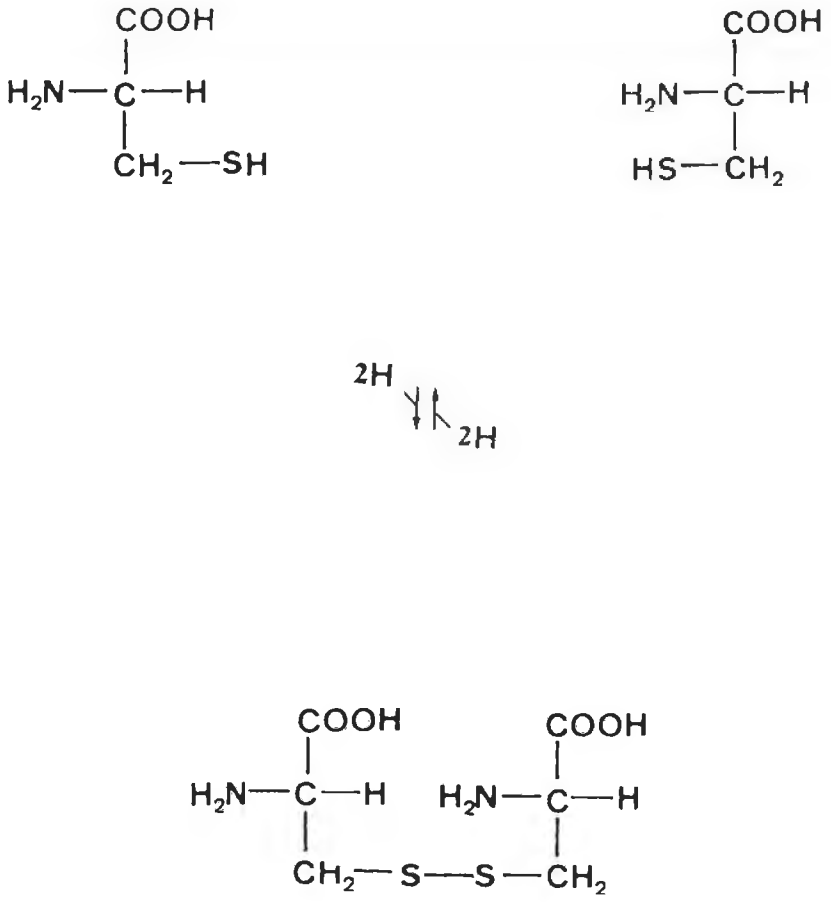

Figure 6.2. The formation of cystine. The thiol groups of two cysteine residues are readily oxidised to yield the disulphide molecule, cystine.

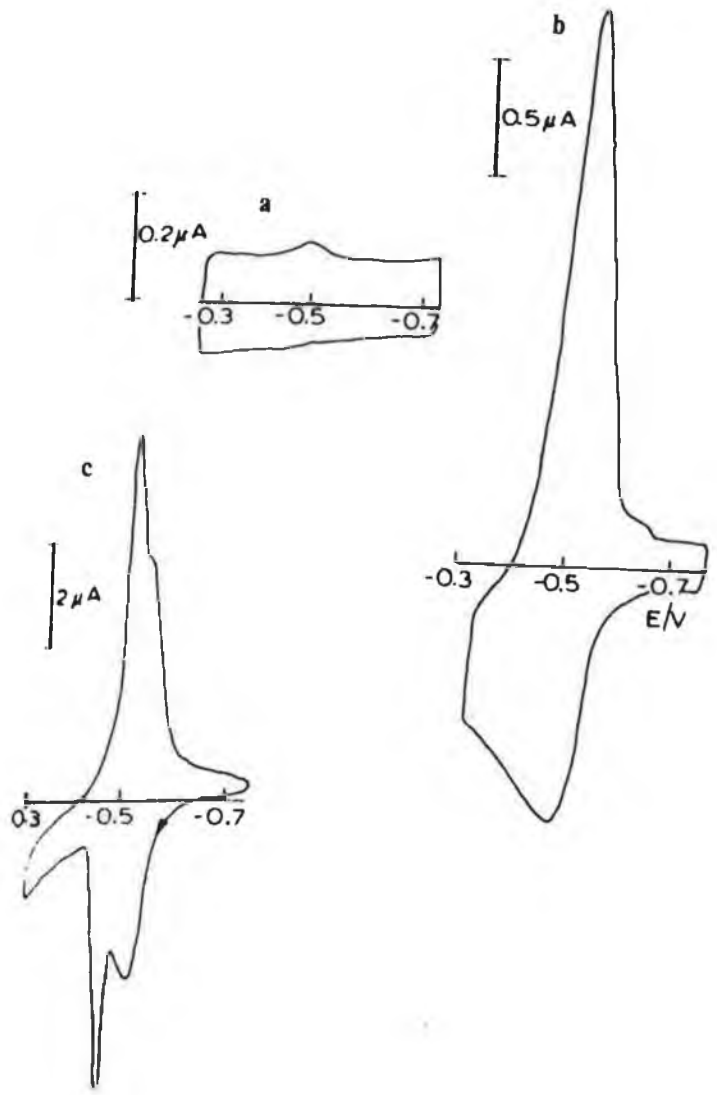

Figure 6.3. Typical cyclic voltammograms of cysteine at pH 7.4, accumulated for 60 s at +0.65 V. (a) 9 x 10^{-7} M; (b) 9 x 10^{-5} M; (c)3 x 10^{-4} M.

Adsorbed reactant. A very small anodic wave was also observed at -0.47 V (vs SCE). Stankovich and Bard[16] suggested that the reduction wave of cystine on the first scan is due to the reduction of adsorbed cystine through breaking of the disulphide bond and formation of dissolved cysteine;

$$(RSSR)_{ads} + 2H^+ + 2e^- \rightleftharpoons 2(RSH)_{soln} \qquad 6.1.$$

Mercuric cysteinate was not formed from the direct reaction of mercury and cystine. Stankovich and Bard predicted a monolayer coverage of the electrode following adsorption of cystine and suggested that the hydrophobicity of the disulphide bond facilitated its strong adsorption to the mercury surface. When the scan was reversed, the cysteine (RSH) in solution was reoxidised:

$$2(RSH)_{soln} + Hg \rightleftharpoons [Hg(RS)_2]_{ads} + 2H^+ + 2e \qquad 6.2.$$

The species $Hg(RS)_2$ is more strongly adsorbed than cystine (RSSR), and therefore subsequent scans show only RSH behaviour. A mechanism for oxidised glutathione (GSSG) has also been proposed by Stricks and Kolthoff[17]:

$$GSSG + e^- + H^+ \rightleftharpoons GS^{\cdot} + GSH \qquad 6.3.$$

$$GS^{\cdot} + e^- + H^+ \rightleftharpoons GSH^{\cdot} \qquad 6.4.$$

Polarography has also been used to study the electroreduction

of the disulphide bonds of insulin and other disulphide proteins by Cecil and Weitzmann at different pH's[18]. At pH 1.0 insulin gave rise to a single cathodic wave at -0.25 V (vs SCE). At pH 7.1, two cathodic waves were observed, the first (wave I) at -0.65 V (vs SCE), and the second (wave II) at -1.02 V. The first wave was apparent at very low concentrations of insulin, and unlike the second wave it increased linearly in height with concentration to a limiting value. The effect of temperature was different for each wave: wave I shifted to a more negative potential and wave II to a more positive potential. At pH 9.2, similar waves were obtained but had $E_{1/2}$ values closer together. On increasing the temperature from 25° to 45°C, the waves merged into one single wave at -1.75 V. These waves were attributed to the reduction of disulphide bonds, of which there are three in the molecule. It was suggested that the appearance of the second cathodic wave (as wave I reached its limiting value) was facilitated by the formation of a second layer of adsorbed protein molecules. Trijueque et al.[19] have used alternating current (AC) polarography to study the reduction of insulin. AC polarograms of amorphous zinc insulin showed three peaks A, B and C. At high concentrations, only peaks A and C were apparent; these waves corresponded to the same faradaic processes discussed by Cecil and Weitzman. The second wave, B, was attributed to a non-faradaic process; this wave was not found using DC or DP polarography. The peak intensity of peak B decreased with pH described by the equation:

$$\log i_p\ (\mu A) = -1.28 - 0.076\ pH \qquad 6.5.$$

Substance	M.w.	Charge ($\mu C\ cm^{-2}$)
Ribonuclease	12.640	8
Somatostatin	1.639	22
Felypressin	1.040	20
Oxytocin	1.007	26
Ox. glutathione	612	60

Table 6.1. Correlation between molecular weight and charge at full coverage.

At pH 3.2, the peak intensity with respect to concentration of protein could be described by:

$$i_p\ (\mu A) = 0.034 - 460\ (Cp\ (M)) \qquad 6.6.$$

where i_p is the peak height, and Cp is the protein concentration. The results obtained corresponded to a desorption of the protein with wholly or partially reduced disulphide bonds. Ribonuclease, oxidised glutathione and insulin were among the disulphide proteins of different sizes studied by Forsman[20] using a stripping voltammetric technique, in the presence and absence of Cu(II) ions. Peaks were obtained for each of these proteins and attributed to the reduction of the disulphide bond. However, the proteins reacted differently on the addition of Cu(II). Oxidised glutathione yielded a peak 100 mV more positive than that of the other proteins, its voltammetric behaviour being very similar to cysteine. This is not really surprising as glutathione is a tripeptide containing L-glutamic acid, L-cysteine and glycine. There was a correlation between amino acid content and voltammetric response; three polypeptides that do not contain any disulphide linkages were also studied and did not give rise to an electrochemical response. Data on the charge obtained from the stripping peak at full coverage is shown in Table 6.1. where it can be seen that their is a relationship between charge and molecular weight. Hertl[21] exploited the electroactivity of disulphide proteins in a differential pulse polarographic serum protein assay. Both human serum and human serum albumin gave rise to a peak near

-0.60 V (vs Ag/AgCl) which was found to be linear with respect to concentration. The optimum pH for studying these proteins was pH 7.0. At pH 3.0 and pH 12.6 the peak had a low initial current which slowly increased but did not reach the intensity of that at pH 7.0 until incubated for sixteen hours. A series of concentrations of bovine serum albumin to 7 μg/ml were assessed for total protein concentration by this method and compared to a standard curve. Linear regression analysis gave a correlation coefficient of 0.894. The assay was also tested for whole blood samples, and cellular constituents were found not to interfere.

6.4. ADSORPTION OF PROTEINS

Throughout this work, the main analytical technique used was adsorptive stripping voltammetry. The electrochemical response of the protein is dependent primarily on the adsorption of the protein onto the electrode surface. Adsorption of such large biological macromolecules is very complex and often difficult to interpret. Reynaud et al. stated "the literature pertaining to the study of protein adsorption at solid/liquid interfaces is often confused; contradictory and unclear laws seem to emerge".[22] Before looking at the adsorption of a protein onto a polarised electrode surface, the physical and conformational changes a protein undergoes at any solid surface must be described.

6.4.1. General Features Of Protein Adsorption

The adsorption of a typical globular protein onto an electrode surface is a competitive process, since the protein must displace solvent molecules or ions already at the surface. The overall adsorption is a combination of various processes:

(i) redistribution of charged groups;
(ii) Van der Waals interactions between the protein and sorbent; and
(iii) structural rearrangements in the protein molecule.

A typical polymer molecule generally attaches many segments to the sorbent surface, i.e. "trains loops and tails" (Figure 6.4.).

6.4.1.1. Role Of Hydrophobicity

Adsorption may be classified as hydrophobic or hydrophilic. It is further complicated by the fact that the solid surface may also have both hydrophobic and hydrophilic sites[23]. At a hydrophilic surface, polar interactions dominate the process, and at hydrophobic surfaces apolar interactions take precedence[24,25]. The hydrophobicity of the protein molecule adds yet another complex factor to the process. The hydrophobicity of an amino acid is derived from the measurement of the solubility of that amino acid between water and an organic solvent. The data obtained is converted into molar free energy of transfer of the amino acid sequence from the

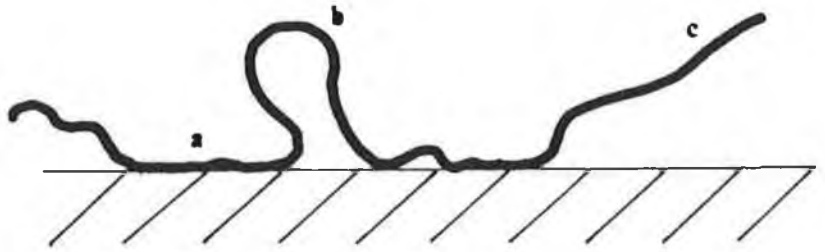

Figure 6.4. "Trains, loops and tails" a model of a biological macromolecule adsorbed at an electrode surface[34]. (a) Train, (b) loop, (c) tail.

aqueous solution to the organic solvent at the same mole fraction at the limit of infinite dilution (ΔF_t). The hydrophobicity ($H\phi$), in calories mol^{-1}, is determined by subtracting ΔF_t for glycine. The hydrophobicity of the protein itself is calculated from:

$$H\phi_{ave} = (\sum_i n_i H\phi_i) / \sum_i n_i . \qquad 6.7.$$

where n_i is the number of residues to the i_{th} amino acid and $H\phi_{ave}$ the amino acid hydrophobicity[26]. A globular protein in an aqueous solution has a hydrophobic core and a hydrophilic shell. In solution, however, it is not always possible to completely bury the hydrophobic regions. In the case where a large degree of the tertiary structure stabilisation of a protein is dependent upon intramolecular hydrophobic interactions, that protein is more likely to rearrange its structure upon adsorption. The loss of these bonds are compensated for by the attachment of these residues to the sorbent surface. Adsorption isotherms usually develop plateau values at around 1 and 5 mg m^{-2}. A very low plateau value (0.6 mg m^{-2}) would indicate that the protein is completely unfolded; although such a case is very rare[27].

6.4.1.3. Role Of Charge

Proteins contain both negatively and positively charged amino acid residues in solution. The isoelectric point (P_i) of a protein is the pH at which that protein has no net charge. At pH's below the isoelectric point, the protein has a net

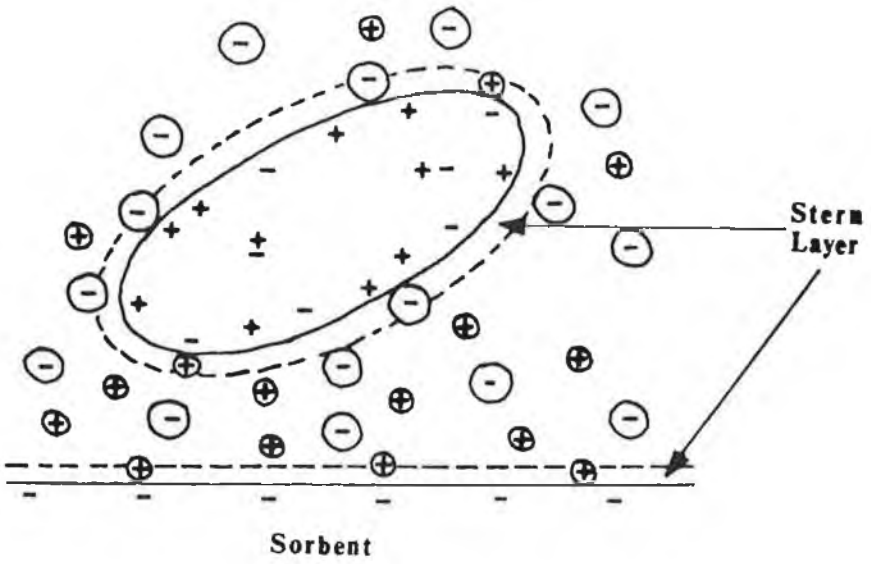

Figure 6.5. Schematic representation of the charge distribution in and around a dissolved protein molecule and at a sorbent/water interface.

results did not give information on the actual configuration of the adsorbed molecule, a possible transition from a Y-shape to a T-shape under the action of external factors was suggested. Brabec and Vucelic[32] suggested that for some proteins there is an extensive perturbation and unfolding at the electrode surface. The adsorption of a simple protein, β_2-microglobulin, consisting of a single polypeptide chain and one interchain disulphide bond buried within the protein, onto a polarised mercury electrode was studied. The diffusion-controlled adsorption was measured by differential capacitance measurements and the surface excess of the solute (Γ) was given by:

$$\Gamma = 1.13 D^{1/2} t^{1/2} C^{b} \qquad 6.8.$$

where D is the diffusion coefficient, t, the time allowed for adsorption and C^b the bulk concentration. Where the protein was adsorbed onto an electrode polarised to potentials corresponding to zero or very small surface charge density, the area taken up by the molecule was large relative to its calculated cross-sectional area, indicating flattening or unfolding of the molecule under the influence of interface energy. These authors noticed that throughout the study, the protein was adsorbed as an almost electroneutral surface active compound. The isoelectric point of β_2-microglobulin was reported to be 5.8. Such compounds are adsorbed at the mercury surface most strongly if that surface is polarised to potentials around the electrode "abandoned potential"[33]. If the electrode was then polarised either positively or

negatively, a decrease in the conformational change was observed. This agrees with the observation made in chapter 5 regarding the preferential adsorption of streptavidin (virtually uncharged at the working pH 7.4) to an electrode held at the abandoned potential. Avidin, which is positively charged at pH 7.4, exhibits no such preference.

Such flattening or unfolding of a protein molecule would allow hydrophobic groups (such as disulphide linkages) buried within the tertiary structure of the protein be exposed and therefore adhere to the electrode surface. Extensive work has been done on the adsorption of nucleic acids which act similarily to proteins at the electrode surface, and which are electroreducible at the mercury electrode, by Palecek[34] and Sequaris[35].

6.5. POSSIBLE EXPLAINATION OF ADSORPTIVE VOLTAMMETRIC BEHAVIOUR OF PROTEINS

An important question that arises from the work carried out in this thesis, is what processes actually give rise to the similar cathodic peaks exhibited by all of the proteins studied in this work and others? Three sets of proteins were studied:

(i) immunoglobulin G (mouse IgG and donkey anti-mouse IgG);

(ii) the antigen binding fragments of IgG (Fab and $F(ab')_2$); and

(iii) the binding proteins avidin and streptavidin.

All of these proteins gave rise to very similar responses when

studied by differential pulse adsorptive stripping voltammetry. They all gave a cathodic peak at around -0.55 V to -0.65 V (vs Ag/AgCl). This variation in peak potential is not considered significant, since variations were found between work carried out at different times i.e. after the reference electrode had been cleaned or the frit changed; this was done frequently as proteins adsorb non-specifically to glass and plastics, making it necessary to change the reference electrode sleeve regularly and silanise the cell to avoid contamination.

Similarly constructed proteins have been studied previously. Fontaine et al.[36,37] have studied various immunoglobulins, i.e. IgG, IgM and IgA. These proteins exhibited both adsorption waves and diffusion waves, the latter being attributed to the reduction of disulphide linkages. The cathodic peak observed at around -0.6 V (vs Ag/AgCl) for many proteins has been attributed to the reduction of this disulphide bond. Lecompte et al.[38] have studied the adsorption rate of the blood clotting protein prothrombin at the HMDE. These authors concluded that in all adsorption states, only a fraction of the total number of disulphide bonds are reduced, implying that only those cystine residues in direct contact with the mercury electrode are electroactive; this protein did not completely unfold at the electrode surface.

In view of this (easy) adsorption of disulphide links and the cathodic peak (at -0.60 V), it would seem (suitable) to apply the proposed model of Stankovich and Bard[16] for the reduction of cystine to these proteins. A typical differential pulse adsorptive stripping voltammogram of cystine is illustrated in

Figure 6.6. It exhibits one main, symmetrical cathodic wave at -0.50 vs Ag/AgCl. This wave is at a slightly more positive potential than those obtained for the proteins. However, of the proteins studied in this work, one, streptavidin had no disulphide bonds or sulphydryl groups present in its structure at all. This protein was chosen for both its importance in immunoassay and its structural similarity to avidin. Both avidin and streptavidin have very similar electrochemical behaviour (chapter 5), both giving rise to a cathodic peak at around -0.55 to -0.60 V vs Ag/AgCl. To avoid confusion, this peak shall be referred to as the "analytical wave" for the rest of this discussion, as it has been found to be analytically useful for both quantitative[21] and qualitative work[39].

A differential pulse adsorptive stripping voltammogram of the carbohydrate binding lectin, concanavalin A, was reported by Rodriguez Flores et al. in a paper investigating the interaction of concanavalin A with mannose[40]. This protein gave rise to two peaks, peak A at -0.21 V (vs Ag/AgCl) and peak B at -0.53 V (vs Ag/AgCl) (Figure 6.7.). It is likely that this second peak is due to the same process or processes that generate the main cathodic peaks of the proteins studied in this work. Concanavalin A is structurally very similar to insulin, except that it has no cysteine residues and therefore no disulphide bonds[41]. This would seem to indicate that "the analytical wave" exhibited by the proteins studied in this work is not neccessarily or entirely due to the reduction of disulphide bonds in contact with the HMDE. The peak is in the same potential region as that of cystine reduction, and therefore some contribution of disulphide bond reduction (from

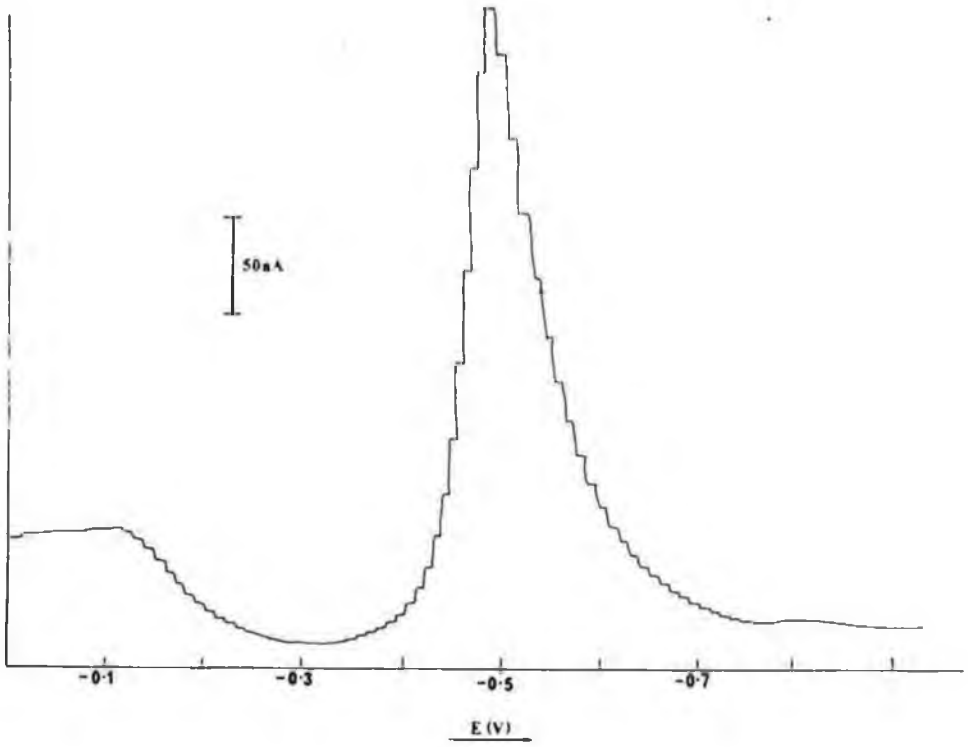

Figure 6.6. A typical adsorptive stripping voltammogram of cystine in 0.1 M phosphate buffer, accumulated at +0.00 V vs. Ag/AgCl.

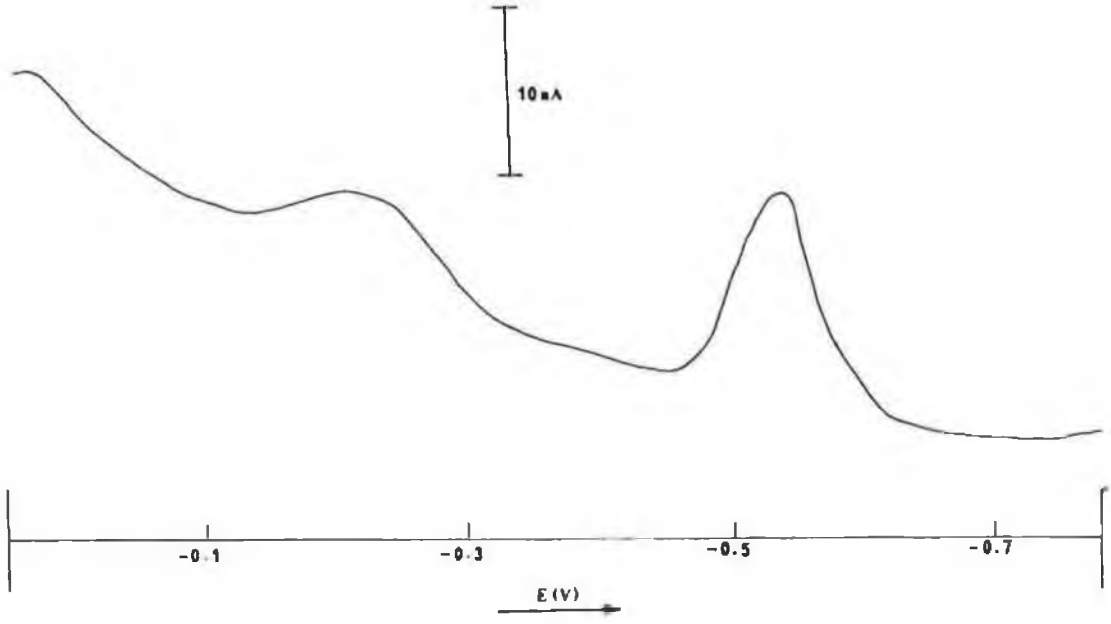

Figure 6.7. A typical adsorptive stripping voltammogram of concanavalin A in 0.05 M phosphate buffer, accumulated at +0.05 vs Ag/AgCl.

those proteins containing disulphide bonds) cannot be ruled out.

It is also unlikely that any chemical reaction of the molecule with mercury occurs in these cases. Stankovich and Bard have compared the behaviour of cystine using (i) a HMDE under electrolysic conditions, and (ii) a mercury pool without electrolysis[16]. After a solution of cystine was stirred over a pool of mercury it was analysed for Hg(II). Stirring for thirty minutes gave rise to a "slight positive test" and indicated a very slow formation of the Hg(II) compound, $Hg(RS)_2$. This same reaction was found to be negligible at the HMDE without electrolysis, and implies that organomercuric compounds are not formed under conditions without electrolysis. Both avidin and streptavidin were investigated with and without electrolysis at the HMDE, and both gave rise to a strong cathodic wave without electrolysis. Indeed, streptavidin gave rise to an enhanced signal, ruling out the formation of an organomercuric compound. It may be seen from the cyclic voltammetric behaviour of those proteins (chapter 5) that the "analytical wave" is due in each case to an irreversible process. This is not consistant with the behaviour reported for insulin or ribonuclease by Forsman[20] or the disulphide proteins trypsin and chymotrypsin, investigated by Wang et al.[42] Similar behaviour was, however, reported for BSA and HSA by Flores et al.[43,44] Cyclic voltammetry at the HMDE, after accumulation with stirring, gave rise for HSA to two cathodic peaks: peak I at -0.68 V (vs Ag/AgCl) and peak II at -0.53 V (vs Ag/AgCl). Peak II disappeared after the first cycle and peak I decreased

gradually on repetitive scanning. Peak II corresponds to the "analytical wave" in this work. This second peak was found to be adsorption controlled as is the "analytical wave" reported here. The profile of the decrease in the "analytical wave" shown in Figure 5.13. (for the protein streptavidin) indicates that the adsorbed protein is stripped from the electrode surface and that the small waves apparent in subsequent scans are due to protein from the vicinity of the double layer adsorbing back onto the electrode surface and that these waves are diffusion controlled.

If the process resulting in the "analytical wave" is not entirely due to either the reduction of the disulphide bonds or the formation of an organomercuric process, the adsorption of the protein onto the mercury drop may have some contribution to the wave formation. Conformational changes of the adsorbed protein, or re-orientation of the molecule leading to some perturbation of the double layer (hence resulting in a charging current), must all be considered.

Desorption of an uncharged surface active compound, that has been adsorbed onto an uncharged electrode may be measured by AC voltammetry. The AC base current in the absence of the surfactant is a measure of the capacity of the double layer. The sharp AC wave that is obtained at the potential of desorption is called a tensammetric wave[45]. Kalvoda[46] has described a protocol to distinguish a pure tensammetric process from a faradaic one. The voltammogram is recorded after accumulation of the surface active species onto the electrode; repetitive scans are then carried out on the same drop without further accumulation. An example of this protocol using a

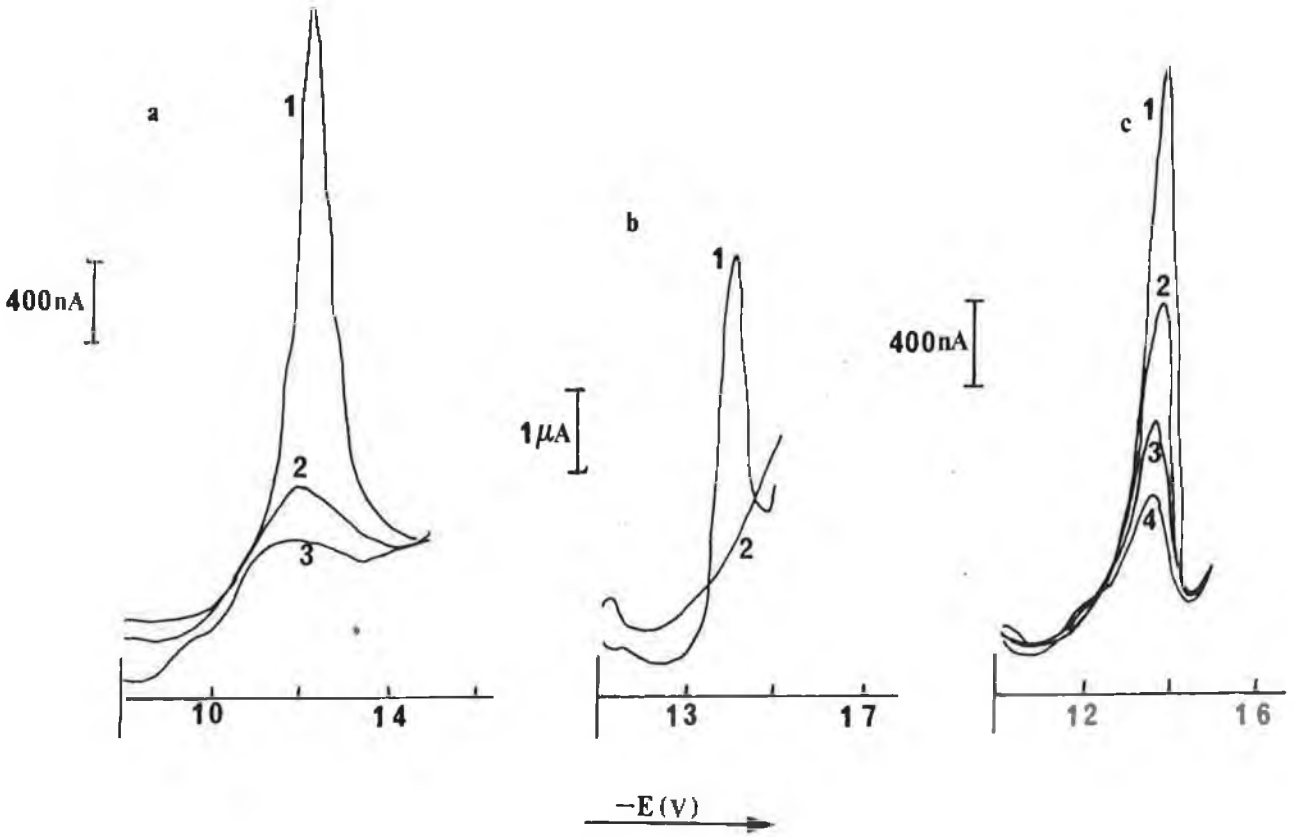

Figure 6.8. The effect of repetitive scans on the same mercury drop for tensammetric and faradaic processes.

(a) diazepam, (1) E_{acc} -0.8 V; t_{acc} 120 s. (2) and (3) succesive scans at the same drop.

(b) papaverine, (1) E_{acc} -1.1 V; t_{acc} 120 s. (2) succesive scan at same drop.

(c) monensin, (1) E_{acc} -1.0 V; t_{acc} 120 s. (2),(3) and (4) succesive scans at same drop.

polyether antibiotic, monensin, diazepam and papaverine, is illustrated in Figure 6.12. The behaviour exhibited in Figure 6.12, a and b are typical of an irreversible reduction, i.e. the waves in subsequent scans are the same as if no accumulation had taken place. If on the other hand successively lower peaks are obtained (as in Figure 6.12, c) the wave may be attributed to a tensammetric process.

The decreases in peak current noticed in the cyclic voltammograms (with adsorptive accumulation) described above show similar behaviour to that described for monensin. The "analytical wave" decreases substantially after the initial scan. The conditions of the CV experiment are of course different, and a linear scan even with accumulation is not as sensitive as AC voltammetry. AC waves are often accompanied by DC waves, and although it is more usual that a tensammetric wave is seen in an AC voltammogram, there may be kinks in the DC curve at potentials where tensammetric waves would occur in the corresponding AC voltammogram. This is due to differences in the double layer capacity at potentials where the surface is covered by the surface active substance and where the normal electrical double layer subsists. If a tensammetric wave was detected using DC methods, it would be likely that it was due to a solution containing a reducible substrate with a surface compound[46].

6.6. CONCLUSION

The cathodic peak exhibited by the proteins studied in this work at around -0.55 V to -0.66 V (vs Ag/AgCl), is an

irreversible, adsorption controlled wave. This wave is useful analytically as it increases linearly with concentration, thereby facilitating the construction of calibration curves. As the proteins studied included streptavidin, a protein that does not contain any sulphydryl groups, it would seem that the models proposed in the literature for the cathodic stripping waves of proteins (at around -0.55 V) involving reduction of disulphide bonds, do not satisfactorily explain the experimental results obtained here. The contribution of a tensammetric process has also been ruled out. It would seem that the wave is due to some faradaic process. There may also be some contribution from structural changes or reorientation at the electrode surface. Further studies on the adsorption profile of proteins at the mercury electrode, particularly proteins without disulphide bonds, and AC voltammetric investigations of such proteins may throw further light on this complex problem.

6.7. REFERENCES

1. Lehninger, A.L., "Principles of Biochemistry" (Worth Publishers Inc., New York, 1882)
2. Berg, H., in "Comprehensive Treatise of Electrochemistry" Volume 10, eds. Srinivasan, S., Chiznadzhev, Y.A., Bockris, J.O'M., Conway, B.E. and Yeager, E., (Plenun Press, New York, 1985).
3. Norde, W. in "Adhesion and Adsorption of Polymers" part B. ed, Lieng-Huang, L., (Plenum publishing corporation, New York, 1980).
4. Herles, F. and Vancura, A. Rozpr. II tr ces. akad. (1932).
5. Heyrovsky, J. and Babicka, J. Coll. Czech. Comm. 2(1930)370.
6. Brdicka, R., Coll. Czech. Comm., 5(1933)112.
7. Brdicka, R., Coll. Czech. Comm., 5(1933)238.
8. Kano, K., Ikeda, T. and Senda, M., Agric. Biol. Chem. 5(1983)1043.
9. Senda, M., Ikeda, T., Kakutani, T., Kano, K. and Kinushita, H. Bioelectrochem, bioenerg. 8(1981)151.
10. Armstrong, F.A., Hill HAO. and Walton, N.J. Acc. Chem. Res. 21(1988)151.
11. Heineman, W.R., Norris, B.J., Goeltz, J.F., Anal. chem. 47(1975)79.
12. Scheller, F., Janchen, M., Lampe, J., Prumke, H-J., Blanck, J. and Palecek, E. Biochem et Biophys. acta. 412(1975)157.

13. Kolthoff, I.M. and Barnum, C. J., Amer. Chem. Soc., 63(1941)520.

14. Kolthoff, I.M., Stricks, W. and Tanaka, N., J. Amer. Chem. Soc., 57(1955)5211.

15. Van den Berg, C.M.G., Househam, B.C. and Riely, J.P. J. Electroanal. Chem., 239(1988)137.

16. Stankovich, M.J. and Bard, A.J., J. Electroanal. Chem., 75(1977)487.

17. Stricks, W. and Kolthoff, I.M., J. Am. Chem. Soc., 75(1953)5673.

18. Cecil, R., and Weitsman, P.D.J., Biochem. J., 93(1964)1.

19. Trijuque, J., Sanz, C., Monleon, C. and Vincente, F., J. Electroanal. Chem., 251(1988)173.

20. Forsman, U., Anal. Chim. Acta., 106(1984)141.

21. Hertl, W., Anal. Biochem., 164(1987)1.

22. Reynaud, J.A., Tavernier, I., Yu, L.T. and Cochet, J.M., Bioelectrochem. Bioenerg., 15(1986)275.

23. Bull, H.B., Biochem. Biophys. Acta. 19(1956)464.

24. Brash, J.L. and Lyman, D.J. in "The Chemistry of Biosurfaces" ed. Hair, M.L., (Marcel Dekker, New York, 1971).

25. Miller, I.R. and Bach, D. in "Surface and Colloid Science" Volume 6. ed. Matijevic, E. (Wiley-Interscience, New York, 1973).

26. Bigelow, C.C. and Channon, M., in "The Handbook of Biochemistry and Molecular biology: Proteins volume 3" ed. Fasman, G.D., (CRC Press, 1976, Ohio)

27. Norde, W. in "Adhesion and Adsorption of Polymers" ed. Lee, L. -H (Plenum Press, New York, 1980).

28. Morrissey, B.W. and Stromberg, J., J. Colloid. Interface. Sci., 46(1974)6.

29. Norde, W., Commun. Agric. Univ. Wageningen., 76(1976)6.

30. Morrissey, B.W., Smith, L.E., Stromberg, R.R. and Fenstermaker, C.A., J. Colloid. Interface. Sci. 66(1978)266.

31. Lavrentev, V.V., Chasovnikaa, L. and Sorokin, J., in "Adhesion and Adsorption of Polymers" ed. Lee, L.H., (Plenum Press, New York, 1980).

32. Brabec, V. and Vucelic, D., Biophys. Chem., 29(1988)271.

33. Mohilner, D.M., in "Electroanalytical Chemistry" Volume 1. ed. Bard, A. J. (Marcel Dekker, New York, 1966).

34. Palecek, E., Bioelectrochem. Bioenerg., 15(1986)103.

35. Sequaris, J.M. in "Electrochemistry, Sensors and Analysis" ed. Smyth, M.R. and Vos, J.G., (Elsevier, Amsterdam, 1986).

36. Fontaine, M., Rivat, C., Ropartz, C. and Coullet, C., Ann. Inst. Pasteur, Paris, 120(1971)313.

37. Fontaine, M., Rivat, C., Ropartz, C. and Coullet, C. Bull. Soc. Chem. Fr. 6(1973)1873.

38. Lecompte, M.F., Clavilier, J., Dode, C., Elion, J. and Miller, J.R., J. Electronnal chem. 163(1984)345.

39. Ryan, E., Vos, J.G. and O'Kennedy, R., unpublished work.

40. Flores, J.R., O'Kennedy, R. and Smyth, M.R., Analyst., 113(1988)525.

41. Edelman, G.M., Cunningham, B.A., Reeke, G.N., Becker, J.W., Waxdal, M.J. and Wang, J.L., Proc. Nat. Acad. Sci. USA. 69(1972)2580.

42. Wang, J., Villa, V. and Tapia, T., Bioelectrochem. Bioenerg., 19(1988)39.

43. Flores, J.R., O'Kennedy, R. and Smyth, M.R., Anal, Chim. Acta (in press).

44. Flores, J.R. and Smyth, M.R., J. Electro. Anal. Chem., 235(1987)317.

45. Kalvoda, R., J, Electrochem., 180(1984)307.

46. Breyer, B. and Bauer, H.H. "Alternating Current Polarography and Tensammetry" (Interscience Publishers, New York, 1936).